Decoding Interactions of the Nematophagous Fungus, *Pochonia chlamydosporia,* with Black Pepper

Thesis submitted to the

University of Calicut

For the award of degree of

Doctor of Philosophy

(Biotechnology)

By

Mery Rincy. K
(U.O.No.4923/2018.Admn.dated 20-04-2018)

Under the guidance of

Dr. Santhosh J. Eapen

ICAR- INDIAN INSTITUTE OF SPICES RESEARCH
Marikunnu (P.O.), Kozhikode, Kerala
December 2024

भाकृअनुप - भारतीय मसाला फसल अनुसंधान संस्थान
ICAR - INDIAN INSTITUTE OF SPICES RESEARCH
(भारतीय कृषि अनुसंधान परिषद *Indian Council of Agricultural Research)*
पोस्ट बैग संख्या: *Post Bag No: 1701,* मेरिकुन्नु पोस्ट *Marikunnu Post,*
कोषिक्कोड *Kozhikode-673012,* केरल, *Kerala,* भारत *India*
(ISO 9001: 2015 Certified Institute)

CERTIFICATE

This is to certify that the thesis entitled **'Decoding interactions of the nematophagous fungus, *Pochonia chlamydosporia,* with black pepper'** submitted to the University of Calicut **by Mrs. Mery Rincy K.** for the award of the degree of **Doctor of Philosophy** in **Biotechnology** is a bonafide record of research work carried out by her at ICAR- Indian Institute of Spices Research, Kozhikode, Kerala, under my supervision and guidance. No part of the work has formed the basis for the award of any degree or diploma previously. The plagiarism has been checked at CHMK library, University of Calicut and the values are well within the acceptable limit.

Place: Thiruvananthapuram
Date: 18 December 2024

Dr. Santhosh J. Eapen

पीएबीएक्स PABX: 0495-2731410/2731753/2731345 निदेशक का कार्यालय Director's Office: 0495-2730294 परियोजना समन्वयक Project Coordinator: 0495-2731794, एटिक ATIC: 0495 - 2730704. आई आई एस आर प्रायोगिक प्रक्षेत्र, पेरुवण्णामुषि IISR Experimental Farm, Peruvannamuzhi: 0496 2249371 कृषि विज्ञान केन्द्र Krishi Vigyan Kendra, पेरुवण्णामुषि Peruvannamuzhi: 0496-2666041, फैक्स Fax: 0091-495-2731187 ई-मेल Email: director.spices@icar.gov.in वेबसाईट Website: www.spices.res.in

DECLARATION

I hereby declare that the thesis entitled **'Decoding interactions of the nematophagous fungus, *Pochonia chlamydosporia,* with black pepper'** submitted by me for the award of the degree of **Doctor of Philosophy** in **Biotechnology** at the **University of Calicut**, is a bonafide record of research work carried out at **ICAR-Indian Institute of Spices Research**, Kozhikode under the guidance of **Dr. Santhosh J. Eapen**, Former Head and Principal Scientist, Nematology, Division of Crop Protection, ICAR-Indian Institute of Spices Research, Kozhikode, Kerala. This thesis or part of it has not been submitted to any other university for the award of another degree or diploma previously. The contents of the thesis are undergone plagiarism check using iThenticate software at C.H.M.K. Library, University of Calicut, and the similarity index found within the permissible limit. I also declare that the thesis is free from AI generated contents.

Mery Rincy. K

Dr. Santhosh J. Eapen
(*Research Supervisor*)

Place:

Date:

To my dear Amma and Appachan,
whose love and support sustained me
throughout my work.

ACKNOWLEDGEMENTS

I take this opportunity to convey my immense gratitude to all people who spend their valuable time, affection, advices and guidance all that enabled me to complete my research in a creative way. First and foremost, praises to the ***God, Almighty****, for his blessings to complete my research work.*

It is difficult to accurately evaluate the assistance, support, and advice provided by a group of people. However, I am revealing the names of the petals that, together with the flower, filled my life with an elegant smell.

With immense pleasure and pride, I express my gratitude and indebtedness to my research guide, ***Dr. Santhosh J. Eapen****, Former Head and Principal Scientist, Nematology, Division of Crop Protection, ICAR-Indian Institute of Spices Research, Kozhikode, Kerala. His intellectual guidance, valuable advice, abundant and inspiring support and care, made my task easy and his vast knowledge and experience have contributed a lot in completing the study successfully. I express my sincere gratitude for encouraging my freedom of thought and constant support he showered towards me go beyond words.*

I sincerely thank, ***Dr. R. Dinesh*** *the Director, ICAR-IISR for his support, encouragement, and also for providing excellent lab facilities.*

I am thankful to ***Dr. K. Nirmal Babu****, the Former Director, ICAR-IISR for giving me this opportunity to do Ph.D. in ICAR-IISR.*

I express my sincere thanks to ***Dr. A. Ishwara Bhat****, Head, Division of Crop Protection, ICAR-IISR for the valuable suggestions and timely advice during the course of my study.*

I owe a huge debt of gratitude to ***Dr. R. Praveena*** *and* ***Dr. Sona Charles*** *for being a mental support throughout my research and also for their important*

suggestions and timely advice during the course which help me to improve my research work.

I express my sincere gratitude to scientists of the Division of Crop Protection, ICAR-IISR, ***Dr. C.M. Senthil Kumar, Dr. C.N. Biju, Dr. C. Sarathambal, Dr. Manimaran B, Dr. Mohammed Faisal Peeran*** *and* ***Dr. C. Sellaperumal*** *for their support and encouragement.*

My deepest and genuine thanks to scientists of the Division of Crop Production and Post-Harvest Technology, ***Dr. C.K. Thankamani, Dr. N.K. Leela, Dr. K. Kandiannan, Dr. K.S. Krishnamoorthy, Dr. V. Srinivasan, Dr. E. Jayashree, Dr. K. Anees, Dr. P. Alagupalamuthirsolai*** *and* ***Dr.. R. Sivaranjani*** *for various favors received during my study at ICAR-IISR.*

I am grateful to scientists of the Division of Crop Improvement and Biotechnology, ***Dr. K.V. Saji, Dr. T.E. Sheeja, Dr. D. Prasath, Dr. Sharon Aravind, Dr. P. Umadevi,*** *and* ***Dr. S. Aarthi****, for their kind support and help which encouraged me to improve the work.*

I thank scientists of the section of Social Sciences, ***Dr. P. Rajeev****, and* ***Dr. Lijo Thomas*** *for their kind support.*

I express my gratitude towards ***Dr. Manimaran B,*** *Secretary HRD and* ***Dr. E. Jayashree*** *former Secretary HRD, ICAR-IISR, Kozhikode for their help and support during the end and starting of my research.* ***Dr. D. Prasath*** *and* ***Dr. C. Sarathambal,*** *for their advices support and encouragement during the course and I thank* ***Vishnu*** *and all members of HRD and PME for all the help rendered.*

I express my heartfelt gratitude to all the ***doctoral committee members and research advisory committee members*** *especially* ***Dr. KK Elyas*** *and* ***Dr. Santhosh Nampy*** *for evaluating my research and their valuable suggestions to improve my work. I would like to thank* ***Dr. Anu Augustine*** *for evaluating and conducting PQE viva. I express my sincere gratitude to the all-staff members at* ***Directorate of Research and CHMK Library****, University of Calicut for their support. Special thanks to* ***Dr.Nasirudheen.T*** *who carried out the plagiarism check in my thesis.*

The financial and administrative support extended by the ***Kerala State Council for Science, Technology and Environment, Kerala,*** *through* ***KSCSTE research fellowship*** *is greatly acknowledged.*

I would like to express my sincere gratitude to ***Dr. S. Hamza****, Chief technical officer for his immense support and advices and also, I thank* ***Mrs. Chandravally*** *and* ***Dr. Priya George*** *for their support and care.*

I thank ***Mr. M.P. Ramesh Kumar****, former Librarian, ICAR-IISR, who allowed me to access library facilities. I am thankful to* ***Mr. K. Jayarajan****, Chief Technical Officer for the statistical helps rendered. I thank* ***Mr. A. Sudhakaran****, Technical Assistant, ICAR-IISR for assisting me in photography. I thank* ***Mrs. C.K. Beena****, PS to Director, for the moral support and encouragement given all the time. The help rendered by the staff members of accounts and administration sections, ICAR-IISR is also gratefully acknowledged.*

I thank all the ***contract labours and supporting staffs*** *at ICAR-IISR. I express my gratitude to* ***Mrs. Nisha, Mrs. Prabha, Mrs. Reeja, Mr. Sreedharan, Mrs. Indira, Mrs. Sujatha*** *and* ***Mrs. Divya*** *for their immense support and help. I express my gratitude to all the* ***security staffs*** *for their care and support.*

I express my deepest gratitude to my best friends, ***Subila K.P, Aiswarya, Anju, Alka*** *and* ***Sumayya Hassan*** *for their constant support, encouragement, and unconditional helps rendered.*

I extend my sincere gratitude towards my dear friend ***Ambilly sarath*** *for the love, support, and concern during my research journey.*

I owe my sincere thanks to ***Fayad*** *for the technical help and moral support given throughout the period.*

I thank my colleagues ***Prashina, Aparna, Shajna, Lijina, Hemesh, Vadivukarasi, Atheena, Ahmed Mujtaba, Asha, Naveen, Karthika, Sumaila, Megha, Rugma, Blessy, Nasmin, Neenu, Vijayashanthi, Theertha, Ashwathy, Greeshma, P.B. Krishna,*** *and* ***Jitheesh*** *for their help and support.*

Finally, words fail to acknowledge the cherishing love and care of ***my family*** *and* ***relatives.*** *I owe my loving thanks to my parents,* ***Rosy K.S, K.J Wilson, Thimothy, Kunjethy*** *and my siblings* ***John wins, Emerin, Shinoj and Shelly*** *for their endless affection, support and encouragement.*

Last but not least I thank my dear ***Shijoy*** *who saw all my bitterness and constantly stood by my side during the entire journey with utmost patience.*

I am indebted toward to my son ***Neslin*** *for giving me happiness during all phases of the research.*

I am thankful to all other staff members of the Indian Institute of Spices Research, Kozhikode for their assistance and care.

I thank one and all who have directly or indirectly involved in my work.

Thank you…

Mery Rincy. K

CONTENTS

LIST OF FIGURES

LIST OF TABLES

ABBREVIATIONS

AAS	Atomic absorption spectrophotometer
ABA	Abscisic acid
ACC	1- aminocyclopropane-1-carboxylate
ANOVA	Analysis of variance
APX	Ascorbate peroxidase
BCA	Biocontrol agent
BLAST	Basic Local Alignment Search Tool
BP	Biological Process
bZIP	basic leucine zipper
Ca	Calcium
$CaCl_2$	Calcium chloride
CAS	Chrome azurol S
CC	Cellular Component
CD-HIT	Cluster Database at High Identity with Tolerance
cDNA	Complementary DNA
CDS	Coding sequences
CFU	Colony forming unit
CMC	Carboxymethyl cellulose
Ct	Cycle Threshold
CTAB	Cetyltrimethylammonium bromide
Cu	Copper
CMV	Cucumber mosaic virus
DEG	Differentially expressed gene
DIR	Dirigent proteins

DMSO	Dimethyl sulphoxide
DNA	Deoxyribonucleic acid
dpi	Days post inoculation
DTPA	Diethylene triamine pentaacetic acid
EC	Enzyme Commission
ED	Effective dose
EN	Enniatin
ERT	Ethylene-responsive transcription factor
ES	Excretory/secretory
ETI	Effector-triggered immunity
FC	Fold change
Fe	Iron
Fig.	Figure
FLAs	Fasciclin-like arabinogalactan proteins
FP	Forward Primer
g	Gram
GO	Gene ontology
GRP	Gibberellin-regulated protein
GST	Glutathione S-transferase
H	Hour
H_2SO_4	Sulphuric acid
HCl	Hydrochloric acid
HSV	Herpes simplex virus
IAA	Indole-3-acetic acid
ICAR	Indian Council of Agricultural Research
IISR	Indian Institute of Spices Research
IPM	Integrated pest management

ISR	Induced systemic resistance
JA	Jasmonic acid
K	Potassium
KAAS	KEGG Automatic Annotation Server
KEGG	Kyoto Encyclopedia of Genes and Genomes
KO	KEGG Orthology
l	Litre
LEA	Late embryogenesis abundant
LEA	Late embryogenesis abundant
LRR	Leucine-rich repeats
M	Molar
m	Metre
MAPK	Mitogen-activated protein kinases
MF	Molecular Function
Mg	Magnesium
mg	Milligram
mg/ml	Milligram per milliliter
min	Minute
MIP	Major intrinsic protein
Ml	Millilitre
MLPs	Major latex-like proteins
mM	Millimolar
mm	Millimetre
Mn	Manganese
mRNA	Messenger RNA
MTCC	Microbial type culture collection
N	Normal

N	Nitrogen
Na	Sodium
NaCl	Sodium chloride
NaOH	Sodium hydroxide
NBS	Nucleotide-binding site
NCBI	National Center for Biotechnology Information
NGS	Next generation Sequencing
NH_3	Ammonia
NH_4F	Ammonium fluoride
NIPs	Nodulin 26-like intrinsic proteins
nm	Nanometer
NPR1	Nonexpressor of Pathogenesis-Related Protein 1
ORF	Open reading frames
P	Phosphorus
PAL	Phenylalanine ammonia lyase
PBS	Phosphate-buffered saline
PCK	Potassium transporter
PCR	Polymerase chain reaction
PDA	Potato dextrose agar
PDB	Protein Data Bank
PDB	Potato Dextrose Broth
Pg	Picogram
PGP	Plant growth promoting
PGPF	Plant growth-promoting fungi
PYMoV	Piper yellow mottle virus
PIPES	Piperazine-N,N’-bis(2-ethanesulfonic acid)
PIPs	Plasma membrane intrinsic proteins

PIRG	Percentage inhibition of radial growth
Ppm	Parts per million
PPNs	Plant-parasitic nematodes
PR	Pathogenesis-related
psi	Pounds per square inch
PTI	Pattern-triggered immunity
QC	Quality check
qPCR	Quantitative polymerase chain reaction.
qRT- PCR	Quantitative Reverse Transcription PCR
RAL	Resorcylic acid lactone
Rf	Retention factor
RH	Relative humidity
RKN	Root-knot nematode
RNA	Ribonucleic acid
RNA-Seq	RNA sequencing
ROS	Reactive oxygen species
RP	Reverse Primer
rpm	Revolutions per minute
SA	Salicylic acid
SAR	Systemic acquired resistance
SAS	Statistical Analysis System
SE	Standard error
SCP1	Serine protease carboxypeptidase
sec	Second
SI	Solubilization Index
SM	Secondary metabolites
SMILES	Simplified molecular input line entry system.

SRA	Sequence Read Archive
$SrCl_2$	Strontium chloride
TIPs	Tonoplast intrinsic proteins
TLC	Thin-layer chromatography
UPL	Ubiquitin-protein ligase
UPLC- (ESI)-QToF-MS	Ultra Performance Liquid Chromatography coupled with Electrospray Ionization-Quadrupole-Time Of Flight-Mass Spectrometry
UV	Ultraviolet
VAP	Venom allergen-like protein
W	Weight
w/v	Weight in volume
WP	Wettable powder
YPD	Yeast peptone dextrose
ZEP	zeaxanthin epoxidase
Zn	Zinc
ZnO	Zinc oxide
ZT	Zinc transporter
°C	Degree Celsius
µmol	Micromole

Abstract

Biological control agents like *Pochonia chlamydosporia* are gaining prominence as eco-friendly alternatives to chemical pesticides in sustainable agriculture. This nematophagous fungus not only parasitizes nematode eggs but also promotes plant growth, making it valuable for crops like black pepper. This study investigates the biocontrol potential of *P. chlamydosporia* through its secondary metabolites, assessing their antifungal and nematicidal properties, while exploring the fungus's ability to enhance plant growth and defence.

The nematophagous fungus *Pochonia chlamydosporia* was evaluated for its plant growth-promoting properties in black pepper (*Piper nigrum* L.). The fungal isolate, *P. chlamydosporia* strain IISR-MTCC5412, was tested for its ability to produce plant growth-promoting substances, including indole-3-acetic acid (IAA), ammonia, and its capacity to solubilize inorganic phosphate and zinc. Results showed that the strain produced IAA (9.8 µg/ml), ammonia, and solubilised both phosphate (1.3 ± 0.07 response units) and zinc (1.1 ± 0.01 response units). The fungus also exhibited indirect plant growth-promoting effects, such as siderophore production (2 ± 0.04 response units) and the synthesis of extracellular enzymes, including α-amylases, cellulases, and pectinases. Pot culture studies demonstrated that *P. chlamydosporia* significantly enhanced shoot and root growth, biomass, and nutrient uptake (nitrogen, phosphorus, potassium, calcium, magnesium, copper, manganese, iron and zinc) in black pepper plants. These findings underscore the agronomic potential of *P. chlamydosporia* strain IISR-MTCC5412 as both a biocontrol agent and a plant growth promoter.

Secondary metabolites of *P. chlamydosporia* were extracted using ethyl acetate, and their activity against pathogens and plant parasitic nematodes was tested. The crude extract showed strong antifungal activity against pathogens such as *Pythium myriotylum* (99.54%) and *Phytophthora* spp. (99.99%) while the lowest percentage inhibition was observed with *Macrophomina* spp. (40%). The ethyl acetate extract also exhibited nematicidal activity against *Radopholus similis,* with the highest mortality observed at the crude extract concentration. High-resolution UPLC- (ESI)-QToF-MS analysis identified several bioactive compounds, including bisevertinol, enniatin I, and enniatin H.

To identify potential lead compounds, an *in-silico* virtual screening, including molecular docking and binding free energy computation, was performed. The results indicated that three compounds - bisevertinol, enniatin I, and enniatin H - could serve

as lead molecules for the development of nematicidal chemicals against plant parasitic nematodes.

Furthermore, transcriptome analysis was conducted to study the interaction between *P. chlamydosporia* and black pepper roots at 14 and 28 days post-inoculation (dpi). Using next generation sequencing (NGS) technologies (HiSeq 500 platforms), 2,03,092 transcripts and 65,354 differentially expressed genes (DEG) were identified, revealing significant changes in gene expression related to plant growth promotion and induced systemic resistance (ISR). Genes involved in phytohormone biosynthesis (auxin, ethylene, cytokinin, abscisic acid, and gibberellin), nutrient uptake (nitrogen, phosphorous, potassium, calcium, iron, boron, and zinc) and plant defence-related genes (including pathogenesis-related (PR) proteins, lipid-transfer protein (DIR1), endochitinase, germin-like proteins, late embryogenesis abundant (LEA) proteins, LURP1, thaumatin and Major Latex-like Proteins (MLPs)) were upregulated in black pepper plants colonised by *P. chlamydosporia*.

Functional gene ontology (GO) analysis showed enrichment in stress resistance and ISR signalling pathways, indicating that the fungus enhances the plant's ability to withstand biotic and abiotic stress. KEGG enrichment analysis also highlighted upregulation of pathways related to plant hormone signal transduction. This transcriptomic data provides molecular evidence that *P. chlamydosporia* promotes plant growth and strengthens defence mechanisms of black pepper, offering new insights into its dual role as a biocontrol agent and endophyte.

This study confirms *P. chlamydosporia* as a promising biocontrol agent with dual functions: suppressing plant pathogens and promoting growth in black pepper. Key bioactive compounds, such as bisevertinol, enniatin I, and enniatin H, were identified with potential for nematicidal use. Transcriptomic analysis provided molecular insights into how the fungus boosts plant growth and defence, emphasising its potential in sustainable pest management and crop resilience strategies.

Keywords: Biocontrol agent, *Pochonia chlamydosporia,* Secondary metabolites, Transcriptome, bioactive compounds, endophyte and Next generation sequencing (NGS) technologies.

സംഗ്രഹം

സുസ്ഥിര കൃഷിയിൽ രാസ കീടനാശിനികൾക്ക് പരിസ്ഥിതി സൗഹൃദ ബദലായി *പോച്ചോണിയ ക്ലമൈഡോസ്പോറിയ* പോലുള്ള ജൈവ നിയന്ത്രണ ഏജൻറുകൾ പ്രാധാന്യം നേടുന്നു. ഈ നെമറ്റോഫാഗസ് കുമിൾ നിമാവിരകളുടെ മുട്ടകളെ പരാന്നഭോജിയാക്കുക മാത്രമല്ല, ചെടികളുടെ വളർച്ചയെ പ്രോത്സാഹിപ്പിക്കുകയും ചെയ്യുന്നു, ഇത് കുരുമുളക് പോലുള്ള വിളകൾക്ക് വിലപ്പെട്ടതാക്കുന്നു. ഈ പഠനം *പോച്ചോണിയ ക്ലമൈഡോസ്പോറിയ*യുടെ ദ്വിതീയ ഉപാപചയ പ്രവർത്തനങ്ങളിലൂടെയുള്ള ജൈവനിയന്ത്രണ സാധ്യതയെക്കുറിച്ച് അന്വേഷിക്കുന്നു, അവയുടെ ആൻറി ഫംഗൽ, നെമാറ്റിസൈഡൽ ഗുണങ്ങൾ വിലയിരുത്തുന്നു, അതേസമയം ചെടികളുടെ വളർച്ചയും പ്രതിരോധവും വർദ്ധിപ്പിക്കുന്നതിനുള്ള ഫംഗസിൻറെ കഴിവ് പര്യവേക്ഷണം ചെയ്യുന്നു.

നെമറ്റോഫാഗസ് കുമിളായ *പോച്ചോണിയ ക്ലമൈഡോസ്പോറിയ* കുരുമുളകിൽ ചെടികളുടെ വളർച്ചയെ പ്രോത്സാഹിപ്പിക്കുന്ന ഗുണങ്ങളെ വിലയിരുത്തി. ഇൻഡോൾ-3-അസറ്റിക് ആസിഡ്, അമോണിയ, അജൈവ ഫോസ്ഫേറ്റും സിങ്കും ലയിപ്പിക്കാനുള്ള കഴിവ് എന്നിവയുൾപ്പെടെ സസ്യവളർച്ചയെ പ്രോത്സാഹിപ്പിക്കുന്ന പദാർത്ഥങ്ങൾ ഉൽപ്പാദിപ്പിക്കുന്നതിനുള്ള കഴിവ്, *പോച്ചോണിയ ക്ലമൈഡോസ്പോറിയ* കാണിച്ചു. സ്ട്രെയിൻ IAA (9.8 µg/ml), അമോണിയ എന്നിവ ഉൽപ്പാദിപ്പിക്കുകയും ഫോസ്ഫേറ്റും (1.3 ± 0.07 റെസ്പോൺസ് യൂണിറ്റുകൾ) സിങ്കും (1.1 ± 0.01 റെസ്പോൺസ് യൂണിറ്റുകൾ) ലയിപ്പിച്ചതായും ഫലങ്ങൾ കാണിച്ചു. സൈഡറോഫോർ ഉത്പാദനം (2 ± 0.04 റെസ്പോൺസ് യൂണിറ്റുകൾ), α-അമൈലേസ്, സെല്ലുലേസ്, പെക്റ്റിനേസുകൾ എന്നിവയുൾപ്പെടെയുള്ള എക്സ്ട്രാ സെല്ലുലാർ എൻസൈമുകളുടെ സമന്വയം പോലെയുള്ള പരോക്ഷമായ സസ്യവളർച്ചയെ പ്രോത്സാഹിപ്പിക്കുന്ന ഫലങ്ങളും ഫംഗസ് പ്രദർശിപ്പിച്ചു. കുരുമുളക് ചെടികളിൽ

പി.ക്ലാമിഡോസ്പോറിയ, ചിനപ്പുപൊട്ടലും വേരുവളർച്ചയും, ജൈവാംശവും, പോഷകങ്ങളും (നൈട്രജൻ, ഫോസ്ഫറസ്, പൊട്ടാസ്യം, കാൽസ്യം, മഗ്നീഷ്യം, ചെമ്പ്, മാംഗനീസ്, ഇരുമ്പ്, സിങ്ക്) എന്നിവ ഗണ്യമായി വർധിപ്പിച്ചതായി പോട്ട് കൾച്ചർ പഠനങ്ങൾ തെളിയിച്ചു. ഈ കണ്ടെത്തലുകൾ *പോച്ചോണിയ ക്ലമൈഡോസ്പോറിയ*യുടെ അഗ്രോണമിക് സാധ്യതകൾക്ക് അടിവരയിടുന്നു.

പി.ക്ലാമിഡോസ്പോറിയയുടെ ദ്വിതീയ ഉപാപചയങ്ങൾ എഥൈൽ അസറ്റേറ്റ് ഉപയോഗിച്ച് വേർതിരിച്ചെടുക്കുകയും രോഗകാരികൾക്കും സസ്യ പരാന്നഭോജികളായ നെമറ്റോഡുകൾക്കുമെതിരായ അവയുടെ പ്രവർത്തനം പരീക്ഷിച്ചു. പൈത്തിയം മൈരിയോടൈലം (99.54%), ഫൈറ്റോഫ്തോറ എസ്പിപി തുടങ്ങിയ രോഗകാരികൾക്കെതിരെ ശക്തമായ ആന്റിഫംഗൽ പ്രവർത്തനം ക്രൂഡ് എക്സ്ട്രാക്റ്റ് കാണിച്ചു. (99.99%) മാക്രോഫോമിന എസ്പിപിയിൽ ഏറ്റവും കുറഞ്ഞ ശതമാനം നിരോധനം നിരീക്ഷിക്കപ്പെട്ടു. (40%). എഥൈൽ അസറ്റേറ്റ് എക്സ്ട്രാക്റ്റ് റാഡോഫോലസ് സിമിലിസിനെതിരെ നെമാറ്റിസൈഡൽ പ്രവർത്തനവും പ്രകടമാക്കി, ക്രൂഡ് എക്സ്ട്രാക്റ്റ് സാന്ദ്രതയിൽ ഏറ്റവും ഉയർന്ന മരണനിരക്ക് നിരീക്ഷിക്കപ്പെട്ടു. UPLC- (ESI)-QToF-MS അനാലിസിസ് ഉപയോഗിച്ച് ബിസെവെർട്ടിനോൾ, എന്നാറ്റിൻ I, എനിയാറ്റിൻ എച്ച് എന്നിവയുൾപ്പെടെ നിരവധി ബയോ ആക്റ്റീവ് സംയുക്തങ്ങൾ തിരിച്ചറിഞ്ഞു.

സാധ്യതയുള്ള ലീഡ് സംയുക്തങ്ങൾ തിരിച്ചറിയാൻ, മോളിക്യുലാർ ഡോക്കിംഗും ബൈൻഡിംഗ് ഫ്രീ എനർജി കമ്പ്യൂട്ടേഷനും ഉൾപ്പെടെയുള്ള ഇൻ-സിലിക്കോ വെർച്വൽ സ്ക്രീനിംഗ് നടത്തി. ബിസെവെർട്ടിനോൾ, എനിയാറ്റിൻ I, എന്നാറ്റിൻ എച്ച് എന്നീ മൂന്ന് സംയുക്തങ്ങൾക്ക് സസ്യ പരാന്നഭോജികളായ നിമാവിരകൾക്കെതിരെ നെമാറ്റിസൈഡൽ രാസവസ്തുക്കൾ വികസിപ്പിക്കുന്നതിനുള്ള ലീഡ് തന്മാത്രകളായി വർത്തിക്കുമെന്ന് ഫലങ്ങൾ സൂചിപ്പിച്ചു.

കൂടാതെ, 14, 28 ദിവസങ്ങളിൽ കുത്തിവയ്പ്പിന് ശേഷമുള്ള (ഡിപിഐ) പി.ക്ലാമിഡോസ്പോറിയയും കുരുമുളക് വേരുകളും തമ്മിലുള്ള പ്രതിപ്രവർത്തനത്തെക്കുറിച്ച് പഠിക്കാൻ ട്രാൻസ്ക്രിപ്റ്റം വിശകലനം നടത്തി. നെക്സ്റ്റ്

ജനറേഷൻ സീകവൻസിംഗ് (എൻജിഎസ്) സാങ്കേതികവിദ്യകൾ (ഹൈസെക് 500 പ്ലാറ്റ്ഫോമുകൾ) ഉപയോഗിച്ച്, 2,03,092 ട്രാൻസ്ക്രിപ്റ്റുകളും 65,354 ഡിഫറൻഷ്യലി എക്സ്പ്രസ്സ് ജീനുകളും (ഡിഇജി) തിരിച്ചറിഞ്ഞു, ഇത് സസ്യവളർച്ച പ്രോത്സാഹിപ്പിക്കലും ഇൻഡ്യൂസ്ഡ് സിസ്റ്റമിക് റെസിസ്റ്റൻസുമായി (ഐഎസ്ആർ) ബന്ധപ്പെട്ട ജീൻ എക്സ്പ്രഷനിൽ കാര്യമായ മാറ്റങ്ങൾ വെളിപ്പെടുത്തുന്നു. ഫൈറ്റോഹോർമോൺ ബയോസിന്തസിസ് (ഓക്സിൻ, എഥിലീൻ, സൈറ്റോകിനിൻ, അബ്സിസിക് ആസിഡ്, ഗിബ്ബെറെലിൻ), പോഷകങ്ങൾ സ്വീകരിക്കൽ (നൈട്രജൻ, ഫോസ്ഫറസ്, പൊട്ടാസ്യം, കാൽസ്യം, ഇരുമ്പ്, ബോറോൺ, സിങ്ക്), സസ്യസംരക്ഷണവുമായി ബന്ധപ്പെട്ട രോഗകാരികൾ (അതുൾപ്പെടെ) എന്നിവയിൽ ഉൾപ്പെട്ടിരിക്കുന്ന ജീനുകൾ, പ്രോട്ടീനുകൾ, ലിപിഡ് ട്രാൻസ്ഫർ പ്രോട്ടീൻ (ഡിഐആർ1), എൻഡോചിറ്റിനേസ്, ജെർമിൻ പോലുള്ള പ്രോട്ടീനുകൾ, ലേറ്റ് എംബ്രിയോജെനിസിസ് അബൻഡൻറ് (എൽഇഎ) പ്രോട്ടീനുകൾ, എൽയുആർപി1, തൗമാറ്റിൻ, മേജർ ലാറ്റക്സ് പോലുള്ള പ്രോട്ടീനുകൾ (എംഎൽപികൾ) എന്നിവ *പോച്ചോണിയ ക്ലമൈഡോസ്പോറിയ* കൊളനൈസായ കുരുമുളക് ചെടികളിൽ നന്നായി എക്സ്പ്രസ് ചെയ്തു.

ഫങ്ഷണൽ ജീൻ ഓൻറോളജി (GO) വിശകലനം സമ്മർദ്ദ പ്രതിരോധത്തിലും ISR സിഗ്നലിംഗ് പാതകളിലും സമ്പുഷ്ടീകരണം കാണിക്കുന്നു, ഇത് ഫംഗസ് ബയോട്ടിക്, അബയോട്ടിക് സമ്മർദ്ദത്തെ ചെറുക്കാനുള്ള ചെടിയുടെ കഴിവ് വർദ്ധിപ്പിക്കുന്നുവെന്ന് സൂചിപ്പിക്കുന്നു. കെഇജിജി സമ്പുഷ്ടീകരണ വിശകലനം സസ്യ ഹോർമോൺ സിഗ്നൽ ട്രാൻസ്ഡക്ഷനുമായി ബന്ധപ്പെട്ട പാതകളുടെ നിയന്ത്രണം ഉയർത്തിക്കാട്ടുന്നു. ഈ ട്രാൻസ്ക്രിപ്റ്റോമിക് ഡാറ്റ, *പോച്ചോണിയ ക്ലമൈഡോസ്പോറിയ* ചെടികളുടെ വളർച്ചയെ പ്രോത്സാഹിപ്പിക്കുകയും കുരുമുളകിൻറെ പ്രതിരോധ സംവിധാനങ്ങളെ ശക്തിപ്പെടുത്തുകയും ചെയ്യുന്നു എന്നതിന് തന്മാത്രാ തെളിവുകൾ നൽകുന്നു, ഇത് ഒരു ബയോകൺട്രോൾ ഏജൻറും എൻഡോഫൈറ്റും എന്ന നിലയിലുള്ള അതിൻറെ ഇരട്ട റോളിനെക്കുറിച്ചുള്ള പുതിയ ഉൾക്കാഴ്ചകൾ നൽകുന്നു.

ഈ പഠനം *പോച്ചോണിയ ക്ലമൈഡോസ്പോറിയ*യെ ഇരട്ട പ്രവർത്തനങ്ങളുള്ള ഒരു വാഗ്ദാനമായ ബയോകൺട്രോൾ ഏജൻറായി സ്ഥിരീകരിക്കുന്നു: ചെടികളുടെ രോഗകാരികളെ

അടിച്ചമർത്തുക, കുരുമുളക് വളർച്ചയെ പ്രോത്സാഹിപ്പിക്കുക. ബയോആക്ടീവ് സംയുക്തങ്ങളായ ബിസെവെർട്ടിനോൾ, എനിയാറ്റിൻ ഐ, എനിയാറ്റിൻ എച്ച് എന്നിവ നെമാറ്റിസൈഡൽ ഉപയോഗത്തിന് സാധ്യതയുള്ളതായി തിരിച്ചറിഞ്ഞു. ട്രാൻസ്ക്രിപ്റ്റോമിക് വിശകലനം, കുമിൾ ചെടികളുടെ വളർച്ചയെയും പ്രതിരോധത്തെയും എങ്ങനെ ഉത്തേജിപ്പിക്കുന്നു എന്നതിനെക്കുറിച്ചുള്ള തന്മാത്രാ ഉൾക്കാഴ്ചകൾ നൽകി, സുസ്ഥിര കീട പരിപാലനത്തിലും വിള പ്രതിരോധശേഷി തന്ത്രങ്ങളിലും അതിന്റെ സാധ്യതകളെ ഊന്നിപ്പറയുന്നു.

പ്രധാന വാക്കുകൾ: ബയോകൺട്രോൾ ഏജന്റ്, പോച്ചോണിയ ക്ലമൈഡോസ്പോറിയ, സെക്കൻഡറി മെറ്റബോളിറ്റുകൾ, ട്രാൻസ്ക്രിപ്റ്റ്, ബയോ ആക്റ്റീവ് സംയുക്തങ്ങൾ, എൻഡോഫൈറ്റ്, നെക്സ്റ്റ് ജനറേഷൻ സീക്വൻസിങ് (NGS) സാങ്കേതികവിദ്യകൾ.

Chapter 1

Introduction

1. Black Pepper, *Piper nigrum* L.

Black pepper, known as king of spices or black gold, is the most important and widely used culinary spice crop in the world. It is a member of the Piperaceae family and is known botanically as *Piper nigrum* L. The fruit or berry, commonly known as pepper, is the economically valuable portion of the plant. It originated in the Western Ghats of southern India, specifically in Malabar (Hammouti et al., 2019). Black pepper was the first eastern spice brought to the Western world and was popular among the Romans and Greeks. It is essential in medicine and has a wide range of culinary purposes, including flavoring and preserving processed goods. Black pepper has a variety of pharmacological properties, including antioxidant, anti-inflammatory, anti-tubercular, antibacterial, antipyretic, allelopathy, radical scavenging, and anti-insecticidal properties (Ahmad et al., 2012).

1.1 *Global distribution and economic importance*

Black pepper is a crucial crop cultivated in tropical regions worldwide, including India, China, Brazil, Mexico, Indonesia, and several other countries (Lawless, 1989). Global demand for pepper is projected to rise significantly, from approximately 280,000 metric tons in 2020 to an estimated 360,000 metric tons by 2050. Currently, black pepper accounts for about 34% of all spices traded internationally, with demand continuing to grow (Weil et al., 2021). India is a leading producer, buyer, and exporter of black pepper in the world. It is grown extensively in Kerala and Karnataka. India exports 17,600 tonnes of black pepper worth Rs. 1143.13 crore in 2016–17, accounting for 11% of the world market (www.indianspices.com/statistics).

1.2 *Challenges in black pepper cultivation*

A wide range of biotic and abiotic factors influence black pepper cultivation globally. Although India was the world's top producer of black pepper until 2001, it now ranks

third. Diseases and insect pests are causes of reduced production and crop loss in India. Besides nutritional problems, black pepper is affected by several diseases caused by nematodes, bacteria, viruses, fungi, and mycoplasma. Among these, slow decline and foot rot disease caused by *Phytophthora capsici* are the main diseases (Anandaraj and Sarma, 1995). Damage from plant-parasitic nematodes is a significant issue in black pepper cultivation (Ramana et al., 1995). Losses due to nematode infestation are estimated to range from 50% to 60%. The root-knot (*Meloidogyne* spp.) and burrowing (*Radopholus similis*) nematodes are the two most devastating pests affecting black pepper production (Saad et al., 2022).

2. Nematode Interactions and Disease Complexes

Nematodes interact with other species, leading to complex diseases and sometimes breaking down resistance to fungal and bacterial pathogens in many crops (Ramana and Eapen, 2000). Slow-wilt disease or slow decline (yellows disease) of black pepper is mainly caused by the association of *R. similis* (Ramana and Mohandas, 1987). The infection in slow decline disease is typically limited to feeder roots. *R. similis* are migratory endoparasites that perform most of their essential functions inside the roots. Due to their movement and feeding habits, they cause cell death and interfere with the normal function of roots. Sessile endoparasitism is another form of obligatory endoparasitism. Symptoms appear after the rain stops, when vines begin to show signs such as yellowing, withering, defoliation, and drying out. Affected vines display varying levels of root deterioration due to infestation by *M. incognita* and *R. similis.* Once the monsoon is over, the unhealthy vines may recover but eventually lose their strength and yield. Root systems of diseased vines exhibit varying degrees of necrosis and the feeder roots rot and disintegrate. *Ph. capsici* and these nematodes can damage the feeder root system separately or together (Nambiar and Sarma, 1977).

Meloidogyne incognita, a root-knot nematode (RKN), is a highly persistent pest due to its damage-revealing abilities (Ravindra et al., 2014). An obligatory endoparasite that only dwells in plant roots are the RKN. After penetrating the plant roots, the RKN induces "giant cells" to swell in the vascular tissues (Jones et al., 2011). The feeding habits of the RKN cause disturbances to the uptake of water and nutrients through

plant roots, whereas the gigantic, metabolically active cells function as feed sinks to fulfill the increasing nutritional needs of the nematode females for reproduction (Mhatre et al., 2015). *M. incognita* causes yellowing and wilt disease in pepper plants. Wilting occurs two to three months following a serious infection when the weather is sunny, warm, and dry (Shahnazi et al., 2012).

Ph. capsici infects every section of the vine. The severity of the disease is determined by the plant section affected and the level of damage. The infection manifests as one or more black spots on the leaves with characteristic fine fiber-like fimbriations at the advancing borders that quickly expand and cause defoliation. From diseased runner shoots and leaves, the disease spreads throughout the entire vine. Afterwards, the vine exhibits rapid wilting, and the branches break off at the nodes. Rain can cause these vines to regenerate new roots, allowing them to live for several more years until the infection spreads to the collar area, where it causes collar rot and eventually kills the vine. Pathogens can thrive in both diseased plant waste and soil (Anandaraj, 2000).

3. Challenges in Nematode Management

Nematode management is challenging, often relying on chemical pesticides (nematicides). While effective, these chemicals pose environmental risks and potential health hazards. For many years, chemical nematicides were employed to control plant parasitic nematodes; but, due to limited availability in underdeveloped nations and health and environmental concerns, their use is gradually being reassessed. Compared to other pests, nematodes are more difficult to cure since they primarily damage plant roots and obstruct the soil (Mian, 1998). It is more difficult to manage endoparasitic species with pesticides once they have reached a root since nematicidal drugs must be non-phytotoxic and ideally systemic. Currently, there is no nematicide that is safe to apply to growing plants and that can be translocated to the roots in sufficient amounts to eradicate endoparasitic or ectoparasitic nematodes. The only commercial substance used as a foliar treatment is a systemic chemical called oxamyl, which translocates basipetally. However, due to toxicological concerns, its usage as a liquid formulation is prohibited in many countries (Gowen, 1997). While there are a number of nematicides that are useful in controlling nematode pests in

annual crops, there doesn't seem to be much hope for controlling nematodes in many sensitive perennial crops without repeatedly applying nematicides. Such treatments will only be financially justified in specific circumstances (Van Berkum and Hoestra, 1979).

Many products and formulations have been developed for use against many nematode pests since the discovery and widespread use of fumigant nematicides 50 to 60 years ago. These are accessible in most parts of the world (Hague and Gowen, 1987). The risks connected with the production and usage of these items have just recently come to light. As a result, there have been usage limitations and occasionally market withdrawals. It appears that the days of using synthetic pesticides with broad biocidal action to manage nematodes are fading, and traditional fumigants and nematicides are becoming less and less effective. It may be an idealistic desire to produce new classes of nematicides with innovative action that are particular to target pests, environmentally benign, and effective when sprayed directly on crops or in soil (Wright, 1981). Public concern over pesticide residues in food and the environment, along with the development of resistance to numerous pesticides in postharvest pathogens and major crop diseases, has sparked interest in alternate approaches to disease management (Chaudhry and Riazuddin, 2003).

3.1 *Biological control as an alternative*

Biological control is an environmentally friendly and effective method of minimizing or mitigating pests and pest effects by employing natural enemies. Biological control has recently emerged as a significant alternative in managing soil-borne plant diseases (Bowen and Rovira, 1999; Whipps, 1997). Biological control is the front-runner in the effort to lessen reliance on chemical pesticides because of its advantageous qualities, which include target specificity and the absence of adverse effects on humans. The switch from chemical to biological management results in a significant decrease in environmental pollution and helps to preserve natural resources. It increases biodiversity, makes production systems more sustainable, and removes harmful chemical exposure for humans.

Over the course of several decades, research on the biological control of soilborne diseases has focused largely on the prospect of introducing mass-produced antagonists into soil or establishing them on seeds or roots (Davies and Spiegel, 2011). The application of several antagonistic biocontrol agents (BCAs), specifically *Pseudomonas* spp., *Bacillus* spp., *Burkholderia* spp., and *Trichoderma* sp., against pathogens causing foliar and soilborne diseases, has resulted in promising advances in biological control (Compant et al., 2005).

BCAs are used in the disease management of plant diseases, where they suppress plant pathogens through a range of distinct mechanisms of action. By directly opposing the pathogen, BCAs impede its growth and spread by a variety of means, including antibiosis, parasitism, virulence reduction, and competition for infection (Kohl et al., 2019). BCAs work indirectly by inducing resistance through promoting defense responses in plants as well as encouraging plant development and soil fertilization. BCAs have the ability to cause plants to develop systemic resistance, which builds up structural barriers and triggers a variety of biochemical and molecular defense mechanisms in the host. To do this, the pathway of phytohormones, phytoalexins, and defense enzymes such chitinase, phenylalanine ammonia-lyase, PR-proteins, and phenolic compounds must be signaled (Olanrewaju et al., 2017). Over the past ten years, there has been a significant increase in the need for alternate management strategies to control plant-parasitic nematodes. This is mostly due to the prohibition of the most significant nematicides

3.1.1 *Pochonia chlamydosporia* as a biocontrol agent

Suppressing plant-parasitic nematodes using nematode predators, parasites, or disease agents is a key biocontrol strategy. Exploiting beneficial microbes in tropical soils is critical for developing effective biocontrol agents. Predominantly, fungal antagonists that parasitize or prey on nematodes are used for biological suppression (Eapen et al., 2005). A large number of fungi are known to trap or prey on nematodes, but the most important genera include *Paecilomyces, Pochonia, Hirsutella, Nematophthora, Arthrobotrys, Drechmeria*, *Fusarium* and *Monacrosporium* (Siddiqui et al., 1996).

Pochonia chlamydosporia, a significant endophytic, saprophytic, and nematophagous fungus, was initially identified by Goddard (1913) as *Verticillium chlamydosporium* in the genus *Verticillium*. Petch (1939) identified the fungus, *Pochonia chlamydosporia* as *Stemphyliopsis ovorum* and separated it from the egg masses of the African snail (*Achatina fulica*) in Sri Lanka. The fungus is categorized under the genus *Stemphyliopsis*. Barron and Onions (1966) recognized the specimen placed by Petch in the Fungarium of the Royal Botanic Gardens, which they had previously called *S. ovorum*, as *Verticillium chlamydosporium*.

In 1965, Batista and Fonseca in Brazil established the genus *Pochonia* to encompass the recently discovered *Pochonia humicola*, which was isolated from the northeastern soils of the nation. Barron (1984) initially identified *Pochonia humicola* as a synonym for *V. chlamydosporium*, drawing on the description and examples provided by Batista and Fonseca (1965). Molecular approaches enabled the use of ITS and LSU + SSU sequences from *Verticillium* rDNA in phylogenetic investigations. Three clades were identified: B, C, and D. Clade D was subdivided into D1-3. According to Zare et al. (2000) and Sung et al. (2001), the species in group D2, *V. chlamydosporium,* differed more from other taxa. Gams and Zare (2001) classed all D2 species as *Pochonia* based on the oldest nomenclature (Batista and Fonseca, 1965).

Pochonia chlamydosporia is the sole species now recognized as belonging to the genus *Pochonia*. It is distinguished by its capacity to both endophytically establish itself in the root tissues of plants and parasitize plant-parasitic nematodes, while also stimulating plant growth. The fungus *Pochonia chlamydosporia* is a member of the Clavicipitaceae family (Fungi: Ascomycota: Pezizomycotina: Sordariomycetes: Hypocreomycetidae: Hypocreales). Using phylogenetic morphological and multigenic analyses, five different types of *P. chlamydosporia* (SSU, LSU, tef, rpb1, and rpb2) were proposed: *P. chlamydosporia* vars. *chlamydosporia, catenulata, ellipsospora, spinulospora, and mexicana.*

3.1.2 *Pochonia chlamydosporia*: *Mechanisms and potential*

The nematophagous fungus *P.chlamydosporia* var. *chlamydosporia* is capable of parasitizing and destroying the eggs of female nematodes, making it one of the most

promising biological control agents against plant endo-parasitic nematodes. *P. chlamydosporia* promotes plant growth through various mechanisms, including the synthesis of indole-3-acetic acid (IAA), secondary metabolites, antibiotics, solubilization of mineral phosphate, and induction of systemic resistance (Zavala-Gonzalez et al., 2015; Timper, 2014).

3.1.3 *The role of fungal metabolites*

P. chlamydosporia is capable of colonising the endophytic roots of economically important crops, enhancing plants, boosting their plant growth and activating plant defense mechanisms. This multitrophic behavior positions it as a potentially beneficial organism for sustainable agricultural approaches. The chemical ecology of nematophagous fungi is still poorly understood. Few studies have focused on screening metabolites in nematophagous fungi (Stadler et al., 1993a, b; 1994). Extracellular hydrolytic enzymes such as serine protease, chitinase, lipase, and collagenase are thought to play important roles in the infection process of nematophagous fungi against plant-parasitic nematodes (Yang et al., 2007). A thorough screening of fungal natural products of *P. chlamydosporia* may reveal previously unknown nematicidal or anti-helminthic properties.

3.1.4 *Genomic insights into Pochonia chlamydosporia*

Genomics is the study of a live organism's genome, attempting to determine its evolutionary links with other organisms and considering its basic structure to comprehend gene activities and organization. Studying the genomes of these fungi is a valuable tool for identifying the molecular causes of pathogenicity to plant parasitic nematodes. The genome of this fungus is significantly enriched with genes encoding hydrolytic enzymes, which are expressed during their endophytic behaviour. Understanding the molecular processes underlying this multitrophic lifestyle of *P. chlamydosporia* is critical (Macia-Vicente et al., 2009a; Escudero et al., 2012). However, there is limited knowledge about the molecular underpinnings of the infection process in nematode eggs by *Pochonia* species. Therefore, investigating the genomic information is necessary to enhance the capabilities of this fungus as a promoter of plant growth (Larriba et al., 2012).

3.1.5 *The importance of transcriptomic studies*

The entire collection of transcripts in a cell, together with their abundance, for a particular physiological state or developmental stage is known as the transcriptome. Comprehending the transcriptome is crucial for deciphering the functional components of the genome, uncovering the molecular components of cells and tissues, and comprehending both growth and disease. Transcriptomics aims to catalogue all transcript species, including mRNAs, non-coding RNAs, and small RNAs; identify the transcriptional structure of genes, including their start sites, 5′ and 3′ ends, splicing patterns, and other post-transcriptional modifications; and measure the variations in each transcript's expression levels over the course of development and under various environmental conditions (Wang et al., 2009). Several studies utilizing transcriptome analyses have shown that *P. chlamydosporia* induces significant changes during root colonization, including differential regulation of several genes (Rosso et al., 2011; Ciancio et al., 2013; Larriba et al., 2015). The advantage of NGS technology may help in elucidating the interactions between plants and their phytobiomes (Klosterman et al., 2016). Fungus transcriptome studies may also facilitate the creation of industrial and commercial bioformulations for plant protection by inducing natural plant defense mechanisms

4. Research Gaps and Objectives

P. chlamydosporia was isolated from the semi-endoparasitic nematode, *Trophotylenchulus piperis,* infecting black pepper from a garden in Kozhikode District of Kerala (Sreeja et al., 1996). It was recommended by ICAR-Indian Institute of Spices Research as per package of practices recommendations (Director, 1990) for the management of plant parasitic nematodes, especially RKNs and *R. similis*, after extensive laboratory and field studies. Nevertheless, there is no information available on their plant-beneficial properties, synthesis of bioactive secondary metabolites, and their mode of action against nematodes and fungi that infect black pepper. A better knowledge of the tritrophic interaction among plant, fungus, and nematodes is crucial to improve the effectiveness of the biocontrol agents (Manzanilla-Lopez et al., 2013). Typically, researches are focused on the interaction with plant beneficial bacteria, and

little is known about the plant growth promoting ability of such fungi. Plant growth-promoting fungi (PGPF) are a type of non-pathogenic, soil-borne filamentous fungus that benefits plants. They contribute to the growth, morphology, nitrogen assimilation, and mineral uptake of host plants (Murali et al., 2012). The present study was undertaken to get an in-depth knowledge about the plant-beneficial properties of *P. chlamydosporia* which is recommended as a biocontrol agent for suppressing plant parasitic nematodes in black pepper and other spices. The objectives of this study are:

1. To characterize the plant-beneficial properties of *P. chalmydosporia* for black pepper.

2. To identify the secondary metabolites produced by *P. chlamydosporia.*

3. To study and understand the interaction of *P. chlamydosporia* with black pepper using transcriptome approaches.

The thesis is organized into seven sections, with chapters three to five consisting of an abstract, an introduction, materials and methods, results, and a discussion. A list of all the references cited is provided at the end.

Chapter 1 : Introduction

Chapter 2 : Review of literature

Chapter 3 : Plant growth promotion by *P. chlamydosporia.*

Chapter 4 : Identification of secondary metabolites produced by *P. chlamydosporia.*

Chapter 5 : Transcriptome Profiling of black pepper roots colonised by *P. chlamydosporia*

Chapter 6 : Summary and Conclusions

Chapter 7 : Recommendations

Chapter 2

Review of Literature

2.1 Plant-Parasitic Nematodes

Nematodes, commonly known as roundworms, are a highly diverse group within the phylum Nematoda, showcasing remarkable adaptability to various environments. They can be either free-living or parasitic, affecting both plants and animals. Despite their varied habitats, nematodes share a similar external morphology, characterised by an unsegmented, bilaterally symmetrical, elongated body. Their life cycle typically consists of three stages: eggs, juveniles, and adults. While most nematodes are free-living organisms that thrive in soil, freshwater, and marine environments. They play an essential role in nutrient cycling.

Plant-parasitic nematodes (PPNs) are of significant concern due to their detrimental impact on agriculture. PPNs are known to feed on plant tissues, causing substantial economic losses by reducing crop yields and contributing to plant diseases (Kiontke and Fitch, 2013). According to Chitwood (2003) PPN-related losses in agriculture account for approximately 14% of global crop production losses, valued at nearly 125 billion dollars annually.

PPNs are a diverse group comprising around 4,100 species, primarily within the Tylenchida and Dorylaimida orders. They vary in size, typically ranging from 250 µm to 12 mm in length and 15 to 35 µm in width (Jasmer et al., 2003). These nematodes attack a wide range of crops, causing symptoms such as yellowing, stunted growth, and wilting, which can lead to severe yield reductions, especially under high infestation levels (Sasanelli et al., 2008).

2.1.1 *Feeding strategies of plant-parasitic nematodes*

PPNs possess a specialised feeding apparatus called stylet, which allows them to penetrate plant cell walls, inject digestive enzymes, and absorb nutrients. Based on

their feeding behaviour, PPNs are classified into three main categories: ectoparasites, semi-endoparasites and endoparasites (Mesa-Valle et al., 2020).

Ectoparasitic nematodes

Ectoparasites complete their life cycle outside the plant while feeding on root cells using their stylet. This feeding strategy allows them to feed on a wide range of hosts but leaves them vulnerable to environmental changes. Notable ectoparasites include *Xiphinema*, *Trichodorus*, and *Paratrichodorus* species which are also known as vectors of plant viruses (Hewitt et al., 1958).

Semi-endoparasitic nematodes

Semi-endoparasites partially enter the plant tissue, with their head embedded in the root to establish a permanent feeding site. They can lay eggs outside the plant, and once established, they lose mobility but gain the advantage of a consistent nutrient source. Examples include *Helycotylenchus, Sphaeronema* and *Hoplolaimus* species (Wubben et al., 2010).

Endoparasitic nematodes

Endoparasites penetrate plant tissues and can be either migratory or sedentary. Migratory endoparasites, such as *Pratylenchus* and *Radopholus*, cause extensive tissue damage as they move through the roots, resulting in necrosis and secondary infections (Fosu-Nyarko & Jones, 2016). In contrast, sedentary endoparasites, including root-knot nematodes *(Meloidogyne* spp.) and cyst nematodes *(Heterodera* spp., *Globodera* spp.), establish feeding cells that serve as nutrient sources throughout their life cycle (Barker et al., 1985; Schmitt et al., 2004).

2.1.2 *Impact of plant-parasitic nematodes in agriculture*

PPNs are one of the most well-known and underestimated hazards to plant health and food security in the world, lowering crop yields and costing billions of dollars in losses every year. PPN infection commonly goes untreated because its symptoms are largely non-specific and are frequently confused with abiotic stress. PPNs pose a significant threat to global agriculture, causing billions of dollars in losses annually (Jones et al.,

2013). The most detrimental nematodes for agricultural crops are typically RKNs (*Meloidogyne* spp.), root-lesion nematodes (*Pratylenchus* spp.) and burrowing nematodes (*Radopholus similis*) (Jones et al., 2013; Kantor et al., 2022). These pests affect a wide range of crops, including cereals, legumes, vegetables, and spices, leading to reduced yields and poor-quality produce. In wheat, cereal cyst nematodes (*Heterodera* spp.) and root-lesion nematodes (*Pratylenchus* spp.) are major pests, causing significant yield losses (Nicol et al., 2007) as well as seed gall or ear-cockle nematode, *Anguina tritici* (Lasserre et al., 1994). Potato cyst nematodes (*Globodera rostochiensis* and *Globodera. pallida*) are the most significant nematode pests of potatoes. They are also known to affect other solanaceous plants (Jones et al., 2017). Similarly, *Meloidogyne* species are notorious found all over the world and are important pests of rice, maize, sweet potato and potato crops, leading to substantial yield reductions and other crops grown in tropical and temperate regions (Trudgill et al., 2001, Decraemer and Hunt, 2006; Nicol et al., 2011).

2.1.3 *Nematode infestation in black pepper cultivation*

Black pepper (*Piper nigrum* L.), known as the "King of Spices," is highly susceptible to PPNs, which significantly impact its productivity. Studies have identified PPNs from 29 genera and 48 species infesting black pepper in India (Sundararaju et al., 1979).

The association of black pepper with RKNs (*Meloidogyne* spp.) was first reported by Butler (1906). Extensive surveys in the key black pepper-growing regions revealed that *Meloidogyne incognita*, *Radopholus similis*, *Trophotylenchulus piperis,* and *Helicotylenchus* spp. are the most common nematodes identified (Ramana et al., 1987). D'Souza et al. (1970) were the first to report the association of burrowing nematodes, *R. similis,* with black pepper in India. Infection by these nematodes causes the devastating disease, slow decline or slow wilt disease, in all black pepper growing countries. Infected plants exhibit symptoms like slow decline, wilting, and yellowing, primarily due to damage to the feeder roots caused by nematodes and secondary pathogens like *Phytophthora capsici* (Koshy et al., 2005). Recent studies have also identified a new species, *Meloidogyne piperi*, affecting black pepper roots in Kerala,

India (Nisha et al., 2019). International studies have documented similar impacts of nematode infestations on black pepper in Brazil (De Souza et al., 2021), Malaysia (Leong et al., 2021), and Vietnam (Thuy et al., 2012). In these regions, *Meloidogyne*, *Radopholus*, and *Hoplolaimus* species have been identified as major threats to pepper cultivation. These infestations not only reduce plant height and root growth but also cause leaf yellowing and reduced yields (De Souza et al., 2021).

2.2 Nematophagous Fungi: An Overview

Fungi exhibit a wide range of interactions with other organisms, including harmful, parasitic, or symbiotic relationships. However, their interaction with soil-dwelling nematodes extends beyond parasitism into predation. Nematophagous fungi are specialised microfungi capable of trapping, killing, and consuming nematodes, serving as natural antagonists against soil-borne nematodes. These fungi can inhabit both the external and internal environments of the nematode host, exploiting it for survival. Notably, they are facultative parasites that can switch between saprophytic and parasitic phases depending on the presence of a suitable host. Over 200 species of taxonomically diverse fungi have been classified as nematophagous, with the ability to attack and digest nematode eggs, juveniles, and adults (Barron, 1977). These fungi exhibit infection mechanisms and are recognized as natural biocontrol agents against nematodes. Nematophagous fungi are taxonomically dispersed across several groups, including Zygomycota, Pleurotaceae (Basidiomycota), Ascomycota, Oomycota, and Chytridiomycetes (Gams and Zare, 2003).

2.2.1 *Mechanisms of nematode predation by nematophagous fungi*

Nematophagous fungi deploy various mechanisms to capture, immobilize, and parasitize nematodes. These include using specialized traps, conidia for attachment, toxins to immobilize prey, and hyphal tips to parasitize nematode eggs and females. Based on these strategies, they are classified into four main groups (Fig. 2.1): (1) fungi with specialised trapping structures, (2) fungi parasitic to nematode eggs and females, (3) endoparasitic fungi using spores, and (4) fungi that produce toxins immobilize nematodes prior to invasion (Liu et al., 2009).

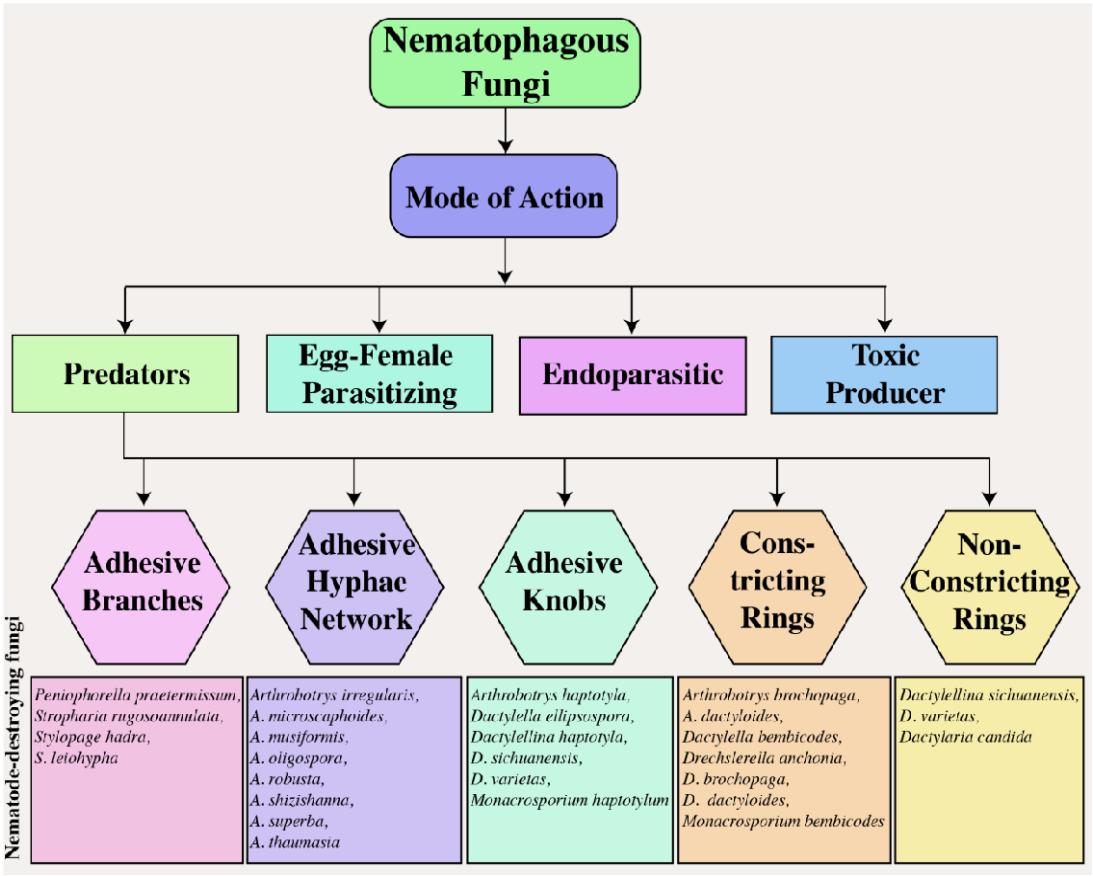

Fig. 2.1: *Mode of action of nematophagous fungi*

Predatory fungi

Predatory fungi utilise specialised hyphal structures to trap nematodes, showcasing a diversity of trapping mechanisms. These structures, developed from the fungal mycelium, disrupt the nematode cuticle, allowing penetration by a penetration peg, followed by the spread of hyphae both internally and externally on the nematode body (Veenhuis et al., 1985). These fungi are independent of a specific host and attract a wide range of soil-dwelling nematodes. The formation of traps, which may occur spontaneously or in response to the presence of nematodes, is a critical phase of fungal mycelium development. Predatory structures include adhesive branches, adhesive networks, adhesive hyphae, adhesive knobs, constricting rings, and non-constricting rings (Moosavi and Zare, 2020).

Adhesive branches: Adhesive branches, also known as adhesive columns, are less complex than that of other capture organs. These vertical branches, which are made

up of one to three cells, unite through anastomosis to form networks or adhesive hoops with two-dimensional structures that resemble lines or crochet. The branch is completely covered in a thin film of adhesive, making it simple to catch the nematode when it comes into contact with it. Nematodes usually struggle to separate themselves from more sticky hyphae after coming into touch with them because of the close proximity of adhesive branches. The species *Dactylella cionopaga* is frequently found in temperate soils with established adhesive branches (Poinar and Jansson, 1988). These branches are common trapping strategies for *Monacrosporium gephyrophagum* and *Monacrosporium cionopagum*. The sugar beet cyst nematode, *Heterodera schachtii*, is trapped and rendered immobile by the sticky branches produced by *M. cionopagum* (Andersson et al., 2014).

Adhesive hyphal network: Adhesive networks are constructed using upright lateral branches that extend from the parent hyphae, forming three-dimensional structures. These networks are coated with adhesives that attract nematodes. The most widely studied species utilising this trapping mechanism is *Arthrobotrys oligospora,* which is found globally (Niu and Zhang, 2011).

Adhesive knobs: Adhesive knobs are specialised cells coated with a thin adhesive layer. Upon contact, these knobs expand the adhesion surface, securing the nematode and allowing fungal penetration through enzymatic and mechanical processes. Hyphae subsequently develop to consume the internal contents of the nematodem (Gray, 2018). Species like *Dactylellina copepodii* and *Dactylellina arcuata*, employ adhesive knobs for trapping nematodes (Li et al., 2005).

Constricting rings: Constricting rings are highly specialised structures composed of three cells that actively capture nematodes. Upon nematode entry, these cells rapidly expand, constricting and immobilising the nematode. The hyphae then penetrate the trapped nematode to absorb its nutrients (Heintz and Pramer, 1972). Constricting rings are a distinctive trapping strategy observed in multiple hyphomycetes (Poinar and Jansson, 1988).

Non-constricting rings: Non-constricting rings are composed of three cells attached to a supporting stalk. These rings passively capture nematodes, which inadvertently

carry the rings, enabling the fungus to spread in the soil (Askary and Martinelli, 2015). *Dactylaria lysipaga* and *Dactylaria candida*, are examples of fungi that utilise this mechanism (Drechsler, 1937).

Egg- and female-parasitic fungi

These fungi parasitize eggs, females, and other stages using specialised structures like appressoria and hyphal pegs. *Pochonia* spp. and *Purpureocillium* spp. are known for targeting nematode eggs by forming appressoria on the egg surface, leading to the degradation of egg contents (Lopez-Llorca et al., 2008). Studies have demonstrated that *P. chlamydosporia* isolates exhibit significant pathogenicity against *Globodera pallida* eggs, with parasitism rates varying between 34% to 49% (Vieira Dos Santos et al., 2019).

Endoparasitic fungi

Endoparasitic fungi infect nematodes using spores, which either penetrate through the cuticle or are ingested by the nematode. These fungi remain inside the host throughout their vegetative life cycle. Spores attach to the nematode cuticle and release a penetration tube that injects fungal contents into the nematode, eventually leading to the nematode's death (Dijksterhuis et al., 1991). In greenhouse studies, these fungi have been shown to reduce RKN populations in crops like tomatoes and alfalfa (Liu et al., 2009). *Drechmeria coniospora* is a prominent example of an aggressive endoparasitic fungus that targets nematodes (Wan et al., 2021).

Toxin producing fungi

Certain nematophagous fungi produce toxins that immobilise nematodes, enhancing the fungi's ability to parasitize their hosts. These fungi secrete low-molecular-weight metabolites and enzymes, such as proteases and chitinases, which degrade nematode cuticles and prevent egg hatching (Sarker et al., 2020). The culture filtrates of these fungi contain non-volatile compounds that are effective in inhibiting nematode development (Westphal and Becker, 2001). Additionally, fungi can produce toxins that impair nematode mobility, facilitating their capture and digestion (Satou et al., 2008).

2.3 *Pochonia chlamydosporia*: A Key Nematophagous Fungus

Pochonia chlamydosporia is a well-documented biological control agent (BCA) with significant potential against PPNs, particularly RKNs (*Meloidogyne* spp.) and cyst nematodes (*Globodera* spp. and *Heterodera* spp.). This multitrophic species, *P. chlamydosporia* exhibits a versatile lifestyle, functioning as a symbiont in plants while acting as a parasite or antagonist to nematodes and certain invertebrates. Its saprophytic nature enables it to thrive in the soil, producing resilient chalmydospores that enhance its ecological persistence. Moreover, as an endophyte, *P. chlamydosporia* colonises plant rhizoplanes and internal root tissues, providing it with a competitive edge in nematode biocontrol and facilitating plant growth across monocot and dicot crops.

2.3.1 *Taxonomy and biology*

The initial scientific description of what is now recognized as *P. chlamydosporia* was provided by Goddard (1913) during a study of mycobiota in Michigan, USA. Goddard classified the fungus under the genus *Verticillium* as *V. chlamydosporium*, based on its distinctive verticillate conidial structures and the production of characteristic chlamydospores. Subsequently, Petch (1939) described the same organism as *Stemphyliopsis ovorum,* isolating it from egg masses of the African land snail (*Achatina fullica*) in Sri Lanka. Further taxonomic studies, including those by Barron and Onions (1966), revealed that these isolates were synonymous with *V. chlamydosporium.* The genus *Pochonia* was later established by Batista and Fonseca (1965) to accommodate species like *P. humicola*.

Significant advancements in molecular phylogenetics refined the taxonomy of *P. chlamydosporia*. Gams and Zare (2001) proposed its reclassification under the genus *Pochonia* based on phylogenetic analysis of ribosomal genes, distinguishing it from closely related genera such as *Metapochonia* (Kepler et al., 2014). Further studies based on multigenic analyses (SSU, LSU, tef, rpb1, and rpb2) identified five varieties of *P. chlamydosporia*: var. *chlamydosporia,* var. *mexicana*, var. *spinulospora*, var. *catenulata*, and var. *ellipsospora* (Zare et al., 2001).

Morphologically, *P. chlamydosporia* produces slow-growing, white to yellowish colonies (approximately 0.3 cm/day) with temperature-dependent growth rates. It forms both erect and prostrate conidiophores, with globular conidia aggregating into chains or heads. Dictyochlamydospores, a hallmark of the species, serve as resistant, dispersal structures. Appressoria develops upon contact with nematode eggs or plant root tissues, facilitating infection (Manzanilla-López et al., 2017).

***Pochonia chlamydosporia* (Goddard) Zare & W. Gam**

Kingdom	**:**	**Ascomycota**
Division	**:**	**Pezizomycotina**
Class	**:**	**Sordariomycetes**
Subclass	**:**	**Hypocreomycetidae**
Order	**:**	**Hypocreales**
Family	**:**	**Clavicipitaceae**
Genus	**:**	***Pochonia***
Species	**:**	***Chlamydosporia***

2.3.2 *Mechanisms of nematode control*

P. chlamydosporia resides in the rhizosphere, a complex microenvironment comprising plant roots and associated microbial communities. The fungus's ability to transition between saprophytic, endophytic, and parasitic phases underscores its ecological adaptability and effectiveness as a BCA. The shift from saprophytism to parasitism is often triggered by the presence of nematodes, with root exudates playing a critical role in modulating fungal behaviour (Kerry, 2000; Manzanilla-López et al., 2011). Its parasitism targets PPN eggs and females, proceeding through three distinct stages: adhesion, penetration, and colonisation (Manzanilla-López et al., 2013).

Adhesion: Adhesion is critical for fungal infection, ensuring stable attachment to the nematode substrate. Conidia and hyphae of *P. chlamydosporia* adhere to nematode

eggs via glycoproteins that the fungus secretes, which also protect the hyphae from desiccation (Lopez-Llorca et al., 2002). The adhesion process is influenced by environmental factors such as moisture and substrate properties like hydrophobicity and hardness (Nicholson and Moraes, 1980; Tucker and Talbot, 2001). Studies reveal that hydrophobic surfaces enhance appressoria formation compared to hydrophilic ones. Although *P. chlamydosporia* can form appressoria on various surfaces, hydrophobic cues significantly increase differentiation (Lopez-Llorca et al. 2002).

Penetration: Penetration involves mechanical and enzymatic processes mediated by appressoria. The fungus secretes extracellular enzymes to degrade the vitelline membrane and expose the chitin layer of the nematode eggshell, enabling germ tube ingress. The shape and density of appressoria vary depending on the nematode host. For example, *M. incognita* eggs exhibit more extensive appressoria formation compared to *Globodera rostochiensis* (Segers et al., 1996). The appressoria of *P. chlamydosporia* share similarities with necrotrophic plant pathogens like *Bipolaris sorokiniana* (Kumar et al., 2002). However, the fungus also relies on secreted enzymes, reducing dependence on appressoria and conserving energy.

Colonisation: Following penetration, *P. chlamydosporia* colonises nematode eggs and female tissues to extract nutrients and proliferate. Trehalose, a disaccharide found in nematode egg shells and juveniles, serves as a carbon source for fungal growth and reproduction. This sugar is associated with anhydrobiosis, aiding the nematode's resistance to desiccation (Yen et al., 1996). The fungus colonises not only nematode eggs but also embryos and juveniles (Morgan-Jones et al., 1984). Additionally, *P. chlamydosporia* targets specialized feeding cells of sedentary endoparasitic nematodes, disrupting nutrient storage and parasitising females.

2.3.3 *Enzymatic and molecular mechanisms via interaction with nematodes*

P. chlamydosporia secretes extracellular enzymes that are crucial to the infection process of eggs because they allow the fungus to break down the nematode eggshell, which serves as the host's main defence against infection. It has been shown that certain proteases and chitinases are active against the nematode eggshell after being isolated, purified, and tested (Segers, 1996; Tikhonov et al., 2002). These enzymes

are regarded as virulence factors and participants in the infection process (Huang et al., 2004; Mi et al., 2010)

In the rhizosphere, *P. chlamydosporia* produces vegetative hyphae, which can parasitize female nematodes and eggs by producing an appressorium without the need for additional specific infectious structures. Environmental signalling must occur prior to appressorium development and egg infection (Lopez-Llorca et al., 2002). According to them, prepenetration events entail thigmotropic reactions and adhesion processes mediated by glycoproteins and enzymes. In many plants and entomopathogenic fungi, the production of appressoria is believed to represent a nutritional response (Blakeman and Parbery, 1977; Jackson and Schisler, 1992). Low C:N ratios, low quantities of complex nitrogen sources, and nutrient depletion all contribute to favorable conditions. *P. chlamydosporia* egg pathogenicity is influenced by low C:N ratios (Segers, 1996), but conidia production appears to be enhanced by conditions with relatively high C: N (Mo et al., 2005). Therefore, nutrients (such as C and N) that are either released by plants into the rhizosphere or available in eggs, egg masses, and galls may be linked to the transition, or "switch," of the fungus from the saprophytic to the parasitic phase.

Serine Proteases (Enzymes)

The *P. chlamydosporia* genome encodes the greatest number of proteases, known as serine proteases (Larriba et al., 2014). There are already known serine proteases in *Pochonia*, including P32 (Lopez-Llorca, 1990), VCP1 (Segers et al., 1994), and SCP1 (Lopez-Llorca et al., 2010).

The P32 Serine Protease enzyme was initially isolated in 1990, with an empirical molecular mass of 32 kDa (Lopez-Llorca, 1990). Two years later, it was revealed that P32 affected *P. suchlasporia*'s pathogenicity to *Heterodera schachtii* eggs (Lopez-Llorca and Robertson, 1992). According to Lopez-Llorca (1990), P32 is a member of the subtilisin family, also referred to as the S8 family. Throughout the infection process, nematophagous and entomopathogenic fungi break down the outer layers of their hosts by producing subtilisin-like serine proteases (Li et al., 2010). According to Larriba et al. (2012), P32 exhibits similarity with the subtilisin-like serine proteases

Pr1A (86%) of the entomopathogenic fungus *Metarhizium anisopliae* and VCP1 (76%) of *P. chlamydosporia*. Therefore, P32 aids in *P. rubescens* parasitism by removing the egg shell's vitelline membrane.

The serine protease carboxypeptidase (SCP1) was first isolated in 2010 and is a member of the S10 family of serine carboxypeptidases (Lopez-Llorca et al., 2010). This enzyme's molecular mass in its secreted form is 60.5 kDa (Larriba et al., 2012). It shows 88.1% and 86.5% homology with the serine carboxypeptidases of *Metarhizium acridum* and *M. anisopliae*, respectively, and is a member of a distinct protease subfamily (Lopez-Llorca et al., 2010; Larriba et al., 2012). When *P. chlamydosporia* colonizes roots endophytically (Lopez-Llorca et al., 2010) and parasitizes RKN eggs (Escudero et al., 2016), SCP1 is generated.

VCP1 Serine Protease, a 33 kDa protein, was initially isolated in 1994 by Segers et al. and belongs to the S8 family. In the early phases of egg infection, *P. chlamydosporia* produces it, which disrupts the vitelline layer and makes it easier for hyphal penetration and nematode infection to follow (Segers et al., 1994; Ward et al., 2012). This enzyme may therefore function as a pathogenicity factor. Purified VCP1-pretreated *M. incognita* eggs colonize more quickly than untreated ones (Segers et al., 1996). According to Lopez-Llorca et al. (2010), VCP1 plays a significant role in the fungus's endophytic phase as well.

Many extracellular enzymes generated by fungi are regulated by pH, carbon, and nitrogen sources (Aro et al., 2005). VCP1 expression is first decreased by ammonium chloride, but its synthesis is quickly increased (Ward et al., 2012). In an environment with a lot of glucose, the fungus lowers VCP1 synthesis. According to Ward et al. (2012), *P. chlamydosporia* would rather exploit the easily accessible carbon supply than inhabit nematode eggs. Therefore, *P. chlamydosporia'*s ability to parasitise nematodes may be compromised by rapidly metabolized carbon sources and low environmental pH (Ward et al., 2012).

Host preference in *P. chlamydosporia* may be explained by genetic diversity in VCP1 among isolates from various nematode hosts. Amino acid variations between VCP1 were discovered in fungal isolates derived from cyst nematodes (*Globodera*

rostochiensis and *Heterodera schachtii*) and RKNs (*Meloidogyne* spp.). Morton et al. (2003) found that isolates from RKNs include glycine instead of alanine, which alters the amino acid affinities at the S3 substrate-binding area. The characteristics of enzymes and the utilization of substrates are impacted by variations in amino acid sequences (Segers et al., 1995; Liu et al., 2007). Thus, host selection among *P. chlamydosporia* biotypes may be influenced by amino acid variations in VCP1.

Chitinases

The intermediate layer of nematode egg shell contains a polymer of N-acetylglucosamine called chitin (Yang et al., 2007). To get past this barrier, the fungus must produce endochitinase, exochitinase, and N-acetyl-β-D-glucosaminidase (Khan et al., 2004; Palma-Guerrero et al., 2010). An endochitinase weighing 43 kDa was the first chitinase to be isolated from *Pochonia*. It was demonstrated that this enzyme and the serine protease P32 worked in concert to harm *Globodera pallida* eggs. However, *M. rubescens's* N-acetyl-β-D-glucosaminidases have a stronger action on *Globodera* egg shells than *P. chlamydosporia*'s, despite both species producing chitinases (Tikhonov et al., 2002). This variation in chitinase expression between these two fungal species could account for the apparent specialization of *P. chlamydosporia* and *M. rubescens* for *Globodera* and *Meloidogyne* infection, respectively.

Mi et al. (2010) cloned the 44 kDa endochitinase PCCHI44 from *P. chlamydosporia* and observed that this enzyme might be a possible virulence factor. This chitinase can disrupt the normal development of nematodes by causing the shell of *M. incognita* eggs to flake and furrow, followed by the formation of huge vacuoles (Mi et al., 2010). Using chitin deacetylases, entomopathogenic fungi can convert chitin from their hosts' cuticles into chitosan. During host penetration, fungal chitinases subsequently break down the chitosan that has been produced (Nahar et al., 2004). Given that *P. chlamydosporia* can make chitosanases in vitro and that the composition of worm egg shells is comparable to that of insect cuticles, it is possible that this process also takes place during nematode parasitism (Palma-Guerrero et al., 2010).

2.3.4 *Factors impacting the parasitic activity of P. chlamydosporia*

P. chlamydosporia's biological control efficacy against nematodes is established and guaranteed by a number of elements. Numerous facts exist on the conditions that promote *P. chlamydosporia* growth in soil, increasing its effectiveness. For appropriate nematode management, further research into the factors influencing the interaction between fungi and nematodes is also required. The main elements that affect a fungus's pathogenicity include its kind, temperature, pH, antifungal qualities, application techniques, and timing.

pH is essential for the effective development of the fungal-nematode interaction. Since each enzyme has an ideal pH value that maximizes activity, pH indirectly controls enzyme activity. *P. chlamydosporia* secretes the well-studied and described enzyme VCP1, which contributes to the pathogenicity of nematode eggs at higher pH levels (Ward et al., 2012). *P. chlamydosporia* was found to infect *M. incognita* eggs five times more frequently at pH 6.5 than at pH 5.7 or 7.0 in a different investigation (Luambano et al., 2015). *P. chlamydosporia* thrives in artificial environments with a pH range of 3.0 to 7.0 (Olivares-Bernabeu and Lopez-Llorca, 2002). It has been demonstrated that pH variability leads to complex outcomes. Additionally, it should be noted that distinct *P. chlamydosporia* isolates need various ideal circumstances for growth and development (Kerry et al., 1986). Therefore, more research is necessary to fully comprehend this component and enhance nematode treatment overall.

In relation to the pathogenicity of the fungus, temperature also has a significant impact on its proliferation, parasitism, and enzymatic activity. *P. chlamydosporia* isolates from tropical soil were shown to thrive successfully at 30^0C in one investigation (Nagesh et al., 2007). Additionally, it was shown that the ideal temperatures for each isolate's growth and parasitism vary. Kery et al. (1986) showed that an isolate of *P. chlamydosporia* develops well at 25^0C, but optimum parasitism was observed at 12^0C. The environmental conditions in which the nematode and fungus coevolve determine the climatic needs of *P. chlamydosporia* isolates. However, the fungus is typically less effective at controlling nematodes if the soil temperature is too low or higher than 30^0C. The fungus's low efficacy is caused by decreased fungal development at low

temperatures, whereas higher temperatures encourage nematode embryonic development and increase nematode escape after hatching, which lowers fungal efficiency (Verdejo-Lucas et al., 2003).

One of the primary factors influencing the production of a specific enzyme needed for infection is the chemical makeup of the nematode surface (Tunlid et al., 1994). The primary source of information regarding the fungus metabolism in the interaction between *P. chlamydosporia* and RKN is VCP1, a particular enzyme that breaks down the eggshell proteins. Ammonium chloride, a short duration, fast-metabolizing carbon sources like glucose, and an unfavorable acidic pH in the rhizosphere or egg masses appear to influence the development of VCP1, which in turn affects the fungus's pathogenicity to RKN (Ward et al., 2012).

The soil provides water and nutrients to its inhabitants, including plants and bacteria. Microorganisms depend on soil so much that their existence is determined by the type and characteristics of the soil. For instance, nematodes thrive in sandy soil, making crops grown there more susceptible to nematodes. The comparatively easy mobility in sandy soils and the decreased organic matter, which lowers the quantity of nematode natural enemies, are thought to be the causes of this phenomenon. *P. chlamydosporia* exhibits soil type selectivity, just like other soil microorganisms. Although it may grow in clay and saline soils, this fungus thrives in sandy soil (Ceiro et al., 2014). Numerous factors, including improved aeration, drainage, and porosity, which aid in the fungus's mobility and survival, may contribute to the preference for sandy soils. Since nematodes thrive in sandy soil, parasitism is most common there, increasing the amount of fungal inoculum in the soil. Since *P. chlamydosporia* can grow in soil with a greater NaCl concentration, it is also a viable option for the biocontrol of nematodes in saline soil (Ceiro et al., 2014).

The growth of biocontrol fungi in various environments for nematode control is determined by the soil's antifungal capability. The biotic or abiotic characteristics of the soil that prevent the fungus propagules from germinating are linked to this activity. In sterile soil, *P. chlamydosporia* grows more effectively and controls the nematode more effectively than in natural soil (Podestá et al., 2009). The pathogenicity of *P.*

chlamydosporia to nematodes is greatly influenced by management strategies in addition to environmental factors. Successful fungal establishment in the soil and nematode management depend on the application technique and time. This is because the fungus kills the nematode and takes longer to develop in the soil (Podestá et al., 2009).

2.4. Biological Control of Nematodes in Agriculture

PPNs significantly harm crops by feeding on roots, causing symptoms such as wilting, stunted growth, and reduced yields. This results in substantial agricultural losses, as crops damaged by nematodes are also more susceptible to secondary diseases. Annually, PPN infestations cost global agriculture billions of dollars in lost productivity, reduced yields, and increased production costs, including the expenses of management techniques such as chemical treatments (Abd-Elgawad, 2021). Synthetic nematicides remain a widely used and effective control strategy for managing PPNs. However, their overuse poses serious risks to human health and the environment, leading to restrictions and driving the need for alternative control methods (Gao et al., 2016).

BCAs present a sustainable and environmentally friendly alternative for managing PPNs (Ali et al., 2023). Biological control involves the use of natural or modified organisms and their gene products to suppress pests, enhancing plant health and productivity. Unlike physical and chemical control methods, biological control focuses on ecological balance and long-term sustainability (Kroschel, 2002). BCAs promote plant growth under stress and reduce dependence on agrochemicals by supporting beneficial soil organisms. Fungal and bacterial species dominate the ranks of BCAs for PPN management, employing direct antagonistic effects or indirectly promoting plant growth (Abd-Elgawad and Askary, 2018). They can be endoparasitic, produce toxins, trap nematodes, or parasitize eggs, juveniles, or adults. Additionally, these BCAs are capable of producing plant growth promoters (Glick, 2012). They can directly help plants by facilitating the synthesis of active chemicals and hormones (like auxin, cytokinin and gibberellins) that are essential for plant growth. They can indirectly reduce infections and pests by producing antibiotics and lytic enzymes.

Additionally, BCAs can prime plants against infection by upregulating endogenous defence genes, including those linked to salicylic acid (SA)-dependent systemic acquired resistance, such as PR-1, PR-3, and PR-5 (Molinari and Leonetti, 2019). Enhanced activity of defence enzymes such as endochitinase and glucanase further supports nematode management.

2.4.1 *Bacterial biocontrol agents*

Bacteria serve as effective BCAs by suppressing nematodes in the plant rhizosphere and promoting plant growth. Genera such as *Pseudomonas*, *Serratia*, and *Bacillus* have shown substantial efficacy in reducing PPN populations (Khabbaz et al., 2019). For instance, strains of *Bacillus* produce secondary metabolites and volatile organic compounds (VOCs) with nematicidal activity. *B. cereus* 09B18 and *B. subtilis* OKB105 culture filtrates have demonstrated up to 95% mortality of *M. javanica* and *Heterodera filipjevi* juveniles (Zhang et al., 2016). Similarly, *B. subtilis* OKB105 and *B. amyloliquefaciens* B3, which demonstrated high nematicidal activity against *Ditylenchus destructor, Aphelenchoides besseyi* and *Bursaphelenchus xylophilus,* While the endophytic bacterium K6, isolated from coffee leaves, caused 65% mortality of *P. coffea* and *Serratia plymuthica* M24T3 caused 100% death rate against pinewood nematodes (Proença et al., 2019; Migunova and Sasanelli, 2021).

Certain bacterial strains suppress nematode reproduction through novel mechanisms. *Bacillus thuringiensis* produces Cry proteins that disrupt nematode physiology, while *Serratia proteamaculans* Sneb 851 has shown strong activity against *M. incognita* (Jisha et al., 2013; Zhao et al., 2018). VOCs such as dimethyl disulfide (DMDS) and 2-undecanone (2-UD), produced by *B. atrophaeus* GBSC56, exhibited nematicidal effects and induced systemic resistance (Ayaz et al., 2021). Additionally, *Pseudomonas fluorescens* F113 reduces egg hatching in *G. rostochiensis* J2 stage nematodes. In cotton, *B. firmus* GB-126 has also been observed to reduce egg hatching and significantly impacts nematode motility (Cronin et al., 1997; Castillo et al., 2013).

2.4.2 *Fungal biocontrol agents*

Fungal BCAs play a pivotal role in managing PPNs by reducing nematode populations and enhancing crop productivity. *Trichoderma* species, for example, are well-known for their nematode-suppressing abilities. *Trichoderma* strain TH dramatically reduced the RKNs in tomatoes by increasing flavonoids, phenol, lignin, jasmonic acid (JA), cellulose, and salicylic acid (SA), while lowering malondialdehyde (MDA), hydrogen peroxide (H2O2), and electrolyte leakage levels (Yan et al., 2021). *T. asperellum* T00 significantly reduces *Pratylenchus brachyurus* infestations in soybeans by modulating defence enzymes (de Oliveira et al., 2021). *T. harzianum* effectively suppressed *M. incognita* infection in tomato and brinjal plants (Yan et al., 2021). Tomatoes developed systemic resistance to the RKN by *P. chlamydosporia* M10.43.2, which resulted in decreased female reproduction (14.7–27.6%) and reduced infection (32–43%) (Dababat et al., 2006; Ghahremani et al., 2019). Other fungi, such as *Acremonium sclerotigenum* cause 95% mortality of *M. incognita* juveniles and inhibit egg hatching (Yao et al., 2023). A new endophytic fungus, *Chaetomium ascotrichoides,* from *Pinus massoniana* was reported to be effective against *Bursaphelenchus xylophilus* with a 99% mortality (Kamaruzzaman et al., 2024). Nematophagous fungi employ diverse strategies, including predation, parasitism, and toxin production. Predatory fungi such as *Drechslerella* spp. and *Arthrobotrys oligospora* create trapping structuress like adhesive hyphal networks and constricting rings, while endoparasitic fungi like *Drechmeria coniospora*directly invade nematodes. Facultative parasitic fungi, including *Pochonia chlamydosporia* and *Paecilomyces lilacinus*, target sedentary stages such as eggs, cysts, and adult females, reducing nematode populations (Al-Ani et al., 2022). Additionally, toxin-producing fungi like *Pleurotus ostreatus* immobilise nematodes with toxic compounds before penetrating their cuticles (Pires et al., 2022).

2.5. Black Pepper: Agronomy, Diseases and Nematode Issues

Black pepper is one of the most extensively used spices globally. Derived from the dried, mature fruits (berries) of *Piper nigrum* L., a tropical perennial climbing plant of the Piperaceae family, black pepper has been an integral part of history, culture, and trade. Its distinctive pungency, attributed to the chemical compound piperine,

makes it a staple in global cuisines and various traditional medicine systems, including Ayurveda (Ravindran, 2000). Historically, India's rich diversity in spices, including black pepper, attracted traders from across the world. The spice has been highly valued across civilizations, serving as a preservative, condiment, and medicinal agent.

India was once the largest producer and exporter of black pepper until the 1990s, when Vietnam emerged as the leading producer. However, black pepper cultivation in India, particularly in Kerala, has witnessed a decline in both production area and yield due to various biotic and abiotic factors, with diseases and pests being major contributors (Zachariah and Parthasarathy, 2008; Sabu et al., 2020).

2.5.1 *Agronomic practices*

Black pepper cultivation requires careful selection of high-yielding, disease-resistant mother plants and appropriate agronomic practices to ensure successful production.

Propagation: Propagation techniques for black pepper include traditional and modern methods such as *in vitro* multiplication, rapid multiplication techniques, and the serpentine method. Rooted cuttings are commonly used, with live standards like *Erythrina lithosperma*, *Erythrina indica*, *Glyricidia*, *Cocos nucifera*, and *Areca catechu* serving as supports for the climbing vines (Ravindran et al., 2000). Bush pepper is an alternative for household cultivation (Sadanandan, 2000).

Modern micropropagation methods offer advantages such as disease-free planting material and higher multiplication rates (Kadam et al., 2020). Techniques like somatic embryogenesis, callus culture, and multiple shoot regeneration have been developed (Nirmal Babu et al., 2007). Field trials have demonstrated that micropropagated plants perform comparably to conventionally propagated plants (Ramakrishnan and Dutta Gupta, 2003).

Soil: Black pepper thrives in a variety of soil types, including sandy loam and clayey loam, provided they are well-drained, rich in organic matter, and slightly acidic to neutral (pH 5.0–6.2). High-yielding pepper gardens are often characterized by soils with good moisture retention, high organic carbon content, and adequate micronutrients like zinc (Hamza et al., 2005). Pepper is commonly cultivated as a

monocrop in nutrient-rich soils or as a mixed crop in coconut and areca nut plantations.

Nutrients: Nutrient management plays a crucial role in black pepper productivity. Key nutrients include nitrogen, magnesium, potassium, phosphorus, and micronutrients like zinc and iron. Studies have shown that nitrogen is the most easily absorbed nutrient, followed by potassium and calcium (Mohanakumaran and Cheeran, 1981). Balanced nutrient application, such as 140 kg N, 270 kg K_2O, and 55 kg P_2O_5 per hectare, has been recommended for optimal growth and yield (Sadanandan, 2000).

Rainfall: Black pepper requires a well-distributed annual rainfall of 1000 and 3000 mm for optimal growth. While pepper can tolerate low rainfall, soil moisture retention and drainage are critical. Depending on the kind of soil, 70 to 100 mm rainfall, spread over 20 days, is enough to initiate the flushing and flowering processes of the plant. After flowering has started, there should be regular but moderate rainfall for the best fruit set. A few days of dry weather during this critical time will cause spike shedding and a large reduction in pepper yield (Sadanandan, 2000).

Temperature: Temperature ranges between 20 to 30°C are ideal, with the crop being sensitive to extreme temperatures (Sadanandan, 2000). Normally around 25 - 28°C temperature prevails at 30 cm soil depth which is optimum for pepper growth.

Humidity: Black pepper grows best in hot, humid environments. But suffers from persistent high humidity, which can exacerbate pest and disease issues. High humidity (>90%) during monsoon may have in pepper plantations (Sadanandan, 2000).

2.5.2 *Major diseases of black pepper*

Black pepper is susceptible to a number of diseases caused by oomycetes, fungi, bacteria, mycoplasma, viruses, and parasitic nematodes. Diseases reduce output, which impedes the nation's economic development in which black pepper is a major source of income. The two biggest risks to black pepper are slow decline, which is brought on by the parasitic nematode *Radopholous similis*, and *Phytophthora* foot rot, which is brought on by the oomycetes pathogen *Phytophthora capsici* (Anandaraj, 2000). Black pepper is susceptible to fungal diseases such as pollu (anthracnose) from

Colletotrichum gloeosporioides, basal wilt from *Sclerotium rolfsii*, leaf rot and blight from *Rhizoctonia solani*, and vascular wilt from *Fusarium* spp. Viral diseases include wrinkled leaf disease, stunt disease, and the cucumber mosaic and piper yellow mottle viruses (Sarma et al., 2001; Bhat et al., 2005). Mycoplasma infections are the cause of black pepper phyllody disease (Paily et al., 1981).

Quick wilt (Foot rot)

It is a serious and damaging disease that mostly affects pepper production during the monsoon season and is brought on by the soil fungus *Phytophthora capsici*. Muller (1937), who identified the genesis of the disease and reported its epidemiology and symptoms in Indonesia, Sumatra and Java, came up with the term "foot rot." All plant parts, including leaves, stems, spikes and roots, are impacted by this fungus. During the rainy season, black, water-soaked lesions with a distinctive fimbriate that progresses and enlarges to cause defoliation on the leaves. If the main stem at ground level is damaged, the entire vine may wilt, dropping leaves and spikes with or without black spots. The branches may also break at the nodes, resulting in the vine's collapse within a month. Due to the high susceptibility of black pepper vines to Phytophthora foot rot, which was first observed in Indonesia in 1885, productivity has decreased globally (Erwin and Ribeiro, 1996). The disease is one of the biggest production barriers in Vietnam's black pepper-growing regions (Truong et al., 2008), and it is estimated to cause 5 to 20% vine loss (Manohara et al., 2004). However, it is much higher in India (Shamarao Jahagirdar and Siddaramaiah, 2002) and Indonesia (Sitepu and Mustika, 2000). In certain nations, the disease has been found to impact up to 95% of vines on particular farms (Anandaraj et al., 1989), and Kifelew and Adugna (2018) documented that it exists in Ethiopia.

Pollu disease (Anthracnose)

Young leaves, spikes, and berries are all impacted by this fungal disease, which is brought on by *Colletotrichum gloeosporioides* and manifests towards the conclusion of the monsoon season. Early on, the impacted berries exhibit brown, sunken spots. Later on, they develop discoloration, distinctive cross splitting, and cracks, which not only harms the berry but also lowers the quality of the fruit. On the leaves, the fungus

also produces irregular, brownish lesions that have a chlorotic halo. Defoliation and spike shedding happen in the severe type. The range of damage is 28–34% (Unnikrishnan Nair et al., 1987). As per Kumari and Gopalan (2000), the disease caused a complete loss of yield.

Basal wilt

Basal wilt is another soil-borne infection that is particularly common in black pepper nurseries, where vast quantities of seedlings or rooted black pepper cuttings are generated. Basal rotting of the plants is a characteristic of the disease (Anandaraj and Sarma, 1995). The disease, caused by *Sclerotium rolfsii*, is most visible in nurseries between June and September. The main source of infection, the soil, is where the pathogen is still present. Greyish sores appear on stems and foliage. White mycelium on the leaves can be seen at the lesions' progressing edges. Later, the rooted cuttings dry out and the leaves droop past the point of infection as the mycelial threads wrap the stem. Little, grain-like sclerotial structures that range in color from white to cream develop on more advanced lesions. When *S. rolfsii* invades pepper seedlings in the nursery, the cuttings rot and wilt. The fungus grows as a white mycelium with many sclerotia, and the afflicted plants have greyish lesions on their stems. Sclerotria on lesions and greyish patches with whitish mycelium near the lesion's expanding margins are visible on the leaves (Anandaraj, 2000).

Vascular wilt (Yellow wilt)

Yellow wilt, a systemic disease caused by *Fusarium oxysporum*, is a severe issue in Brazil. It mostly affects the black pepper's root, stem, and leaf. It is found in Brazil and Indonesia, and it is also a major disease in Malaysia (Zakaria and Noor, 2020). The disease enters pepper plants through damaged roots caused by nematodes (*Meloidogyne javanica* and *M. incognita*) or when new roots sprout. It invades the vascular bundles, resulting in necrosis and blocking the absorption of nutrients and water. The vascular necrosis, which is mainly unilateral, spreads to the apical twigs' leaf veins, causing the plants to quickly wilt and die. Diseased plants exhibit yellowing on the outside, as well as the loss of rootlets and the shedding of leaves and internodes. While the vessels in the root stellar section become necrotic, the roots themselves stay

normal in yellow wilt. According to Duarte et al. (2003), triangular lesions are observed at the nodal area. These lesions move upward and cause unilateral necrosis, which turns half of the branches necrotic while the other half remain green. The foliar yellowing is severe, and there may be initial defoliation on one side of the vine before symptoms spread to the entire vine. Throughout the year, it is present and spreads by root contact.

Viral diseases

Cucumber mosaic virus (CMV) and piper yellow mottle virus (PYMoV) are two stunt diseases that are more common in pepper-growing regions. It is also known as a mosaic, tiny leaf, or wrinkled leaf. Higher elevations exacerbate the condition. Whereas aphids carry CMV, mealy bugs spread PYMoV. The diseased vine develops narrow, leathery, puckered, and crinkled leaves, and its internodes decrease. At this stage, the shortage of nutrients causes the plant to die. Conversely, a temperature of 35°C encourages the development of symptoms (Bhat et al., 2018).

Phyllody disease

The majority of cases of phyllody disease occur in the districts of Wayanad and Kozhikode in the state of Kerala. It is brought on by phytoplasma, and infected vines exhibit symptoms of spike deformity at different levels, which causes the flower buds to change into a narrow, leaf-like structure with phyllody symptoms. At later stages, the leaves grow small and chlorotic, which causes the internodes to shorten. The impacted fruiting branches have the look of a witch's broom. Vines that are severely diseased stop producing after two to three years (Paily et al., 1981).

Nematode infestation on black pepper

Black pepper cultivation faces significant threats from PPNs, which are among the leading causes of yield losses (Abd-Elgawad and Askary, 2015). PPNs, including *R. similis* and *M. incognita,* can cause direct damage by feeding on roots and indirect damage by predisposing plants to secondary pathogens like *Fusarium* spp. (Mohandas and Ramana, 1991). The relationship between black pepper vines and the RKN was initially noted in 1906 (Butler, 1906), and then the fungus *Fusarium* sp. was linked to

"wilt sickness". This synergistic interaction between nematodes and pathogens leads to devastating diseases such as slow decline and root rot (Usman et al., 2020).

Slow decline disease

Slow decline, also referred to as "yellows" disease, or slow decline disease is caused by a combination of PPNs (*Meloidogyne* spp., *R. similis)* and fungal pathogens (*Phytophthora capsici*, *Fusarium* spp.). Symptoms include yellowing and defoliation of leaves, dieback, and progressive loss of vigour and productivity, eventually leading to vine death. The disease primarily affects feeder roots, causing lesions, necrosis, rotting primarily due to *R. similis infestation*, and root galls by RKNs, which disrupt nutrient and water uptake (Nambiar and Sharma, 1977). Nematode feeding creates entry points for fungal pathogens, compounding the damage. Infested roots exhibit necrotic lesions, rotting, and a significant reduction in feeder root biomass. Secondary root infections exacerbate the problem, causing above-ground symptoms like stunted growth and wilting. *R. similis* and *Meloidogyne* spp. have been identified as major contributors to slow decline in all black pepper-growing regions, including India, Indonesia, and Brazil (Venkitesan and Setty, 1977).

Root-knot nematodes: RKNs (*Meloidogyne* spp.) are sedentary endoparasites that induce gall formation in fibrous roots. Their feeding causes hypertrophy and hyperplasia of root tissues, leading to nutrient and water uptake disruption. Severely galled roots deteriorate over time, leaving plants unable to recover (Mohandas and Ramana, 1987). Nematodes feed on the vascular tissues in the stelar part of the roots. Over time, the cells disintegrate and merge to form big or giant cells. Above-ground symptoms include foliar yellowing, defoliation, and reduced vigor, ultimately reducing yields (Kueh, 1990).

Burrowing nematodes: *R. similis* is a migratory endoparasite that penetrates root cortical tissues, causing necrotic lesions and rotting. Its host range includes approximately 370 plant species (Peachey, 1969). The nematode’s feeding activity leads to extensive tissue destruction, and the resulting tunnels in root tissues compromise structural integrity. In severe infestations, most feeder roots are lost, resulting in reduced nutrient and water uptake. Above-ground symptoms mirror those

caused by RKNs, including yellowing, defoliation, and dieback (Peachey, 1969; Freire and Bridge, 1985).

Interaction with fungal pathogens: The combined effects of nematodes and fungal pathogens like *Fusarium solani* aggravate root damage. For example, nematode-infected roots are more susceptible to fungal colonization, leading to root rot. In Indonesia and Malaysia, *F. solani* infections, in conjunction with nematodes, result in extensive root necrosis, reducing vine productivity (Freire, 1983). Similarly, in India, *Phytophthora capsici* and nematodes contribute to feeder root mortality and canopy reduction in black pepper vines (Anandaraj, 2000).

2.6 *Pochonia chlamydosporia* in Biocontrol of Nematodes

The interactions between plants and microorganisms, particularly rhizosphere fungi, play a crucial role in modulating plant metabolism, enhancing vigor, and promoting growth and development. Plant growth promoting fungi (PGPF) are rhizosphere fungi that colonise plant roots and stimulate plant growth without causing harm. PGPF can be categorised as endophytic (residing within plant roots and exchanging metabolites), epiphytic (living on the root surface), or free-living (inhabiting the rhizosphere). These fungi establish non-obligate mutualistic relationships with a wide range of host plants facilitating plant productivity, seed germination, seedling vigor and resilience to phytopathogens (Aly et al., 2011).

P. chlamydosporia stands out as an effective BCA due to its adaptability to various soil types, ability to parasitize multiple nematode genera, and ease of mass production. Its versatility allows it to switch between saprophytic and parasitic lifestyles, depending on the presence of nematodes. This fungus preferentially parasitises nematode eggs, particularly those encased in mucilage, which facilitates fungal adhesion and enzymatic degradation (Kerry and Crump, 1977; Esteves & Devonshire, 2017). *P. chlamydosporia* can parasitize various nematode genera, including *Meloidogyne, Rotylenchulus, Naccobus* and *Pratylenchus* (Monteiro et al., 2018).

Numerous studies highlight the efficacy of *P. chlamydosporia* in reducing nematode populations. For example, Viggiano et al. (2014) demonstrated that increasing doses

of *P. chlamydosporia* PC-10 significantly reduced root galls and nematode eggs in cucumber plants. Similarly, Ebadi et al. (2018) reported that isolates Pcc20 and Pcc10 reduced *Meloidogyne javanica* reproduction by 57% and 36%, respectively, in pistachio plants.

Beyond direct parasitism, *P. chlamydosporia* also induces systemic resistance in plants (Medeiros et al., 2015). Studies in *Arabidopsis thaliana* revealed upregulation of salicylic acid-associated defence genes and pathogenesis-related proteins (PR), enhancing plant resistance to nematodes (Zavala-González et al., 2017). Tomato plants treated with different isolates of *P. chlamydosporia* showed improved root systems and higher fruit yields (Zavala-Gonzalez et al., 2015). The effectiveness of *P. chlamydosporia* varies with soil type and environmental conditions. Nasu et al. (2018) found that sandy soils supported better colonization and nematode suppression than clayey soils. Furthermore, the compatibility of *P. chlamydosporia* with chemical fungicides and other beneficial microbes, such as *Trichoderma harzianum* and rhizobacteria, highlights its potential for integrated pest management (Puertas et al., 2006; Podestá et al., 2013).

2.6.1 *Plant growth promotion by Pochonia chlamydosporia*

P. chlamydosporia is a versatile fungus known not only for its nematophagous activity but also for its ability to promote plant growth. As a plant growth-promoting fungus (PGPF), it interacts with host plants through multifaceted mechanisms, enhancing their vigor and productivity. This fungus can colonize plant roots as an endophyte, facilitating nutrient uptake, producing phytohormones, and inducing systemic resistance against pests and pathogens (Zavala-Gonzalez et al., 2017). Its capacity to colonise the plant cortex and outer vascular tissue as an endophyte underpins many of these benefits (Larriba et al., 2015; Ciancio et al., 2017; Monteiro et al., 2018). These traits, coupled with its role as a biocontrol agent, make *P. chlamydosporia* a valuable tool for sustainable agriculture. Understanding the mechanisms underlying its plant growth-promoting effects is essential to fully exploit its potential in crop health management, particularly in black pepper cultivation.

Mechanisms of plant growth promotion

The growth-promoting effects of PGPF are mediated through direct and indirect mechanisms. Direct mechanisms include the production of phytohormones, phosphate solubilization, and siderophore formation, while indirect mechanisms involve the suppression of plant diseases, stress tolerance, and induced systemic resistance (ISR). A single PGPF may employ multiple mechanisms to promote plant growth and development (Glick et al., 2007).

Phytohormone production: Phytohormones play a central role in mediating plant-microbe interactions. Auxins, such as indole-3-acetic acid (IAA), are the most studied phytohormones produced by PGPF. Auxins regulate root architecture by promoting lateral root formation and adventitious root development. Gibberlins (GAs) influence plant developmental processes, including stem elongation, while cytokinins, particularly zeatin, stimulate cell division and growth (Contreras-Cornejo et al., 2009).

In studies on *P. chlamydosporia,* Larriba et al. (2015) observed the up-regulation of genes involved in auxin biosynthesis in barley, such as putative auxin-induced protein, auxin responsive transcription factors and enzymes like arogenate dehydratase, enolase, auxin transporter, prephenate dehydratase and shikimate kinase. Gouveia (2018) assessed the phytohormone production capacity of *P. chlamydosporia* using LC/MS analysis of *in vitro* fungus cultures and found IAA in the extracellular medium of two of the three fungal isolates studied. Additionally, Zavala-Gonzalez et al. (2015) demonstrated that *P. chlamydosporia* inoculation in tomatoes increased fruit production, reduced blooming and fruiting times, and promoted root growth. These effects can be attributed to the production of IAA, enhancing plant growth.

Phosphate solubilization: Phosphorus is a crucial macronutrient that is often limited in plant growth due to its insoluble form in soil. *P. chlamydosporia* is a phosphate-solubilizing fungus that converts insoluble phosphorus into soluble forms, making it more accessible to plants. This mechanism is vital for improving nutrient uptake and promoting plant growth, particularly in phosphorus-deficient soils (Islam and Hossain, 2012). Monteiro et al. (2018) demonstrated that *P. chlamydosporia* enhances

phosphorus uptake of tomato plants, likely through the solubilization of inorganic phosphorus in the soil. The fungus increased uptake of phosphorus by 24.5%, contributing to faster growth and shorter flowering times, which resulted in earlier fruit production (Monteiro, 2013; Zavala-Gonzalez et al., 2015).

Siderophore production: Siderophores are low molecular weight compounds that chelate iron, a critical nutrient often limiting plant growth in soil. These molecules, produced by bacteria, fungi, and plants, facilitate the acquisition of iron by sequestering it from the environment (Hider and Kong, 2010). *P. chlamydosporia* produces siderophores that may enhance iron availability, contributing to plant growth. The production of siderophores by *P. chlamydosporia* in soils could potentially reduce the reliance on synthetic fertilizers and contribute to sustainable agricultural practices (Oberegger et al., 2001; Tamariz-Angeles et al., 2021).

Induced systemic resistance: ISR is a plant defence mechanism triggered by beneficial microorganisms, including *P. chlamydosporia*. It involves a complex network of signalling pathways that prepare the plant to respond more effectively to future pathogen attacks. The primary plant hormones involved in ISR are ethylene (ET), jasmonic acid (JA), and salicylic acid (SA). In plants, ISR is associated with the activation of the JA and ET pathways, while systemic acquired resistance (SAR) is linked to the accumulation of SA and the expression of pathogenesis-related (PR) genes (Kuć, 2001; Campos et al., 2014).

Plant hormones, particularly jasmonic acid (JA), play a crucial role in regulating plant growth and stress responses by activating gene expression to mediate reactions to environmental stressors. Jasmonates, including JA, its methyl ester (MeJA), and isoleucine conjugate (JA-Ile), activate signalling pathways that are vital for plant resistance, primarily through jasmonic acid and salicylic acid (SA)-mediated pathways. These pathways trigger plant defences against pathogens and environmental damage. Additionally, ethylene (ET) and abscisic acid (ABA) interact with the JA signalling pathway through transcription factors like ORA59 and MYC2, which help coordinate plant responses. Systemic acquired resistance (SAR), an induced defence mechanism, provides long-term protection against a variety of

microbes, with SA being essential for its activation. SAR is associated with the upregulation of pathogenesis-related (PR) genes and is driven by the combined actions of multiple PR proteins.

Studies on *P. chlamydosporia* have shown that it can enhance ISR in plants by upregulating genes associated with JA metabolism. For example, Larriba et al. (2015) demonstrated that *P. chlamydosporia* colonization in barley roots resulted in a moderate increase in the expression of ISR-related genes. Similarly, Zavala-Gonzalez et al. (2017) found that *P. chlamydosporia* colonization in *Arabidopsis thaliana* roots induced altered jasmonate signaling, leading to faster blooming and increased fruit yield. Additionally, Escudero et al. (2017) showed that *P. chlamydosporia* can enhance its effectiveness against nematodes by combining it with chitosan, a natural enhancer that stimulates ISR in plants.

Root colonisation and rhizosphere competence: Root colonization is essential for the growth-promoting effects of PGPF. Fungi that can effectively colonise plants are considered to have high rhizosphere competence, which enables them to thrive in the competitive root environment. *P. chlamydosporia* has demonstrated strong rhizosphere competence, which facilitates its colonization of host roots and promotes plant growth. The ability of *P. chlamydosporia* to successfully colonise plant roots and persist within the rhizosphere enhances its effectiveness as a biocontrol agent and plant growth promoter (Hoyos-Carvajal et al., 2009).

In various crops, including bananas, barley, wheat, and tomatoes, *P. chlamydosporia* has been shown to promote plant growth through endophytic colonization (Monfort et al., 2005; Maciá-Vicente et al., 2009; Escudero and Lopez-Llorca, 2012; Mingot-Ureta et al., 2020). The growth-promoting effects of *P. chlamydosporia* vary depending on the plant species and the fungal isolate, highlighting the importance of specific interactions between the fungus and the host plant (Manzanilla-López et al., 2011).

2.6.2 *Potential applications*

The multifunctional roles of *P. chlamydosporia* as a plant growth promoter and nematode biocontrol agent make it a promising candidate for sustainable agricultural practices. Future studies should explore its potential in integrated pest management systems, especially when combined with other beneficial microbes like *Trichoderma* spp. and mycorrhizal fungi. Additionally, understanding the molecular mechanisms underlying *P. chlamydosporia's* interactions with plants will provide insights into optimizing its application in diverse agricultural settings.

Future research could also focus on developing formulations for large-scale applications of *P. chlamydosporia*, enhancing its effectiveness in different soil types and under varying environmental conditions. Moreover, its compatibility with other agrochemicals should be explored to optimize its use alongside conventional crop protection measures, thereby promoting sustainable and resilient agricultural systems.

2.7 Secondary Metabolites of *Pochonia chlamydosporia*

Plants and microbes produce a variety of tiny, unusual compounds called secondary metabolites that dominate the global environment. These compounds are very abundant in plants and fungus. Fungal secondary metabolites (SM) are a broad class of compounds with a variety of chemical characteristics. They perform a wide range of tasks and are frequently linked to the fungus's enhanced fitness in its surroundings, frequently engaging in interactions with plant species or competing with other microorganisms. Numerous beneficial microorganisms employed for crop protection and biofertilization around the world depend on several of these compounds for the biological control of plant diseases (Elhamouly et al., 2022). Natural metabolites can stimulate root and shoot growth and/or disease resistance by triggering host systemic defences, in addition to their direct toxic actions against phytopathogens. Research is increasingly focusing on these microbes' capacity to produce and store physiologically active metabolites, which are a powerful source of new natural substances useful for agriculture. Furthermore, some of these compounds target plant development and metabolism, while others are essential for modulating fungal activity, including sporulation and hyphal extension (Keller et al., 2005).

Resorcylic acid lactone (RAL), phenolics, alkaloid, and pyranones are the primary secondary metabolites of *P. chlamydosporia*, whereas those of the other *Pochonia* species include polycyclic aromatic compounds, phenol-terpenoid hybrids, nonaromatic polyketides, β-carotene-type neurosporaxanthin, daphnane-type diterpenoids, pentanol lanostane triterpenoids, polyhydroxylated pyrrolizidine, cyclodepsipeptides, linear lipopeptide, and verticillin-type diketopiperazines. Numerous natural compounds have garnered significant interest due to their intriguing molecular structures and appealing biological properties, including antimicrobial, antifungal, antioxidant, anti-malarial, antihelminthic, antiviral, and antitumor properties (Niu, 2017).

The three primary groups of secondary metabolites of resorcylic acid lactone are monocillins, pochonins, and radicicol (monordens). A family of substances known as resorcylic acid lactones (RALs) has a resorcylate moiety united within a macrolactone ring with 12 or 14 members. For many years, they have been recognized since monorden was first purified (Delmotte and Delmotte-Plaquee, 1953). Khambay et al. (2000) purified radicicol from *P. chlamydosporia* during their hunt for nematicidal components in nematophagous fungus. Radicicol was discovered to be the main ingredient in *P. chlamydosporia* potato dextrose cultures that were 14 days old. However, a bioassay employing the RKN *M. incognita* revealed that radicicol lacked nematicidal action. However, at 10 ppm, it demonstrated antiviral action against Herpes Simplex Virus 1 (HSV) as well as selectivity for the parasite *Eimeria tenella* (Hellwig et al., 2003).

Initial purification and identification of pochonins came from strains of *P. chlamydosporia* (Hellwig et al., 2003; Shinonaga et al., 2009a, b). Except for pochonins F and J, all of the pochonins were RALs that contained chlorine, and pochonin K was a radicicol derivative that contained 14-aldofuranose. Pochonins L-N are the first three examples of radicicol analogues with a double bond with an E-configuration at C5-C6, whereas pochonins G and H were the first two examples in the radicicol family to feature a furan ring among these secondary metabolites. The macrolide ring of pochonin I has a single benzene moiety. Pochonins B, D, E, F, K, L,

and O demonstrated a potent inhibitory effect on WNT-5A expression, with IC50 values ranging from 8 to 18 μM (Shinonaga et al., 2009a, b). Monocillin I, II, III, and IV were among the class of monocillin metabolites, which were purified from *P. chlamydosporia* and contained non-chlorine-containing RALs. The monocillin I shown strong activity against a broad range of fungi, including *Ceratocystis ulmii*, *Pythium debaryanum*, *Phellinus pini*, and *Phycomyces blaksleeanus*, suggesting that their antifungal properties are general (Ayer et al., 1980, Aver and Peña-Rodriguez, 1987).

The second major class of *P. chlamydosporia* secondary metabolites are pyranones. Bacteria and fungi contain a large number of 2-pyrone (α-pyrone or pyran-2-one) molecules, which are known as pyranone secondary metabolites. They can bind to particular protein domains to provide a variety of biological effects (McGlacken and Fairlamb, 2005). Pyranone class mainly include phomalactone and aurovertin. In 2000, the first investigation on the separation of phomalactone from the fungus *P. chlamydosporia* was published. Phomalactone was isolated as the nematicidal metabolite by a bioassay-directed fractionation of the 14-day-old potato dextrose cultures of the fungus in conjunction with a bioassay against the RKN, *M. incognita.* Phomalactone was also modestly toxic to tephritid fruit flies and showed dose-dependent insecticidal efficacy against apple maggot flies, *Rhagoletis pomonella*. Additionally, it demonstrated inhibitory efficacy against *Metarhizium anisopliae* and *Bacillus bassiana* spores (Krasnoff and Gupta, 1994).

The metabolites of the aurovertin type share certain molecular similarities with phomalactone, which has a carbon skeleton made up of 5-methyl-6-((E)-prop-1-enyl) pyran-2-one. Niu et al. (2010) reported the first isolation of aurovertin-type secondary metabolites (D, E, E, and I) from *P. chlamydosporia* strain YMF 1.00613, a parasitic fungus that parasitizes nematodes and is obtained from tobacco root knots infected with *M. incognita.* It was shown that the nematode-parasitic fungus *P. chlamydosporia* produces the majority of aurovertins, D and F, which are poisonous to the free-living nematode *Panagrellus redivivus*, with IC50 values of 41.7 and 88.6 μg/ml, respectively. The nematodes exposed to aurovertin D or F in the nematicidal bioassay

showed a disintegration of their internal structures and the formation of many vacuoles within their bodies, leaving only the empty cuticles of the deceased nematodes after 48 hours. Additional bioassay demonstrated that aurovertin D inhibited *Caenorhabditis elegans* and significantly killed *M. incognita* second-stage juveniles, suggesting a higher inhibitory effect toward root-knot than free-living nematodes. Additionally, even at subinhibitory concentrations, aurovertin D had significant and negative impacts on *C. elegans* survival. In nematodes, aurovertin D may also activate the DAF-16/FOXO transcription factor (Wang et al., 2015).

The third major class of *P. chlamydosporia* secondary metabolites Spirocyclic Alkaloids which mainly include Pseurotin A. Hellwig et al. (2003) found that the majority of *P. chlamydosporia* isolates grown in Q6-medium (D-glucose 0.2%, cotton seed meal 0.5%, glycerol 1%, pH 7.2) had pseurotin A as a major metabolite. All biological tests conducted with the pochonins in a cellular replication assay against HSV1 were also conducted on the compound, pseurotin A, which was discovered to be inert.

2.8 Genomic and Transcriptomic Insights

Genomics studies an organism's genome to understand its organization, gene functions, and phylogenetic links with other organisms. Genomics has improved understanding of developing biocontrol agents, including their population dynamics, identification, epidemiology, and pathogenicity. Genomics research has led to a better understanding of the genetic events that shape the genomes of BCAs, including recombination, duplications, inversions, mutations, transpositions, deletions, and insertions. These events are used to evaluate the effectiveness of BCAs against plant pests and diseases. The pathogenicity of *P. chlamydosporia* to PPNs has been studied using various methods, including cloning, proteomics, and sequencing (Lopez-Llorca, 1990; Larriba et al., 2014). The transcriptome refers to the complete collection of transcripts in a cell, along with their abundance, at a particular developmental stage or physiological state. Transcriptomics focuses on studying this collection of RNA transcripts generated by the genome under specific conditions. The primary technologies used in transcriptomic studies are sequence-based approaches. Dynamic

data regarding tissue-level gene expression is obtained through transcriptomic studies, enabling the identification of genes exhibiting differential expression in various cell groups or in response to specific treatments (Wang et al., 2009).

2.8.1 *Genomics of P. chlamydosporia*

Recent genomic advances allow scientists to better understand the genetic basis of *P. chlamydosporia* pathogenicity to RKN. Several studies have used genomic methods to examine how chitosanases and chitin deacetylases contribute to *P. chlamydosporia*'s pathogenicity to nematode eggs (Aranda-Martinez et al., 2016). Earlier, culture methods were used to assess the biocontrol agent's efficacy, with inoculum level quantification as a key factor. However, these conventional culture-based methods often overestimate the amount of fungal inoculum in the soil or rhizosphere (Escudero and Lopez-Llorca, 2012). With newer genetic technologies, scientists can more accurately estimate fungal populations in the environment. Quantitative PCR (qPCR), for instance, enhances the quantification of *P. chlamydosporia* in soil and during host root colonisation, enabling more effective application timing and adequate inoculum levels for RKN management (Escudero and Lopez-Llorca, 2012). Recent sequencing and functional analysis of *P. chlamydosporia* have provided valuable insights into its pathogenic mechanisms (Larriba et al., 2014). Genomic studies reveal significant presence of chitin-modifying enzymes, such as chitosanases and deacetylases, which play a critical role in degrading nematode egg shells during infection (Aranda-Martinez et al., 2016). These enzymes facilitate fungal penetration into nematode eggs by degrading the chitin layer of the egg shell.

Genomic analyses have also highlighted the evolutionary relationships and polytrophic nature of *P. chlamydosporia*, shedding light on its dual role as a biocontrol agent and a plant growth promoter. The presence of numerous serine proteases, particularly the S33 prolyl peptidase, has been identified as critical for disrupting nematode egg shells and initiating fungal parasitism by recognizing proline residues in the egg shell (McClure and Bird, 1976; Larriba et al., 2014). Additionally, genes encoding nematicidal secondary metabolites have been identified, enhancing the

fungus's pathogenicity (Reeves et al., 2008). Fungal genome mining can also aid in the development of diagnostic tools for precise identification of *P. chlamydosporia.*

2.8.2 *Transcriptomics of P. chlamydosporia*

Transcriptomic research has progressed significantly since the early use of hybridization-related microarray technology (Casneuf et al., 2007; Shendure and Ji, 2008). Advances in next-generation sequencing and bioinformatics tools have made transcriptome analysis a powerful approach to understanding the pathogenicity and root colonization potential of BCAs. For instance, the genome sequence of *P. chlamydosporia* PC123 has provided a foundation for studying the mechanisms underlying its parasitism (Larriba et al., 2014). A large fraction of secreted proteins identified in the PC123 genome were expressed during its endophytic phase, indicating their importance for the fungus's various lifestyles.

Transcriptomics is a valuable tool for uncovering the molecular basis of host-pathogen interactions and root colonization (Mutz et al., 2013). Additionally, it is a quick and potentially useful technique for identifying molecular markers and large-scale functional genes (Morozova et al., 2009). A study of *P. chlamydosporia* revealed differential gene expression profiles during its parasitic and saprophytic stages. These findings reveal the fungus's ability to rewire gene expression during transitions from saprophytic to parasitic forms, with upregulated genes involved in metabolism, detoxification, and enzymatic activity (Rosso et al., 2011). *P. chlamydosporia* in roots and soil can be estimated by qPCR analysis of parasite-specific genes. It offers a means of quantifying *P. chlamydosporia* abundance in soil and roots, as well as assessing the soil's fungal parasitism potential. Transcriptomic analysis has also shed light on *P. chlamydosporia's* ability to promote plant growth and enhance natural resistance to RKN. When colonising barley roots, the fungus upregulates genes associated with jasmonic acid, auxin and ethylene signalling pathways - key components of plant defence mechanisms (Larriba et al., 2015). Similarly, tomato plants exhibited significant metabolic pathway activation in the presence of endogenous *P. chlamydosporia* (Ciancio et al., 2019). *P. chlamydosporia* activates

WRKY72 transcription factors, linked to defence pathways independent of salicylic acid, on colonising tomato roots (Bhattarai et al., 2010).

2.9 Interactions Between *P. chlamydosporia* and Black Pepper

The biology of *P. chlamydosporia* is complex, as the fungus exhibits symbiotic and multitrophic traits depending on the host, substrate, and environmental conditions. *Pochonia* can persist in its saprophytic stage without nematode or plant hosts, efficiently competing with other soil microorganisms. Once established in soil, its effectiveness depends on factors influencing rhizosphere colonization (Kerry, 1988). Unlike plant pathogenic fungi, *Pochonia* does not inhabit the vascular cylinder but can colonize the epidermis of certain Solanaceae and Gramineae species. Some isolates of *Pochonia* spp. demonstrate endophytic behaviour, potentially enhancing host plant defence against soil-borne pathogens. These endophyte-plant alliances, engaging in rhizosphere tritrophic interactions, represent an evolutionary trait with potential applications in crop management. As an endophytic fungus, *P. chlamydosporia* has dual effects: benefitting the host plant and harming nematodes. According to Kerry et al. (1993), *P. chlamydosporia* establishment and reproduction are more pronounced in naturally suppressive soils infected with nematodes.

Black pepper itself harbours diverse endophytic bacteria and fungi. Prominent bacterial genera include *Burkholderia ubonensis*, *Pseudomonas geniculata*, *Burkholderia territorii, Pseudomonas beteli, Bacillus subtilis, Brevibacillus gelatini* and *Bacillus siamensis* (Lau et al., 2020). Endophytic fungi such as *Alternaria, Cladosporium, Acremonium, Phoma, Chaetomium, Rhizoctonia, Curvularia, Humicola, Fusarium, Colletotrichum*, and non-sporulating types have also been identified in black pepper (Sreeja et al., 2019).

Notably, *P. chlamydosporia* has been isolated from black pepper plantations infested with nematodes. In one investigation, *P. chlamydosporia* was identified from the semi-endoparasitic nematode, *Trophotylenchulus piperis,* in a black pepper garden in Kozhikode District of Kerala, India (Sreeja et al., 1996). *In vitro* bioassays revealed that the fungus inhibited RKN egg hatching by 41.4% within five days, demonstrating its potential for managing RKNs in spice crops.

However, the association between black pepper and *P. chlamydosporia* remains largely unexplored. Critical aspects such as the internal mycobiota, modes of transmission, and biological significance in black pepper are poorly understood. There is limited knowledge about its plant-beneficial properties, production of bioactive secondary metabolites, or mechanisms of action against nematodes and fungi affecting black pepper. A deeper understanding of the tritrophic interaction between plants, fungi, and nematodes is essential for optimising BCAs (Manzanilla-Lopez et al., 2013).

The plant growth-promoting potential of *P. chlamydosporia* is similarly under-researched, with most studies focusing on interactions with plant beneficial bacteria. PGPF are non-pathogenic soil fungi that enhance plant growth, morphology, nitrogen, and mineral uptake (Murali et al., 2012). This study seeks to elucidate the plant-beneficial characteristics of *P. chlamydosporia*, a proposed biocontrol agent for reducing PPNs in black pepper and other spices. Furthermore, the molecular mechanism underlying black pepper's defence responses to endophytic colonization by *P. chlamydosporia* remains unknown. Few studies have explored how endophytic colonization affects gene expression in black pepper. A detailed understanding of these mechanisms is crucial to leveraging *P. chlamydosporia* for effective plant health management in black pepper.

Chapter 3

Plant Growth Promotion by *Pochonia chlamydosporia*

Abstract

The nematophagous fungus, *Pochonia chlamydosporia,* is one of the most promising biological control agents of plant-parasitic nematodes. This study is used for evaluating the root colonization and plant growth promotional potential of *P. chlamydosporia* strain IISR-MTCC5412 in dicotyledonous host plant, black pepper (*Piper nigrum* L.). The fungal isolate was tested for its direct plant growth promoting activities such as production of indole-3-acetic acid (IAA), ammonia and its capacity to solubilize inorganic phosphate and zinc. The isolate was found to be positive for ammonia and IAA production (9.8 µg/ml) as well as phosphate (1.3 ± 0.07 response units) and zinc solubilisation (1.1 ± 0.01 response units). It also revealed indirect plant growth-promoting features such as the synthesis of siderophores (2 ± 0.04 response units) and production of extracellular enzymes such as α-amylases, cellulases, and pectinases. Using readily accessible nutritive media presents a significant challenge in terms of isolating and counting viable colonies of *P. chlamydosporia* from soil and other substrates without contamination. The fungus can be isolated more easily if a suitably selective or semi-selective media is prepared by adding one or more microbial growth inhibitors. The compatibility of several widely used pesticides, including carbendazim, copper oxychloride, metalaxyl, metalaxyl-mancozeb, and chlorpyrifos, with *P. chlamydosporia* was tested *in vitro.* The fungus demonstrated relatively high resistance to higher dosages of metalaxyl and carbendazim, and it was utilized in the modified medium to better inhibit other soil-borne fungi. In order to quantify *P. chlamydosporia* colonisation in black pepper plants, we used culturing techniques, real-time PCR, and bright field microscopy. When the fungus was applied to the root zone of black pepper cuttings in pot culture studies, it dramatically enhanced shoot and root length, shoot and root biomass, number of secondary roots, and leaves compared to uninoculated black pepper plants. The contents of nitrogen, phosphorus, potassium, calcium, magnesium, copper, manganese, iron and zinc in both soil and plant were also enhanced significantly on inoculating with this fungal isolate. Our findings highlight the agronomic significance of *P. chlamydosporia* strain IISR-MTCC5412 as a biocontrol agent for plant-parasitic nematodes with black pepper growth promoting capabilities.

3.1 Introduction

Black pepper (*Piper nigrum*), also known as the 'King of Spices', is the world's most important and widely used spice. Global production of black pepper is influenced by a wide range of biotic and abiotic factors. Plant-parasitic nematodes are key biotic agents that cause large economic losses and disrupt productivity. Many synthetic nematicides were used to control plant nematodes; however, most pesticides have been taken off the market because of substantial unexpected consequences and environmental risks. Because of this, scientists are searching for more ecologically acceptable strategies to control the numbers of plant-parasitic nematodes. An alternative tactic to minimize these unfavourable effects is the use of endophytes and fungal biological control agents (Abd-Elgawad, 2021).

Endophytism is a complex process occurring in all plants and environments, playing a vital part in plant development. It is the ability of an organism to colonise tissues of a host plant without causing visible harm. Fungal endophytes may benefit host plants by adapting to their environments, alleviating biotic and abiotic stresses, stimulating plant growth and root formation through the production of phytohormones such as indole-3-acetic acid (IAA), fixing atmospheric nitrogen, and enabling soil nutrient uptake through the solubilization of minerals such as phosphorus and zinc. Endophytes also protect plants from the adverse effects of phytopathogens through the production of antibiotics, siderophores, and enzymes and protect plants from herbivore pests and plant-parasitic nematodes (Ahemad and Kibret, 2014).

The ubiquitous facultative hyperparasitic fungus *Pochonia chlamydosporia* is one of the most promising biocontrol agents for the management of phytoparasitic nematodes and is commonly found in cyst and root-knot nematode-infested soils worldwide. It has the ability to produce chlamydospores, enabling survival in the soil without the need for additional energy sources. As an endophyte, the *P.*

chlamydosporia can colonise the rhizoplane and internal tissues of the roots of various plants, providing a competitive advantage in nematode biocontrol. *P. chlamydosporia* promotes the growth of various monocot and dicot crops such as tomato (Escudero and Lopez-Llorca, 2012), wheat (Monfort et al., 2005), pistachio (Ebadi et al., 2009), barley (MacIá-Vicente et al., 2009a) and lettuce (Dias-arieira et al., 2011). Additionally, *P. chlamydosporia* increases yields of nematode-infested crops such as potato (Muthulakshmi et al., 2012), cotton (Wang et al., 2005) okra (Chaya & Rao, 2012), chili (Singh et al., 2011), eggplant (Khan et al., 2012) and lemon (Deepa et al., 2011).

P. chalamydosporia has the ability to decrease root knot nematode egg hatching by 41.4% in just five days, suggesting that it may be utilized to control nematodes in spice crops (Ghahremani et al., 2019). Additionally, *P. chlamydosporia* is identified from *Trophotylenchulus piperis*, a semi-endoparasitic nematode, from an infected black pepper garden in Kerala's Kozhikode District (Sreeja et al., 1996). Given the simplicity of mass multiplication, saprophytic character, and durability of the chlamydospores produced, the effectiveness of biocontrol agents in reducing root knot nematodes was demonstrated, but only *P. chlamydosporia* showed superior management of root knot nematodes infesting black pepper (Saad et al., 2022). *P. chlamydosporia* is recommended by the ICAR-Indian Institute of Spices Research (IISR) for the management of plant parasitic nematodes, especially root knot nematodes and *R. similis*, after extensive field trials.

Isolation and counting of *P. chlamydosporia* colonies would be significantly easier and faster with a suitable semi-selective medium established by including one or more microbial growth inhibitors. Using semi-selective media for enumeration and isolation can limit the growth of fast-growing fungal colonies and bacterial contamination and help determine the relative abundance of the fungus in the root rhizosphere infected with nematodes (Mauchline et al., 2002). Enumerating *P. chlamydosporia* from soil and other substrates with Kerry's semi-selective medium contaminates the medium with colonies of other soil-borne fungi. Consequently, in

this work, we created a modified semi-selective medium to isolate and measure the fungus from different substrates as well as wet tropical soils.

In this study, we used the strains of *P. chlamydosporia* (MTCC5412) maintained in the repository of biocontrol agents at ICAR-Indian Institute of Spices Research (IISR) to find out the root colonization potential and plant growth promotion ability of the fungus in black pepper plant. To achieve this, we conducted pot experiments, inoculating the fungal isolate into black pepper roots to ensure endophytic development and cultivating the inoculated plants under greenhouse conditions. We tested this fungal strain for plant growth-promoting properties such as IAA and ammonia production, the ability to solubilize inorganic phosphate and ZnO, siderophore formation, and extracellular enzyme production. Using microscopy, culturing, and quantitative PCR techniques, we periodically checked the occurrence of the fungus, either on the rhizoplane or within the roots.

The goal of this study was to assess how effectively *P. chlamydosporia* can endophytically colonise roots and promote plant growth in a dicotyledonous host plant, black pepper (*Piper nigrum* L.). This study emphasizes the information regarding the plant-beneficial properties of the fungus *P. chlamydosporia* (MTCC5412) in black pepper cultivation. The significance of colonization potential of this fungus in black pepper will open a new insight into the growth and production of the plant. Understanding these features of the fungus, in addition to its biocontrol potential against plant-parasitic nematodes, could help promote it as a plant growth stimulator.

3.2 Materials & Methods

3.2.1 *Fungus*

The fungal strain used in the analysis was *P. chlamydosporia* (MTCC5412) available in the repository for biocontrol agents at ICAR-Indian Institute of Spices Research (IISR), Kozhikode, India. The sequence data of the *P. chlamydosporia* vcp1 (alkaline serine protease p1) gene of this fungus are available in NCBI database under accession number MW553913. The fungal strain was grown on potato dextrose agar (PDA)

plates at 28ºC ± 2°C, 70- 80% RH and a 12:12 h day: night photo phase for 10 days in a microbiological incubator.

3.2.2 *In vitro analysis of plant growth promoting traits of P. chlamydosporia* (MTCC5412)

The fungus was examined for the production of direct and indirect plant growth promoting traits such as IAA, siderophore, ammonia, amylase, pectinase, cellulase as well as its ability to solubilize inorganic phosphate and zinc oxide (ZnO). All assays were performed in triplicate, and the experiments were replicated three times.

Screening for phytohormone production

The production of phytohormone, Indole acetic acid (IAA) by the isolate was quantitatively determined using a colorimetric assay (Patten and Glick, 1996). An agar plug (5 mm diameter) taken from a 10 days old culture of the fungus grown on potato dextrose agar (PDA) medium was inoculated with 20 mL of Potato Dextrose Broth (PDB) supplemented with 0.1 % L-tryptophan (w/v) and incubated for 72 hours at 28 ± 2° C. The cultures were centrifuged at 10,000 g for 5 min. 1 ml of supernatant, in triplicate, was mixed with 2 mL of Salkowski reagent (Gordon and Weber, 1951) and incubated in the dark for 30 min. As a control, PDB without L-tryptophan was used. The production of IAA was indicated by the development of a pink red colour in the medium. The amount of IAA released was estimated from a standard graph prepared using known amounts of pure IAA, and the colour intensity at 530 nm was measured in a UV–vis spectrophotometer (Shimadzu).

Production of siderophores

Siderophore production was screened by CAS plate assay method (Schwyn and Neilands, 1987) by inoculating the cultures on PDA supplemented with 3.02% PIPES and chrome azurol S (CAS) dye. The inoculated culture plates were incubated for 10 days at 28 ± 2°C. The positive results were identified by clear orange halo zones developed around the culture and expressed as activity units (AU). The AU can be found out by the equation, Activity unit (AU) = Diameter of reaction zone ÷ Diameter of colony.

Production of ammonia (NH_3)

Ammonia (NH_3) production was screened by inoculating the 10-day-old culture of the isolate into 5 ml yeast peptone dextrose (YPD) broth and incubated on a rotary shaker at 28 ± 2 °C for 5 days. Adding Nessler's reagent to the fungus revealed its ability to generate NH_3. A positive result for ammonia production was suggested by the formation of a yellow to brown colour (Cappucino and Sherman, 1992).

Phosphate and zinc solubilization

Pikovskaya's agar medium containing tricalcium phosphate was used to monitor the fungus's ability to solubilize phosphate. Zn solubilization activity of the fungus was assayed on mineral salts agar medium supplemented with 0.1% of insoluble ZnO. Agar plugs (5 mm diameter) were inoculated in the centre of the plate and incubated at a temperature of 28 ± 2° C for 10 days after being collected from 10 days old culture of *P. chlamydosporia* isolate. The positive results were identified by the clear halo zones developed around the fungal culture. The phosphate, potassium and ZnO solubilization index (SI) was calculated by the equation, Solubilization Index (SI) = Colony diameter + Halozone diameter ÷ Colony diameter (Pande et al., 2017).

Screening for extracellular enzyme production

The capability of *P.chlamydosporia* to produce extracellular enzymes such as α-amylases was determined by inoculating the culture onto the surface of starch agar (Dinesh et al., 2015). The ability of the isolate to produce these enzymes was determined by the development of a clear zone around the colony. For determining pectinase production, the media was prepared by adding 1% pectin in PDA and inoculating the mycelial disc on the surface of the media, then incubated for 10 days. Gram's iodine solution was poured in the pectin agar, and a zone of clearance was observed against a dark background (Sudeep et al., 2020). The mycelial disc (5 mm diameter) was inoculated on the surface of PDA supplemented with 1% carboxymethyl cellulose (CMC) and incubated at 28 ± 2 °C to assess the cellulolytic activity of the fungus. After 10 days of incubation, 0.01% Congo red solution was poured on the medium for 15 min and the plates were destained using 1% NaCl

solution for 5 min. The capacity of the fungus to produce cellulase was shown by a clear zone against a red background (Dinesh et al., 2015).

3.2.3 *Development of a modified semi-selective medium for the isolation and quantification of P. chlamydosporia*

In order to do this, the compatibility of *P. chlamydosporia* with various concentrations of five distinct pesticides: metalaxyl, metalaxyl-mancozeb, carbendazim, copper oxychloride, and chlorpyrifos, was investigated. The quantity of viable fungal propagules in several substrates (rice, farmyard manure, maize, rice bran, barley, and sorghum) and soil infected with *P. chlamydosporia* was counted in order to assess the medium.

In vitro compatibility of P. chlamydosporia with pesticides

The compatibility of five pesticides with *P. chlamydosporia* was tested using the poisoned food technique (Bruin et al., 1981) at the recommended dose, two lower doses, and two higher doses as listed in Table 3.1. The pesticides are carbendazim (Bavistin 50% WP), metalaxyl-mancozeb (Master 72% WP), metalaxyl (Metalaxyl 35% WP), copper oxychloride (Blitox 50% WP), and chlorpyrifos (Anth 50% EC). A stock solution of each pesticide was made by mixing the necessary amount of the chemical with sterile distilled water, then adding the mixture to melted PDA in Erlenmeyer flasks individually. The poisoned medium was placed into sterile petri dishes with 9 cm diameters and allowed to cool. Five-millimetre diameter mycelial discs, extracted from the periphery of the *P. chlamydosporia* colony, were positioned at the center of each petri dish and cultured for ten days at 28°C ± 2°C. The control was provided by non-poisoned media in petri dishes. There were three replicates of every treatment. The radial growth of the colonies was evaluated for each treatment, and the formula I = (C-T)/C x 100 was used to calculate the percentage growth inhibition where, I stand for percentage growth inhibition, C for radial growth in the control (mm), and T for radial growth in the treated plates (mm). Values were statistically analyzed to determine the pesticide concentration tolerance limit for the fungus.

Table 3.1: Pesticides and doses for *in vitro* compatibility experiments with *P. chlamydosporia*

Pesticide	Concentrations tested (ppm)				
	1/4x	**1/2x**	**x**	**2x**	**4x**
Metalaxyl	250	500	1000	2000	4000
Carbendazim	250	500	1000	2000	4000
Metalaxyl - mancozeb	312.5	625	1250	2500	5000
Copper oxychloride	500	1000	2000	4000	8000
Chlorpyrifos	750	1500	3000	6000	12000

Isolation and quantification of P. chlamydosporia from soil and various solid substrates

Using the leads from the *in vitro* compatibility of *P. chlamydosporia* with pesticides, we modified the semi-selective medium (Kerry et al., 1993) of *P. chlamydosporia.* The semi-selective medium was modified in the present investigation with the following composition: 17 g corn meal agar, 17.5 g NaCl, 75 mg Rose Bengal, 50 mg metalaxyl and carbendazim, 3 mL Triton X-100, and 50 mg each of rifampicin, streptomycin sulphate, and chloramphenicol per liter.

Sorghum, rice, barley, rice bran, maize, farmyard manure, and soil artificially inoculated with *P. chlamydosporia* were among the solid substrates used to study the effectiveness of the modified semi-selective medium. This was accomplished by soaking 40 g of sorghum, rice, barley, rice bran, and maize individually in distilled water for one to two hours. After rinsing the soaked grains with distilled water, the substrates were autoclaved at 15 psi for 20 minutes. To inoculate the solid substrates, a *P. chlamydosporia* liquid inoculum was prepared by inoculating PDB in Erlenmeyer flasks with 5 mm mycelial discs taken from the margins of the colony (5 discs in 250 ml^{-1} medium). The flasks were incubated in an incubator shaker at a temperature of 28 ± 2°C and 180 rpm for 10 days. Each flask containing the solid substrates was sterilised, and then 10 ml of the liquid fungal inoculum were added. To achieve homogeneous fungal growth, the inoculation flasks were shaken regularly. The

experiment was performed three times to verify the findings, and the tests were run in triplicate. Fourteen days following inoculation, *P. chlamydosporia* was measured on several solid substrates and soil. The dilution-plate method was used to assess the modified semi-selective media. In terms of CFU g^{-1} of the substrate, the colonies were enumerated and counted.

3.2.4 *In planta evaluation of P. chlamydosporia for growth promotion in black pepper plants*

Pot experiments were carried out to determine the plant growth promoting potential of *P. chamydosporia* under greenhouse conditions. The experiments were carried out using one-month old black pepper rooted cuttings (variety Sreekara). *P. chlamydosporia* was multiplied on rice as the substrate (10^8 CFU/g) and used invariably as the inoculum.

Fig 3.1: Black pepper rooted cuttings (variety Sreekara) inoculated with *P. chlamydosporia*

T_0: Uninoculated sterile soil, T_1: Sterile soil inoculated with 1g*, T_2: Sterile soil inoculated with 3g, T_3: Sterile soil inoculated with 5g, T_4: Uninoculated nonsterile soil, T_5: Non sterile soil inoculated with 1g, T_6: Non sterile soil inoculated with 3g, T_7: Non sterile soil inoculated with 5g, T_8: Uninoculated vermiculite + farmyard manure, T_9: Vermiculite + farmyard manure inoculated with 1g, T_{10}: Vermiculite +

farmyard manure inoculated with 3g, T_{11}: Vermiculite + farmyard manure inoculated with 5g. * *P. chlamydosporia* (10^8 CFU/g) mass multiplied on rice grains.

Effect of different dosages of P. chlamydosporia on the growth of black pepper

The experiment consisted of 12 treatments with six replications. The potting media used were sterilized soil, non-sterilized soil and vermiculite + farmyard manure. The experiments were carried out using one-month old black pepper rooted cuttings (variety Sreekara) in 1 kg pots of size 13 cm x 8 cm x 12 cm (Fig. 3.1). The *P. chlamydosporia* multiplied on rice substrate was used as the inoculum and the dosages evaluated were 0, 1, 3 and 5 g/plant. All of the treatments were applied to the potting media after 15 days of planting and were replicated six times. Plants that did not receive any inoculum of *P. chlamydosporia* served as control. The plants were irrigated daily and maintained in a greenhouse with temperature ranging from 25 to 32°C, relative humidity 70–80%. After six months, the plants were uprooted, washed thoroughly and growth parameters such as shoot length, root length, shoot and root dry weight (oven-dried at 65-70°C), number of nodes, number of leaves and number of roots were recorded. Also, isolated and quantified the *P. chlamydosporia* from *in planta* studies. For this samples of soil were taken six months after the inoculation, serially diluted, plated in modified semi-selective medium, and then cultured for ten days at 28 ± 2°C and 70–80% relative humidity. Colonies on plates that had been serially diluted were enumerated and represented as CFU mL^{-1}. Nutrient analysis of potting media and plants were observed after 6 months of planting.

Nutrient analysis of potting media: After six months of planting, samples of potting media were collected from pots, cleaned of plant debris, and put into polythene bags. The soil samples were taken to the lab, where they were placed under refrigeration for additional analysis after being passed through a 2.0 mm pore size sieve. The nutrient parameters such as phosphorus, potassium, calcium, magnesium, copper, manganese, iron and zinc were analysed.

Phosphorus determination using the Bray-1 method: A 5 g sample was taken and placed in a 100 mL shaking bottle. The material was mixed with roughly 50 mL of Bray-1 reagent. After adding a little amount of activated charcoal free of phosphorus

and filtering using Whatman 2 filter paper, shake for 30 minutes at 180 oscillations. 3 mL of an aliquot were transferred to a 10 mL test tube, to which 2 mL of colouring reagent were added. Distilled water was then used to make the volume equal. After allowing it to stand for ten minutes to develop colour, a spectrophotometer was used to measure the percentage transmittance or absorbance at 882 nm (Olsen and Sommers, 1982). For around two hours, the colour remained consistent.

$$\text{Soil phosphorus (ppm)} = (50/5)\ (10/3) * X$$

Where, X= concentration (ppm) obtained from the spectrophotometer.

Determination of calcium (Ca), magnesium (Mg), and potassium (K): Five g of the air-dried (2 mm) sample were weighed out into a 100 ml extraction container. 50 ml of the extracting reagent was then added, and the shaker was shaken for 30 minutes at 180 oscillations per minute. Following the shaking process, the filtrate was collected and the solution was filtered. 2 ml of a 12500 ppm $SrCl_2$ solution was added to the filtrate in order to determine the Ca and Mg levels. These solutions were also used to prepare the standards (Helmke and Sparks, 1996; Suarez, 1996). An atomic absorption spectrophotometer (AAS) (Model: Varian AA240FS) was used to determine the exchangeable K, Ca, and Mg in the filtrate.

Reagents used:

Extraction reagent (1 N ammonium acetate, pH 7.0 adjusted): 570 ml of glacial acetic acid (99.5%) were diluted with purified water to make about 5000 ml. After that, add 690 ml of concentrated ammonium hydroxide to the solution kept in a fume hood and stir well. Added acetic acid to bring the pH of the solution to 7.0. The solution was diluted with distilled water to a final volume of 10,000 ml. Ammonium acetate (771 g) was alternatively dissolved in around 9000 ml of clean water. After completely mixing the solution with 3 N ammonium hydroxide, the pH was adjusted to 7.0. Lastly, distilled water was used to dilute the solution to a volume of 10,000 ml.

Determination of Iron (Fe), Manganese (Mn), Copper (Cu), and Zinc (Zn): Zn, Fe, Mn, or Cu were estimated using the DTPA test. The extractant had a pH of 7.3 and was made up of 0.0l M $CaCl_2$, 0.1 M triethanolamine, and 0.005 M DTPA. Ten grams

of air-dried sample material was shaken with 20 ml of extractant for two hours. After filtering the leachate, atomic absorption spectrophotometry was used to detect the amounts of Zn, Fe, Mn, and Cu in the filtrate (Lindsay and Norvell, 1978).

Nutrient analysis of plant samples: Plant samples were taken six months after planting, and they were cleaned using running tap water, 0.1% detergent solution, 0.1N HCl, single distilled water and double distilled water. The sample was cleaned, any remaining water was blotted off the surface with blotting paper, and then it was labelled and placed in a paper cover. Next, the sample was dried for 48 hours or until a consistent weight was achieved in a hot air oven set between 60 and 70^0C. Once the samples have dried, they are crushed in a metal-free mixie or grinding mill and placed in polythene bags for digestion. The nutrient parameters such as nitrogen, phosphorus, potassium, calcium, magnesium, copper, manganese, iron and zinc were analysed.

Mineral nitrogen (N) determination using the steam distillation method:

Digestion: The prepared, finely ground sample (0.5g) should be weighed before being transferred to a 250ml Kjeldahl digestion tube. Mix in 2 or 3g of the digestion mixture with roughly 10 ml of concentrated H_2SO_4 and let it sit overnight. In order to obtain a transparent or bluish green substrate, the tubes are next heated to 410 degrees Celsius for 1.5 to 2 hours in a digesting block (Keeney, 1982). The tubes are removed from the digestion block and given time to cool after the digestion is complete.

Distillation: Place the residue-filled flask into the Kjeldahl distillation apparatus and set the timer for four to five minutes to pass steam, dilute, and neutralize. Gather the distillate in a 250 ml conical flask with a 25 ml boric acid-double indicator solution. Put 10 ml of an aliquot and 10 ml of 40% NaOH into the Kjeldahl distillation unit. Then, distill. Gather the distillate and place it in a 100 ml conical flask with 10 ml of boric acid solution. Titrate the distillate using an automatic burette to obtain the original color of the boric acid mixed indicator solution by comparing it to standard 0.1N H_2SO_4. Take note of the titrate value of sample (X).

Calculation:

$$1 \text{ ml } 0.1 \text{ N } H_2SO_4 = 0.0014 \text{ g N} = 1.4 \text{ mg N};$$

Therefore, X ml 0.1 N H_2SO_4= 1.4 * X mg N, where X is the titre value.

Phosphorus determination using the Vanado molybdate method: 5 ml of diacid extract of plant sample (digested sample) was transferred into a 25 ml volumetric flask. This was made up to the mark after adding 5 ml of the vanadomolybdate reagent and 10 ml of water. Using a blue filter, the reading was taken at 470 nm in the spectrophotometer. To obtain the concentration of 0.4, 0.8, 1.2, 1.6, 2.0, and 2.4 ppm phosphorus solution, the blank and standard were developed using 1, 2, 3, 4, 5, and 6ml aliquot of 10 ppm standard "P" solution. From the standard graph, the concentration of phosphorus was analysed. (Peachey et al., 1973)

Calculation:

From graph find the concentration of sample in ppm (X)

$$P\ (\%) = (100 \times 25 \times X)/ (W \times 5 \times 10000)$$

$$= (0.05 \times X)/W, \text{ where W is weight of sample digested}$$

Determination of calcium (Ca), magnesium (Mg), and potassium (K)

In a 50 ml volumetric flask, 1 ml of the diacid digested sample was diluted. Utilizing a standard solution of 1, 2, 3, 4, and 8 ppm, K and Ca were calculated in a flame photometer or AAS. Similar to that, magnesium was also found in AAS using the previously mentioned solution and standard solutions of 0.5, 1,2, 4, and 6 ppm (Sparks et al., 2020).

Calculation:

Concentration of Ca, Mg and K elements in plant tissue (%) = $(100 \times 50 \times X)/ (W \times 1 \times 10^4)$

Where X is the AAS reading in ppm and W is the weight of the sample.

Determination of iron (Fe), manganese (Mn), copper (Cu), and zinc (Zn)

Utilizing appropriate lamps and standards, a clear solution of the diacid digested plant samples was fed straight into the AAS (Sparks et al., 2020).

Calculation:

Concentration of Fe, Mn, Cu and Zn elements in plant tissue (ppm) = (X x 100)/ W, where X is the AAS reading in ppm and W is the weight of the sample.

Standardisation of higher doses of P. chalmydosporia and frequency of application

The experiment consisted of 24 treatments with four different dosages of inoculum (0, 5 g, 10 g and 15 g) at three different frequencies like single, double and triple applications (Fig. 3.2) with one month interval and 9 replications per treatment. The black pepper rooted cuttings planted in sterilized and unsterilized soil were used as the experimental plants. The treatments were imposed in the soil after 15 days of planting and subsequent applications were made after a one month-interval. Plants without any inoculation with *P. chlamydosporia* served as control plants. The plants were maintained in a greenhouse (temperature 25 to 32°C, relative humidity 70–80%) with daily irrigation and care. After six months, they were uprooted, washed and their growth parameters were recorded as mentioned earlier.

Fig 3.2: Black pepper rooted cuttings (variety Sreekara) inoculated with *P. chlamydosporia* for standardising doses and frequency of application.

T_1: Uninoculated sterile soil, T_2: Sterile soil inoculated with 5 g*; Frequency of application - one time, T_3: Sterile soil inoculated with 5 g ; Frequency - 2 times, T_4: Sterile soil inoculated with 5 g, ; Frequency - 3 times, T_5: Uninoculated sterile soil, T_6:

Sterile soil inoculated with 10 g ; Frequency - one time, T_7: Sterile soil inoculated with 10 g ; Frequency - 2 times, T_8: Sterile soil inoculated with 10 g; Frequency - 3 times , T_9: Uninoculated sterile soil, T_{10} : Sterile soil inoculated with 15 g ; Frequency - one time, T_{11}: Sterile soil inoculated with 15 g ; Frequency - 2 times, T_{12}: Sterile soil inoculated with 15 g ; Frequency - 3 times, T_{13}: Uninoculated non-sterile soil, T_{14}: Non-sterile soil inoculated with 5 g; Frequency - one time, T_{15} : Non-sterile soil inoculated with 5 g; Frequency - 2 times, T_{16} : Non-sterile soil inoculated with 5 g; Frequency - 3 times, T_{17}: Uninoculated non-sterile soil, T_{18}: Non-sterile soil inoculated with 10 g; Frequency - one time, T_{19}: Non sterile soil inoculated with 10 g; Frequency - 2 times, T_{20}: Non-sterile soil inoculated with 10 g; Frequency - 3 times, T_{21}: Uninoculated non-sterile soil, T_{22}: Non sterile soil inoculated with 15 g; Frequency - one time, T_{23}: Non-sterile soil inoculated with 15 g; Frequency - 2 times, T_{24}: Non-sterile soil inoculated with 15 g; Frequency - 3 times,* *P. chlamydosporia* (10^8 CFU/g) mass multiplied on rice grains.

3.2.5 *Evaluation of root colonization by P. chlamydosporia in black pepper*

Pot experiments were conducted with black pepper plants to analyse the root colonization of *P. chlamydosporia* under greenhouse conditions. For this, one-month old, healthy black pepper (variety Sreekara) rooted cuttings were planted in 1 kg pots of size 13 cm x 8 cm x 12 cm containing sterilized soil. The plants were held in a greenhouse with temperatures ranging from 28 - 30ºC with 70-80% humidity. The *P. chlamydosporia* inoculated rice substrates were used as the inoculum. Each plant received 5 g of *P. chlamydosporia* multiplied on rice as the initial inoculum. Plants that did not receive any *P. chlamydosporia* served as the control. Three plants each were taken at intervals of 3, 7, 14, 21 & 28 days after inoculation for studying the extent of colonisation.

Colonization study using microscopy

For assessing the colonization of *P. chlamydosporia* in black pepper plants bright field microscopy was used. For this, the root tissues were hand sectioned with a razor blade and stained in 0.5% Rose Bengal dissolved in 5% aqueous ethyl alcohol (w/v) solution and mounted on glass microscope slides (Jackson et al., 1988). The samples were examined using a Leica DM5000B microscope.

Estimation by dilution plating

Rhizoplane population of *P. chlamydosporia* was evaluated by agitating one gram of root tissue in 100 ml of phosphate-buffered saline (PBS) at 200 rpm for 30 min to release the rhizoplane organisms. The suspension containing the fungal population was serially diluted up to 10^{-6}. One ml of serially diluted sample was poured in modified semi-selective media and incubated at 28 ± 2° C for 10 days. After incubation, colonies were counted and expressed as CFU/g of fresh tissue.

Similarly, the endophytic population of *P. chlamydosporia* in black pepper roots was estimated through dilution plating. For this, one gram each root was taken from each sample and surface sterilized using 0.5% sodium hypochlorite for 5 min, 70% alcohol for 1 min followed by rinsing thoroughly with sterile distilled water for 2-3 times. Sterility checks were carried out for each sample to monitor the efficiency of the surface sterilization procedure. For this, 0.1 mL of the last wash was spread onto a modified semi-selective medium and incubated at 28 ± 2° C for 10 days. The tissue samples (1 g) were ground aseptically with 2 mL of PBS using a pre-cooled sterile mortar and pestle (Aravind et al., 2009). The extracts were serially diluted and pour plated on modified semi-selective media.

Quantification using real time PCR

The surface sterilized roots (1-1.5 g) were used for DNA extraction using CTAB buffer (Maciá-Vicente et al., 2009b). The DNA was extracted with a 25:24:1 mixture of phenol, chloroform, and isoamyl alcohol, then further extracted with a mixture of 24:1 chloroform: isoamyl alcohol and then precipitated with isopropanol. The precipitated DNA pellets were washed two times with 70% ethanol, allowed to air-dry and resuspended in nuclease free water. Further DNA was quantified in a Bio-Photometer (Eppendorf, Germany) and stored at -20^0C. *P. chlamydosporia* specific primers, designed based on the *vcp1* (alkaline serine protease p1) gene to yield 136-bp amplicons were used for the study (Maciá-Vicente et al., 2009b). In this study, primer sequences FP: 5'- CGTTTCCCAGGACTACAAGA -3' and RP: 5'-CGGCAACTGAGAGGAAGA -3' were used. The specificity of primers was checked using DNA of different fungal species such as *P. chlamydosporia*, *Trichoderma, Fusarium, Pythium* and *Phytophthora.* The real-time PCR assays were run using QuantiFast SYBER green mastermix (12.5 µL) in a final volume of 25 µl containing

1 µL template DNA and 0.5 µM forward and reverse primers in a Rotor-Gene Q Real-time PCR system (Qiagen, Germany). Each reaction was duplicated three times. The following were the thermal cycling conditions: an initial denaturation step at 94°C for 5 min, 40 cycles of denaturation at 94°C for 30 s, annealing at 59°C for 30 s, and extension at 72°C for 20 s. Real time PCR runs were analysed using Ct values obtained. For determining the sensitivity of primers, 2.5fold-serial dilutions of *P. chlamydosporia* DNA were used. Real time reactions were carried out using different DNA concentrations ranging from 20 ng to 10 pg per reaction. The real-time PCR runs were analysed; the obtained Ct values were plotted against serial dilutions of template DNA to create a standard curve. The quantification of real-time PCR assays was carried out using the total DNA isolated from the treated black pepper plants using the same protocol described above. Ct values obtained were interpolated in the standard curve to calculate the *P. chlamydosporia* concentration with respect to the total.

3.2.6 *Statistical analysis*

All data are expressed as mean ± standard error (SE). SAS software version 9.3 (SAS Institute Inc., Cary NC) was used for data analysis, including PROC ANOVA and PROC mixed procedures of split plot design. Means were separated using Fisher's least significant difference (LSD) test ($p \leq 0.05$).

3.3 Results

3.3.1 *Plant growth promoting traits of P. chlamydosporia*

The *in vitro* analysis revealed the multifaceted plant growth-promoting capabilities of *P. chlamydosporia*. The ability of the fungus to solubilize phosphate and zinc was found by the formation of clear zones around the fungal colony (Fig. 3.3 a & b). The phosphate and zinc solubilization indices were 1.3 ± 0.07 and 1.1 ± 0.01, respectively, suggesting the potential of the fungus to significantly impact plant nutrient uptake efficiency (Table 3.2).

Further emphasizing its role in plant growth promotion, *P. chlamydosporia* produced 9.8 ± 0.36 µg/ml of IAA in the liquid culture supplemented with 0.1% L-tryptophan (Table 3.2). The standard graph of IAA was represented in Fig. 3.4. The IAA production was calculated from the regression equation of the standard curve. The

medium turning pink red on adding Salkowski reagent indicates the successful synthesis of IAA, a key phytohormone that regulates various aspects of plant growth and development.

Siderophore production, quantified at 2 ± 0.04 activity units (AU) evidenced by an orange halo zone around the colony (Fig. 3.3c). This result highlights *P. chlamydosporia's* potential to enhance plant iron uptake, as siderophores chelate iron from the soil, making it more available to plants. This is particularly beneficial in iron-deficient soils, improving plant health and growth.

The production of ammonia, another plant growth-promoting trait, was confirmed through the appearance of brown colour in the yeast peptone dextrose (YPD) medium following the addition of Nessler's reagent (Fig. 3.3d). Ammonia production by *P. chlamydosporia* suggests its role in nitrogen cycling within the soil, providing an additional nitrogen source for plant uptake.

Enzymatic activity, crucial for breaking down complex organic materials in the soil, making nutrients more accessible to plants, was also observed. The ability of *P. chlamydosporia* to produce α -amylase was demonstrated by a clear zone on starch media (Fig. 3.3e), indicating its role in starch breakdown. Pectinase activity, essential for the hydrolysis of pectin, a major component of plant cell wall was evidenced by clear zones in pectin containing media after application of Gram's iodine (Fig 3.3f). This activity may facilitate plant residue decomposition, contributing to a healthier soil environment. Furthermore, the fungus's cellulolytic activity, involved in cellulose breakdown, was indicated clear zone formation around the colony after staining with 0.01% Congo red and destaining with 1% Nacl solution (Fig 3.3g), underscoring its contribution to the cycling of organic matter in the soil.

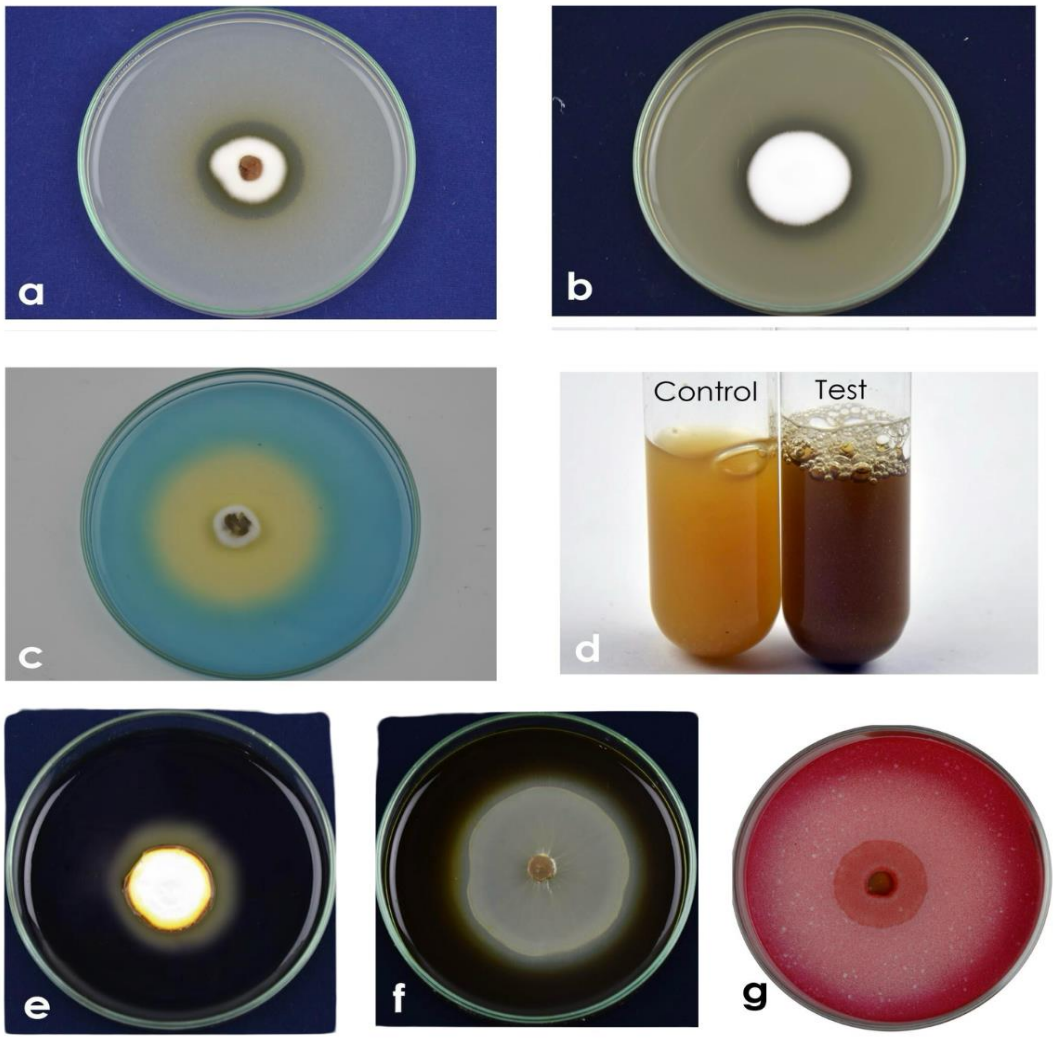

Fig. 3.3: Plant growth promoting traits of the nematode antaonistic *Pochonia chlamydosporia.* (a) Zinc solubilizing efficiency on mineral salts agar medium supplemented with 0.1% of insoluble ZnO (b) Phosphate-solubilizing activity on Pikovskaya's agar medium (c) Siderophore production (d) Ammonia production in YPD both (e) α-amylase activity (f) Pectinase production (g) Cellulase activity by formation of clear zones around the fungal colony.

Table 3.2: *In vitro* plant growth promoting (PGP) traits of *P. chlamydosporia*.

PGP trait	Response units[a]
Phosphate Solubilization Index (SI)	1.3 ± 0.07
Zinc Solubilization Index (SI)	1.1 ± 0.01
Indole acetic acid production (µg/mL)	9.8 ± 0.36
Siderophore production (AU)	2 ± 0.04
Ammonia production	+
α-Amylase activity	+
Cellulase activity	+
Pectinase activity	+

'+' = positive result. [a] Values are means of three replications ± standard error (SE).

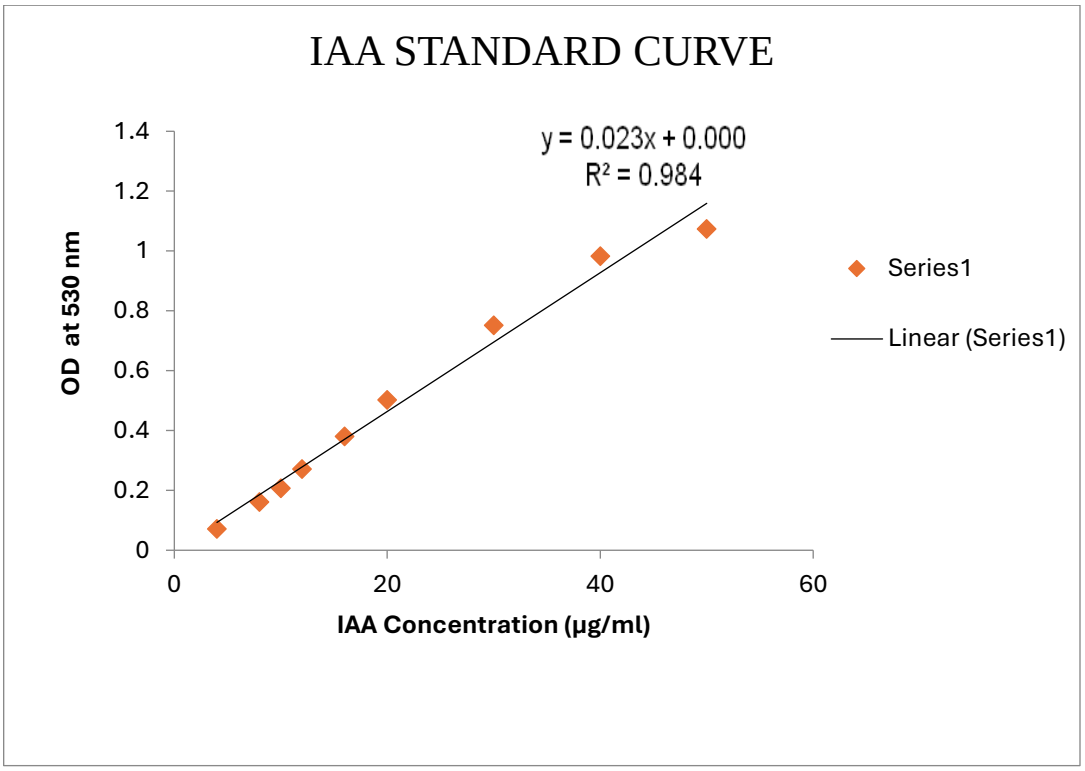

Fig. 3.4 Standard curve of indole-3-acetic acid (IAA) used to quantify IAA production by *P. chlamydosporia*. The regression equation derived from the curve was utilized to calculate the IAA concentration in the culture medium.

3.3.2 *Development of a modified semi-selective medium*

In the pursuit of developing a modified semi-selective medium for the isolation and quantification of *P. chlamydosporia*, *in vitro* compatibility studies were conducted with five pesticides *viz*., copper oxychloride, carbendazim, metalaxyl, metalaxyl-mancozeb, and chlorpyrifos. The study revealed a distinct tolerance of *P. chlamydosporia* to higher concentrations of metalaxyl (0.4%) and carbendazim compared to other pesticides with effective dose concentrations (ED50s) identified at 2.36% for metalaxyl and 1.32% for carbendazim (Table 3.3). This tolerance was visually documented through mycelial growth patterns in Figures 3.5 (metalaxyl) and 3.6 (carbendazim). Conversely, concentrations exceeding 2000 ppm of copper oxychloride, the combination product of metalaxyl-mancozeb, and chlorpyrifos inhibited fungal growth.

Table 3.3: Compatibility of *P. chlamydosporia* with different pesticides

Pesticides	Concentration (ppm)	Percentage growth inhibition (I) (%)*	ED50 (%)
Metalaxyl	250	4.76 ± 0.017^{d}	2.36
	500	9.52 ± 0.011^{c}	
	1000	9.52 ± 0.029^{c}	
	2000	19.04 ± 0.023^{b}	
	4000	23.80 ± 0.005^{a}	
Carbendazim	250	33.3 ± 0.034^{b}	1.32
	500	33.3 ± 0.040^{b}	
	1000	42.85 ± 0.023^{a}	
	2000	42.85 ± 0.017^{a}	
	4000	42.85 ± 0.028^{a}	
Metalaxyl - Mancozeb	312.5	42.85 ± 0.046^{c}	0.06
	625	42.85 ± 0.080^{c}	
	1250	52.38 ± 0.046^{b}	
	2500	100 ± 0^{a}	
	5000	100 ± 0^{a}	

Pesticides	Concentration (ppm)	Percentage growth inhibition (I) (%)*	ED50 (%)
Copper oxychloride	500	33.3 ± 0.069[b]	0.05
	1000	33.3 ± 0.086[b]	
	2000	100 ± 0[a]	
	4000	100 ± 0[a]	
	8000	100 ± 0[a]	
Chlorpyrifos	750	42.8 ± 0.057[c]	0.11
	1500	47.6 ± 0.029[b]	
	3000	100 ± 0[a]	
	6000	100 ± 0[a]	
	12000	100 ± 0[a]	

* Values are means of three replicates ± standard error (SE). I = C - T/C x 100 where, I = Percentage growth inhibition; C = Radial growth in control (mm); T = Radial growth in treated plates (mm), ED50 (Effective dose). Data points with the same letter indicate no significant difference according to Fisher's test at 0.05% confidence level.

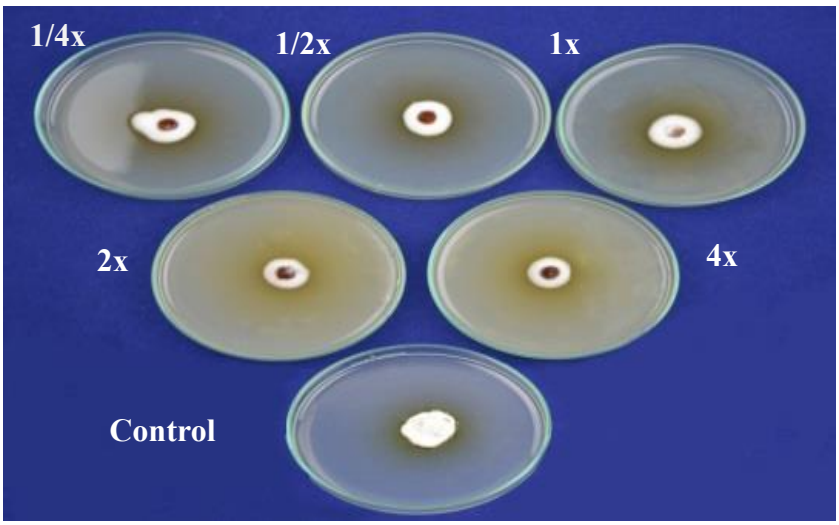

Fig 3.5: *In vitro* evaluation of different concentrations of metalaxyl on mycelial growth of *P. chlamydosporia* (1/4x- 250 ppm, 1/2x-500 ppm, 1x-1000 ppm, 2x- 2000 ppm, 4x- 4000 ppm)

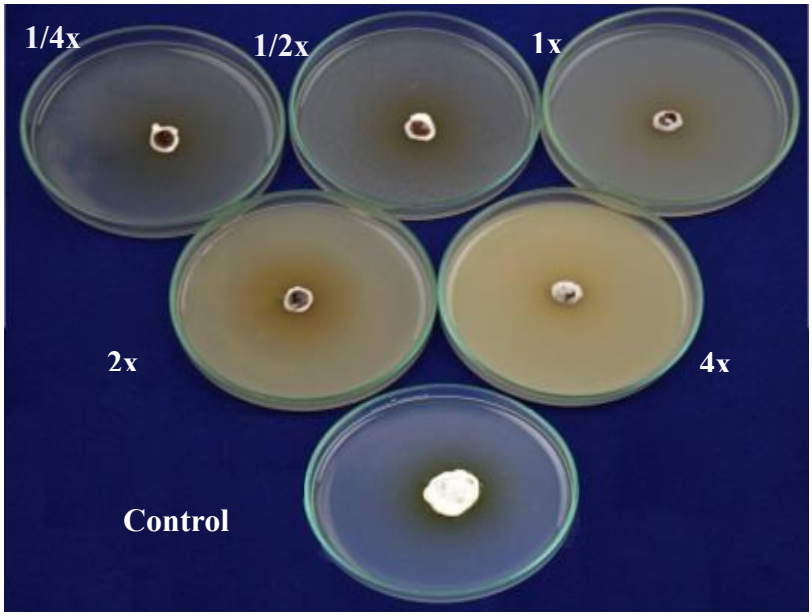

Fig 3.6: *In vitro* evaluation of different concentrations of carbendazim on mycelial growth of *Pochonia chlamydosporia* (1/4x- 250 ppm, 1/2x-500 ppm, 1x-1000 ppm, 2x- 2000 ppm, 4x- 4000 ppm).

Based on these findings, metalaxyl and carbendazim were selected to refine Kerry's semi-selective medium, leading to the creation of a modified medium outlined earlier in the materials and methods. The novel medium incorporates fungicides and antibiotics capable of suppressing non-target fungi and bacteria, respectively. Additions like NaCl and Triton X-100 slowed down colony formation, while Rose Bengal was effective in inhibiting bacterial growth. This strategic formulation allowed for easier identification and enumeration of *P. chlamydosporia* colonies, due to the application of fungicides metalaxyl and carbendazim to prevent the fast-growing fungi like *Pythium* and *Fusarium* species. The colonies of *P. chlamydosporia* appeared as reddish-yellow on the modified medium. To verify the identity of the colonies, those cultivated on the semi-selective media were recultivated on potato dextrose agar, exhibiting the morphological characteristics unique to *P. chlamydosporia* used in this study. This modified medium demonstrated its utility across various solid substrates (sorghum, rice, barley, rice bran, maize, and farmyard manure) and soil, with rice grains showing the highest CFU g^{-1}, indicating a significantly larger *P. chlamydosporia* population (Fig. 3.7a & 3.7b)

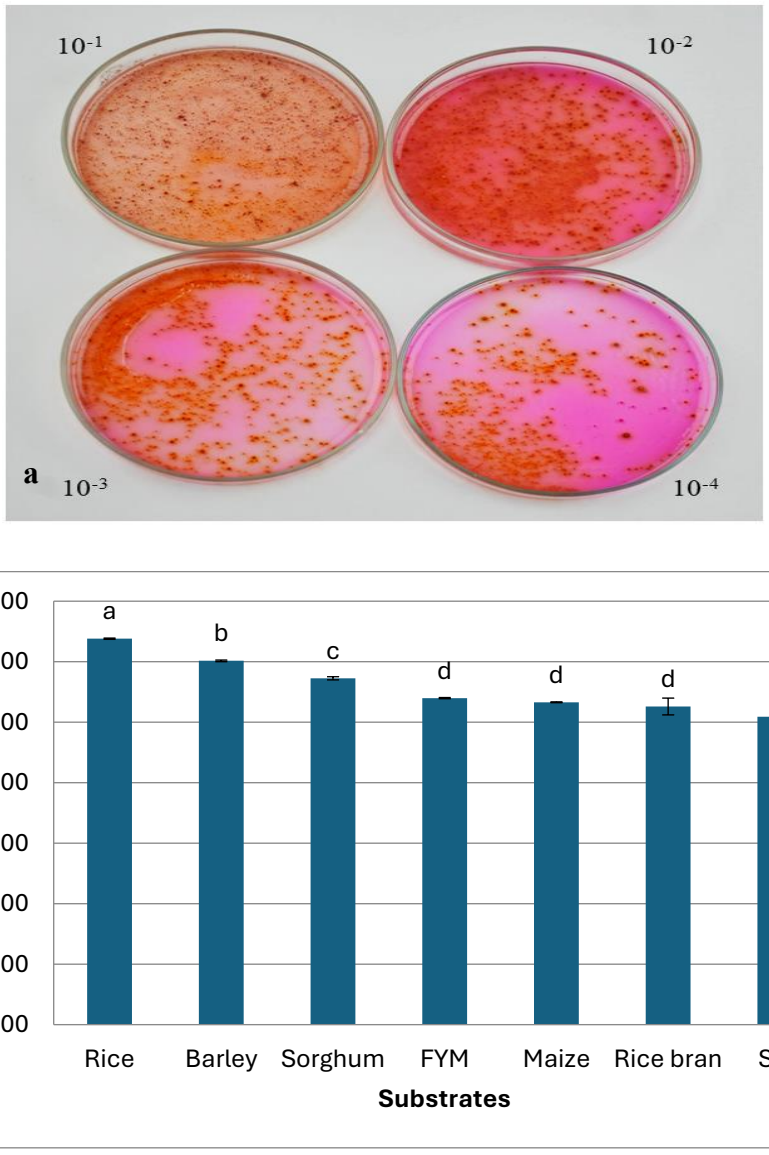

Fig. 3.7 Enumeration of *P. chlamydosporia* mass multiplied on various solid substrates using the modified semi-selective medium. **a**. *P. chlamydosporia* colonies in modified semi-selective medium after serial dilution from rice substrate. **b**. Quantification of *P. chlamydosporia* on different solid substrates and soil after 10 days of post-inoculation.

3.3.3 *In planta evaluation of P. chamydosporia for growth promotion in black pepper plants*

In pot culture experiments, the application of *P. chlamydosporia* at the root zone of black pepper cuttings significantly increased shoot and root lengths, biomass, the number of secondary roots, and leaves compared to untreated control plants. Notably,

growth promotion effects were more prominent in sterilized soil than in non- sterilized soil or a vermiculite + farmyard manure mixture (Table 3.4). Across all potting media, the maximum growth promotion was observed with 5 g application of *Pochonia*, especially in sterile soil.

In this study we isolated and quantified the *P. chlamydosporia* from the *in-planta* studies. Further application of the semi-selective medium to quantify *P. chlamydosporia* growth in soil samples inoculated with varying fungus doses showcased its effectiveness. Six-month post-inoculation, the potting media treated with different doses of the fungus exhibited a larger population, with the highest prevalence observed in sterile soil treated with 5 g of inoculum (Fig. 3.8). Semi-selective medium proved instrumental in estimating *P. chlamydosporia* populations in non-sterile soil samples without succumbing to fungal or bacterial contamination, thus marking a significant advancement in the selective enumeration of this beneficial fungus.

Table 3.4: Growth promoting effects of different dosages of *P. chlamydosporia* on black pepper rooted cuttings planted in different potting media

Potting medium	**Sterilized soil**					**Non-sterilized soil**					**Vermiculite + Farmyard manure**					**Subplot Mean**			
***Pochonia* dosage (g/plant)**	**0**	**1**	**3**	**5**	**MP mean**	**0**	**1**	**3**	**5**	**MP mean**	**0**	**1**	**3**	**5**	**MP mean**	**0**	**1**	**3**	**5**
Shoot length (cm)	51.7	148.3	160.0	195.3	138.8^{A}	41.7	108.3	130.0	136.7	104.2^{B}	91.3	133.3	151.7	166.7	135.6^{A}	61.6^{D}	130.0^{C}	147.2^{B}	166.2^{A}
Root length (cm)	8.3	18.7	23.7	29.7	20.1^{A}	4.7	10.7	15.3	19.7	12.6^{B}	8.7	15.7	21.0	24.0	17.3^{A}	7.2^{D}	15.0^{C}	20.0^{B}	24.4^{A}
Shoot dry weight (g)	2.0	5.1	5.5	6.6	4.8^{A}	1.4	4.0	4.5	5.0	3.7^{C}	1.5	4.9	5.3	5.6	4.3^{B}	1.6^{D}	4.6^{C}	5.1^{B}	5.8^{A}
Root dry weight (g)	0.2	0.7	0.7	1.3	0.7^{A}	0.1	0.4	0.5	0.7	0.4^{C}	0.5	0.7	0.7	0.7	0.6^{B}	0.3^{D}	0.5^{C}	0.6^{B}	0.9^{A}
No of roots	8.0	13.0	18.3	19.0	14.6^{A}	5.0	10.7	12.3	14.3	10.6^{B}	6.0	11.7	13.0	16.7	11.8^{B}	6.3^{D}	11.8^{C}	14.6^{B}	16.7^{A}
No of nodes	11.7	21.0	27.7	33.0	23.3^{A}	8.7	12.3	17.3	20.0	14.6^{C}	8.0	18.0	22.0	27.3	18.8^{B}	9.4^{D}	17.1^{C}	22.3^{B}	26.8^{A}
No of leaves	8.0	18.3	25.3	30.3	20.5^{A}	8.3	13.0	14.7	17.7	13.4^{C}	8.7	16.7	18.7	26.3	17.6^{B}	8.3^{D}	16.0^{C}	19.6^{B}	24.8^{A}

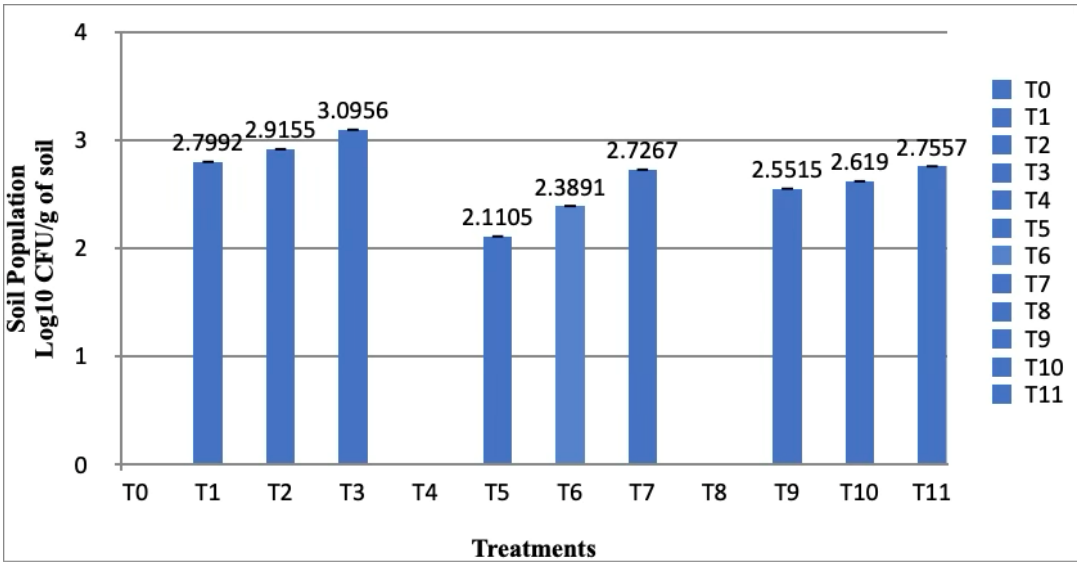

Fig 3.8: Quantification of *P. chlamydosporia* (10^8 CFU g^{-1}) mass multiplied on rice grains in potting mixture after six-month post inoculation**.**

T_0: Uninoculated sterile soil, T_1 : Sterile soil inoculated with 1 g*, T_2 : Sterile soil inoculated with 3 g, T_3 : Sterile soil inoculated with 5 g, T_4 : Uninoculated non sterile soil, T_5 : Non sterile soil inoculated with 1 g, T_6 : Non sterile soil inoculated with 3 g, T_7 : Non sterile soil inoculated with 5g, T_8 : Uninoculated vermiculite + farmyard manure, T_9 : Vermiculite + farmyard manure inoculated with 1 g, T_{10} : Vermiculite + farmyard manure inoculated with 3 g, T_{11} : Vermiculite + farmyard manure inoculated with 5 g. * *P. chlamydosporia* (10^8 CFU/g) mass multiplied on rice grains.

Furthermore, this significant enhancement of nutrient contents such as nitrogen, phosphorus, potassium, calcium, magnesium, copper, manganese, iron and zinc were analysed in both soil (Fig 3.9a & 3.9b) and plant tissues (Fig 3.9c & 3.9d) following treatment with a higher concentration of inoculum (5 g) in each substrate of treatments T_3, T_7 and T_{11}.

To standardise the concentration of inoculum, higher doses of *P. chlamydosporia* were tested to assess their effect on the growth of black pepper plants in sterilized and non-sterilized soil (Table 3.5). The fungal inoculum was administered at one-month intervals, with applications once, twice and thrice. Comparing the different dosages, plant growth increased in relation to the dosage of *P. chlamydosporia.* However, the plants treated with different dosages demonstrated significantly higher growth promotion, regardless of the frequency used. Consequently, from the pot experiments conducted, the optimal plant growth matrices were recorded in the treatment with 5g of *P. chlamydosporia*. Hence the inoculum concentration for the isolate was standardized to single applications of 5 g/plant.

Table 3.5: Evaluation of growth promotion in black pepper plants treated with different dosages and frequency of *P. chlamydosporia*

Unsterilised Soil												
***Pochonia* dosage** (g/plant)	**0**	**5**			**0**	**10**			**0**	**15**		
Application Frequency		**1**	**2**	**3**		**1**	**2**	**3**		**1**	**2**	**3**
Shoot length (cm)	31.00	132.11	130.89	135.11	31.07	144.11	146.00	148.11	31.14	154.89	152.67	156.67
Root length (cm)	5.89	18.00	17.78	18.33	6.33	20.22	21.00	21.44	6.44	22.00	21.56	22.44
Shoot dry weight (g)	1.57	2.96	2.82	2.91	1.57	4.70	4.72	4.77	1.57	5.22	5.20	5.43
Root dry weight (g)	0.15	0.46	0.46	0.47	0.16	0.70	0.71	0.71	0.16	0.82	0.78	0.89
No of roots	5.33	10.67	10.22	11.11	5.58	15.22	16.00	16.44	5.89	20.11	19.89	22.11
No of nodes	6.44	16.11	15.56	16.33	6.56	22.78	23.22	23.89	6.67	27.33	26.67	27.78
No of leaves	6.22	16.00	15.56	16.11	6.33	21.11	22.11	22.44	6.67	26.33	25.67	26.89

Sterilised Soil												
***Pochonia* dosage (g/plant)**	**0**	**5**			**0**	**10**			**0**	**15**		
Application Frequency		**1**	**2**	**3**		**1**	**2**	**3**		**1**	**2**	**3**
Shoot length (cm)	40.11	172.89	174.44	176.00	41.00	181.11	182.22	184.00	41.33	191.00	190.44	192.22
Root length (cm)	7.22	23.00	23.44	23.89	7.78	24.00	24.67	25.67	7.89	26.89	25.44	27.56
Shoot dry weight (g)	1.89	5.76	5.98	6.00	1.91	6.47	6.47	6.60	1.93	6.88	6.92	6.94
Root dry weight (g)	0.18	1.14	1.26	1.39	0.19	1.62	1.63	1.64	0.19	1.95	1.95	1.95
No of roots	8.22	18.78	19.22	19.67	8.33	22.89	23.44	25.00	8.67	25.56	25.00	27.11
No of nodes	8.22	33.89	35.11	36.22	8.56	36.11	36.44	37.22	8.67	37.78	37.44	37.89
No of leaves	7.00	32.89	33.89	35.00	7.33	34.89	35.11	35.78	7.56	36.33	36.11	36.67

Table of Means										
***Pochonia* dosage**	**Unsterilised Soil**					**Sterilised Soil**				
Application Frequency	**0**	**5**	**10**	**15**	**Mean**	**0**	**5**	**10**	**15**	**Mean**
Shoot length (cm)	31.07	143.70	143.19	146.63	**116.15**	40.81	181.67	182.37	184.07	**147.23***
Root length (cm)	6.22	20.07	20.11	20.74	**16.79**	7.63	24.63	24.52	25.70	**20.62***
Shoot dry weight (g)	1.57	4.29	4.25	4.37	**3.62**	1.91	6.37	6.46	6.52	**5.31***
Root dry weight (g)	0.16	0.66	0.65	0.69	**0.54**	0.18	1.57	1.61	1.66	**1.26***
No of roots	5.59	15.33	15.37	16.56	**13.21**	8.41	22.41	22.56	23.93	**19.32***
No of nodes	6.56	22.07	21.81	22.67	**18.28**	8.48	35.93	36.33	37.11	**29.46***
No of leaves	6.41	21.15	21.11	21.81	**17.62**	7.30	34.70	35.04	35.81	**28.21***

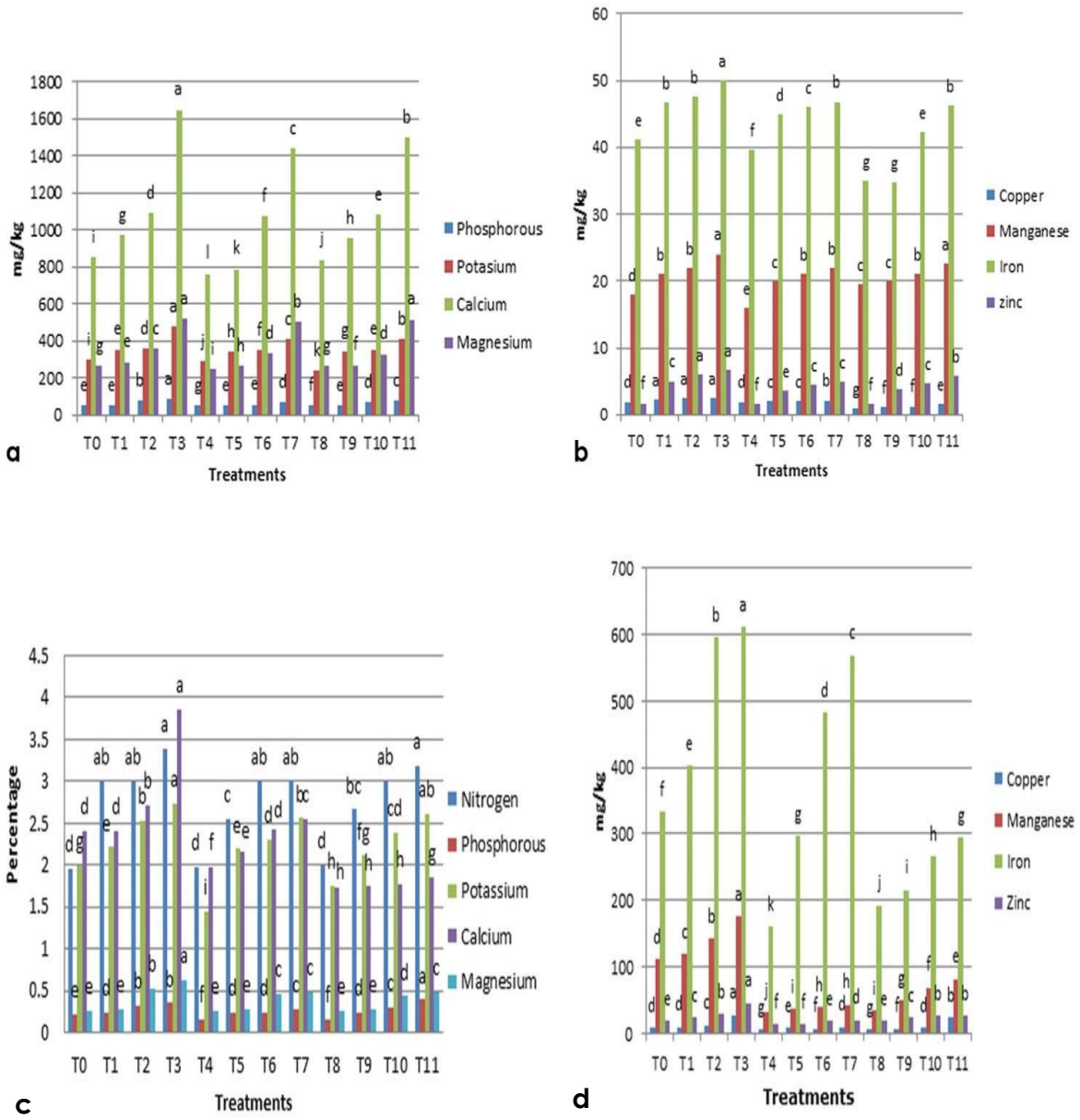

Fig 3.9: Status of major and minor nutrients in potting media and plant tissues after six months of planting *P. chlamydosporia* inoculated black pepper plants. **a.** Major nutrients in soil. **b**. Minor nutrients in soil. **c**. Major nutrients in plant tissues. **d.** Minor nutrients in plant tissues.

T_0: Uninoculated sterile soil, T_1 : Sterile soil inoculated with 1g*, T_2 : Sterile soil inoculated with 3g, T_3 : Sterile soil inoculated with 5g, T_4 : Uninoculated nonsterile soil, T_5 : Non sterile soil inoculated with 1g, T_6 : Non sterile soil inoculated with 3g, T_7 : Non sterile soil inoculated with 5g, T_8 : Uninoculated vermiculite + farmyard manure, T_9 : Vermiculite + farmyard manure inoculated with 1g, T_{10} : Vermiculite + farmyard manure inoculated with 3g, T_{11}: Vermiculite + farmyard manure inoculated with 5g. * *P. chlamydosporia* (10^8 CFU/g) mass multiplied on rice grains.

3.3.4 Evaluation of root colonization of *P. chlamydosporia* in black pepper

Microscopy: Observations of endophytic root colonization of *P.chlamydosporia* were made using bright field microscopy. Penetration of the fungus into the root epidermis was observed on the third day of post-inoculation (Fig 3.10 b). Hyphal growth within the root cortex, indicating intracellular penetration, was visible by the seventh day of inoculation (Fig 3.10 c). Following intracellular penetration, conidial formation was noted on the 14^{th} day of post-inoculation (Fig 3.10 d). Intracellular colonization within the cortical cells intensified by the 21^{th} and 28^{th} days post-inoculation (Fig 3.10 e and Fig 3.10 f).

Dilution plating: The rhizoplane and endophytic populations of *P. chlamydosporia* in black pepper roots were quantified through dilution plating. A high population density of fungus was observed in the rhizoplane region on the 7^{th} and 14^{th} day post-inoculation, with colony counts ranging from 2.8 to 3 log10 CFU per gram of fresh root tissue (Fig 3.11 a). Conversely, the endophytic population density continuously increased, peaking at 3.6 log10 CFU/g of root on the 28^{th} day post-inoculation (Fig 3.11 b). No fungal colonies were detected on plates inoculated with the last wash or in control plants.

qPCR: Real time PCR studies confirmed the specificity of primers designed from the *vcp1* gene, with amplification observed only with *P. chlamydosporia* genomic DNA (Fig. 3.12a). The Ct values ranged from 20.9 to 36.59, showing adequate correlations between Ct and DNA quantity (Fig. 3.12b). The assay's sensitivity was highlighted by its ability to detect DNA concentrations as low as 10 pg. A standard curve plotted using the Ct values against serial dilutions of the template DNA facilitated the estimation of DNA concentrations at various inoculation intervals (Fig. 3.12c). *P. chlamydosporia* DNA was detected in root samples at all the intervals (7, 14, 21, and 28 post inoculation) with Ct values of 33.37 and 32.7 at 21 and 28 post inoculation, respectively. On interpolating the Ct values into the standard curve, DNA concentrations were estimated to be between 0.8 to 1.8 at 21 and 28 post-inoculations (Fig 3.12d).

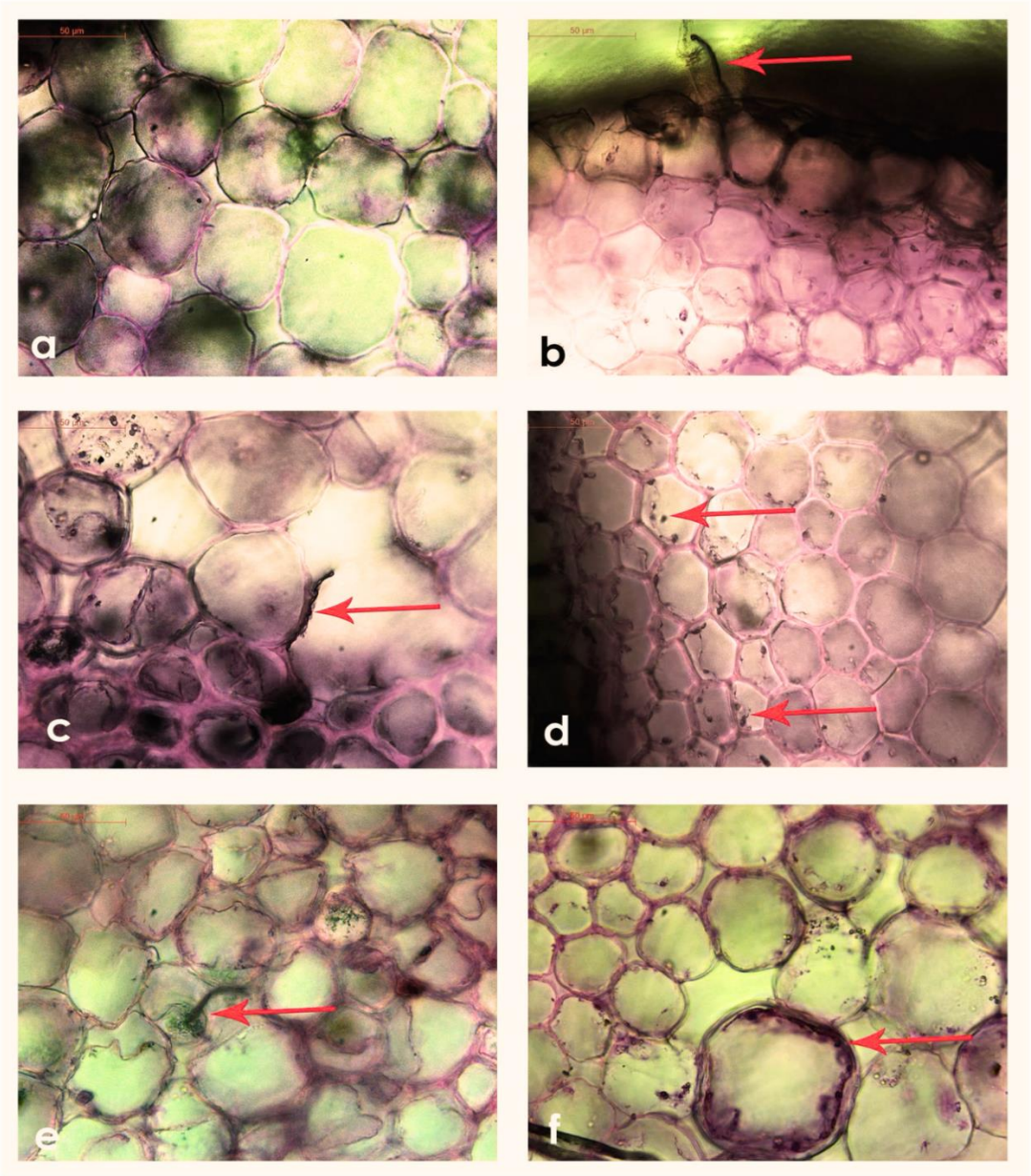

Fig 3.10: Cross section of black pepper roots colonised by *Pochonia chlamydosporia*. (a) Uninoculated control; (b) Root epidermal penetrations at 3rd dpi; (c) Intracellular penetration during 7th dpi; (d) Conidia formation durin 14th dpi; (e) and (f) Increased intracellular colonisation in cortical cells at 21st and 28th dpi. (Bar 50µm)

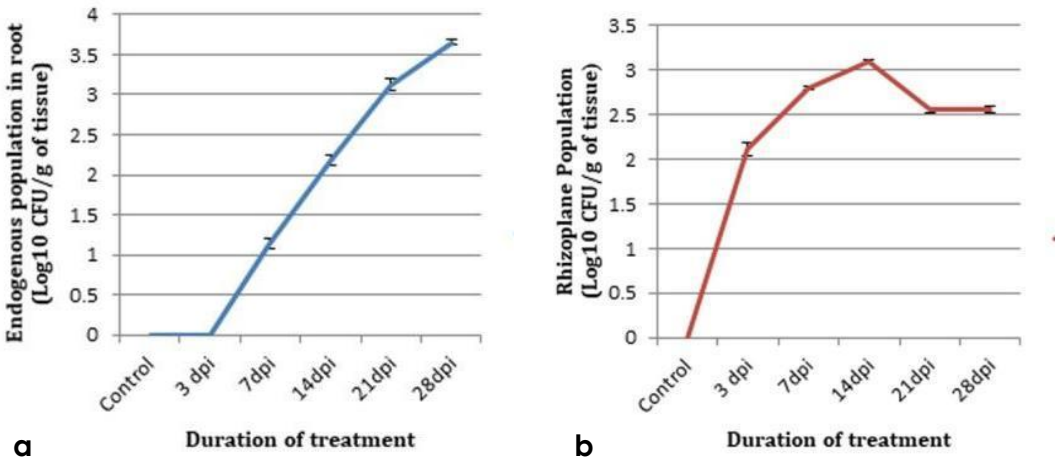

Fig. 3.11: Estimation of *Pochonia chlamydosporia* in black pepper roots by dilution plating. **a.** Rhizoplane population **b.** Endophytic population.

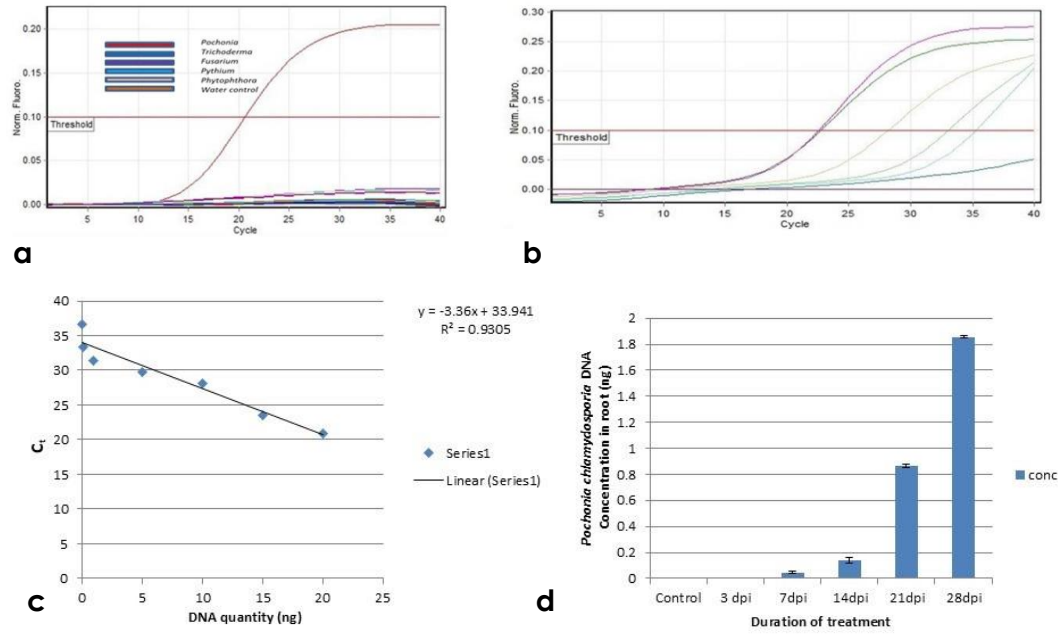

Fig. 3.12 a. Specificity of real time primers. **b**. Amplification plot demonstrating sufficient amplification for various DNA concentrations. **c**. Sensitivity of primers and standard curve **d**. *P. chlamydosporia* DNA concentrations in root (ng).

3.4 Discussion

In this study, we analysed the plant growth promoting effects of *P. chlamydosporia,* on black pepper (*Piper nigrum* L.). Application of the fungus to the root zone significantly enhanced shoot and root weights, biomass, number of secondary roots, and leaf count compared to untreated control plants. The growth promoting ability of this nematophagous fungus has been well documented in several crops, including *Arabidopsis* (Zavala-Gonzalez et al., 2017), tomato (Escudero & Lopez-Llorca, 2012; Zavala-Gonzalez et al., 2015), barley (Macia-Vicente et al., 2009b) and lettuce (Dallemole-giaretta et al., 2015).

This study specifically focused on the impact of different dosages and frequencies of *P. chlamydosporia* inoculation on root colonization, finding that a regimen of 5 g/plant with single application was optimal for promoting growth in black pepper rooted cuttings. Previous research has shown that single inoculation leads to sustained rhizosphere or endophytic colonization, which are critical for long-term crop protection (Macia-Vicente et al., 2009a; Escudero & Lopez-Llorca, 2012).

Our results also indicated a significant increase in the uptake of nutrients such as nitrogen, phosphorus, potassium, calcium, magnesium, copper, manganese, iron, and zinc in treated black pepper plants. Increases in phosphorus uptake have been similarly reported (Monteiro et al., 2018; Gouveia et al., 2019), highlighting the fungus's ability to mineralize and mobilize major and minor nutrients in soil, thereby aiding plant growth.

The root colonization ability of *P. chlamydosporia* is crucial for its effectiveness as a biocontrol agent. In this study, several methods including dilution plating, bright field microscopy and real-time PCR were employed to assess this trait. While the rhizoplane population of the fungus initially increased, peaking by the 14^{th} day post-inoculation before declining, the endophytic population continued to rise through the 28^{th} day. This pattern suggests that intracellular colonization, particularly within the cortical cells, may play a significant role in the plant-fungal symbiosis and was further supported by microscopic observations. Similar observations were made by (Monteiro et al., 2018) in tomato plants. In some studies, scanning and confocal microscopy are

used to monitor the fungal colonization within root tissues (Zavala-Gonzalez et al., 2017; Mingot-Ureta et. al., 2020).

Furthermore, real-time PCR with specifically designed primers confirmed the presence and quantified the colonization of *P. chlamydosporia* in the plant tissues, demonstrating the assay's sensitivity and specificity. These findings correlate with prior research on other plant hosts (Maciá-Vicente et al., 2009b; Escudero & Lopez-Llorca, 2012; Larriba et al., 2015; Zavala-Gonzalez et al., 2015; 2017; Mingot-Ureta et. al., 2020).

Although the growth-promoting effects of *P. chlamydosporia* in black pepper are clear, the precise mechanisms underlying these effects remain to be fully elucidated. The production of IAA, siderophores, ammonia, and extracellular enzymes, alongside the solubilization of phosphorus and zinc, are likely contributing factors. Production of plant hormones like IAA has been previously reported with *P. chlamydosporia* (Zavala-Gonzalez et al., 2015; Zavala-Gonzalez et al., 2017; Junior et al., 2021;). Previous studies have shown that *P. chlamydosporia* solubilizes inorganic phosphates in soil by releasing acid and alkaline phosphatases (Zavala-Gonzalez et al., 2015; Monteiro et al. 2018; Gouveia et al., 2019; Junior et al. 2021). The capability of the *P.chlamydosporia* to produce extracellular enzymes such as cellulases, amylases and pectinases was also proved in our study. Genome sequencing of *P. chlamydosporia* clearly indicated the presence of a number of glycoside hydrolases in its genome in comparison with those of other nematophagous, entomopathogenic or mycoparasitic fungi (Larriba et al., 2014). However, cellulase degrading enzymes in this fungus, though present, are fewer in number compared to fungi like *Trichoderma* spp. Notably, the ability of *P. chlamydosporia* to produce ammonia and siderophores, as well as its role in enhancing nutrient uptake, have been documented for the first time in this study, paralleling findings from other beneficial fungi (Milagres et al., 1999).

3.5 Conclusion

This study supports the hypothesis that *P. chlamydosporia* is a nematophagous fungus with significant agronomic benefits, particularly due to its plant growth-promoting properties. Our investigations focused on evaluating the root colonization potential of

P. chlamydosporia in the dicotyledonous host plant, black pepper (*Piper nigrum* L.). The results demonstrate that the endophytic capabilities of *P. chlamydosporia* effectively promote root and shoot growth in black pepper plants. This enhancement is attributed to the fungus's ability to produce IAA, siderophores, ammonia, and extracellular enzymes, along with its capacity to solubilize phosphorus and zinc.

The use of real-time PCR in this study proved a rapid three-hour quantitative detection method for the fungus, a significant improvement over the traditional two-week growth period required for colony development on selective media. Pot experiments further confirmed that *P. chlamydosporia* not only boosts the growth of black pepper but also holds promise as a biofertilizer that could enhance growth and yield in a variety of agronomically significant crops across different soil types. Our ultimate goal is to optimize the biocontrol efficacy and crop growth enhancement of *P. chlamydosporia* under diverse agricultural conditions, thereby contributing to sustainable farming practices.

Chapter 4

Identification of Secondary Metabolites Produced by *Pochonia chlamydosporia*

Abstract

This study investigated the biocontrol potential of culture filtrates and secondary metabolites from the nematophagous fungus *Pochonia chlamydosporia.* The fungus exhibited antifungal activity against pathogens such as *Pythium myriotylum*, *Macrophomina* sp., *Colletotrichum* sp., *Phytophthora* sp., *Fusarium* sp. and *Exerohilum rostratum*. The highest percentage inhibition of radial growth (PIRG values) was observed with *P. myriotylum* (81.42%) and *Phytophthora* sp. (82.71%), while *Macrophomina* sp. showed the lowest inhibition (40%). The study also aimed to identify the secondary metabolites responsible for the biocontrol activity of *P. chlamydosporia*. Secondary metabolites were extracted using ethyl acetate, and their activity profiles were assessed via thin-layer chromatography (TLC). The ethyl acetate extracts fully inhibited the mycelial growth of *Pythium myriotylum* (99.54%) and *Phytophthora* sp. (99.99%). Moreover, the extract demonstrated significant nematicidal activity against the plant parasitic nematode *Radopholus similis,* with the crude extract showing the highest efficacy among various concentrations tested. High resolution UPLC- (ESI)-QToF-MS analysis of the extract revealed a diverse array of bioactive compounds, including antifungal, antibacterial, antiviral, antitumor, cytotoxic, antimalarial, antitrypanosomal, and nematicidal agents. An *in-silico* screening approach was employed to identify potential lead compounds for nematicidal activity, targeting glutathione S-transferases and venom allergen-like proteins. The results highlighted three compounds bisevertinol, enniatin I, and enniatin H that exhibited strong binding affinities to multiple pharmacological targets, suggesting their potential as lead candidates for developing nematicidal agents against plant-parasitic nematodes. Further research is required to confirm the nematicidal properties of these compounds against phytophagous nematodes.

4.1 Introduction

Nematophagous fungi are natural predators of nematodes in soil and employ several mechanisms to attack their hosts. These fungi can be classified into three primary categories: endoparasitic fungi, nematode-trapping fungi, and egg- and cyst-parasitic fungi (Schmidt et al., 2007) Nematophagous fungi typically use predatory structures and hydrolytic enzymes to capture, kill, and digest nematodes, while some species secrete nematode-toxic secondary metabolites to assault their hosts (Li et al., 2014).

Secondary metabolites are structurally diverse, low molecular weight compounds that are not directly required for the growth of the producer organism but play a crucial role in its interaction with the environment. Soil-dwelling bacteria and fungi produce a variety of secondary metabolites, primarily to compete with other organisms for nutrients and space (Brakhage, 2013). Secondary metabolism typically occurs in the later stages of growth, and although it has a genetic basis, environmental factors can significantly influence its expression (Bibb, 2005). Despite the importance of secondary metabolites in nematophagous fungi, limited information is available on their specific roles in nematode infection. *P. chlamydosporia*, a nematophagous fungus, is one of the most extensively studied biological control agents against nematodes. This fungus plays a vital role in reducing soil-dwelling nematodes in certain agroecosystems (Larriba et al., 2014). It parasitises nematode eggs by secreting hydrolytic enzymes such as chitinases, which degrade the nematode cuticle, and proteases, which penetrate the egg shells (Lopez-Llorca et al., 2010). Some studies suggest that the biocontrol efficacy of nematophagous fungi is partially due to the production of antifungal metabolites (Trifonov et al., 1986). Given the growing interest in natural products, the assessment and commercial development of secondary metabolites from nematophagous fungi, including *P. chlamydosporia*, are gaining importance (Hellwig et al., 2003).

P. chlamydosporia produces a wide range of secondary metabolites, including aromatic compounds (Pochonins A−P, tetrahydromonorden, radicicol, pseurotin A (Shinonaga et al., 2009b), nonaromatic polyketides (vertinolide (Trifonov et al., 1982), lowdenic acid (Angawi et al., 2003), bisvertinols, and bisvertinoqinol

(Trifonov et al., 1983)), cyclopeptides (including epidithiodioxopiperazine- type verticillins (Minato et al., 1973) and bassianolide (Chaturvedi et al., 1988)), β-carotene-type neurosporaxanthin (Valadon et al., 1977), pentanorlanostane triterpenoids (Grove,1984), and aphidicolane-type diterpenoid (Brundret et al., 1972). Many of these compounds exhibit biological activities, including antibacterial, antifungal, antioxidative, antiviral, and anticancer properties. Some have been studied for potential medical applications, such as treatments for cancer and herpes (Moulin et al., 2005; Huang et al., 2008).

Recent genome sequencing of *P. chlamydosporia* has revealed a greater number of gene clusters potentially involved in secondary metabolite production than the number of known metabolites (Larriba et al., 2014). However, only two nematicidal compounds phomalactone and aurovertins have been identified from *P. chlamydosporia* through bioassay-directed fractionation (Khambay et al., 2000; Wang et al., 2015). Despite these findings, the nematicidal activity of the secondary metabolites from this fungus remains largely unexplored, Necessitating further research to understand their roles in nematode control and their potential environmental applications.

Radopholus similis, a globally significant plant-parasitic nematode, is among the top 10 most damaging nematodes. It is a migratory endoparasite that moves through the host plant's root tissues, causing cell damage such as black lesions, tissue necrosis, slow-growth, and plant lodging (Jones et al., 2013). *R. similis* parasitises over 250 plant species, including economically important crops such as citrus, bananas, black pepper, coconut, and many other crops (O'Bannon et al., 1977). During parasitism, *R. similis* secretes various proteins, referred to as effectors, into host plant cells, which play crucial roles in infection by manipulating plant defence mechanisms (Hogenhout et al., 2009; Haegeman et al., 2012). Two major secretory proteins, venom allergen-like proteins (VAPs) and glutathione S-transferases (GSTs) have been identified as critical for parasitism and suppression of plant defenses (Rosana et al., 2016*;* Li et al., 2021*)*. Chemical nematicides are currently the primary method of managing plant parasitic nematodes (PPNs), but their toxicity to non-target organisms and

environmental persistence makes them unsustainable. They are also expensive and hazardous to human health (Siddiqui et al., 2001). Therefore, alternative strategies, including biological control using natural products like secondary metabolites, are essential for sustainable agriculture. Given the role of glutathione S-transferases and venom allergen-like proteins in nematode parasitism, targeting these proteins with bioactive compounds presents a promising approach for developing novel nematicides.

This study aims to investigate the secondary metabolites produced by *P. chlamydosporia* with antifungal activity against pathogens such as *Pythium myriotylum*, *Macrophomina* sp., *Colletotrichum* sp., *Phytophthora* sp., *Fusarium* sp. and *Exerohilum rostratum*. Additionally, the nematicidal activity of these metabolites against the plant parasitic nematode *R. similis* was explored. The study will focus on the extraction, characterisation, and bioactivity profiling of secondary metabolites using thin-layer chromatography (TLC) and ultra-performance liquid chromatography coupled with electrospray ionization quadrupole time-of-flight mass spectrometry (UPLC-(ESI)-QToF-MS). In addition, *in silico* docking will be employed to identify lead compounds that target specific nematode effector proteins, such as venom allergen-like proteins and glutathione S-transferases.

4.2 Materials and Methods

4.2.1 *Fungus*

The fungus strain used in this study was *P. chlamydosporia* (MTCC5412), obtained from the biocontrol agent repository at the Indian Institute of Spices Research (IISR), Kozhikode, India. The strain was cultured on potato dextrose agar (PDA) plates at 28C ± 2°C for ten days.

4.2.2 *Antagonism of P. chlamydosporia against fungal plant pathogens*

The antifungal activity of *P. chlamydosporia* was tested *in vitro* against six plant pathogenic fungi: *Pythium myriotylum*, *Macrophomina* sp., *Colletotrichum* sp., *Phytophthora* sp., *Fusarium* sp. and *Exerohilum rostratum* using the dual culture method. A 5-mm agar plug from a 10-day-old culture of *P. chlamydosporia* was placed

2 cm from the edge of the Petri dish. On the opposite end, an agar disc (5 mm) containing plant pathogenic fungi was placed 2 cm from the dishe's edge. Controls included only the plant pathogenic fungi on a fresh PDA plate. All plates were incubated at 28 ± 2°C in triplicate. After 10 days, the radius of the plant pathogenic fungal colony towards the antagonist colony (R2) and the radius in the control plate (R1) were measured. Antagonistic activity was expressed as the percentage inhibition of radial growth (PIRG), using the formula by Skidmore and Dickinson (1976): PIRG = [(R1-R2) ÷ R1] × 100.

4.2.3 *Extraction of secondary metabolites produced by P. chlamydosporia*

Fermentations were conducted in a 3-L laboratory glass fermentor (Lark Innovative Fine Teknowledge, Chennai). The PDB medium was steam-sterilised in situ for 20 minutes at 121°C. A 250-mL Erlenmeyer flask containing 100 mL of PDB was inoculated with a 5-mm agar plug from a 10-day-old *P. chlamydosporia* culture on PDA. The flask was incubated for 10 days at 28°C in an orbital shaker at 150 rpm in order to generate the primary seed culture. Ten millilitres of the seed culture were transferred to a 3-L fermentor containing sterilised PDB medium. To prevent excessive foaming, 1 mL of Sigma Antifoam A was added. The fermentation was maintained at p^H 6.29, with aeration (1 L/min) and agitation (180 rpm) at 28 °C for 14 days. Daily samples were collected and analysed.

After 14 days, the cultures were filtered through Whatman No. 1 filter paper to separate the mycelia from the culture filtrate. The filtrate was extracted with an equal volume of ethyl acetate using a separatory funnel, then concentrated using a rotary vacuum evaporator (Buchi India Ltd) at 45ºC, yielding an oily residue. The crude ethyl acetate extract was diluted to concentrations of 10, 20, 50 and 100 µg/ml in dimethyl sulphoxide (DMSO) for bioassay-directed monitoring.

Bioassay for antagonistic activity of secondary metabolites

The crude ethyl acetate extract of *P. chlamydosporia* was tested for antagonistic activity *in vitro* against six plant pathogens: *Pythium myriotylum*, *Macrophomina* sp., *Colletotrichum* sp., *Phytophthora* sp., *Fusarium* sp. and *Exerohilum rostratum* using

the agar well diffusion method (Magaldi et al., 2004). Fungal discs (5 mm) were placed in the centre of PDA plates, and four wells (5 mm diameter) were punched aseptically around the disc. Twenty microlitres of the crude extract were added to each well. Plates with diluted DMSO (without extract) served as controls. The plates were incubated at 28°C for four days, and zones of inhibition were measured.

In vitro bioassay for nematicidal activity

The ethyl acetate extract of *P. chlamydosporia* was tested for nematicidal activity *in vitro* against the plant parasitic nematode *Radopholus similis.* Nematodes were cultured on carrot callus, prepared by surface sterilising carrot discs and incubating them at 26°C. Nematodes were surface sterilised using 0.01% Hyamine and 0.02% streptomycin sulphate, then inoculated into the carrot callus and cultured at 26°C for one month. Various concentrations of the ethyl acetate extract (10, 20, 50, 100 µg/ml, 1 mg/ml, and crude extract) were dissolved in 1% DMSO and added to wells of cell culture plates (NEST, 6x4 wells and 1.5 cm diameter each). Each well was inoculated with 25 nematodes. Distilled water served as an absolute control, 1% DMSO as a negative control, and carbosulfan as a positive control. Mortality rates were recorded after 24 and 48 hours of incubation at room temperature, and percentage mortality was calculated. The experiment was repeated three times.

4.2.4 *Thin Layer Chromatography (TLC) fingerprinting of secondary metabolites*

TLC was performed using aluminum sheets coated with silica gel 60 F254 (Merck, Germany). The TLC chamber was saturated with a solvent mixture of ethyl acetate and hexane (9:1 ratio). and securely sealed to avoid any loss of solvent due to evaporation. A 5-μL aliquot of the ethyl acetate extract was spotted onto 10 x 10 cm plates, which were developed in the TLC chamber until the solvent front reached the top. The plates were then removed and dried. They were exposed to iodine vapour in an iodine chamber, and yellow-brown spots were visualised. The plates were examined under white light, and retention factor (Rf) values of the spots were calculated.

4.2.5 *Identification of secondary metabolites using UPLC-(ESI)-QToF-MS*

One liter of the ethyl acetate extract was concentrated to 10 mL and further evaporated under nitrogen. The concentrated extract was diluted with methanol (10X) and injected into an Acquity Ultra Performance Liquid Chromatography (UPLC) coupled to a Quadrupole - Time of Flight mass spectrometer (QToF-MS, Synapt G2 HDMS, Waters Corporation, Manchester, UK). Electrospray ionisation (ESI) was used in MSE mode, with data acquired over the m/z 50–1200 range. MS/MS data were collected using high energy (10–60 V ramping), and full scan MS data were collected at low energy (4 V). Operating parameters included a capillary voltage of 3 kV, source temperature of 120ºC, desolvation temperature of 500ºC, desolvation gas flow rate of 1000 L/h, and cone gas flow rate of 50 L/h. Sodium formate (0.5 mM) was used for calibration, and leucine enkephalin served as the reference mass (m/z 556.2771 in positive mode, m/z 554.2670 in negative mode). An ACQUITY UPLC BEH C_{18} column (2.1 × 100 mm, 1.8 µm, Waters India Pvt. Ltd., Bengaluru) was used for chromatographic separation at 35°C, with a flow rate of 0.4 mL/min). The mobile phases consisted of methanol:water (10:90) (A phase) and methanol:water (90:10) (B phase), both containing 0.1% formic acid. A gradient program was applied, and samples were maintained at 15°C with a 5-µl injection volume. Data were processed using UNIFI software (Waters Corporation, Manchester, UK).

4.2.6 *In silico screening and identification of lead compounds with nematicidal activity*

UPLC-(ESI)-QToF-MS analysis identified 47 bioactive compounds in the ethyl acetate extract of *P. chlamydosporia,* in which 12 compounds with antitumor, antifungal, antibacterial, antiviral, and nematicidal properties were selected for *in-silico* studies. Excretory/secretory (ES) proteins of plant parasitic nematodes were used as receptor molecules to screen for lead compounds with nematicidal activity.

Macromolecule preparation

Two ES proteins, venom allergen-like protein (PDB ID: 5WEE) and glutathione s-transferase (PDB ID: 4Q5F), were selected as receptor molecules. These proteins are

key effectors in plant parasitism by nematodes, aiding in the suppression of plant defenses. The COACH-D (Wu et al., 2018) was used to identify active sites in the protein structures.

Ligand preparation

The chemical compositions, structural information, and canonical simplified molecular input line entry system (SMILES) of the 12 bioactive compounds were obtained from the PubChem database (https://pubchem.ncbi.nlm.nih.gov/) (Table 4.1). PDB structures of the compounds were generated using CORINA, an online tool.

Table 4.1 Selected list of ligand compounds used in docking studies

Ligand molecules	Molecular formula	Molecular weight (g/mol)	Compound CID	Canonical SMILES
Enniatin H	$C_{34}H_{59}N_3O_9$	653.8	11104255	CCC(C)C1C(=O)N(C(C(=O)OC(C(=O)N(C(C(=O)OC(C(=O)N(C(C(=O)O1)C(C)C)C)C(C)C)C(C)C)C)C(C)C)C(C)C)C
Viridin	$C_{20}H_{16}O_6$	352.3	94257	CC12C(C(C(=O)C3=COC(=C31)C(=O)C4=C2C=CC5=C4CCC5=O)OC)O
Pseurotin A	$C_{22}H_{25}NO_8$	431.4	9845622	CCC=CC(C(C1=C(C(=O)C2(O1)C(C(NC2=O)(C(=O)C3=CC=CC=C3)OC)O)C)O)O
Monocillin II	$C_{18}H_{20}O_4$	300.3	6478915	CC1CC=CCCC=CC(=O)CC2=C(C(=CC=C2)O)C(=O)O1
Pyrenocine A	$C_{11}H_{12}O_4$	208.21	6312351	CC=CC(=O)C1=C(OC(=O)C=C1OC)C
Asperlin	$C_{10}H_{12}O_5$	212.2	9859172	CC1C(O1)C2C(C=CC(=O)O2)OC(=O)C
Asteltoxin	$C_{23}H_{30}O_7$	418.5	6438150	CCC1C(C2(C(C(OC2O1)C=CC=CC=CC3=C(C(=CC(=O)O3)OC)C)O)C)(C)O
Pochonin F	$C_{18}H_{20}O_5$	316.3	6478916	CC1CC=CC(CC=CC(=O)CC2=C(C(=CC=C2)O)C(=O)O1)O
Bisvertinol	$C_{28}H_{34}O_8$	498.6	5368914	CC=CC=CC(=C1CC(C2(C(C1=O)(C3C(=C(C=CC=CC)O)C(=C(C(=O)C3(O2)C)C)O)C)O)(C)O)O

Ligand molecules	Molecular formula	Molecular weight (g/mol)	Compound CID	Canonical SMILES
Coniothyriomycin	$C_{13}H_{12}ClNO_5$	297.69	6450543	COC(=O)C=CC(=O)NC(=O)CC1=CC(=C(C=C1)O)Cl
Enniatin I	$C_{35}H_{61}N_3O_9$	667.9	11125230	CCC(C)C1C(=O)N(C(C(=O)OC(C(=O)N(C(C(=O)OC(C(=O)N(C(C(=O)O1)C(C)C)C)C(C)C)C(C)C)C(C)C)C(C)CC)C(C)C)C
Acremine B	$C_{12}H_{16}O_4$	224.25	11356526	CC1(CC(=O)C(=CC1=O)C=CC(C)(C)O)O

Docking

AutoDock 4.2 was used to dock the 12 ligands into the active sites of glutathione s-transferase and venom allergen-like protein following the methodology by Morris et al., (1998). The grid-based approach, with grid spacing of 0.375 A^0 and XYZ dimensions of 60 x 60 x 60, was centred on the active site. Binding affinities were analysed, and potential orientations were ranked by lowest binding energy. A hit molecule was defined as having a binding energy of ≤-5 kcal/mol.

Drug likeness and post dock analysis

The pKCSM tool (Pires et al., 2015) was used to predict the pharmacokinetic properties, absorption, distribution, metabolism, excretion, and toxicity of the potential lead compounds. This early-stage screening facilitated the identification of drug-like molecules suitable for further development.

4.3 Results

4.3.1 *Antagonism of P. chlamydosporia against fungal plant pathogens*

P. chlamydosporia effectively suppressed the radial mycelial growth of six plant pathogenic fungi such as *Pythium myriotylum*, *Macrophomina* sp., *Colletotrichum* sp., *Phytophthora* sp., *Fusarium* sp., and *Exserohilum rostratum* (Fig 4.1). The highest percentage inhibition of radial growth (PIRG) was observed with *P. myriotylum*

(81.42%) and *Phytophthora* sp. (82.71%), while the lowest PIRG was recorded with *Macrophomina s*p. (40%) (Table 4.2).

Table 4.2: Percentage inhibition of radial growth (mean ± S.E.) of *P. chlamydosporia,* against various fungal pathogens.

Plant pathogens	Mean percentage inhibition of radial growth*(PIRG)
Pythium myriotylum	81.42 ± 0.08^{b}
Macrophomina sp.	40.00 ± 0.08^{f}
Colletotrichum sp.	68.90 ± 0.40^{d}
Phytophthora sp.	82.71 ± 0.08^{a}
Fusarium sp.	71.42 ± 0.82^{c}
Exerohilum rostratum	61.42 ± 0.08^{e}

* Values are means of three replicates ± standard error (SE). Data points with the same letter indicate no significant difference according to Fisher's test at 0.05% confidence level.

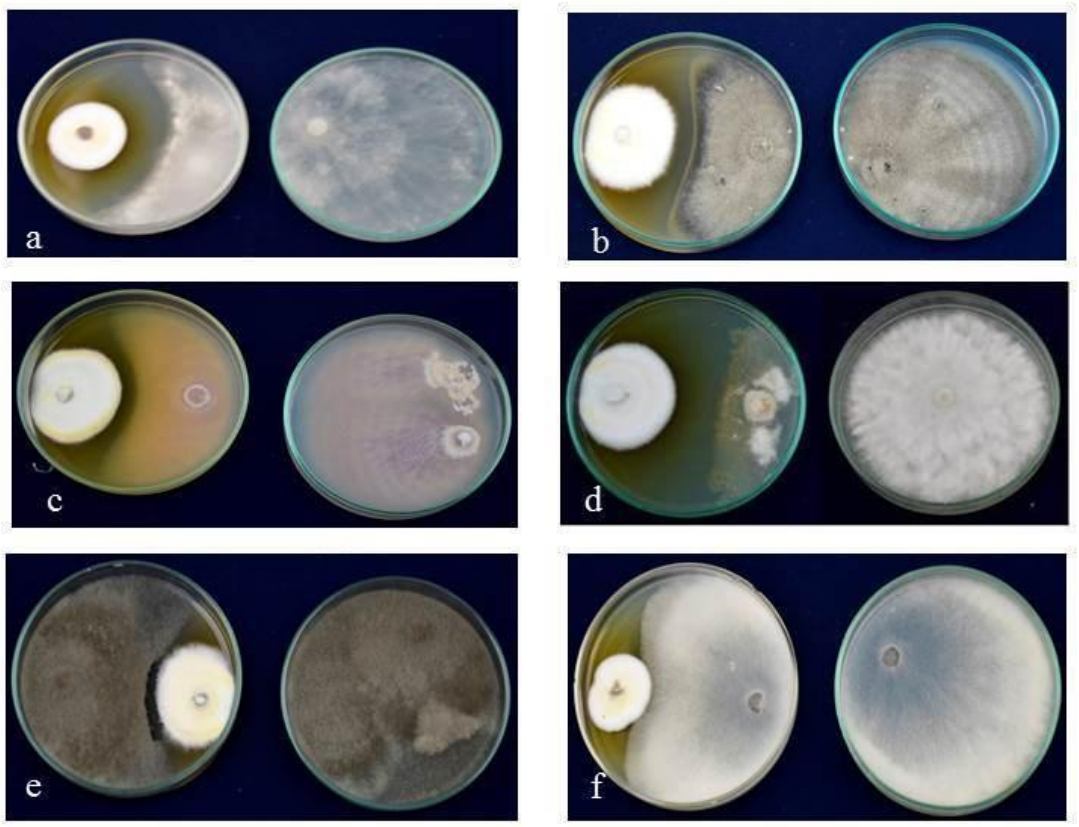

Fig 4.1 Antagonistic effects of *P. chlamydosporia* against fungal plant pathogens in dual culture Method. (a) *Pythium myriotylum* (b) *Colletotrichum* sp. (c) *Fusarium* sp. (d) *Phytophthora* sp. (e) *Exerohilum rostratum* (f) *Macrophomina* sp.

4.3.2 *Extraction and bioassay of secondary metabolites*

The crude extract, weighing 1.2 g, was obtained from the fermentation process in a 3-L glass in situ fermenter (Fig. 4.2a) while the extracellular secondary metabolites of *P. chlamydosporia* were extracted using ethyl acetate in a separatory funnel (Fig 4.2b), followed by concentration using a rotary vacuum evaporator (Fig 4.2c). The crude ethyl acetate extract was dissolved in DMSO, and its bioactivity was tested against six plant pathogenic fungi.

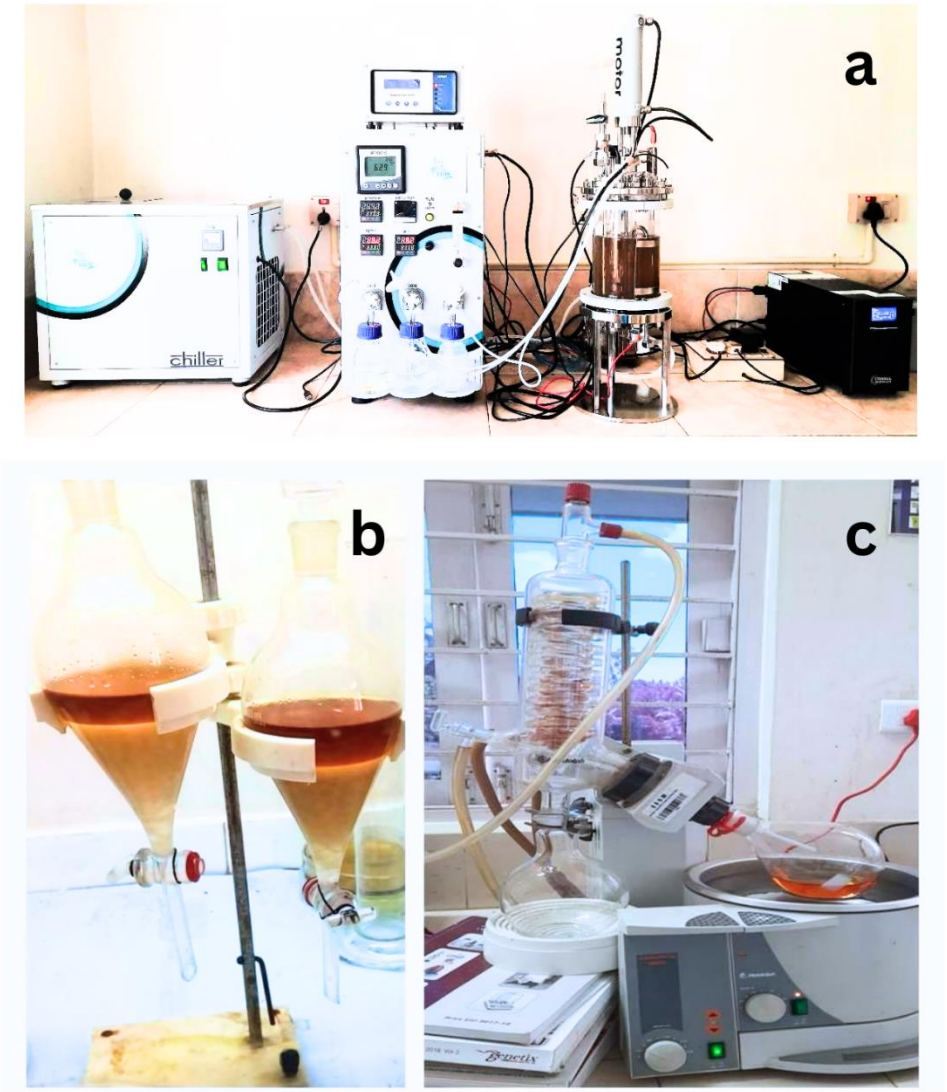

Fig. 4.2: Extraction of secondary metabolites from *Pochonia chlamydosporia.* (a) Cultivation in 3L laboratory glass *in situ* fermentor; (b) Extraction using separatory funnels; (c) Concentration using rotary vacuum evaporator.

The results of the bioassay revealed that the ethyl acetate extract showed the highest activity against *P. myriotylum* (99.54%) and *Phytophthora* sp. (99.99%) (Table 4.3, Fig. 4.3). The extract also demonstrated strong nematicidal activity against *R. similis,* with the highest mortality rate observed with the crude extract (87.9% after 48 h) (Table 4.4, Fig. 4.4).

Table 4.3: Antifungal activity of crude extracts of *P. chlamydosporia* against fungal plant pathogens

Plant pathogens	Mean percentage inhibition*
Pythium myriotylum	99.54 ± 0.39^{a}
Macrophomina sp.	30.86 ± 0.31^{d}
Colletotrichum sp.	31.39 ± 0.66^{d}
Phytophthora sp.	99.99 ± 0.005^{a}
Fusarium sp.	47.49 ± 0.48^{c}
Exerohilum rostratum	55.71 ± 0.82^{b}

* Values are means of three replicates ± standard error (SE). Data points with the same letter indicate no significant difference according to Fisher's test at 0.05% confidence level.

Table 4.4: Nematicidal actions of secondary metabolites produced by *P. chlamydosporia* against *R. similis*

Concentration of ethyl acetate extract	Mortality (%) after 24 hrs	Mortality (%) after 48 hrs
10 µg/ml	35.33 ± 0.66^{g}	43 ± 0.57^{g}
20 µg/ml	47.33 ± 0.33^{f}	50.66 ± 0.88^{f}
50 µg/ml	55.5 ± 0.76^{e}	59.06 ± 0.58^{e}
100 µg/ml	63.63 ± 0.27^{d}	67.46 ± 0.31^{d}
1 mg/ml	71.4 ± 0.50^{c}	75.43 ± 0.28^{c}
Crude	84.06 ± 0.12^{b}	87.9 ± 0.37^{b}
Carbosulfan (Positive control)	91.56 ± 0.23^{a}	91.63 ± 0.18^{a}

* Values are means of three replicates ± standard error (SE). Data points with the same letter indicate no significant difference according to Fisher's test at 0.05% confidence level.

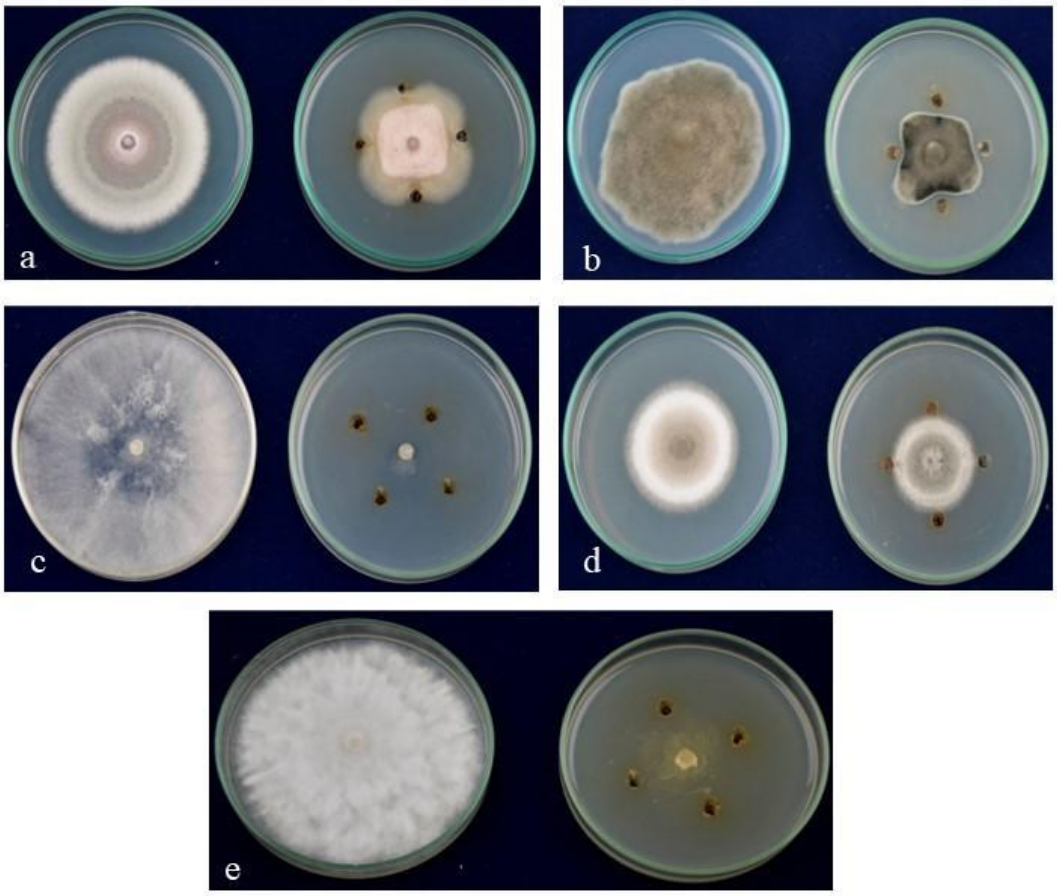

Fig 4.3 Activity profile of crude ethyl acetate extracts of *P. chlamydosporia* against fungal plant pathogens. (a) *Fusarium* sp. (b) *Exerohilum rostratum* (c) *Pythium myriotylum* (d) *Colletotrichum* sp. (e) *Phytophthora* sp.

4.3.3 *Thin Layer Chromatograhy (TLC) fingerprinting of secondary metabolites*

The ethyl acetate extract of *P. chlamydosporia* was fractionated using Thin Layer Chromatography (TLC) to identify and isolate active compounds. Seven distinct compounds were observed with varying retention factor (Rf) values such as P1 (0.12), P2 (0.18), P3 (0.5), P4 (0.56), P5 (0.7), P6 (0.8) and P7 (0.87). The TLC plate image is shown in Fig. 4.5.

4.3.4 Identification of Secondary metabolite using UPLC-(ESI)-QToF-MS analysis

The UPLC-(ESI)-QToF-MS analysis of the ethyl acetate extract of *P. chlamydosporia* identified 47 bioactive chemical compounds (Table 4.5). Among these, enniatin,

viridin, and pseurotin A were the primary nematicidal compounds. Various enniatin analogues with potent nematicidal activity, such as enniatin B3, enniatin H, enniatin I, and enniatin K1, were detected. Viridin, a well-known nematicidal compound produced by *Trichoderma spp*., and pseurotin A, which inhibits the growth of *Bursaphelenchus xylophilus* and *Pratylenchus penetrans,* were also identified.

In addition to nematicidal compounds, several bioactive metabolites with antifungal properties were found, including Acremine B, Acremine I, Acremine M, and Coniothyriomycin. Coniothyriomycin, a known antifungal metabolite produced by *Coniothyrium* spp., has been reported to be effective against *Plasmopara viticola* and *Phytophthora infestans.* Our analysis also revealed important antibiotics like Salfredin B11, Penicillin V, Pyrenocine A, and various enniatin analogues.

Enniatins (ENs), known for their antibacterial, antifungal, antileishmanial, and antimalarial properties, were among the prominent compounds identified. Monocillin II and III, with demonstrated antibacterial, antiviral, and antifungal activities, were also detected. Additionally, pyrenocines, which have shown phytotoxicity, antifungal, antibacterial, antimalarial properties, were identified in the extract. The extract contained antibacterial chemicals that were identified as acetoxyanthecotulide, acremonol, asperlin, cycloepoxylactone, penicillanthranin B, rhodolamprometrin, sorbicillinol, and verimol J.

Several antiviral compounds were also detected, including asteltoxin, asteltoxin B, epoxysorbicillinol, pochonins F and J. Pochonins, members of the resorcylic acid lactone (RAL) family, were originally isolated from *P. chlamydosporia* and exhibit antiviral and antiparasitic properties.

Moreover, cytotoxic and antitumor compounds, such as bisvertinol, enniatin B3, migrastatin, and phomenone were identified. Bisvertinol, a dimeric vertinoid, exhibited notable cytotoxic and anticancer effects. Other identified compounds with bioactive potential included adenosine, which acts as a vasoactive agent, and several antiprotozoal substances such as acetoxyanthecotulide and enniatin H and I.

This comprehensive profiling highlights the potential of *P. chlamydosporia* as a source of diverse bioactive compounds with applications in agriculture and medicine.

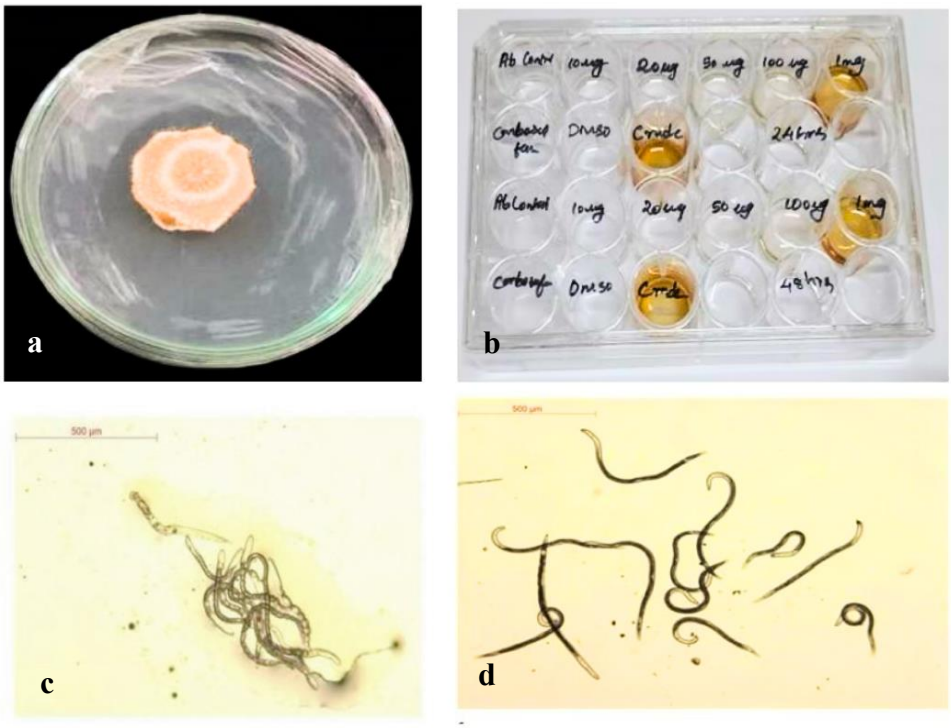

Fig. 4.4: Nematicidal action of secondary metabolites generated by *Pochonia chlamydosporia* against *Radopholus similis.* **a)** Carrot disc culture of *R. similis*; **b)** Cell culture plate for nematicidal bioassay; **c)** Dead nemotodes in crude extract after 45 h of inoculation, **d)** Control showing live nematodes.

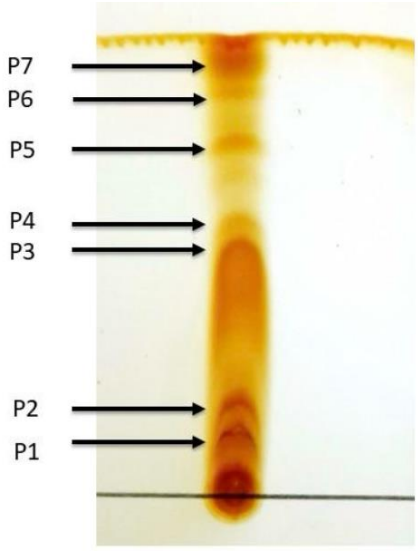

Fig. 4.5: TLC plate image of the ethyl acetate extract of *Pochonia chlamydosporia*

Table 4.5: UPLC-(ESI)-QToF-MS profiling of ethyl acetate extract of *P. chlamydosporia*

Component	Expected mass (Da)	Observed mass (Da)	Mass error (mDa)	Observed RT (min)	Response	Adducts
(2R)-2-Hydroxy-3-[(9Z)-9-octadecenoyloxy] propyl 2-(trimethylammonio)ethyl phosphate	521.348	521.347	-1.08	9.91	70161.23	-e, +H
2-Ammonioethyl (2R)-2-hydroxy-3-[(9Z)-9-octadecenoyloxy]propyl phosphate	479.301	479.298	-2.56	8.14	14957.82	-e, +H
2R)-3-[(9Z)-9-Hexadecenoyloxy]-2-hydroxypropyl 2-(trimethylammonio)ethyl phosphate	493.316	493.31	-2.68	9.29	25152.57	-e, +H
Acetoxyanthecotulide	306.1467	306.1462	-0.51	6.40	1203.41	+H
Acremeremophilane D	372.193	372.191	-1.761	8.39	2118.772	+H
Acremine B	224.104	224.105	0.99	4.44	33824.66	+Na
Acremine I	240.099	240.100	1.00	2.77	45892.83	+Na
Acremine M	256.094	256.095	0.65	2.22	1218.743	+H
Acremonol	282.110	282.111	1.47	6.25	8843.87	+Na, +H
Acremonone G	252.063	252.064	1.39	5.32	945080.3	+H
Acremonone H	222.052	222.053	0.52	3.59	1010.238	+H
Acremostrictin, rel-	252.099	252.101	1.58	5.68	814.181	+Na
Adenosine	267.096	267.098	1.39	0.85	57989.53	+H
Aselacin B	922.4800	922.4803	0.36	8.19	110628.8	+Na, +H, -e
Asperlin	212.068	212.069	0.95	2.95	5288.179	+H
Asteltoxin	418.199	418.197	-1.43	7.88	8510.974	+H
Asteltoxin B	434.194	434.192	-1.86	7.23	6918.021	+H
Bisvertinol	498.2253	498.2258	0.48	10.15	7279.996	-e, +H
Coniothyriomycin	297.040	297.041	0.80	6.89	92751.1	-e, +H
Cordyheptapeptide C	865.473	865.478	4.51	9.26	1744.358	+Na, -e
Cycloepoxylactone	240.099	240.1	0.86	4.59	3068.635	+H

Component	Expected mass (Da)	Observed mass (Da)	Mass error (mDa)	Observed RT (min)	Response	Adducts
Enniatin analog	653.425	653.423	-1.30	10.08	89707.8	-e, +H
Enniatin B3	499.252	499.254	1.67	8.99	19014.17	+H
Enniatin H	653.425	653.424	-0.85	9.94	106129.9	-e, +H
Enniatin I	667.440	667.439	-1.13	10.44	2319.854	-e, +H
Enniatin K1	625.393	625.392	-1.72	9.20	60364.23	-e, +H
Epoxysorbicillinol	264.099	264.100	0.81	6.33	49482.38	+H, +Na
Ercalcitriol	428.3290	428.3295	0.51	11.910	23584.54	+Na, +H
Leukotriene A4	318.219	318.2204	1.08	9.84	81296.85	+Na, +H
Migrastatin	489.272	489.273	0.49	10.35	85601.98	+Na, +H
Migrastatin	489.272	489.273	0.39	10.11	4288.39	+Na
Monocillin II	300.136	300.135	-1.15	8.73	62876.56	+H
Monocillin III	332.125	332.127	1.83	7.38	630.9197	+H
Mycotoxin T-2_insariotoxin	466.220	466.221	0.85	9.14	16150.8	-e, +H
Penicillanthranin B	536.131	536.134	2.90	8.09	61200.58	+Na
Penicillin V	350.093	350.092	-1.08	3.38	51711.13	-e, +H
Phomenone	264.136	264.137	0.95	5.73	4002.389	+Na, +H
Pochonin F	332.125	332.127	1.73	5.38	632.2116	+Na
Pochonin J	350.136	350.137	0.83	7.09	9101.404	+H, +Na
Pseurotin A	431.1580	431.1583	0.34	5.79	6644.967	+Na
Pyrenocine A	208.073	208.074	0.99	2.37	34043.92	+Na
Rhodolamprometrin	314.042	314.044	1.38	6.89	7216.092	+Na
Salfredin B11	232.073	232.0734	1.01	4.75	41062.23	+H, +Na
Sorbicillinol	248.104	248.103	-1.48	2.57	27146.92	+H
Trichodermone	415.235	415.234	-1.30	8.04	2168.256	+H
Verimol J	182.094	182.095	1.01	2.74	36577.03	+H
Viridin	352.094	352.095	1.04	6.92	1679.545	+Na

4.3.5 *In silico* screening and identification of lead molecules with nematicidal activity

The *in silico* docking study was performed on twelve bioactive ligand molecules identified from the ethyl acetate extract of *P. chlamydosporia* against two excretory/secretory (ES) proteins of plant-parasitic nematodes, glutathione S-transferase and venom allergen-like protein. The study aimed to identify potential lead molecules for nematicidal activity. The best hits were defined as compounds with ΔG_{bind} (binding energy) values less than -5 kcal/mol. All twelve ligand molecules showed negative binding energies, confirming their potential to interact with the target proteins.

Table 4.6 presents the binding affinities of these ligand molecules with venom allergen-like protein and glutathione S-transferase. Among the tested ligands, bisevertinol exhibited the highest binding affinity with glutathione S-transferase (−8.59 kcal/mol), followed by enniatin I (-8.06 kcal/mol) and enniatin H (-7.77 kcal/mol). These results suggest that bisevertinol, enniatin I, and enniatin H are the most promising candidates for nematicidal activity. Figure 4.6 illustrates the molecular interactions of lead compounds bisevertinol (a), enniatinI (b) and enniatin H (c) with glutathione S-transferase.

Similarly, when docked against venom allergen-like protein, enniatin H showed the strongest binding affinity (-11.42 kcal/mol), followed by enniatin I (-10.9 kcal/mol) and bisevertinol (-10.17 kcal/mol). Figure 4.7 depicts the molecular interactions of lead compounds enniatin H (a), enniatin I (b) and bisevertinol (c) with venom allergen-like protein. The strong binding affinities of these compounds with both proteins suggest their potential as nematicidal agents. These results confirm that bisevertinol, enniatin H, and enniatin I could serve as lead compounds for developing nematicides to control plant-parasitic nematodes. Table 4.7 provides the drug-likeness properties of the lead molecules, further validating their potential as nematicidal agents.

Table 4.6: Molecular interaction of lead molecules identified from ethyl acetate extract of *Pochonia chlamydosporia* with glutathione s-transferase and venom allergen-like protein of plant-parasitic nematodes.

Ligand Molecules	Receptor Molecules (ES Proteins)							
	Glutathione S-transferase				Venom allergen-like protein			
	Binding energy (kcal/mol)	Inhibition constant	H- Bond	Bond type	Binding energy (kcal/mol)	Inhibition constant	H-Bond	Bond type
Acremine B	-5.32	126.41	3	N..H; N..H; N..O	-6.5	17.16	3	O..H; N..O; O..H
Asperlin	-4.69	366.63	No. H- bonds	-	-5.57	82.12	1	OH..O
Asteltoxin	-6.33	22.73	1	N..H	-8.7	420.88	1	O..H
Bisevertinol	-8.59	502.45	1	O..H	-10.17	35.35	No H-bonds	-
Coniothyriomycin	-6.57	15.38	1	O..H	-7.35	4.1	2	OH..H ; N..H
Enniatin H	-7.77	2.02	1	NE..O	-11.42	4.26	1	OH..O
Enniatin I	-8.06	1.23	No. H- bonds	-	-10.9	10.24	2	N..O ; OH..O
Monocillin II	-7.19	5.34	1	O..H	-8.8	356.05	1	OH..O
Pochonin F	-7.37	3.99	1	N..O	-8.47	613.7	2	N..O ; OH..O,
Pseurotin A	-6.58	15.05	2	N..H; N..O	-8.29	841.71	4	O..H ; O..H ; OH..H ; OH..O
Pyrenocine A	-4.81	297.65	No H-bonds	-	-5.52	90.52	1	N..O
Viridin	-7.55	2.92	1	N..O	-8.46	632.74	1	O..H

Table 4.7: Drug-likeness evaluation of lead molecules identified from ethyl acetate extract of *P. chlamydosporia*

Lead molecules	**Water solubility** (log mol/L)	**Caco2 permeability** (Log Papp in 10^{-6} cm/s)	**Intestinal absorption** (human-%)	**P-glycoprotein substrate** (yes/no)	**VDss** (human) (logL/kg)	**BBB permeability** (log BB)	**CYP2D6 substrate** (yes/no)	**AMES toxicity**	**Hepato-toxicity**
Enniatin H	-3.092	0.798	48.269	Yes	-0.082	-1.16	No	No	No
Bisvertinol	-4.65	0.292	51.341	Yes	-0.425	-0.945	No	No	No
Enniatin I	-3.218	0.823	48.508	Yes	-0.074	-1.228	No	No	No

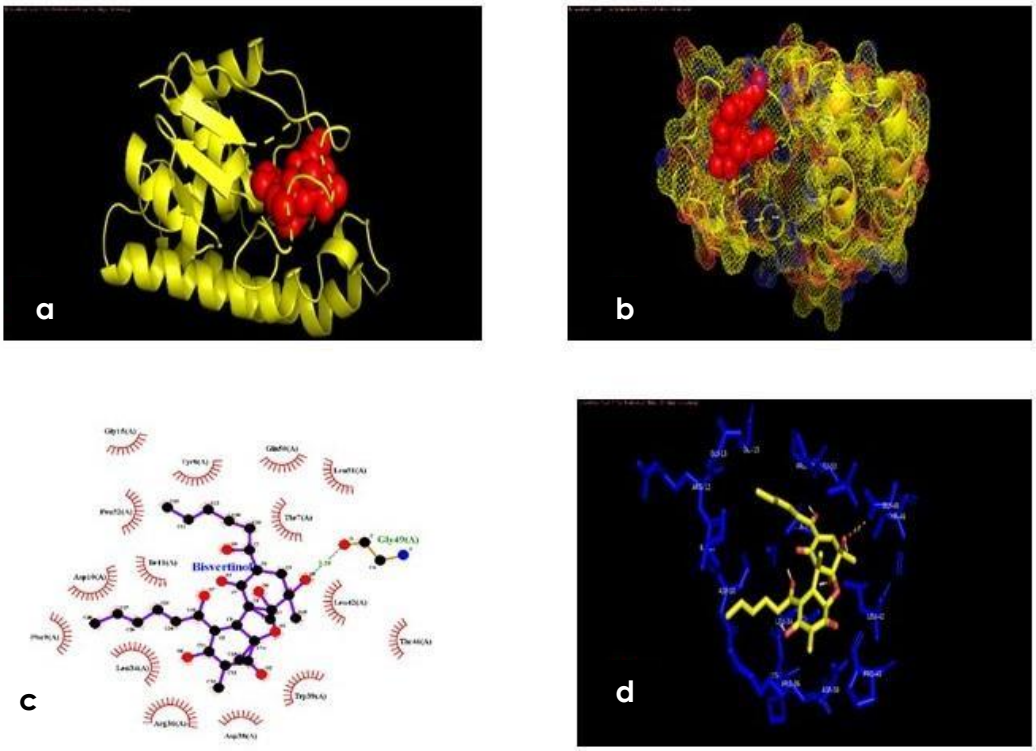

Fig. 4.6a: Docking images of lead molecule, bisevertinol from *P. chlamydosporia* with the target protein glutathione S-transferase, of plant parasitic nematodes. **a)** Ribbon model **b)** 3D mesh model **c)** 2D diagram showing interaction **d)** 3D diagram showing interaction

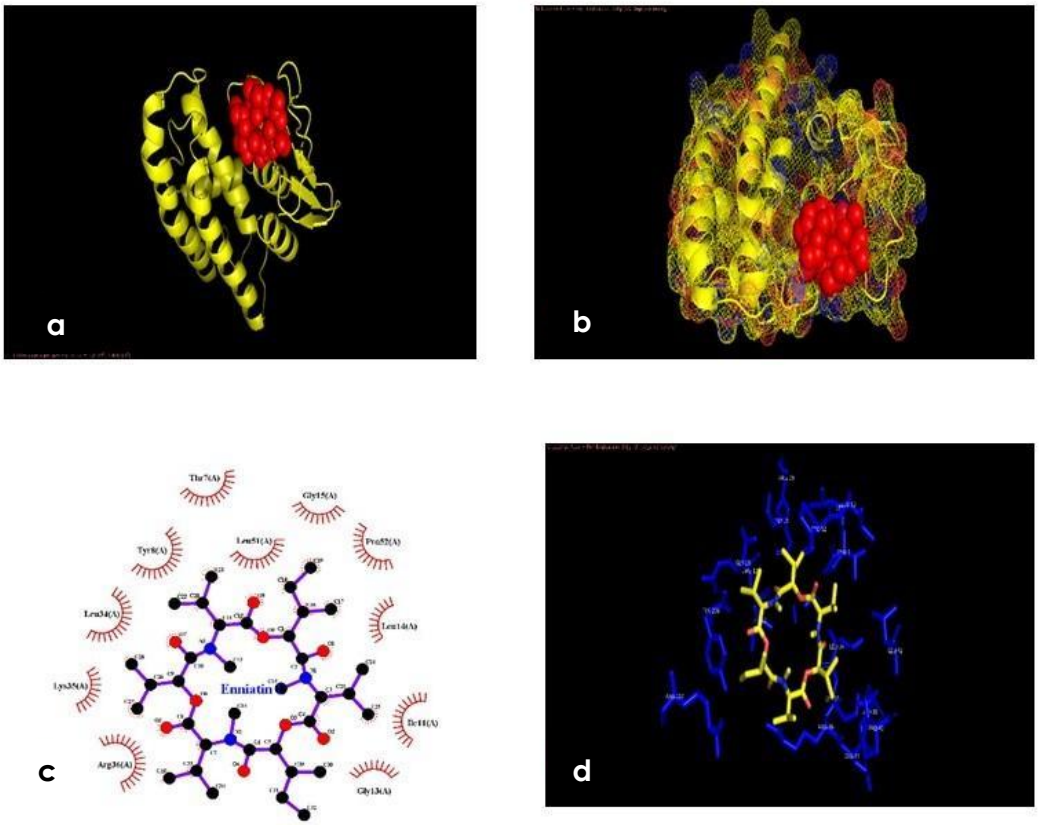

Fig. 4.6b Docking images of lead molecule, Enniatin I from *P. chlamydosporia* with the target protein glutathione S-transferase, of plant parasitic nematodes. **a)** Ribbon model **b)** 3D mesh model **c)** 2D diagram showing interaction **d)** 3D diagram showing interaction

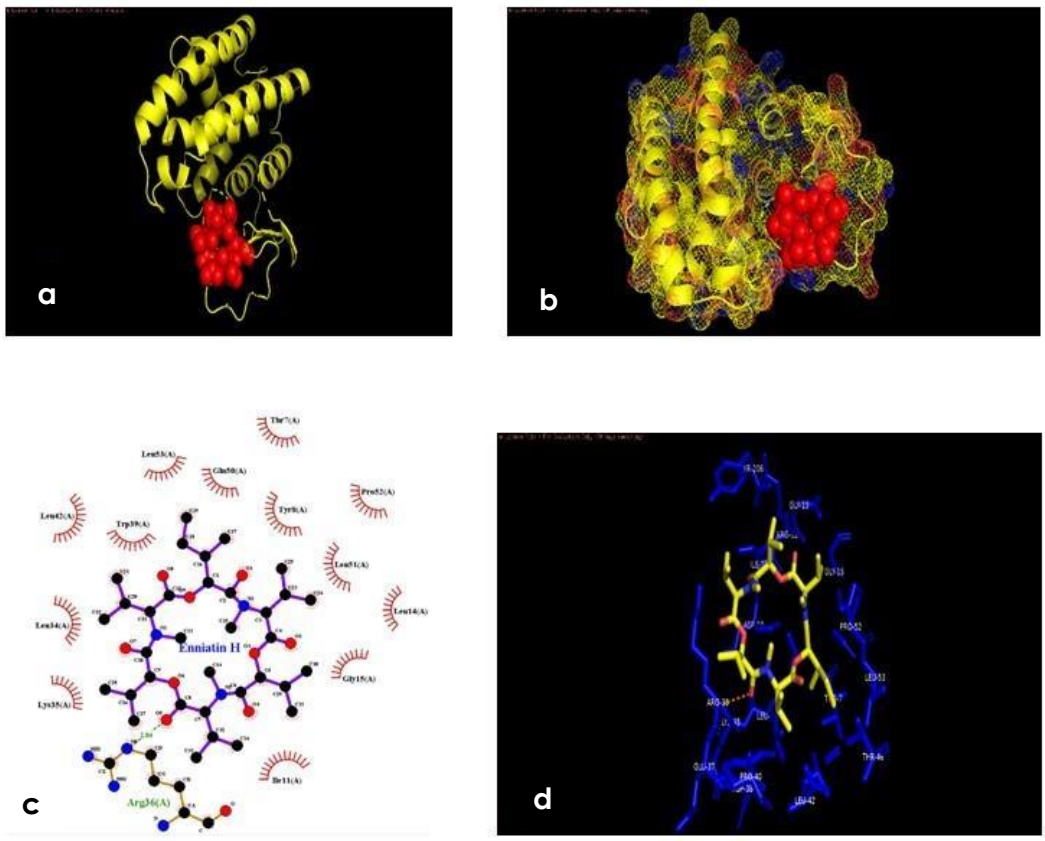

Fig. 4.6c Docking images of lead molecule, Enniatin H from *P. chlamydosporia* with the target protein glutathione S-transferase, of plant parasitic nematodes. **a)** Ribbon model **b)** 3D mesh model **c)** 2D diagram showing interaction **d)** 3D diagram showing interaction

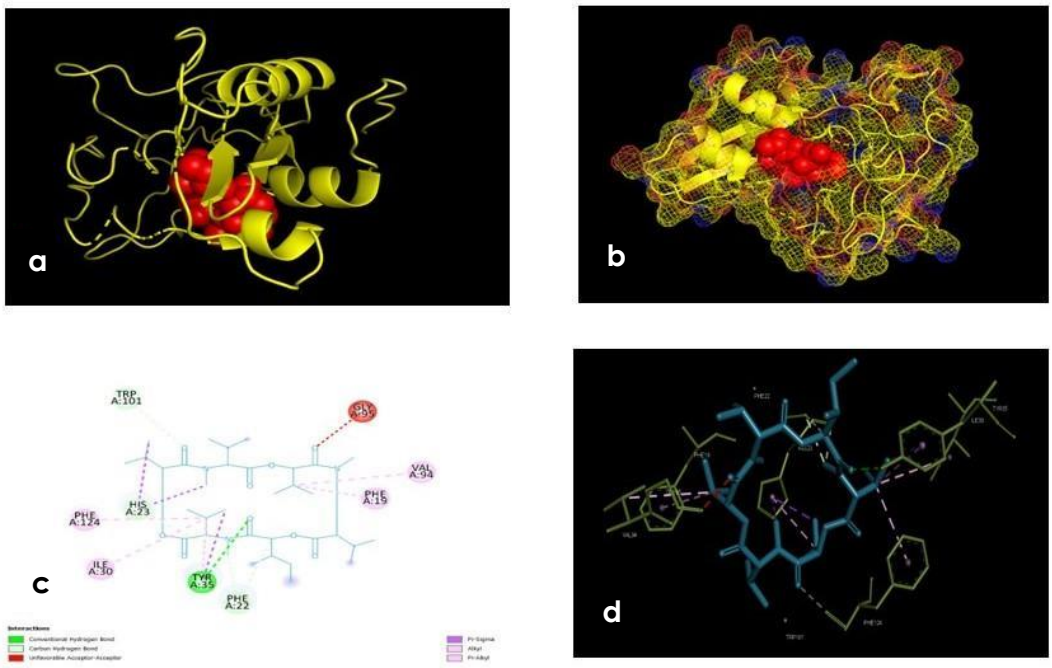

Fig. 4.7a Docking images of lead molecule, Enniatin H from *P. chlamydosporia* with the target protein, venom allergen-like protein of plant parasitic nematodes **a)** Ribbon model **b)** 3D mesh model **c)** 2D diagram showing interaction **d)** 3D diagram showing interaction

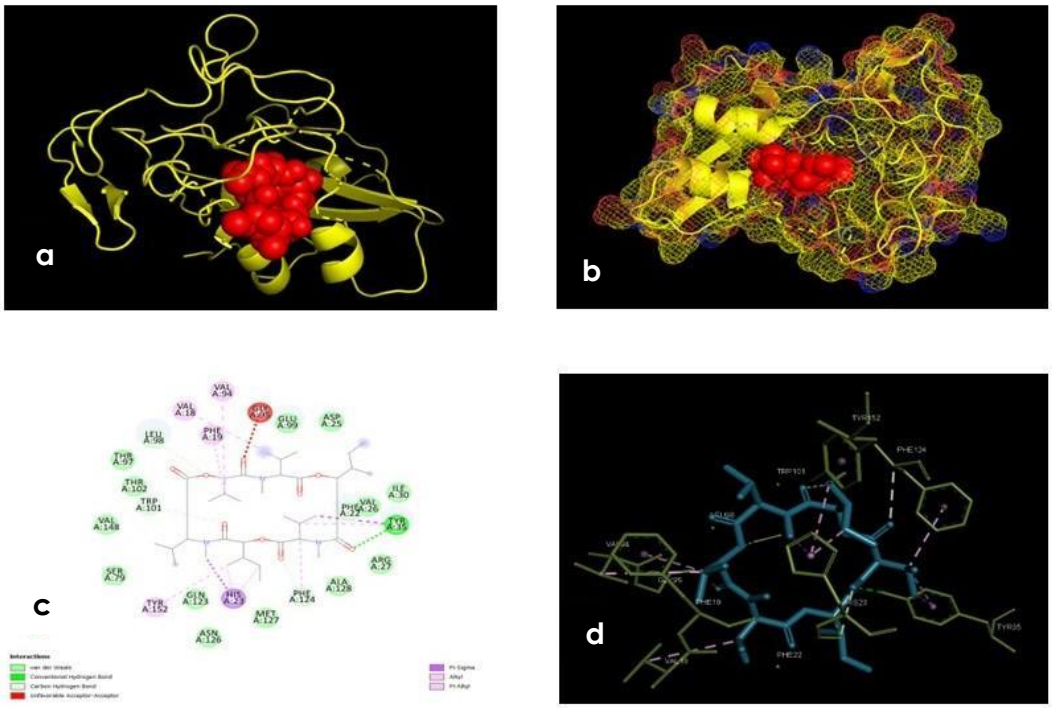

Fig. 4.7 b Docking images of lead molecule, Enniatin I from *P. chlamydosporia* with the target protein, venom allergen-like protein of plant parasitic nematodes **a)** Ribbon model **b)** 3D mesh model **c)** 2D diagram showing interaction **d)** 3D diagram showing interaction

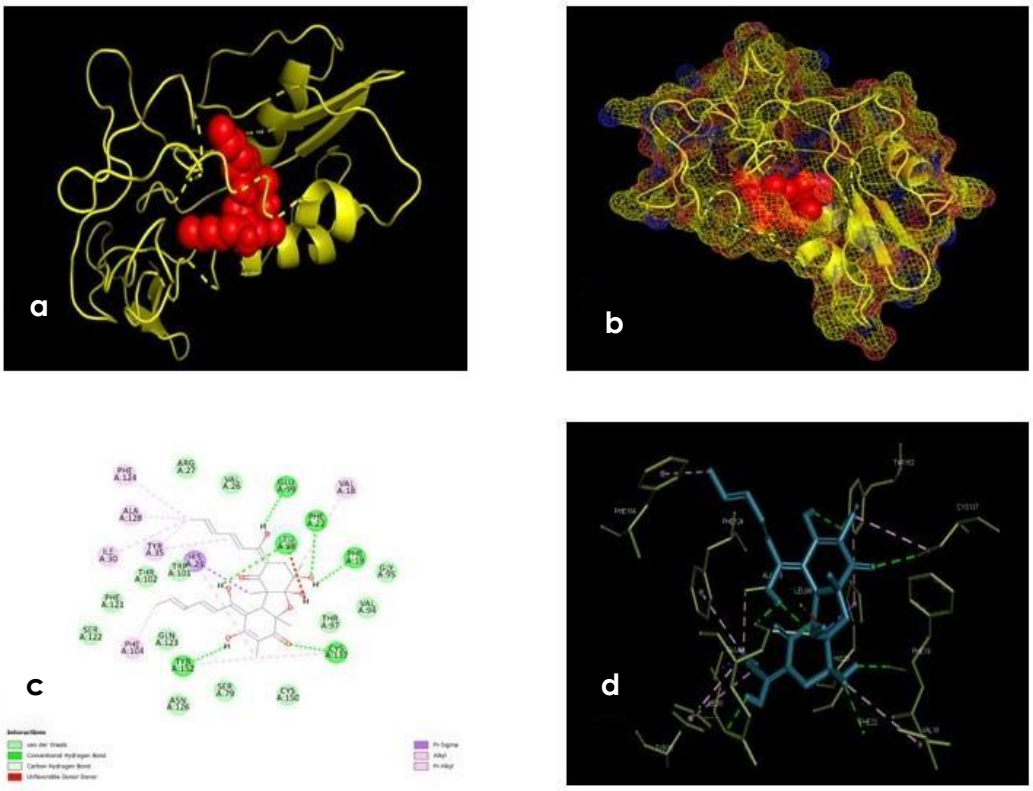

Fig.4.7c Docking images of lead molecule, bisevertinol from *P. chlamydosporia* with the target protein, venom allergen-like protein of plant parasitic nematodes **a)** Ribbon model **b)** 3D mesh model **c)** 2D diagram showing interaction **d)** 3D diagram showing interaction.

4.4 Discussion

Plants and microbes produce a variety of secondary metabolites, small organic compounds that play significant roles in ecological interactions. These compounds, particularly abundant in plants and fungi, often exhibit diverse chemical properties, although their precise physiological roles remain largely unknown. Fungal secondary metabolites (SM) are a broad class of compounds essential for biological control in agriculture. Many beneficial microorganisms depend on these metabolites for biofertilization and crop protection, as they possess direct toxic effects on phytopathogens and can stimulate host systemic defences, promoting root and shoot development or disease resistance (Elhamouly et al., 2022).

Nematophagous fungi, known for their ability to produce various secondary metabolites, exhibit a range of biological activities. The production of these metabolites can vary across different strains and environmental conditions. For instance, secondary metabolite production in *P. chlamydosporia* can differ depending on the geographic region (Manzanilla-López et al., 2017). The primary goal of this study was to investigate the secondary metabolites produced by *P. chlamydosporia,* particularly from humid tropical soils, and evaluate their potential as biocontrol agents.

In this study, *P. chlamydosporia* exhibited strong antagonistic activity against several pathogens, including *Pythium myriotylum*, *Macrophomina* sp., *Colletotrichum* sp., *Phytophthora* sp., *Fusarium* sp., and *Exerohilum rostratum*. The highest percentage inhibition of radial growth (PIRG) was observed for *P. myriotylum* and *Phytophthora* sp. exhibited. These results are consistent with previous research that demonstrated the antagonistic effects of *P. chlamydosporia* against soil-borne fungal plant pathogens such as *Rhizoctonia solani* (Jacobs et al., 2003), *Fusarium oxysporum* (Monfort et al., 2005), and *Pythium aphanidermatum* (Lumsden et al., 1982). Furthermore, *P. chlamydosporia* has been reported to suppress *Phytophthora capsici* when used as a root dip treatment (Sutherland and Papavizas, 1991).

The ethyl acetate extract of *P. chlamydosporia* in this study demonstrated significant nematicidal activity against *Radopholus similis*, with the crude extract showing the strongest activity. The secondary metabolites extracted are likely responsible for the biocontrol efficacy of *P. chlamydosporia*. Previous studies have shown that *P. chlamydosporia* can act as a root endophyte, producing toxins or inducing resistance in plants such as bananas to control migratory nematodes like *Pratylenchus* spp. and *R. similis* (Freitas et al., 2009). Similar studies have isolated nematicidal compounds from *P. chlamydosporia,* such as phomalactone, which was reported to be effective against *Meloidogyne incognita* (Khambay et al., 2000). Other secondary metabolites, including lowdenic acid and pochonins, have been identified from the ethyl acetate extract of *P. chlamydosporia* (Angawi et al., 2003; Hellwig et al., 2003; Shinonaga et al., 2009a). The chemical profile of *P. chlamydosporia* was further analysed using thin-layer chromatography (TLC) and UPLC-(ESI)-QToF-MS, identifying 47 bioactive compounds. The three primary nematicidal compounds were enniatin, viridin, and pseurotin A. Enniatins are well-known for their nematicidal, antibacterial, herbicidal, and insecticidal properties (Hyun et al., 2009; Sy-Cordero et al., 2012). Enniatin B, in particular, has demonstrated nematicidal activity against *Meloidogyne javanica* (Ciancio, 1995). Similarly, pseurotin A, produced by *Aspergillus fumigatus* and *Penicillium janczewskii*, has potent nematicidal properties (Schmeda-Hirschmann et al., 2008). According to Hellwig (2003), the majority of *P. chlamydosporia* isolates grown in Q6-medium included pseurotin A as a major metabolite. Hayashi et al. (2007) reported that pseurotin A demonstrated potent nematicidal actions against *Bursaphelenchus xylophilus* without causing any inhibition of plant growth. Viridin, a metabolite of *Trichoderma viride,* has shown significant nematicidal activity (Khan et al., 1989). In addition to these nematicidal compounds, the study identified enniatin, coniothyriomycin, and acremine as major antifungal metabolites. Acremines, produced by members of the *Acremonium* genus, have antifungal properties and can suppress sporangia germination of oomycetous pathogens (Yao et al., 2015). Coniothyriomycin has been shown to be effective against *Phytophthora infestans* (Krohn et al., 2003). Furthermore, monocillin, pyrenocine A, and enniatin were

identified as important antibiotic compounds in the extract. Monocillin has broad-spectrum activity against fungi and bacteria (Ayer et al., 1980; Aver and Peña-Rodriguez, 1987; Qin et al., 2019), while pyrenocine A exhibits antifungal, antibacterial, and cytotoxicproperties (Sparace et al., 1987; Nilanonta et al., 2003, Krohn et al., 2008).

Asperlin is one of the major antimicrobial chemicals in our ethyl acetate extract. A broad variety of microorganisms, including bacteria, fungi, and protozoa, were inhibited in their growth by asperlin. It was also discovered to possess antitumor properties (Owen and Bhuyan, 1965). The extract also contained notable antiviral chemicals, such as pochonins and asteltoxin, which have demonstrated activity against H1N1 and H3N2 viruses (Tian et al., 2015). Pochonins, in particular, have been shown to inhibit herpes simplex virus (HSV-1) and protozoan parasites (Hellwig et al., 2003). Enniatin and bisvertinol were the primary cytotoxic and antitumor compounds identified. Bisvertinol, isolated from *Trichoderma* species, has strong anticancer, and radical scavenging activities (Abe et al., 1999; Abdel Lateff et al., 2009; Meng et al., 2016).

In silico screening was performed on 12 bioactive compounds from the ethyl acetate extract to assess their potential as nematicidal agents. Molecular docking studies revealed strong interactions between bisevertinol, enniatin I, enniatin H, and two ES proteins glutathione s-transferase and venom allergen-like protein from *R. similis*. These proteins play key roles in nematode parasitism, making them important targets for nematicidal drug development (Li et al., 2021; Rosana et al., 2016). Similar virtual screening techniques have been employed to identify nematicidal compounds in other studies (Shanmugam et al., 2018; Sharma et al., 2012; Taylor et al., 2013). The strong binding affinities of bisevertinol, enniatin I, and enniatin H suggest that these compounds are promising candidates for the development of novel nematicidal drugs.

4.5 Conclusion

This study highlights the potential of *P. chlamydosporia* as a source of bioactive secondary metabolites with nematicidal, antifungal, and antiviral properties. The

identification of key compounds, including bisevertinol, enniatin I, and enniatin H, offers promising leads for the development of novel nematicidal agents. These findings suggest that *P. chlamydosporia* could be effectively utilised in sustainable agricultural practices, particularly in black pepper cultivation, to control plant-parasitic nematodes and enhance crop growth. Further studies on the mechanisms of action and field trials are warranted to optimise the application of these metabolites for agricultural pest management.

Chapter 5

Transcriptome Profiling of Black Pepper Roots Colonised by *Pochonia chlamydosporia*

Abstract

Pochonia chlamydosporia, an egg-parasitic fungus, has long been studied for its potential as a biological control agent for plant-parasitic nematodes. This fungus has been demonstrated to stimulate plant growth in a variety of agronomic crops and can also function as an endophyte in monocot and dicot plants. In the current work, a transcriptome analysis was carried out on the study of the time-dependent effect of endophytic fungus *P. chlamydosporia* inoculated on black pepper roots. A next generation Sequencing (NGS) using Illumina HiSeq500 platform was applied for the study at two different time intervals (14 and 28 dpi (day after post inoculation). *De novo* transcriptome assembly and analysis of differential gene expression discovered 2,03,092 transcripts and 65,354 differentially expressed genes (DEG) between the inoculated and uninoculated control samples, in which 289 and 37 were consistently up-and downregulated across all time points, offering light on the growth promotion and endophytism process. Genes associated with stress resistance and induced systemic resistance (ISR) signalling was found to be enriched in the black pepper transcriptome under endophytism, according to functional gene ontology (GO) analysis. In addition, we discovered an up-regulation of genes involved in the biosynthesis of plant hormones such as auxin, ethylene, cytokinin, abscisic acid, and gibberelin in our transcriptome analysis. The genes associated with nutrient (nitrogen, phosphorus, potassium, calcium, iron, boron, and zinc) availability, were also found to be upregulated, supporting the plant growth promotion. The upregulation of defence-related genes such as pathogenesis-related (PR) proteins, lipid-transfer protein (DIR1), endochitinase (a hydrolytic enzyme), germin like proteins, late embryogenesis abundant (LEA) proteins, LURP1, thaumatin and Major latex-like proteins (MLPs) showed the endophytic and biocontrol ability of the fungus. Furthermore, KEGG enrichment analysis revealed that differentially expressed genes were classified a larger extend into Plant hormone signal transduction pathways. Our research provides molecular evidence that *P. chlamydosporia* has a growth-promoting effect on plants that are colonised endophytically. This finding paves the way for future research on the fungus's ability to reduce the damaging effects of biotic and abiotic factors on plant crops.

5.1. Introduction

Black pepper (*Piper nigrum*) known as 'King of Spices', is among the most significant and widely used spices globally. Black pepper production is influenced by numerous biotic and abiotic factors, with plant-parasitic nematodes being a critical biotic factor that causes substantial economic losses and impacts overall crop yield. Synthetic nematicides have been extensively used to manage these nematode populations; however, many majorities of these pesticides have been withdrawn due to adverse environmental impacts and unintended consequences. This has led researchers to seek more sustainable, eco-friendly methods for controlling plant-parasitic nematodes, with endophytes and fungal biological control agents emerging as promising alternatives (De Zelicourt et al., 2013).

P. chlamydosporia, an egg-parasitic fungus, has been traditionally studied for its potential as a biological control agent against plant-parasitic nematodes. Isolated from soils, rhizospheres, and infected eggs of cyst and root-knot nematodes worldwide, *P. chlamydosporia* is a beneficial species with potential for industrial application due to its role in the rhizosphere and its contribution to plant health. This fungus exhibits a tritrophic lifestyle, encompassing root endophytism, root-knot nematode parasitism, and saprotrophic metabolism, which collectively enhance plant growth (Manzanilla-López et al., 2013; Zavala-Gonzalez et al., 2017). As a root endophyte, *P. chlamydosporia* colonises a wide range of plant species, promoting growth in crops such as lettuce, tomato, wheat, pistachio, and barley (Larriba et al., 2015).

P. chlamydosporia supports colonisation by modulating plant defence mechanisms at both structural and biochemical levels, such as forming root papillae and secreting phenolic compounds (Escudero and Lopez-Llorca, 2012). Recent studies on *Arabidopsis* indicate that jasmonate signalling is a critical pathway in managing the progression of plant colonisation by this fungus (Zavala-Gonzalez et al., 2017). In tomatoes, *P. chlamydosporia* endophytism has been shown to influence the expression of miRNAs and their target genes, which are vital for plant signalling and perception, thereby enabling the plant to recognise and accommodate the fungus as an endosymbiont (Pentimone et al., 2018). Furthermore, the root transcriptome of barley

in response to *P. chlamydosporia* colonisation displays upregulation of genes associated with plant growth hormones, as well as genes involved in defence and stress responses (Larriba et al., 2015).

In this study, black pepper was chosen as a model crop to identify black pepper genes involved in promoting plant growth and regulating defensive responses, thereby enhancing our understanding of the molecular interactions between *P. chlamydosporia* and its host plants.

5.2. Materials & Methods

5.2.1. *Fungal strain and plant material*

The fungal strain used for this study was *P. chlamydosporia* (MTCC5412), obtained from the biocontrol agent repository at the ICAR-Indian Institute of Spices Research (IISR), Kozhikode, India. Sequence data for the *P. chlamydosporia vcp1* (alkaline serine protease p1) gene is available in the NCBI database under accession number MW553913. The strain was cultured on potato dextrose agar (PDA) plates at 28ºC ± 2° C for 10 days. The experiment used healthy, one-month-old black pepper (variety Sreekara) rooted cuttings, grown in 1kg pots (dimensions: 13 cm x 8 cm x 12 cm) with sterilised soil. The plants were maintained in a greenhouse at 28 - 30^0C with 70-80% humidity. The inoculum consisted of *P. chlamydosporia* grown on rice substrates (10^8 CFU/g), with each plant receiving 5 g of this inoculum. Uninoculated plants served as controls. Three plants each were sampled at intervals of 14 and 28days post-inoculation to study the transcriptomic response to fungal colonisation.

5.2.2 *Isolation of total RNA from black pepper roots*

Root samples were collected 14 and 28 days after *P. chlamydosporia* inoculation, as well as from uninoculated plants at corresponding growth stages. Each RNA-Seq sample consisted of roots from three plants. Total RNA was extracted using the Norgen Total RNA Purification Kit (NorgenBiotek, Canada) following the manufacturer's protocol. RNA quantity and quality were assessed using a Nanodrop Spectrophotometer (DeNovix, Wilmington, DE, USA).

5.2.3 *Library preparation and sequencing*

RNA-seq paired-end libraries were prepared from QC passed RNA samples using the Illumina TruSeq Stranded mRNA sample preparation kit. Library preparation and sequencing were conducted by M/s Eurofins Genomics India Pvt. Ltd. Briefly, mRNA was enriched from total RNA using Poly-T attached magnetic beads, followed by fragmentation, first-strand cDNA synthesis, and conversion to second-strand cDNA. Purified cDNA was then subjected to adapter ligation and PCR enrichment. Libraries were analyzed on Agilant 4200 TapeStation system with D1000 ScreenTape. The Illumina libraries were sequenced on HiSeq500 platforms to generate paired-end reads.

5.2.4 *De novo transcriptome assembly*

The generated sequences have been added to the NCBI Sequence Read Archive (SRA) under accession number PRJNA1187805. Raw sequencing data were processed with Trimmomatic v0.38 (Bolger et al., 2014) to remove adapters, ambiguous reads, and low-quality sequences (threshold QV < 20). High-quality paired-end reads (QV>20) were used for *de novo* assembly with Trinity (version 2.8.4) (Henschel et al., 2012) with a kmer size of 25. To remove isoforms, transcripts were clustered using CD-HIT-EST-4.6 (http://weizhong-lab.ucsd.edu/cd-hit/). Only unigenes with >85% coverage at 3X read depth were included for further analysis.

5.2.5 *Coding sequence (CDS) prediction*

Coding sequences were predicted from the unigenes using TransDecoder v5.3.0 (http://transdecoder.github.io/), which identifies candidate ORFs. In cases of nested ORFs, the longest was retained. A single unigene could report multiple ORFs, supporting operons and chimeras.

5.2.6 *Functional annotation*

The DIAMOND program (BLASTX mode) (Buchfink et al. 2015) was used for functional annotation of the predicted CDS by mapping them against the NR protein database from NCBI to identify homologous sequences.

5.2.7 *Gene ontology (GO) analysis*

Gene ontology (GO) analysis of the CDS was conducted using Blast2GO (Conesa et al. 2005), classifying predicted CDS into Biological Process (BP), Molecular Function (MF) and Cellular Component (CC) categories.

5.2.8 *Functional annotation of KEGG pathways*

To determine the potential involvement in biological pathways, CDSs were mapped to canonical pathways in KEGG (Kyoto Encyclopedia of Genes and Genomes) database using the KEGG Automatic Annotation Server, KAAS (http://www.genome.jp/kaas-bin/kaas_main) (Moriya et al., 2007). Outputs included KEGG Orthology (KO) assignments, Enzyme Commission (EC) numbers, and pathway annotations.

5.2.9 *Differential gene expression analysis*

Differential expression analysis between control and treated samples was performed using DESeq (version 1.22.1) (Anders and Huber, 2012). Dispersion was estimated with parameters: method = "blind", sharingMode = "fit-only" and fitType = "local". Log2 fold change (FC) value was calculated as: $FC = Log2\ (Treated/Control)$. CDSs with log2 FC >0 was considered up-regulated, while those with log2 FC < 0 were down-regulated. A P-value threshold of 0.05 was applied for statistical significance.

5.2.10 *Expression validation of RNA-Seq analysis by qRT-PCR*

Quantitative RT-PCR (qRT-PCR) was performed to validate RNA-Seq results for selected differentially expressed genes (DEGs) at 14 and 28 dpi. Nine genes associated with defence (UPL and WRKY), hormone metabolism (WAT and GRP), signalling (ERT), stress tolerance (MYB), and plant growth mechanisms (MIP, ZT and PCK) were analysed. Total RNA from roots (both treated and control) at 14 and 28 dpi was extracted using the Norgen Purification Kit (NorgenBiotek, Canada). RNA was quantified and quality-checked with a Nanodrop Spectrophotometer (DeNovix, Wilmington, DE, USA). cDNA synthesis was done using RevertAid First- Strand

cDNA synthesis kit (Thermo Fisher Scientific assachusetts, USA). Primers were designed with PrimerQuest™ (IDT, USA) and listed in Table 5.1. qRT-PCR was conducted in triplicate on three biological samples using QuantiFast SYBR Green PCR kit (Qiagen, Germany) on a Rotor-Gene Q real-time PCR machine (Qiagen, USA). Transcript fold change relative to control (0 dpi) was calculated by the $2^{-\Delta\Delta Ct}$ method using ubiquitin conjugating enzyme as the reference gene (Umadevi et al. 2019).

Table 5.1: List of primers used in qRT-PCR analysis for validation of RNA-Seq results

Gene ID	Primer sequence (5' – 3')	Encoding protein	Product size (bp)
MIP	ACGGTTGCTCATGGCTATAC / GAATCTCTGGCACTCCTCTTG	Major intrinsic protein PIPB	116
MYB	GTAACAGGTGGTCGGCAATA / GCCCATCTTCTCTAACCTCTTC	Myb family transcription factor	104
UPL	GATGTGGAGATTCCTTCGTTCT / TCCAACTCTCTATGCTCTCTCT	Ubiquitin-protein ligase	112
WAT	GAGATGGTGTGGTCCAAGTATG / CCAAAGTGGCTATGATGAGAAGA	WAT1-related protein	115
ZT	ACATTTCCACCTCCCTCCT / CATACCTTGACCCTGATCAACC	zinc transporter	127
WRKY	ACTTTGGGCACACAGAAGAA / GATGGAGCCATGGAGGTATTG	WRKY transcription factor 13	106
PCK	GTGATGGGAGCAGAGATACAAG / GGAAGCCTAAGACAGCTCAAA	potassium transporter	98
GRP	TGTTCAAGGAGGTGCAGTAAG / CAAACTTCCTTGTTGCCGTAAG	Gibberellin-regulated protein	116
ERT	GAAGTGGGTGGCTGAGATT / GCCGCGGAGGATAAACA	Ethylene-responsive transcription factor	118

5.3 Results

5.3.1 *RNA-seq evaluation and de novo transcriptome assembly*

The RNA-seq analysis of all three sample groups (control, 14 and 28 dpi) yielded a combined total of 43,350,878 high-quality paired-end reads (QV>20), resulting in approximately 12.7 GB of transcriptome data. The high-quality reads were assembled into contigs, which were then further processed into transcripts. The Trinity de novo assembler, using a kmer size of 25, combined the high-quality mapped reads across all samples to produce 203,092 transcripts. To reduce redundancy and remove isoforms, the assembled transcripts were clustered using CD-HIT-EST-4.6, resulting in 94,345 unigenes, representing 85% of the original transcripts. Coding regions within these unigenes were identified using TransDecoder, predicting 51,712 coding sequences (CDS) that were subsequently used for functional annotation. Table 5.2 summarises the key statistics of the de novo transcriptome assembly, including the number of contigs, contig N50, and other relevant metrics.

Table 5.2: Summary statistics of transcriptome assembly of *P. chlamydosporia*-inoculated black pepper samples

Sequence type	Count	Contig N50	Shortest contig	Longest contig	Mean contig size
Transcripts	2,03,092	1,886	182	16,664	1074
Unigenes	94,345	1,974	201	16,664	1,243
Coding sequences	51,712	3,046	255	14,721	1,239

This assembly data provides a comprehensive foundation for further functional analysis of *P. chlamydosporia's* influence on black pepper root transcriptome, facilitating insights into genes involved in plant growth promotion and defence responses during fungal colonization.

5.3.2 *Functional annotation and differential gene expression analysis*

The functional annotation of the pooled CDS identified 43,378 annotated sequences (83.88%). Transcriptome analysis across two time points (14 and 28 dpi) revealed

65,354 differentially expressed genes (DEGs) during *P. chlamydosporia* colonisation in black pepper roots. At 14 dpi, 27,353 DEGs were observed, with 737 significantly (Supplementary Table 1) upregulated and 667 downregulated. In contrast, at 28 dpi, 38,001 DEGs were recorded, with 1,668 (Supplementary Table 2) upregulated and 488 downregulated. Figure 5.1 displays the volcano plots of DEGs for 14 and 28 dpi. Notably, 289 genes were consistently upregulated and 37 downregulated across both time points, highlighting genes potentially involved in growth promotion and endophytism.

Four primary categories of upregulated genes emerged: signalling, defence proteins, stress tolerance, and plant growth promotion. Genes in the plant growth and development category were grouped into three main areas: aquaporins, nutrient uptake, and plant hormone synthesis. Aquaporins, including MIPs (major intrinsic proteins), TIPs (tonoplast intrinsic proteins), PIPs (plasma membrane intrinsic proteins), and NIPs (nodulin 26-like intrinsic proteins) play essential roles in cell wall reconstruction, photosynthesis, and water homeostasis (Fig. 5.2A). Genes associated with nutrient uptake (nitrogen, phosphorus, potassium, calcium, iron, boron, and zinc) were also significantly expressed (Table 5.3). Additionally, genes for auxin, gibberellin, and cytokinin biosynthesis were upregulated at both time points, underscoring their involvement in growth regulation (Table 5.4).

Signalling genes: Signalling-related genes primarily associated with ethylene, jasmonic acid (JA), and abscisic acid (ABA) pathways showed significant upregulation. Among ethylene-responsive genes, 1- aminocyclopropane-1-carboxylate (ACC) synthases and the ERF subfamily of AP2 transcription factors were notably expressed, suggesting ethylene's role in stress responses (Fig. 5.2B). JA biosynthesis-related genes, such as ω-3 fatty acid desaturase, JAZ/TIFY transcription factors, were also upregulated, indicating the importance of JA in defence signalling (Fig. 5.2C). Additionally, genes linked to ABA signalling, zeaxanthin epoxidase (ZEP) and 9-cis-epoxycarotenoid dioxygenase (NCED), were expressed, hinting at ABA's role in stress tolerance.

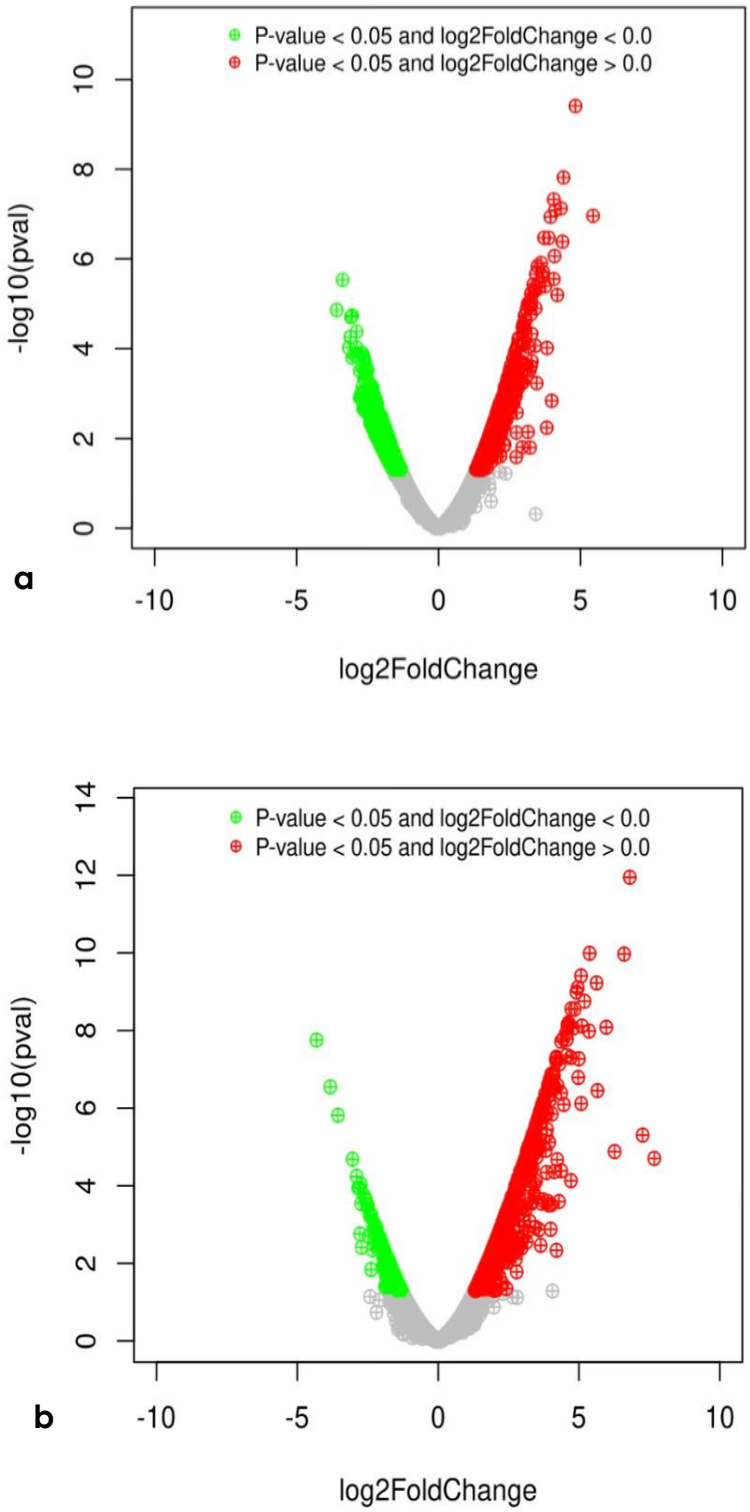

Fig. 5.1: Volcano plots of differentially expressed genes (DEGs) during *Pochonia chlamydosporia* colonisation in black pepper roots **(a)** At 14 dpi; **(b)** At 28 dpi.

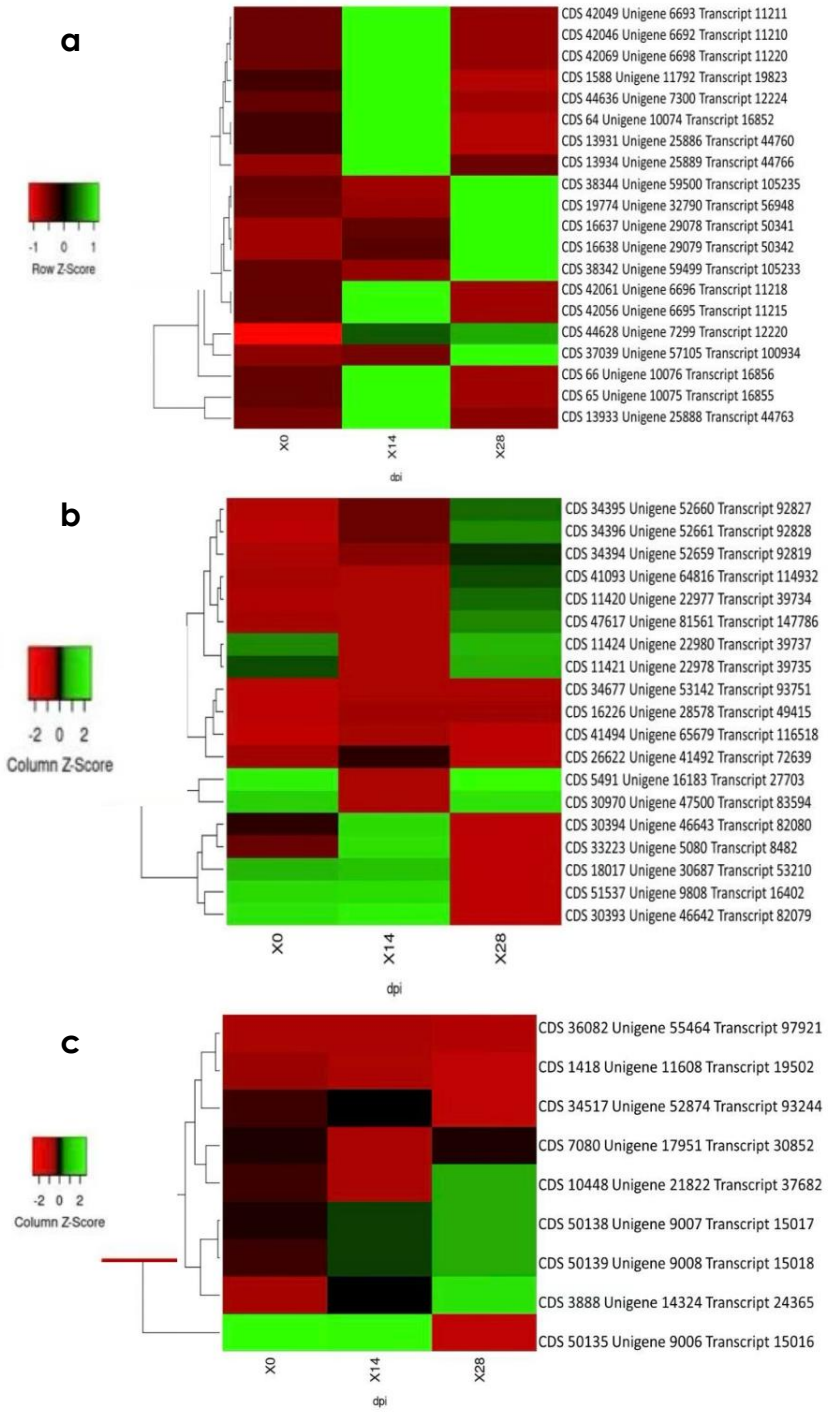

Fig. 5.2: Heatmaps displaying expression levels of three genes in black pepper roots at 14 dpi (X14), 25 dpi (X28), and control (X0). **(a)** Aquaporin; **(b)** Ethylene; and **(c)** Jasmonic acid. Relative abundance is indicated by the color code, which goes from red (low abundance) to green (high abundance).

Table 5.3: Differentially expressed genes that encode proteins involved in the uptake of nutrients in *P. chlamydosporia*-treated black pepper roots.

Group	Transcript ID	Annotation	Log2 fold change	Expression Patterns[a]
Nitrogen	CDS_26477_Unigene_41301_Transcript_72275	glutamate dehydrogenase	2.696	14 dpi
	CDS_43449_Unigene_70077_Transcript_124761	cationic amino acid transporter	2.102	14 dpi
	CDS_4088_Unigene_14558_Transcript_24805	nodulation-signaling pathway protein	1.931	14 dpi
	CDS_3137_Unigene_134_Transcript_208	vacuolar amino acid transporter	1.812	14 dpi
	CDS_2966_Unigene_132_Transcript_206	vacuolar amino acid transporter	1.548	14 dpi
	CDS_26477_Unigene_41301_Transcript_72275	glutamate dehydrogenase	2.369	28 dpi
	CDS_28302_Unigene_43741_Transcript_76804	glutamate dehydrogenase	2.266	28 dpi
	CDS_2509_Unigene_127_Transcript_197	vacuolar amino acid transporter	1.682	28 dpi
	CDS_3137_Unigene_134_Transcript_208	vacuolar amino acid transporter	1.596	28 dpi
	CDS_2966_Unigene_132_Transcript_206	vacuolar amino acid transporter	1.574	28 dpi
	CDS_3309_Unigene_136_Transcript_210	vacuolar amino acid transporter	1.567	28 dpi
	CDS_2883_Unigene_131_Transcript_205	vacuolar amino acid transporter	1.480	28 dpi
	CDS_2597_Unigene_128_Transcript_198	vacuolar amino acid transporter	1.475	28 dpi
	CDS_2696_Unigene_129_Transcript_199	vacuolar amino acid transporter	1.418	28 dpi

Group	Transcript ID	Annotation	Log2 fold change	Expression Patterns[a]
Phosphorous	CDS_41383_Unigene_6540_Transcript_10934	purple acid phosphatase	2.502	14 dpi
	CDS_41378_Unigene_6539_Transcript_10933	purple acid phosphatase	2.267	14 dpi
	CDS_41367_Unigene_6535_Transcript_10928	Purple acid phosphatase	2.049	14 dpi
	CDS_40853_Unigene_6426_Transcript_10714	Purple acid phosphatase	2.044	14 dpi
	CDS_41362_Unigene_6534_Transcript_10927	Purple acid phosphatase	2.036	14 dpi
	CDS_41377_Unigene_6538_Transcript_10932	Purple acid phosphatase	1.977	28 dpi
	CDS_41372_Unigene_6537_Transcript_10931	purple acid phosphatase	1.690	28 dpi
	CDS_41370_Unigene_6536_Transcript_10930	purple acid phosphatase	1.538	28 dpi
	CDS_9171_Unigene_20357_Transcript_35067	SPX domain-containing protein	2.395	28 dpi
	CDS_42463_Unigene_6788_Transcript_11353	SPX domain-containing protein	1.528	28 dpi
	CDS_41370_Unigene_6536_Transcript_10930	purple acid phosphatase	1.811	28 dpi
	CDS_41383_Unigene_6540_Transcript_10934	purple acid phosphatase	1.773	28 dpi
	CDS_41378_Unigene_6539_Transcript_10933	purple acid phosphatase	1.641	28 dpi
	CDS_41362_Unigene_6534_Transcript_10927	Purple acid phosphatase	1.559	28 dpi
	CDS_41377_Unigene_6538_Transcript_10932	Purple acid phosphatase	1.449	28 dpi
Potassium	CDS_15454_Unigene_27681_Transcript_47865	potassium channel KOR2	1.663	14 dpi
	CDS_12751_Unigene_24529_Transcript_42410	potassium transporter	1.427	14 dpi
	CDS_18661_Unigene_31429_Transcript_54526	potassium channel SKOR	1.451	28 dpi
	CDS_12751_Unigene_24529_Transcript_42410	potassium transporter	1.749	28 dpi
	CDS_31593_Unigene_48421_Transcript_85285	potassium transporter	1.379	28 dpi

Group	Transcript ID	Annotation	Log2 fold change	Expression Patterns[a]
Calcium	CDS_18777_Unigene_31566_Transcript_54808	calcium-binding protein	1.976	14 dpi
	CDS_26361_Unigene_41133_Transcript_71973	calmodulin-binding protein	2.090	14 dpi
	CDS_32325_Unigene_49559_Transcript_87293	calcium uniporter protein	1.836	14 dpi
	CDS_29037_Unigene_44723_Transcript_78610	calcium-transporting ATPase	1.568	14 dpi
	CDS_18777_Unigene_31566_Transcript_54808	calcium-binding protein	2.035	28 dpi
	CDS_22983_Unigene_36653_Transcript_63909	calmodulin-like protein	2.030	28 dpi
	CDS_33128_Unigene_50684_Transcript_89254	calmodulin-like protein	1.919	28 dpi
	CDS_33129_Unigene_50685_Transcript_89255	calmodulin-like protein	1.811	28 dpi
	CDS_39301_Unigene_61310_Transcript_108526	calmodulin-binding protein	1.414	28 dpi
	CDS_26361_Unigene_41133_Transcript_71973	calmodulin-binding protein	1.383	28 dpi
	CDS_22984_Unigene_36654_Transcript_63910	calmodulin-like protein	1.375	28 dpi
	CDS_9886_Unigene_21172_Transcript_36523	Calreticulin/calnexin	1.919	28 dpi
	CDS_9887_Unigene_21173_Transcript_36524	Calreticulin/calnexin	2.243	28 dpi
	CDS_15610_Unigene_27868_Transcript_48214	calcium-dependent membrane targeting	1.472	28 dpi

Group	Transcript ID	Annotation	Log2 fold change	Expression Patterns[a]
Iron	CDS_50976_Unigene_9331_Transcript_15615	transcription factor bHLH66	2.432	14 dpi
	CDS_29126_Unigene_44843_Transcript_78800	transcription factor bHLH96]	2.300	14 dpi
	CDS_36274_Unigene_55774_Transcript_98469	transcription factor bHLH123	1.728	14 dpi
	CDS_50969_Unigene_9329_Transcript_15612	transcription factor bHLH66	1.982	14 dpi
	CDS_50960_Unigene_9326_Transcript_15607	transcription factor bHLH66	1.726	14 dpi
	CDS_5691_Unigene_16399_Transcript_28120	transcription factor bHLH47	1.427	14 dpi
	CDS_49254_Unigene_8690_Transcript_14468	transcription factor bHLH155	1.476	14 dpi
	CDS_5690_Unigene_16398_Transcript_28119	transcription factor bHLH47	1.347	28 dpi
	CDS_50964_Unigene_9327_Transcript_15608	transcription factor bHLH82	1.652	28 dpi
	CDS_50973_Unigene_9330_Transcript_15614	transcription factor bHLH82	1.644	28 dpi
	CDS_48273_Unigene_835_Transcript_1408	transcription factor bHLH112	2.109	28 dpi
	CDS_48299_Unigene_836_Transcript_1410	transcription factor bHLH112	1.468	28 dpi
	CDS_11607_Unigene_23191_Transcript_40067	transcription factor bHLH93	4.596	28 dpi
	CDS_29122_Unigene_44838_Transcript_78795	transcription factor bHLH96	2.961	28 dpi
	CDS_29126_Unigene_44843_Transcript_78800	transcription factor bHLH96	2.922	28 dpi
	CDS_30628_Unigene_47003_Transcript_82726	transcription factor bHLH30	1.813	28 dpi
	CDS_24789_Unigene_39061_Transcript_68114	transcription factor bHLH74	1.725	28 dpi
	CDS_11606_Unigene_23190_Transcript_40065	transcription factor bHLH93	1.628	28 dpi
	CDS_49264_Unigene_8694_Transcript_14475	transcription factor bHLH155	1.338	28 dpi

Group	Transcript ID	Annotation	Log2 fold change	Expression Patterns[a]
Boron transporter	CDS_7341_Unigene_18237_Transcript_31402	Boron transporter	3.839	28 dpi
Zinc transporters	CDS_34801_Unigene_53358_Transcript_94166	zinc transporter	1.927	14 dpi
	CDS_50708_Unigene_92230_Transcript_190874	Zinc transporter	1.538	14 dpi
	CDS_23720_Unigene_37652_Transcript_65617	zinc transporter	1.522	14 dpi
	CDS_20500_Unigene_33636_Transcript_58429	zinc transporter	1.435	14 dpi
	CDS_50708_Unigene_92230_Transcript_190874	Zinc transporter	1.975	28 dpi
	CDS_34801_Unigene_53358_Transcript_94166	zinc transporter	2.311	28 dpi
	CDS_48694_Unigene_84966_Transcript_156428	zinc transporter	1.402	28 dpi
	CDS_23720_Unigene_37652_Transcript_65617	zinc transporter	1.367	28 dpi

[a] represents the expression pattern demonstrated the time after *P. chlamydosporia* inoculation when the relevant genes were upregulated

Table 5.4: Differentially expressed genes related to plant hormone biosynthesis in *P. chlamydosporia* treated black pepper roots.

Hormone	Transcript ID	Annotation	Log2 fold change	Expression Patterns[a]
Auxin	CDS_18131_Unigene_30822_Transcript_53447	WAT1-related protein	2.791	14 dpi
	CDS_9679_Unigene_20941_Transcript_36125	WAT1-related-like protein	2.753	14 dpi
	CDS_18130_Unigene_30821_Transcript_53446	WAT1-related protein	2.504	14 dpi
	CDS_18132_Unigene_30823_Transcript_53448	WAT1-related protein	2.239	14 dpi
	CDS_50650_Unigene_92077_Transcript_190198	auxin-responsive protein	1.497	14 dpi
	CDS_12189_Unigene_23866_Transcript_41240	MOB kinase activator	2.398	14 dpi
	CDS_51035_Unigene_9348_Transcript_15641	protein NRT1/ PTR FAMILY	2.251	14 dpi
	CDS_18130_Unigene_30821_Transcript_53446	WAT1-related protein	4.012	28 dpi
	CDS_9679_Unigene_20941_Transcript_36125	WAT1-related-like protein	3.960	28 dpi
	CDS_18131_Unigene_30822_Transcript_53447	WAT1-related protein	3.268	28 dpi
	CDS_18132_Unigene_30823_Transcript_53448	WAT1-related protein	3.234	28 dpi
	CDS_46838_Unigene_7907_Transcript_13184	auxin-responsive protein	2.886	28 dpi
	CDS_48226_Unigene_83427_Transcript_152385	auxin transporter-like protein	2.346	28 dpi
	CDS_39651_Unigene_61966_Transcript_109713	Auxin-induced protein	1.995	28 dpi
	CDS_35608_Unigene_54677_Transcript_96478	Auxin-induced protein	1.662	28 dpi
	CDS_44430_Unigene_72517_Transcript_129555	Arogenate dehydratase/prephenate dehydratase	3.092	28 dpi

Hormone	Transcript ID	Annotation	Log2 fold change	Expression Patterns[a]
	CDS_32975_Unigene_50490_Transcript_88918	arogenate dehydratase/prephenate dehydratase	1.910	28 dpi
	CDS_10459_Unigene_21832_Transcript_37700	arogenate dehydrogenase	1.653	28 dpi
	CDS_10457_Unigene_21830_Transcript_37697	arogenate dehydrogenase	1.622	28 dpi
	CDS_10458_Unigene_21831_Transcript_37699	arogenate dehydrogenase	1.536	28 dpi
	CDS_49066_Unigene_8622_Transcript_14344	protein NRT1/ PTR FAMILY	3.960	28 dpi
	CDS_27945_Unigene_4325_Transcript_7235	protein NRT1/ PTR FAMILY	1.655	28 dpi
Cytokinin	CDS_15594_Unigene_27838_Transcript_48167	cytokinin riboside 5'monophosphate phosphoribohydrolase	2.590	14 dpi
	CDS_12441_Unigene_24146_Transcript_41730	cytokinin riboside 5'monophosphate phosphoribohydrolase	2.600	28 dpi
	CDS_15594_Unigene_27838_Transcript_48167	cytokinin riboside 5'monophosphate phosphoribohydrolase	1.438	28 dpi
Gibberellin	CDS_44123_Unigene_7177_Transcript_12013	F-box protein	2.958	14 dpi
	CDS_44140_Unigene_7181_Transcript_12019	F-box protein	2.202	14 dpi
	CDS_28950_Unigene_4459_Transcript_7460	gibberellin-regulated protein	1.852	14 dpi
	CDS_43304_Unigene_69730_Transcript_124102	gibberellin 3-beta-dioxygenase	2.038	14 dpi
	CDS_8424_Unigene_19514_Transcript_33596	ent-kaurene oxidase	1.713	28 dpi
	CDS_44123_Unigene_7177_Transcript_12013	F-box protein	1.563	28 dpi

Hormone	Transcript ID	Annotation	Log2 fold change	Expression Patterns[a]
	CDS_44128_Unigene_7178_Transcript_12014	F-box protein	1.360	28 dpi
	CDS_28950_Unigene_4459_Transcript_7460	gibberellin-regulated protein	2.576	28 dpi
	CDS_8424_Unigene_19514_Transcript_33596	ent-kaurene oxidase	1.777	28 dpi
Abscisic acid	CDS_8276_Unigene_19331_Transcript_33271	Zeaxanthin epoxidase	2.378	14 dpi
	CDS_42731_Unigene_6845_Transcript_11465	Abscisic acid-Insensitive 5	2.302	14 dpi
	CDS_42726_Unigene_6843_Transcript_11462	Abscisic acid-Insensitive 5	1.658	14 dpi
	CDS_42742_Unigene_6847_Transcript_11469	Abscisic acid-Insensitive 5	1.653	28 dpi
	CDS_42728_Unigene_6844_Transcript_11463	Abscisic acid-Insensitive 5	1.561	28 dpi
	CDS_48350_Unigene_83861_Transcript_153520	protein ABA Deficient 4	1.667	28 dpi
	CDS_8693_Unigene_19827_Transcript_34172	abscisic acid receptor PYL8	1.398	28 dpi
	CDS_22549_Unigene_36115_Transcript_62878	9-cis-epoxycarotenoid dioxygenase	2.051	28 dpi

[a] represents the expression pattern demonstrated the time after *P. chlamydosporia* inoculation when the relevant genes were upregulated.

Defence-related genes: Defence response genes included pathogenesis-related (PR) proteins, lipid-transfer protein (DIR1), endochitinase (hydrolytic enzyme), germin like proteins, major latex-like proteins (MLPs), among others. Several disease-resistance proteins with leucine-rich repeats (LRRs) and a nucleotide-binding site (NBS) domains were upregulated, pointing to enhanced plant immunity. Cytochrome P450 enzymes involved in lipid metabolism also showed elevated expression, supporting their involvement in defence mechanisms (Table 5.5). Nonexpressor of Pathogenesis-Related Protein 1 (NPR1), a crucial regulator of systemic acquired resistance (SAR), and dirigent proteins (DIR) were upregulated, indicating enhanced systemic defences and pathogen resistance.

Stress tolerance genes: Stress tolerance genes such as ascorbate peroxidase (APX), which toxifies reactive oxygen species (ROS) were notably upregulated (Table 5.6). Additionally, fasciclin-like arabinogalactan proteins (FLAs), essential for cell wall biosynthesis and abiotic stress tolerance, showed increased expression. Other consistently upregulated stress tolerance genes included basic leucine zipper (bZIP) transcription factors, PLAT domain-containing proteins, and LOB domain-containing proteins, all involved in stress response regulation. Conversely, certain MYB transcription factors known to regulate abiotic stress responses, were downregulated.

Table 5.3 to Table 5.6 provide detailed descriptions of DEGs related to nutrient uptake, plant hormone biosynthesis, defence proteins, and stress tolerance proteins, respectively, while Figures 1 to 5 illustrate key differential gene expression patterns in aquaporins, ethylene, and JA signalling pathways. These results provide insights into the transcriptional reprogramming induced *by P. chlamydosporia* colonization, highlighting key pathways in growth promotion, defence, and stress adaptation in black pepper roots.

5.3.3 *Gene ontology analysis*

Gene ontology (GO) analysis was conducted on the DEGs across control, 14 dpi, and 28 dpi samples. A total of 28,766, 39,806, and 46,631 CDS from these respective samples were categorized into three primary GO domains: Biological Process (BP), Molecular Function (MF) and Cellular Component (Table 5.7). Fig. 5.3 illustrates GO term distributions at 14 dpi for BP, CC, and MF categories while Fig. 5.4 displays the GO term distributions at 28 dpi.

Table 5.5: Differentially expressed genes related to plant defence proteins in *P. chlamydosporia* treated black pepper roots.

Transcript ID	Annotation	Log2 fold change	Expression Patterns[a]
CDS_16795_Unigene_29250_Transcript_50657	pathogenesis-related protein PR-4B	4.400	14 dpi
CDS_6662_Unigene_17476_Transcript_30081	pathogenesis-related protein 1	1.705	14 dpi
CDS_38218_Unigene_59275_Transcript_104841	Pathogenesis-related transcriptional activator PTI6	1.811	14 dpi
CDS_16795_Unigene_29250_Transcript_50657	pathogenesis-related protein PR-4B-like	4.197	28 dpi
CDS_18071_Unigene_30748_Transcript_53312	lipid-transfer protein DIR1	2.327	14 dpi
CDS_20852_Unigene_34054_Transcript_59212	LURP1	2.301	14 dpi
CDS_17291_Unigene_29841_Transcript_51728	LURP1	2.127	14 dpi
CDS_29043_Unigene_44734_Transcript_78626	LURP1	1.565	14 dpi
CDS_17206_Unigene_29728_Transcript_51508	LURP1	1.988	14 dpi
CDS_20852_Unigene_34054_Transcript_59212	LURP1	3.350	28 dpi
CDS_44783_Unigene_73318_Transcript_131104	MLP	2.077	14 dpi
CDS_44783_Unigene_73318_Transcript_131104	MLP	1.820	28 dpi
CDS_8069_Unigene_19096_Transcript_32867	thaumatin	1.790	14 dpi
CDS_19494_Unigene_32420_Transcript_56317	thaumatin	3.427	28 dpi

Transcript ID	Annotation	Log2 fold change	Expression Patterns[a]
CDS_8069_Unigene_19096_Transcript_32867	thaumatin	1.700	28 dpi
CDS_43629_Unigene_70538_Transcript_125636	endochitinase	1.396	14 dpi
CDS_23565_Unigene_3745_Transcript_6182	germin-like protein	2.246	14 dpi
CDS_23526_Unigene_3740_Transcript_6169	germin-like protein	2.131	14 dpi
CDS_23551_Unigene_3743_Transcript_6175	germin-like protein	1.701	14 dpi
CDS_23556_Unigene_3744_Transcript_6177	germin-like protein	1.522	14 dpi
CDS_23565_Unigene_3745_Transcript_6182	germin-like protein	4.021	28 dpi
CDS_23551_Unigene_3743_Transcript_6175	germin-like protein	3.412	28 dpi
CDS_23526_Unigene_3740_Transcript_6169	germin-like protein	2.976	28 dpi
CDS_23556_Unigene_3744_Transcript_6177	germin-like protein	2.582	28 dpi
CDS_29382_Unigene_451_Transcript_738	late embryogenesis abundant protein	2.071	14 dpi
CDS_29233_Unigene_449_Transcript_733	late embryogenesis abundant protein	1.890	14 dpi
CDS_26684_Unigene_41567_Transcript_72767	late embryogenesis abundant protein	1.575	28 dpi
CDS_44054_Unigene_71620_Transcript_127762	LRR domain containing protein	2.387	14 dpi
CDS_33584_Unigene_51403_Transcript_90547	LRR receptor-like serine/threonine-protein kinase	2.917	28 dpi

Transcript ID	Annotation	Log2 fold change	Expression Patterns[a]
CDS_38222_Unigene_59282_Transcript_104852	LRR receptor-like serine/threonine-protein kinase	2.115	28 dpi
CDS_40004_Unigene_62628_Transcript_110916	LRR receptor-like serine/threonine-protein kinase	1.808	28 dpi
CDS_14588_Unigene_26670_Transcript_46165	NBS-LRR disease resistance protein,	1.537	28 dpi
CDS_49654_Unigene_88413_Transcript_169193	cytochrome P450	2.021	14 dpi
CDS_50425_Unigene_9118_Transcript_15224	cytochrome b-c1 complex subunit 8	1.371	14 dpi
CDS_8688_Unigene_19821_Transcript_34160	cytochrome b5	2.906	28 dpi
CDS_33756_Unigene_51660_Transcript_90984	cytochrome P450	2.772	28 dpi
CDS_14437_Unigene_26484_Transcript_45808	Cytochrome P450	2.154	28 dpi
CDS_36017_Unigene_55354_Transcript_97705	cytochrome P450	2.087	28 dpi
CDS_30433_Unigene_46688_Transcript_82173	Cytochrome P450	2.075	28 dpi
CDS_30434_Unigene_46689_Transcript_82174	Cytochrome P450	1.889	28 dpi
CDS_13669_Unigene_25599_Transcript_44290	cytochrome P450	1.838	28 dpi
CDS_35381_Unigene_54300_Transcript_95821	cytochrome b561	1.718	28 dpi
CDS_36601_Unigene_56318_Transcript_99503	Cytochrome b245	1.626	28 dpi
CDS_44112_Unigene_71757_Transcript_128041	cytochrome P450	1.382	28 dpi

Transcript ID	Annotation	Log2 fold change	Expression Patterns[a]
CDS_31551_Unigene_48356_Transcript_85153	nonexpressor of pathogenesis-related protein	1.340	14 dpi
CDS_20531_Unigene_33669_Transcript_58482	dirigent protein	1.510	14 dpi
CDS_35484_Unigene_54446_Transcript_96085	dirigent protein	1.770	14 dpi
CDS_38621_Unigene_59992_Transcript_106124	dirigent protein	2.442	14 dpi
CDS_35484_Unigene_54446_Transcript_96085	dirigent protein	2.722	28 dpi
CDS_20531_Unigene_33669_Transcript_58482	dirigent protein	2.771	28 dpi
CDS_47932_Unigene_82509_Transcript_149889	dirigent protein	2.287	28 dpi
CDS_20604_Unigene_33746_Transcript_58620	dirigent protein	2.0791	28 dpi
CDS_38621_Unigene_59992_Transcript_106124	dirigent protein	3.598	28 dpi
CDS_2220_Unigene_12482_Transcript_21078	WRKY transcription factor 22	1.460	14 dpi
CDS_15573_Unigene_27811_Transcript_48099	WRKY transcription factor 13	-1.727	14 dpi
CDS_27569_Unigene_42755_Transcript_75012	WRKY transcription factor 4	1.701	28 dpi
CDS_47160_Unigene_80047_Transcript_144648	WRKY transcription factor 25	1.451	28 dpi
CDS_15573_Unigene_27811_Transcript_48099	WRKY transcription factor 13	-2.203	28 dpi
CDS_50021_Unigene_8977_Transcript_14971	DNA-binding WRKY	-2.061	28 dpi
CDS_48867_Unigene_85572_Transcript_157914	WRKY family protein	-2.031	28 dpi

Transcript ID	Annotation	Log2 fold change	Expression Patterns[a]
CDS_50027_Unigene_8978_Transcript_14972	DNA-binding WRKY	-1.959	28 dpi
CDS_44877_Unigene_73561_Transcript_131624	DNA-binding WRKY	-1.794	28 dpi
CDS_14406_Unigene_26447_Transcript_45747	WRKY transcription factor 13	-1.645	28 dpi
CDS_21163_Unigene_34408_Transcript_59855	WRKY transcription factor 41	-1.359	28 dpi
CDS_29395_Unigene_45221_Transcript_79484	WRKY transcription factor 16	-1.315	28 dpi
CDS_27256_Unigene_42342_Transcript_74211	WRKY71 31	-1.422	28 dpi
CDS_18836_Unigene_3161_Transcript_5196	BTB/POZ domain-containing protein	-2.213	14 dpi
CDS_10051_Unigene_21367_Transcript_36868	BTB/POZ domain-containing protein	-1.614	28 dpi
CDS_37633_Unigene_58181_Transcript_102831	E3 ubiquitin-protein ligase	2.819	14 dpi
CDS_22444_Unigene_35975_Transcript_62652	E3 ubiquitin-protein ligase	2.610	14 dpi
CDS_33762_Unigene_51669_Transcript_91007	E3 ubiquitin-protein ligase	1.976	14 dpi
CDS_39175_Unigene_6103_Transcript_10152	E3 ubiquitin-protein ligase	1.559	14 dpi
CDS_2724_Unigene_13029_Transcript_22052	ubiquitin-protein ligase	1.440	14 dpi
CDS_39484_Unigene_6165_Transcript_10244	ubiquitin-conjugating enzyme E2	2.517	14 dpi
CDS_39485_Unigene_6166_Transcript_10246	ubiquitin-conjugating enzyme E2	2.345	14 dpi
CDS_33659_Unigene_51521_Transcript_90751	E3 ubiquitin-protein	1.431	14 dpi

Transcript ID	Annotation	Log2 fold change	Expression Patterns[a]
CDS_42514_Unigene_6799_Transcript_11373	U-box domain-containing protein	1.646	14 dpi
CDS_42515_Unigene_67_Transcript_113	U-box domain-containing protein	1.514	14 dpi
CDS_23841_Unigene_37809_Transcript_65881	U-box domain-containing protein	1.488	14 dpi
CDS_39485_Unigene_6166_Transcript_10246	ubiquitin-conjugating enzyme E2	2.539	28 dpi
CDS_39484_Unigene_6165_Transcript_10244	ubiquitin-conjugating enzyme E2	2.513	28 dpi
CDS_22444_Unigene_35975_Transcript_62652	ubiquitin-protein ligase	2.311	28 dpi
CDS_27045_Unigene_42038_Transcript_73675	BOI-related E3 ubiquitin-protein ligase	1.965	28 dpi
CDS_21405_Unigene_34699_Transcript_60328	E3 ubiquitin-protein	1.753	28 dpi
CDS_36689_Unigene_56465_Transcript_99816	E3 ubiquitin-protein ligase	1.689	28 dpi
CDS_2724_Unigene_13029_Transcript_22052	E3 ubiquitin-protein ligase BOI-like	1.664	28 dpi
CDS_39175_Unigene_6103_Transcript_10152	E3 ubiquitin-protein ligase	1.597	28 dpi
CDS_43671_Unigene_70661_Transcript_125846	BOI-related E3 ubiquitin-protein ligase	1.519	28 dpi
CDS_22649_Unigene_36246_Transcript_63134	E3 ubiquitin-protein ligase	1.418	28 dpi
CDS_26898_Unigene_41839_Transcript_73271	E3 ubiquitin-protein ligase	1.371	28 dpi
CDS_2729_Unigene_13033_Transcript_22058	E3 ubiquitin-protein ligase BOI-like	1.371	28 dpi

[a] represents the expression pattern demonstrated the time after *P. chlamydosporia* inoculation when the relevant genes were upregulated.

Table 5.6: Differentially expressed genes related to stress tolerance proteins in *P. chlamydosporia* treated black pepper roots.

Transcript ID	Annotation	Log2 fold change	Expression Pattern[a]
CDS_36998_Unigene_57039_Transcript_100817	L-ascorbate peroxidase	2.025	14 dpi
CDS_2948_Unigene_13279_Transcript_22489	L-ascorbate oxidase	5.109	28 dpi
CDS_13746_Unigene_25682_Transcript_44422	fasciclin-like arabinogalactan protein	3.796	28 dpi
CDS_13747_Unigene_25683_Transcript_44423	fasciclin-like arabinogalactan protein	4.594	28 dpi
CDS_20005_Unigene_33060_Transcript_57416	fasciclin-like arabinogalactan protein	1.510	28 dpi
CDS_20006_Unigene_33061_Transcript_57418	fasciclin-like arabinogalactan protein	1.973	28 dpi
CDS_24724_Unigene_38979_Transcript_67983	fasciclin-like arabinogalactan protein	3.056	28 dpi
CDS_423_Unigene_10481_Transcript_17531	fasciclin-like arabinogalactan protein	1.680	28 dpi
CDS_424_Unigene_10482_Transcript_17532	fasciclin-like arabinogalactan protein	1.751	28 dpi
CDS_13643_Unigene_25560_Transcript_44227	fasciclin-like arabinogalactan protein	3.111	28 dpi
CDS_46226_Unigene_7717_Transcript_12867	PLAT domain-containing protein	6.803	28 dpi
CDS_18377_Unigene_31094_Transcript_53924	PLAT domain-containing protein	1.520	28 dpi
CDS_18375_Unigene_31092_Transcript_53922	PLAT domain-containing protein	1.335	28 dpi
CDS_33093_Unigene_50643_Transcript_89185	LOB domain-containing protein	1.778	28 dpi
CDS_6488_Unigene_17285_Transcript_29730	LOB domain-containing protein	4.628	28 dpi

Transcript ID	Annotation	Log2 fold change	Expression Pattern[a]
CDS_45855_Unigene_76177_Transcript_136696	LOB domain-containing protein	1.695	28 dpi
CDS_8614_Unigene_19743_Transcript_34020	LOB domain-containing protein	1.788	28 dpi
CDS_31460_Unigene_4821_Transcript_8039	myb family transcription factor EFM	3.431	14 dpi
CDS_38330_Unigene_59475_Transcript_105189	transcription factor MYB16	2.405	14 dpi
CDS_17638_Unigene_30221_Transcript_52376	myb-related protein Hv1	2.233	14 dpi
CDS_17641_Unigene_30224_Transcript_52379	myb-related protein Zm38	2.0420	14 dpi
CDS_17640_Unigene_30223_Transcript_52378	myb-related protein Hv1	1.849	14 dpi
CDS_17639_Unigene_30222_Transcript_52377	myb-related protein Hv1	1.674	14 dpi
CDS_4900_Unigene_15500_Transcript_26498	myb family transcription factor PHL11	1.649	14 dpi
CDS_34760_Unigene_53273_Transcript_94011	myb family transcription factor APL	1.515	14 dpi
CDS_16012_Unigene_28331_Transcript_48991	transcription factor MYB12	1.3591	14 dpi
CDS_7982_Unigene_19002_Transcript_32699	myb family transcription factor	-1.538	14 dpi
CDS_4900_Unigene_15500_Transcript_26498	myb family transcription factor PHL11	3.313	28 dpi
CDS_17638_Unigene_30221_Transcript_52376	myb-related protein Hv1	2.409	28 dpi
CDS_31460_Unigene_4821_Transcript_8039	myb family transcription factor EFM	2.326	28 dpi
CDS_17640_Unigene_30223_Transcript_52378	myb-related protein Hv1	2.325	28 dpi

Transcript ID	Annotation	Log2 fold change	Expression Pattern[a]
CDS_17639_Unigene_30222_Transcript_52377	myb-related protein Hv1	2.318	28 dpi
CDS_16012_Unigene_28331_Transcript_48991	transcription factor MYB12	1.627	28 dpi
CDS_47849_Unigene_8224_Transcript_13684	myb family transcription factor EFM	1.423	28 dpi
CDS_27788_Unigene_43039_Transcript_75494	transcription factor MYB41	-1.953	28 dpi
CDS_42958_Unigene_69006_Transcript_122650	transcription factor MYB4	-1.756	28 dpi
CDS_7982_Unigene_19002_Transcript_32699	myb family transcription factor	-1.608	28 dpi
CDS_45555_Unigene_75356_Transcript_135064	transcription factor MYB10	-1.469	28 dpi
CDS_45556_Unigene_75357_Transcript_135065	transcription factor MYB10	-1.451	28 dpi
CDS_33414_Unigene_51088_Transcript_89961	transcription factor MYB41	-1.611	28 dpi

[a] represents the expression pattern demonstrated the time after *P. chlamydosporia* inoculation when the relevant genes were upregula

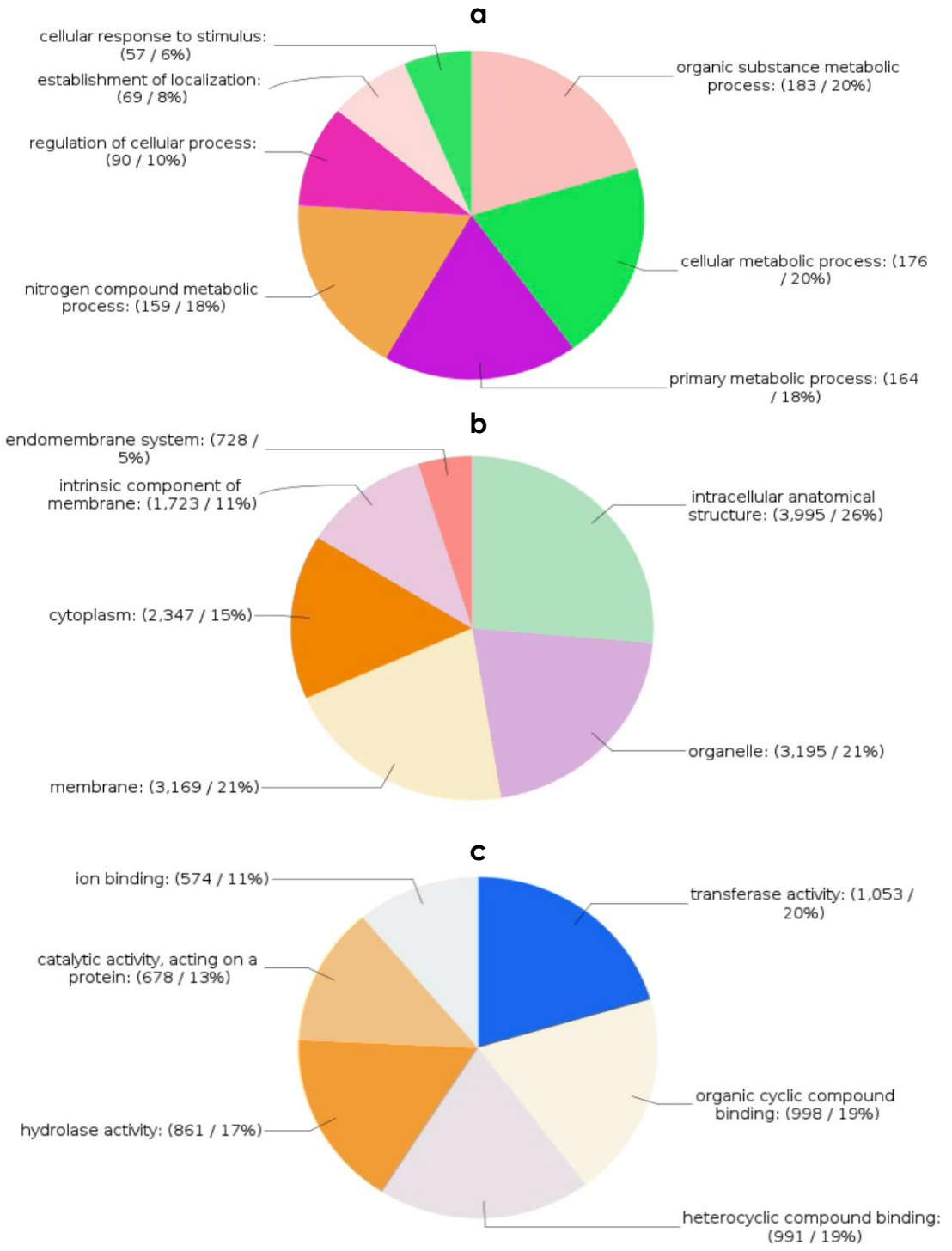

Fig. 5.3: GO term distribution of differentially expressed genes in black pepper roots colonised by *Pachonia chlamydosporia* at 14 dpi. **(a)** Biological process, **(b)** Cellular component, **(c)** Molecular function.

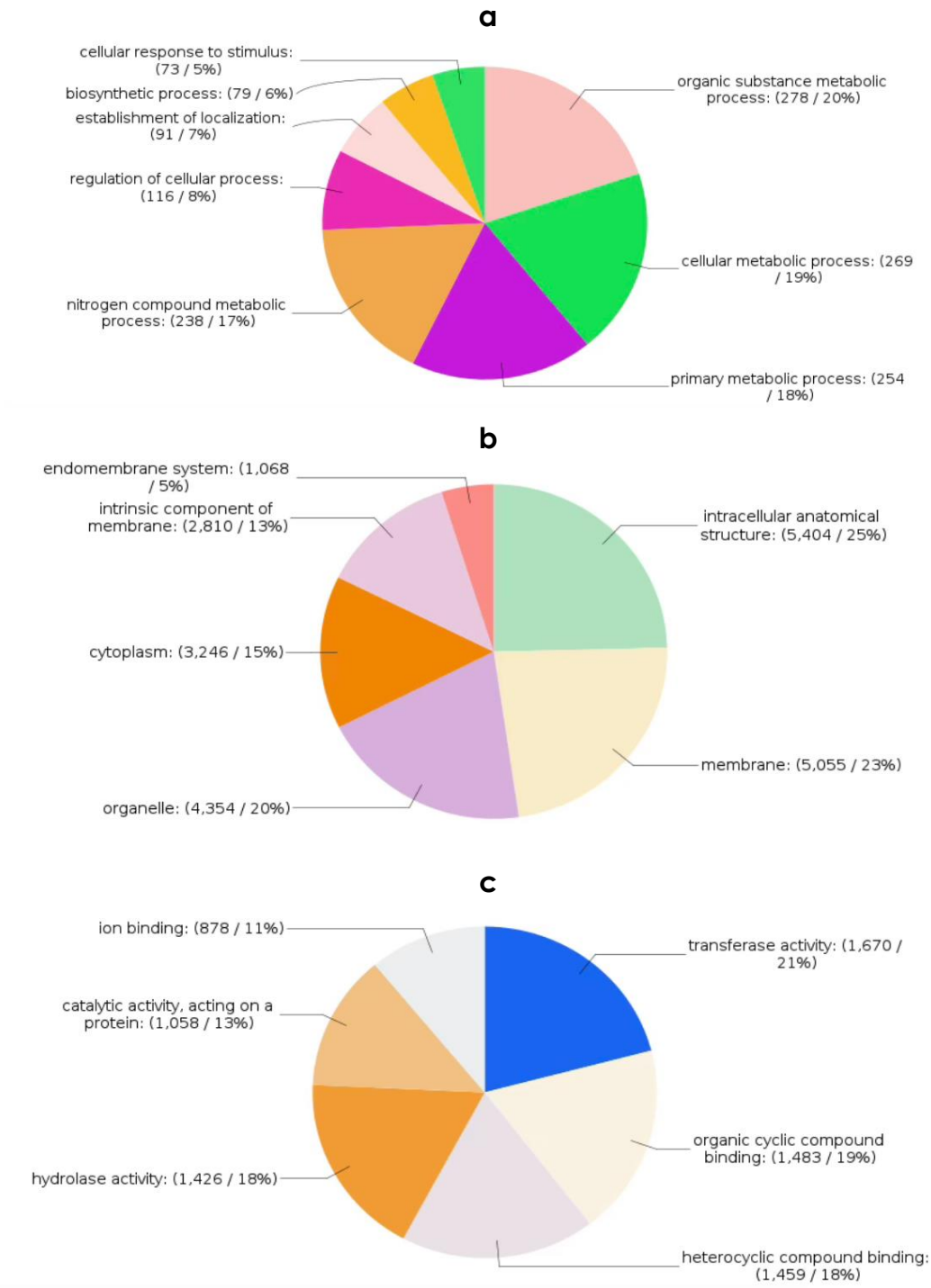

Fig. 5.4: GO term distribution of differentially expressed genes in black pepper roots colonised by *Pachonia chlamydosporia* at 28 dpi. **(a)** Biological process, **(b)** Cellular component, **(c)** Molecular function.

Table 5.7: GO category distribution of CDS across treatments: Control, 14 dpi, and 28 dpi in *Pochonia chlamydosporia*-colonized black pepper roots.

Sample	Biological Process	Cellular Component	Molecular Function
Control	7,919	6,893	9,067
14 dpi	10,468	9,117	12,098
28 dpi	11,801	10,209	13,763

GO term enrichment analysis identified 91 significantly enriched terms across both 14 and 28 dpi time points (Fig. 5.5). In the CC category, "intrinsic to membrane" and "membrane part" were prominent, indicating an enrichment in membrane-related activities during fungal colonisation. For MF, "ion binding" and "transmembrane transporter" were highly annotated, reflecting active roles in ion transport and signalling. The BP category was dominated by "single-organism cellular process" and "organic substance metabolic process" underscoring metabolic and cellular responses at both time points (Fig. 5.5).

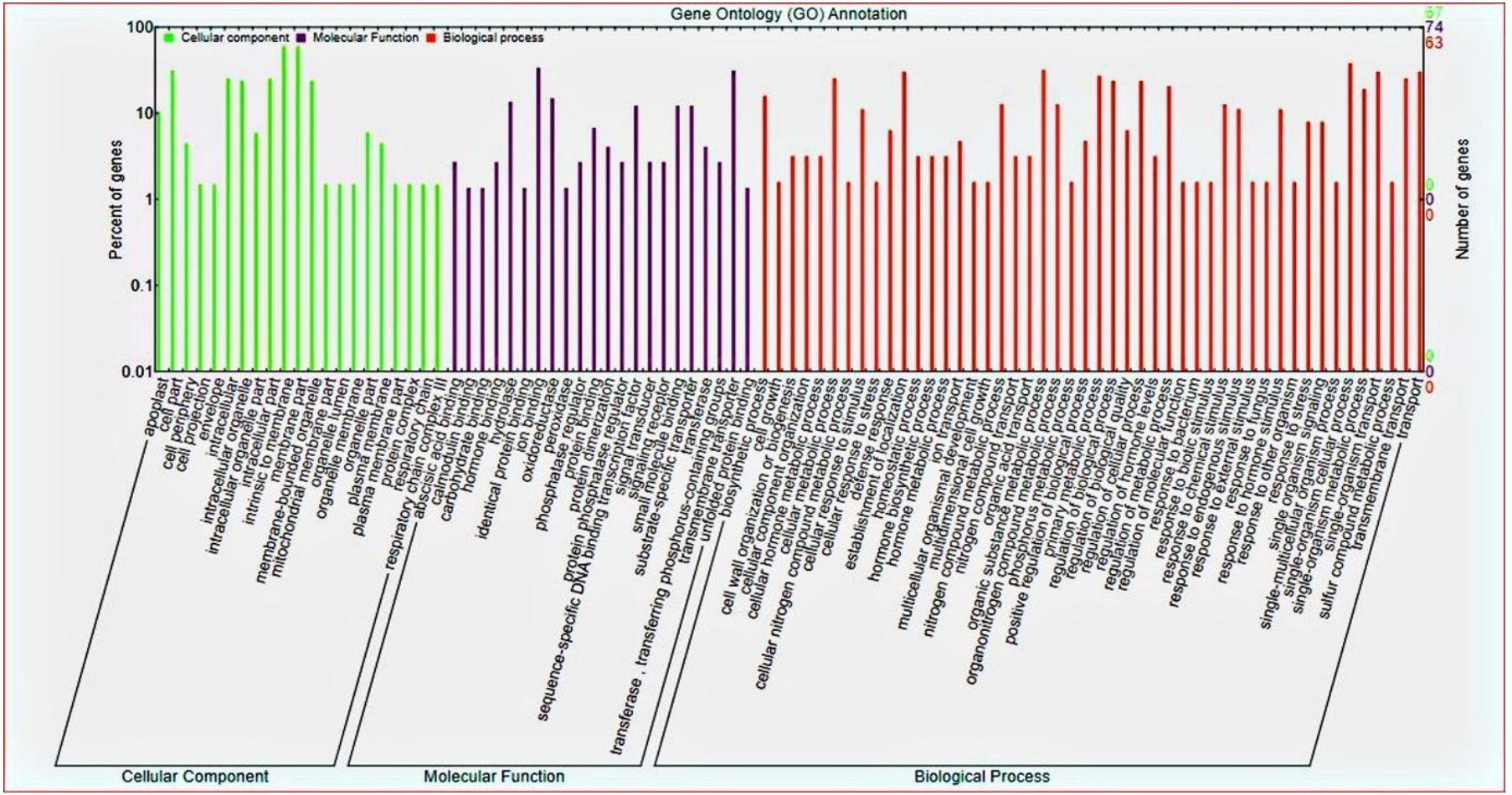

Fig. 5.5 GO functional annotation of black pepper genes that were differentially expressed during *P. chlamydosporia* root colonization together at both time points (14 and 28 dpi). GO terms were classified into the three categories shown: cellular component, molecular function and biological process. The Web Gene Annotation Plot (WEGO) tool was used to plot histograms (Ye et al., 2006).

Table 5.8: Top 20 significantly enriched GO terms for growth promotion and endophytism. Upregulated GO terms are denoted by the plus sign (+).

GO Term	Description	LogSize P- Value	Frequency	Uniqueness	Dispensability	14 dpi	28 dpi
GO:0004601	Peroxidase activity	5.161955	0.420800564	0.865147762	0.262297	+	+
GO:0005516	Calmodulin binding	4.712734	0.149571929	0.920876226	0.045843	+	+
GO:0010427	Abscisic acid binding	3.547652	0.010224762	0.934390038	0.037062	+	+
GO:0004842	Ubiquitin-protein transferase activity	5.270411	0.540173506	0.91601638	0.460893	+	+
GO:0005385	Zinc ion transmembrane transporter activity	3.902547	0.023153523	0.876140057	0.593945	+	+
GO:0005388	P-type calcium transporter activity	4.123917	0.03854863	0.851776993	0.618443	+	+
GO:0008198	Ferrous iron binding	4.200768	0.046011431	0.885571471	0.234891	+	+
GO:0030145	Manganese ion binding	4.933761	0.248817045	0.877126898	0.389227	+	+
GO:0052615	Ent-kaurene oxidase activity	2.588832	0.001121594	0.899042482	0.171053	+	+
GO:0006813	Potassium ion transport	5.237875	0.598802603	0.963045276	0.846222	+	+
GO:0006865	Amino acid transport	5.317865	0.719902483	0.962478125	0.2787638	+	+
GO:0006952	Defense response	5.475132	1.034049555	0.865718505	0.42143085	+	+
GO:0009686	Gibberellin biosynthetic process	3.015779	0.003587324	0.828767483	0.47992059	+	+

GO Term	Description	LogSize P- Value	Frequency	Uniqueness	Dispensability	14 dpi	28 dpi
GO:0009691	Cytokinin biosynthetic process	4.157457	0.049755073	0.823224826	0.4884579	+	+
GO:0009699	Phenylpropanoid biosynthetic process	4.099439	0.043532659	0.90734914	0.15857389	+	+
GO:0009734	Auxin-activated signaling pathway	4.616717	0.143257492	0.836493449	0.21156052	+	+
GO:0009738	Abscisic acid-activated signaling pathway	4.05618	0.039405159	0.813987197	0.3933499	+	+
GO:0055072	Iron ion homeostasis	4.638859	0.150750705	0.892284078	0.13019204	+	+
GO:0004672	Protein kinase activity	6.090873	3.572702423	0.935472625	0.215222	+	+
GO:0038023	Signaling receptor activity	5.791147	1.79172153	1	0	+	+

Distinct GO terms were enriched at each time point, highlighting time-dependent functional shifts in response to *P. chlamydosporia* colonisation. Significant GO terms at 14 dpi included "Gibberellin biosynthetic process" (GO:0009686), "Cytokinin biosynthetic process" (GO:0009691), "P-type calcium transporter activity" (GO:0005388), "Ferrous iron binding" (GO:0008198), "Manganese ion binding" (GO:0030145) and "Potassium ion transport" (GO:0006813). At 28-dpi, key terms included "Peroxidase activity" (GO:0004601), "Ubiquitin-protein transferase activity" (GO:0004842), "Amino acid transport" (GO:0006865), "Defence response" (GO:0006952), "Phenylpropanoid biosynthetic process" (GO:0009699), "Auxin-activated signalling pathway" (GO:0009734), "Abscisic acid-activated signalling pathway" (GO:0009738), "Iron ion homeostasis" (GO:0055072) and "Signalling receptor activity" (GO:0038023) (Table 5.8).

The GO analysis highlights essential functional changes occurring over time, illustrating pathways involved in growth, stress response, and defence processes as *P. chlamydosporia* colonizes black pepper roots. These enriched GO terms offer a deeper understanding of the molecular mechanisms behind growth promotion and endophytism.

5.3.4 *KEGG pathway analysis and functional insights*

To better understand the biological functions of differentially expressed genes (DEGs), KEGG (Kyoto Encyclopedia of Genes and Genomes) pathway analysis was conducted on the CDS (coding sequences) identified in the transcriptome data. The analysis aimed to elucidate the roles of highly expressed DEGs in various metabolic pathways, emphasizing their involvement in plant growth, stress responses, and defence mechanisms.

The identified CDS from control, 14 dpi, and 28 dpi samples were mapped to 21 KEGG pathways, classified into four major categories: Metabolism, Genetic Information Processing, Cellular Processes, and Organismal Systems (Table 5.9). The enrichment analysis revealed that a significantly higher number of pathways associated with growth promotion and stress resistance were activated at 28 dpi

compared to 14 dpi, indicating that prolonged colonization by *P. chlamydosporia* enhances its growth-promoting and endophytic effects.

Functional Categorization of KEGG Pathways: The KEGG pathway classification revealed distinct patterns across the three sample conditions, with a notable increase in CDS counts in various pathways at 28 dpi, highlighting the dynamic impact of *P. chlamydosporia* colonization over time (Table 5.10).

Table 5.9: KEGG pathway annotation summary of CDS in *Pochonia chlamydosporia*-colonized black pepper roots across treatments: Control, 14 dpi, and 28 dpi.

Sample Name	No. of Identified CDS	No. of Annotated CDS	No. of Annotated Categories
Control	28,766	6,176	21
14dpi	39,806	6,302	21
28dpi	46,631	7,528	21

Table 5.10: KEGG pathway classification summary of CDS in *Pochonia chlamydosporia*-colonized black pepper roots: Control, 14 dpi, and 28 dpi.

Pathways	CDS counts		
	Control	14 dpi	28 dpi
Metabolism			
Carbohydrate metabolism	561	632	736
Energy metabolism	331	342	363
Lipid metabolism	274	304	344
Nucleotide metabolism	135	168	181
Amino acid metabolism	375	427	465
Metabolism of other amino acids	179	194	213
Glycan biosynthesis and metabolism	156	211	220

Pathways	CDS counts		
	Control	**14 dpi**	**28 dpi**
Metabolism of cofactors and vitamins	270	317	337
Metabolism of terpenoids and polyketides	112	127	154
Biosynthesis of other secondary metabolites	153	164	212
Xenobiotics biodegradation and metabolism	97	104	112
Carbohydrate metabolism	561	632	736
Energy metabolism	331	342	363
Lipid metabolism	274	304	344
Genetic Information Processing			
Transcription	354	384	387
Translation	706	779	776
Folding, sorting and degradation	583	621	640
Replication and repair	143	201	247
Environmental Information Processing			
Membrane transport	29	36	40
Signal transduction	743	812	911
Cellular Processes			
Transport and catabolism	507	560	581
Cell growth and death	308	371	421
Cellular community - eukaryotes	95	102	111
Cell motility	65	67	77

Enriched pathways related to growth promotion and defence: The KEGG analysis identified the top ten pathways significantly enriched during *P. chlamydosporia* colonisation, which are crucial for growth promotion and plant defense (Fig. 5.6). Notably, the pathway "Plant hormone signal transduction" was highly enriched, suggesting that hormonal signaling plays a central role in the interaction between black pepper roots and *P. chlamydosporia*. The enrichment of pathways involved in ascorbate and aldarate metabolism, brassinosteroid biosynthesis, phenylpropanoid

biosynthesis, cutin, suberine, and wax biosynthesis, as well as the MAPK signaling pathway, further underscores the fungus's role in enhancing plant immunity and defense. At 28 dpi, the number of pathways associated with growth and defence mechanisms increased significantly compared to 14 dpi. This indicates that prolonged fungal colonization enhances the metabolic and signalling networks involved in plant growth promotion, stress tolerance, and disease resistance.

The results demonstrate that *P. chlamydosporia* induces a wide range of metabolic pathways that are critical for promoting plant growth and enhancing stress tolerance. The increased activation of these pathways over time suggests a progressive enhancement of the symbiotic relationship, contributing to improved plant health and resilience.

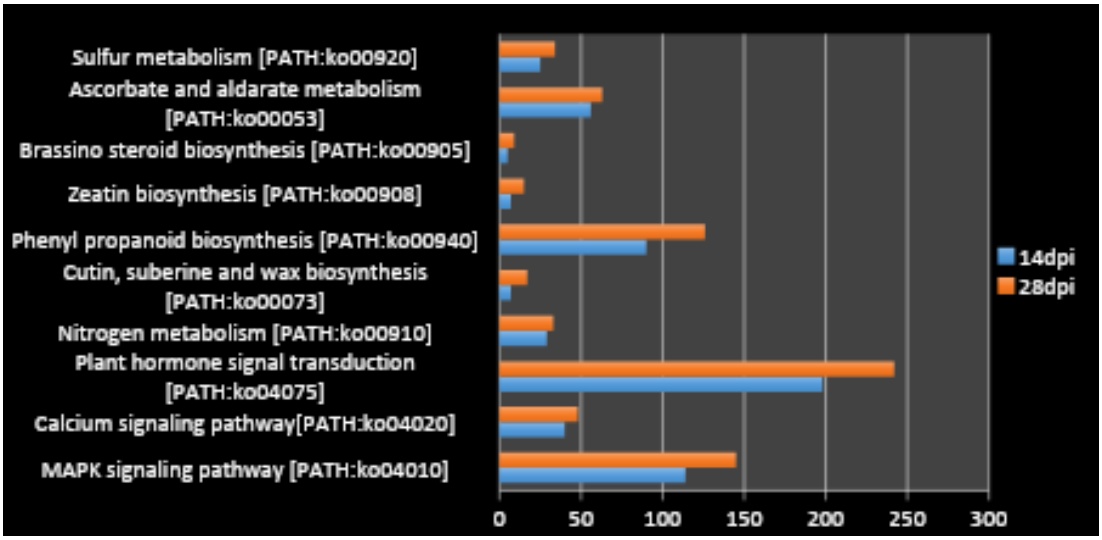

Fig. 5.6 The top ten KEGG pathways enriched for growth promotion and endophytism processes of black pepper genes during *P. chlamydosporia* root colonization. These pathways highlight critical interactions and adaptive responses that contribute to the enhanced growth and defence capabilities of black pepper.

5.3.5 *Validation of RNA-Seq results using qRT-PCR*

To confirm the accuracy and reliability of the RNA-Seq data, quantitative RT-PCR (qRT-PCR) analysis was performed on nine DEGs selected based on their functional roles in hormone metabolism, signalling, stress tolerance, defence, and plant growth.

Selected genes for validation:

- *Hormone metabolism*: WAT (WAT1-related protein) and GRP (Gibberellin-regulated protein)
- *Signalling*: ERT (Ethylene-responsive transcription factor)
- *Stress tolerance*: MYB (Myb family transcription factor)
- *Defence mechanisms*: UPL (Ubiquitin-protein ligase) and WRKY (WRKY transcription factor)
- *Plant growth*: MIP (Major intrinsic protein PIPB), ZT (Zinc transporter), and PCK (Potassium transporter)

The qRT-PCR analysis confirmed the RNA-Seq results by showing consistent expression patterns across the two sampling times (14 and 28 dpi). Up-regulated genes validated through qRT-PCR included UPL, WAT, GRP, ERT, MIP, ZT, and PCK, while down-regulated genes were confirmed for WRKY and MYB.

Expression patterns observed:

- *Overall expression*: All examined transcripts showed increased expression in black pepper roots inoculated with *P. chlamydosporia,* with a more pronounced induction observed at 28 dpi compared to 14 dpi.
- *Consistency with RNA-Seq data*: The gene expression patterns derived from qRT-PCR were highly consistent with those obtained through RNA-Seq analysis, thus validating the reliability of the next-generation sequencing (NGS) results.

Fig. 5.7 illustrates the fold-change expression levels of the nine DEGs. The bar graph represents the relative expression levels, confirming that the transcriptomic analysis effectively captured the temporal dynamics of gene expression associated with *P. chlamydosporia* colonization.

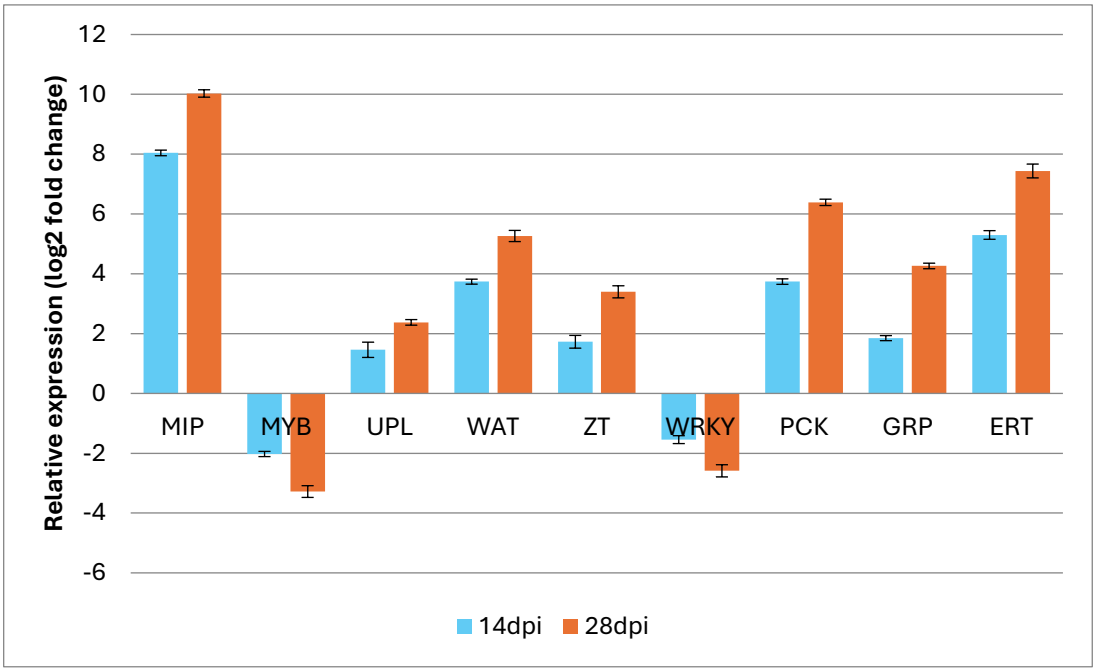

Fig. 5.7 Validation of differentially expressed genes in black pepper using qRT-PCR. The expression levels of selected genes are depicted as bars, showing fold changes at 14 and 28 dpi.Genes include: MIP- Major intrinsic protein (PIPB), MYB- Myb family transcription factor, UPL- Ubiquitin-protein ligase, WAT- WAT1-related protein, ZT, WRKY- WRKY transcription factor 1, PCK- potassium transporter, GRP- Gibberellin-regulated protein and ERT (Ethylene-responsive transcription factor).

This validation confirms the robustness of the transcriptome profiling, highlighting the functional roles of these genes in enhancing plant growth, stress tolerance, and defence responses in black pepper colonized by *P. chlamydosporia*.

5.4 Discussion

Endophytic fungi like *P. chlamydosporia* must overcome host defence mechanisms to establish a symbiotic relationship without triggering adverse effects. The capacity of endophytes to bypass plant immunity while facilitating colonisation is critical for effective symbiosis. Despite considerable research, the molecular mechanisms underlying the endophytic phase remain complex and not fully understood. This study explored the transcriptional responses in black pepper roots to inoculation with *P. chlamydosporia* at 14 and 28 dpi periods that mark significant stages in root colonisation. *P. chlamydosporia* exhibits the minimum incubation period to achieve

root endophytism, an increasing degree of colonization (forming appressoria and hyphal coils in cells, colonized trichomes, epidermal and cortical root cells), and the maximum degree of root colonization, with conidia and chlamydospores in the rhizoplane (Escudero and Lopez-Llorca, 2012).

5.4.1 *Modulation of host defence mechanisms*

Our results demonstrate that *P. chlamydosporia* alters the black pepper root transcriptome, regulating metabolism through sophisticated defence and stress response pathways. Colonisation induced moderate up-regulation of defence-related genes, particularly those linked to jasmonic acid (JA) and ethylene (ET) signalling pathways, which plays a crucial role in plant defence against biotic stress (Wasternack and Hause, 2013; Pieterse et al., 2014). The elevated expression of genes related to JA biosynthesis, including fatty acid desaturases and lipoxygenases, suggest that *P. chlamydosporia* induces systemic resistance mechanisms in the host plant (Li et al., 2003; Larriba et al., 2015; Zavala-Gonzalez et al., 2017). Previous studies have shown that *P. chlamydosporia* can trigger JA-mediated defences in barley (Larriba et al. 2015) and tomato (Pentimone et al., 2019), enhancing resistance against pathogens. The JA pathway has also been linked to systemically induced defence against nematode infection, implying that *P. chlamydosporia* has a protective role against nematode invasion (Nahar et al., 2011; Ozalvo et al., 2014).

P. chlamydosporia has been shown to activate defence pathways like effector-triggered immunity (ETI) and pattern-triggered immunity (PTI), as evidenced by the upregulation of NBS-LRR genes, which are crucial for recognising pathogen effectors (Boller and Felix, 2009; Dodds and Rathjen, 2010). This suggests that *P. chlamydosporia* not only promotes growth but also provides enhanced protection against nematode invasion. Additionally, our results highlight the role of ethylene response factors (ERFs) in mediating defence responses. The upregulation of ERF genes, particularly ERF1 and ERF2, is associated with enhanced resistance against pathogens by activating plant defensins (Thirugnanasambantham et al. 2015). The findings align with studies showing that *P. chlamydosporia* colonisation in tomato

roots promotes ethylene signalling, thereby bolstering plant defences (Maruyama et al., 2013; Pentimone et al., 2019).

5.4.2 *Hormonal regulation and immune response pathways*

Our transcriptome data revealed significant upregulation of genes involved in the biosynthesis of auxins, gibberellins, cytokinins, and brassinosteroids, highlighting the multifaceted role of *P. chlamydosporia* in promoting plant growth and development (Benková and Hejátko, 2009; Maruyama et al., 2013). The "Plant hormone signal transduction" pathway was one of the most enriched in our KEGG pathway analysis, suggesting that these hormones play a critical role in the interaction between *P. chlamydosporia* and black pepper roots. KEGG Pathway Analysis revealed that the brassinosteroid biosynthesis pathway, a key regulator of plant immunity linked to PTI regulation, was also up-regulated in the roots of black pepper (Dodds and Rathjen, 2010).

The upregulation of genes encoding proteins with NBS-LRR proteins and the protein kinase activator responsible for triggering the ETI response, the oxidative burst and many MAPK family kinases are activated together with a rapid influx of Ca2+ ions (Dodds and Rathjen, 2010). Several mitogen-activated protein kinases (MAPK) signalling pathways and protein kinase activities linked to various biological processes are upregulated in this study as in barley (Larriba et al., 2015). MAPKs are a potential convergence site in the defensive signalling network (Zhang and Klessig, 2001). The effect of *P. chlamydosporia* colonization also resulted in a considerable overexpression of several ubiquitin genes at all time points in the analysis. U-box-type ubiquitin ligases inactivate plant receptors that sense pathogen effectors and start the immune response signaling process (Zhou et al., 2017). *P. chlamydosporia* colonization in tomato plant roots caused ubiquitin gene overexpression (Pentimone et al., 2019).

5.4.3 *Enhanced nutrient uptake and plant growth promotion*

The interaction of *P. chlamydosporia* with black pepper roots not only enhances plant defence mechanisms but also significantly promotes plant growth, highlighting its

dual role as a biocontrol agent and a plant growth promoter. Previous studies have demonstrated the ability of *P. chlamydosporia* to enhance root and shoot growth in barley (Maciá-Vicente et al., 2009a). In our study, transcriptomic analyses revealed that *P. chlamydosporia* colonisation upregulated multiple black pepper genes involved in auxin biosynthesis (which is involved in apical dominance, root growth and development) and signalling in black pepper roots. Auxins play a critical role in regulating root growth, apical dominance, and the formation of lateral roots (Benkova and Hejátko, 2009). The induction of genes encoding auxin-responsive proteins and auxin efflux carriers indicates enhanced auxin transport, which facilitates root elongation and development (De Zelicourt, 2013). This auxin-mediated regulation is particularly significant in enhancing the formation of lateral roots, which was observed in black pepper plants colonized by *P. chlamydosporia*. The increased lateral root growth contributes to a larger root surface area, improving the plant's capacity to absorb water and nutrients from the soil. Additionally, this increased root branching can enhance plant tolerance to nematode infestations (Escudero and Lopez-Llorca, 2012) and provides a fertilizer-like effect, supporting plant vigour (Maciá-Vicente et al., 2009b).

Our study also found that *P. chlamydosporia* significantly influences the expression of genes related to gibberellin and cytokinin biosynthesis, which are known to regulate cell division, elongation, and nutrient mobilization. The upregulation of gibberellin receptor genes in black pepper roots is consistent with previous findings in tomato plants colonized by *P. chlamydosporia* (Pentimone et al., 2019). Studies in *P. chlamydosporia* colonized barley roots have shown that the overexpression of genes encoding GA2 oxidase and chitin-inducible GA-responsive protein is responsible for the metabolism of gibberellin (GA) (Larriba et al., 2015). Gibberellins, together with cytokinins, play a pivotal role in promoting shoot and root growth, thereby enhancing overall plant biomass.Auxin plays a central role in root development by promoting cell elongation, division, and differentiation. The upregulation of auxin-responsive genes, including auxin efflux carriers, indicates that *P. chlamydosporia* enhances root architecture, thereby increasing nutrient uptake and stress tolerance (Escudero & Lopez-Llorca, 2012).

Additionally, our study identified significant upregulation of genes involved in the uptake of key nutrients such as nitrogen, phosphorus, potassium, calcium, and iron. This aligns with previous research demonstrating that *P. chlamydosporia* promotes nutrient acquisition, potentially reducing the need for chemical fertilizers (Maciá-Vicente et al., 2009a).

Aquaporins, which were significantly upregulated in our study, are vital for water transport and cellular homeostasis. These proteins enhance water uptake, improve drought tolerance, and facilitate nutrient transport, thus supporting plant growth under stress conditions (Wang et al. 2020). Enhanced expression of aquaporins further supports improved water transport and resistance to abiotic stress (Wang et al., 2018). The increased expression of aquaporin genes in black pepper roots suggests that *P. chlamydosporia* may improve water use efficiency and overall plant resilience, making it a valuable bioinoculant for sustainable agriculture.

5.4.4 *Stress tolerance and defence protein induction*

The upregulation of phenylpropanoid biosynthesis genes in black pepper roots suggests that *P. chlamydosporia* enhances the production of defense-related metabolites, including lignin, flavonoids, salicylic acid (SA), and hydroxycinnamic acid esters, which are essential for plant defence and systemic acquired resistance (SAR) (Kuźniak et al., 2017). Additionally, the increased expression of WRKY transcription factors, known to regulate stress responses, further confirms the role of *P. chlamydosporia* in priming the plant's immune system (Bakshi and Oelmüller, 2014). Pentimone et al. (2019) reported that *P. chlamydosporia*-colonized tomato roots expressed 15 phenylalanine ammonia lyase (PAL) genes and impacted many SA-response WRKY genes. PAL, the initial enzyme in the phenylpropanoid pathway, leads to SA biosynthesis.

Endochitinase, germin like proteins, and late embryogenesis abundant (LEA) proteins are among the defense-responsive genes that are overexpressed as a result of *P. chlamydosporia* colonisation in black pepper roots. Larriba et al. (2015) reported that the colonization of barley roots by *P. chlamydosporia* resulted in the identification of five probesets encoding hydrolytic enzymes associated with response to pathogens

(three methyl esterases and two chitinases), as well as other pathogen-induced genes, including four germin A-like proteins, two pathogenesis-related (PR) proteins, and one late embryogenesis abundant protein. Pentimone et al. (2019) observed similar outcomes from *P. chlamydosporia* colonizing tomato roots, including the upregulation of chitinases, germin-like proteins, and pathogenesis-related proteins (PR).

Our results indicate that *P. chlamydosporia* colonization triggers the expression of stress-responsive proteins such as ascorbate peroxidase (APX), which which plays a crucial role in scavenging reactive oxygen species (ROS) generated during stress (Caverzan et al., 2012). This supports previous findings that *P. chlamydosporia* enhances the stress tolerance in tomato (Pentimone et al., 2019) and barley roots (Larriba et al., 2015). Based on the RNASeq, another DEG that was either overexpressed or underexpressed was a transcription factor belonging to the MYB family. According to Pentimone et al. (2019), the colonization of *P. chlamydosporia* in tomato roots results in the 91-fold repression of a MYB family transcription factor at 21 dpi. MYBs help to activate the genes and PR proteins that produce ROS (Cheong et al., 2002).

5.5 Conclusion

The findings of this study reveal that *P. chlamydosporia* colonization modulates the transcriptome of black pepper roots, resulting in a dual benefit: enhanced defence responses and improved growth promotion. The upregulation of genes involved in hormone signalling, nutrient uptake, and stress responses underscores the potential of *P. chlamydosporia* as both a biocontrol agent and a biofertilizer. By enhancing plant growth and resilience, *P. chlamydosporia* offers a promising alternative to chemical treatments, aligning with sustainable agricultural practices. Future studies should focus on validating these transcriptomic findings in field conditions to explore the practical applications of *P. chlamydosporia* in crop management. This work lays the foundation for using beneficial endophytes to enhance crop productivity while minimizing environmental impacts.

Supplementary Table 1

Functional Annotation of Significantly upregulated DEGs at 14 dpi

Transcript ID	Log2 Fold Change	Hit desc.
CDS_13934_Unigene_25889_Transcript_44766	5.444135642	XP_031262629.1 aquaporin TIP2-2
CDS_22546_Unigene_36109_Transcript_62871	4.8225031	No Blast Hit
CDS_16795_Unigene_29250_Transcript_50657	4.400130412	XP_013626871.1: pathogenesis-related protein PR-4B-like
CDS_19935_Unigene_3297_Transcript_5433	4.365555027	XP_010262131.1: beta-galactosidase isoform X1
CDS_49932_Unigene_8951_Transcript_14921	4.310874512	TVT98964.1 EJB05_55700, partial
CDS_32813_Unigene_50279_Transcript_88567	4.182842676	No Blast Hit
CDS_43769_Unigene_7091_Transcript_11865	4.102535066	PIA50475.1 AQUCO_01300896v1
CDS_36285_Unigene_55797_Transcript_98511	4.086491526	KVI03138.1Phloem protein 2-like protein
CDS_19940_Unigene_3298_Transcript_5434	4.05796323	XP_010262132.1: beta-galactosidase isoform X2
CDS_4102_Unigene_14573_Transcript_24838	4.056649049	No Blast Hit
CDS_16243_Unigene_285_Transcript_474	3.984647837	No Blast Hit
CDS_7052_Unigene_17922_Transcript_30802	3.942761415	OVA04007.1Protein of unknown function DUF761
CDS_47236_Unigene_80320_Transcript_145233	3.880305542	XP_021911467.1protein FAF-like, chloroplastic
CDS_4104_Unigene_14575_Transcript_24840	3.819783795	No Blast Hit
CDS_13933_Unigene_25888_Transcript_44763	3.809720867	NP_001289647.1 aquaporin TIP-type
CDS_49630_Unigene_8833_Transcript_14700	3.762700492	No Blast Hit
CDS_20118_Unigene_33188_Transcript_57650	3.718319784	RWR81931.1protein PHLOEM PROTEIN 2-LIKE A1
CDS_19851_Unigene_32895_Transcript_57117	3.68589724	AAP92160.2chlorophyllase
CDS_9656_Unigene_20917_Transcript_36084	3.684730168	ABX71220.1osmotin
CDS_24252_Unigene_38366_Transcript_66850	3.651394277	XP_023917839.1uncharacterized protein LOC112029389
CDS_42951_Unigene_6898_Transcript_11543	3.610053482	No Blast Hit
CDS_15927_Unigene_28221_Transcript_48804	3.539280407	OVA00651.1Mlo-related protein
CDS_36818_Unigene_56698_Transcript_100224	3.488190248	No Blast Hit
CDS_31572_Unigene_48398_Transcript_85237	3.455959663	No Blast Hit
CDS_31460_Unigene_4821_Transcript_8039	3.431849916	XP_010263063.1: myb family transcription factor EFM-like isoform X2
CDS_7051_Unigene_17921_Transcript_30800	3.429481236	OVA04007.1Protein of unknown function DUF761

Transcript ID	Log2 Fold Change	Hit desc.
CDS_2772_Unigene_13080_Transcript_22131	3.418474041	XP_017243480.1: uncharacterized protein LOC108215483
CDS_51576_Unigene_9857_Transcript_16481	3.417408404	No Blast Hit
CDS_12152_Unigene_23824_Transcript_41172	3.40523369	XP_013736391.1 galactinol--sucrose galactosyltransferase 6
CDS_36598_Unigene_56310_Transcript_99484	3.36296062	XP_030956067.1uncharacterized protein LOC115978188
CDS_29321_Unigene_45115_Transcript_79287	3.3415988	No Blast Hit
CDS_29322_Unigene_45116_Transcript_79288	3.282315569	No Blast Hit
CDS_37653_Unigene_58213_Transcript_102897	3.275186331	ACV88635.1SUPRESSOR OF OVEREXPRESSION OF CONSTANS1
CDS_3737_Unigene_14154_Transcript_24052	3.257751738	XP_007031572.1: uncharacterized protein LOC18600830
CDS_3738_Unigene_14155_Transcript_24053	3.254887438	OMO59275.1 CCACVL1_24955
CDS_20799_Unigene_33998_Transcript_59099	3.254350122	XP_018730850.1: uncharacterized protein LOC108960255
CDS_25174_Unigene_39563_Transcript_69040	3.253289024	RZS23073.1 BHM03_00055927, partial
CDS_42046_Unigene_6692_Transcript_11210	3.249794584	CAA04653.1major intrinsic protein PIPB
CDS_19772_Unigene_32788_Transcript_56946	3.225930096	MQL99914.1
CDS_42049_Unigene_6693_Transcript_11211	3.215690636	CAA04653.1major intrinsic protein PIPB
CDS_3888_Unigene_14324_Transcript_24365	3.208025043	XP_011080226.1omega-6 fatty acid desaturase, endoplasmic reticulum isozyme 2 isoform X1
CDS_12222_Unigene_23903_Transcript_41295	3.183238815	GAY35854.1 CUMW_018960
CDS_20876_Unigene_34078_Transcript_59246	3.160250564	XP_002533873.1uncharacterized protein LOC8284795
CDS_31571_Unigene_48397_Transcript_85235	3.150289753	No Blast Hit
CDS_694_Unigene_10782_Transcript_18092	3.145914292	XP_010277896.1: uncharacterized protein LOC104612242
CDS_41323_Unigene_65254_Transcript_115692	3.116406148	XP_011007843.1: uncharacterized protein LOC105113384
CDS_42069_Unigene_6698_Transcript_11220	3.1126761	CAA04653.1major intrinsic protein PIPB
CDS_33223_Unigene_5080_Transcript_8482	3.097991528	XP_002878679.1ethylene-responsive transcription factor ERF008
CDS_7253_Unigene_18138_Transcript_31205	3.068235473	XP_010273111.1: uncharacterized protein LOC104608736
CDS_22625_Unigene_36218_Transcript_63081	3.038425619	RWR86677.1proline-rich protein DC2.15-like protein
CDS_37474_Unigene_5787_Transcript_9658	3.036318236	No Blast Hit

Transcript ID	Log2 Fold Change	Hit desc.
CDS_42946_Unigene_6897_Transcript_11542	3.033264912	No Blast Hit
CDS_17637_Unigene_30220_Transcript_52375	3.022031181	XP_016695900.1: galactinol synthase 1-like
CDS_37465_Unigene_5786_Transcript_9657	3.004822383	XP_016746493.1: FK506-binding protein 4-like isoform X2
CDS_20783_Unigene_33971_Transcript_59026	2.986582019	BAJ97607.1 protein
CDS_25732_Unigene_40295_Transcript_70375	2.983029182	No Blast Hit
CDS_46701_Unigene_78639_Transcript_141726	2.969949427	EFL06024.1conserved
CDS_44123_Unigene_7177_Transcript_12013	2.958373075	XP_010268836.1: F-box protein At1g61340-like
CDS_2489_Unigene_12774_Transcript_21595	2.954007883	RWR73773.1Glycosyl hydrolases 36
CDS_20875_Unigene_34077_Transcript_59245	2.952445679	XP_002533873.1uncharacterized protein LOC8284795
CDS_7587_Unigene_18543_Transcript_31973	2.9493995	No Blast Hit
CDS_42516_Unigene_68002_Transcript_120733	2.949363655	OVA04715.1Protein of unknown function DUF4228
CDS_38525_Unigene_59847_Transcript_105855	2.945187115	PIA62780.1 AQUCO_00200653v1
CDS_31801_Unigene_48734_Transcript_85819	2.931981577	XP_034912327.1uncharacterized protein LOC118047209
CDS_11203_Unigene_22731_Transcript_39267	2.920695769	XP_020092748.1protein DMR6-LIKE OXYGENASE 2
CDS_43397_Unigene_69955_Transcript_124541	2.906670488	NP_001236302.2alpha crystallin domain-containing protein precursor
CDS_35619_Unigene_54701_Transcript_96517	2.904236586	PIM98415.1Germacradienol synthase
CDS_20447_Unigene_3356_Transcript_5521	2.857980995	KCW50407.1 EUGRSUZ_J00155, partial
CDS_37481_Unigene_5788_Transcript_9659	2.822622821	No Blast Hit
CDS_37633_Unigene_58181_Transcript_102831	2.819506847	RWR85261.1E3 ubiquitin-protein ligase PUB23
CDS_11204_Unigene_22732_Transcript_39268	2.815622863	XP_026398549.1protein DMR6-LIKE OXYGENASE 2-like
CDS_19103_Unigene_31947_Transcript_55509	2.811687343	RXI05536.1 DVH24_017578
CDS_11196_Unigene_22725_Transcript_39261	2.809144804	XP_010255099.1: protein DMR6-LIKE OXYGENASE 1-like
CDS_12223_Unigene_23904_Transcript_41296	2.802004789	XP_016554141.1: bifunctional epoxide hydrolase 2-like
CDS_18131_Unigene_30822_Transcript_53447	2.791383246	XP_020085665.1WAT1-related protein At5g07050-like
CDS_24251_Unigene_38365_Transcript_66849	2.790283492	XP_023917839.1uncharacterized protein LOC112029389
CDS_38785_Unigene_60260_Transcript_106646	2.7886957	RWR95791.1 CKAN_02514700
CDS_11231_Unigene_22765_Transcript_39343	2.784190734	XP_027909364.1S-norcoclaurine synthase 2-like

Transcript ID	Log2 Fold Change	Hit desc.
CDS_44636_Unigene_7300_Transcript_12224	2.759409961	OVA17962.1Major intrinsic protein
CDS_12139_Unigene_23807_Transcript_41138	2.757952177	XP_034916658.1putative glucose-6-phosphate 1-epimerase isoform X2
CDS_9679_Unigene_20941_Transcript_36125	2.753889254	RWR90134.1WAT1-related-like protein
CDS_30573_Unigene_46909_Transcript_82555	2.751827443	PIA47352.1 AQUCO_01400195v1
CDS_42056_Unigene_6695_Transcript_11215	2.747044594	CAA04653.1major intrinsic protein PIPB
CDS_17041_Unigene_29545_Transcript_51194	2.745568452	PNS94102.2 POPTR_018G126400
CDS_66_Unigene_10076_Transcript_16856	2.743127618	XP_010544738.1: aquaporin PIP1-1-like
CDS_65_Unigene_10075_Transcript_16855	2.734362636	RWR96672.1putative aquaporin PIP2-2
CDS_11200_Unigene_22729_Transcript_39265	2.732537488	XP_020092748.1protein DMR6-LIKE OXYGENASE 2
CDS_48486_Unigene_84315_Transcript_154628	2.721084794	KAA8522140.1 F0562_012546
CDS_30394_Unigene_46643_Transcript_82080	2.718151169	XP_010260299.1: ethylene-responsive transcription factor 4-like
CDS_17292_Unigene_29842_Transcript_51730	2.712415199	OVA17154.1LURP1-like domain
CDS_5867_Unigene_16591_Transcript_28498	2.708355555	XP_010278431.1: uncharacterized protein LOC104612634
CDS_44275_Unigene_7214_Transcript_12066	2.704877028	KMT10440.1 BVRB_5g115660
CDS_14700_Unigene_26799_Transcript_46351	2.70249973	CDP01705.1unnamed protein product
CDS_18365_Unigene_31083_Transcript_53907	2.702276126	XP_006363788.1: xyloglucan endotransglucosylase/hydrolase protein 7
CDS_42061_Unigene_6696_Transcript_11218	2.701452022	CAA04653.1major intrinsic protein PIPB
CDS_26477_Unigene_41301_Transcript_72275	2.696026705	XP_010276380.1: glutamate dehydrogenase 1
CDS_5868_Unigene_16592_Transcript_28499	2.690973477	XP_010278431.1: uncharacterized protein LOC104612634
CDS_2490_Unigene_12775_Transcript_21596	2.687497567	RWR73773.1Glycosyl hydrolases 36
CDS_37462_Unigene_5785_Transcript_9656	2.684600435	XP_026664832.1LOW QUALITY PROTEIN: heavy metal-associated isoprenylated plant protein 39
CDS_2488_Unigene_12773_Transcript_21593	2.673543617	RWR73774.1Glycosyl hydrolases 36
CDS_15813_Unigene_2809_Transcript_4631	2.668947171	KAA8521005.1 F0562_011707
CDS_30572_Unigene_46905_Transcript_82548	2.652095253	XP_006421608.1expansin-B15
CDS_34993_Unigene_53660_Transcript_94680	2.642474959	PSS33124.1Spore coat assembly protein like
CDS_51575_Unigene_9853_Transcript_16477	2.641080377	KDO57968.1 CISIN_1g031376mg
CDS_30396_Unigene_46645_Transcript_82083	2.623600014	KAF4350625.1 F8388_002085
CDS_15783_Unigene_2806_Transcript_4627	2.622437206	KAA8521005.1 F0562_011707

Transcript ID	Log2 Fold Change	Hit desc.
CDS_9583_Unigene_20831_Transcript_35915	2.618581753	No Blast Hit
CDS_22444_Unigene_35975_Transcript_62652	2.610053482	XP_010275692.1: E3 ubiquitin-protein ligase RHA1B-like
CDS_29663_Unigene_45580_Transcript_80128	2.610053482	XP_008373624.1FCS-Like Zinc finger 2
CDS_19224_Unigene_32087_Transcript_55747	2.599711537	PSS17867.1Metallothiol transferase
CDS_6319_Unigene_17094_Transcript_29397	2.59235148	XP_034692772.1histone H2A
CDS_15594_Unigene_27838_Transcript_48167	2.590245001	RWR79201.1cytokinin riboside 5'-monophosphate phosphoribohydrolase LOG1 isoform X1
CDS_7261_Unigene_18145_Transcript_31214	2.579910608	XP_010273111.1: uncharacterized protein LOC104608736
CDS_41950_Unigene_66729_Transcript_118413	2.575619985	XP_012093337.1protein YLS3
CDS_19104_Unigene_31948_Transcript_55513	2.570525117	XP_010251393.1: BTB/POZ and TAZ domain-containing protein 3-like
CDS_1827_Unigene_12040_Transcript_20266	2.554344049	RWR83263.1phospholipase A2-alpha isoform X2
CDS_20020_Unigene_3307_Transcript_5446	2.552363631	XP_034677299.1uncharacterized protein LOC117907762
CDS_8318_Unigene_19383_Transcript_33360	2.547350983	PIA64590.1 AQUCO_00100221v1
CDS_30395_Unigene_46644_Transcript_82082	2.5360529	KAF4350625.1 F8388_002085
CDS_8612_Unigene_19741_Transcript_34015	2.53000023	XP_021283467.1uncharacterized protein LOC110415978
CDS_28194_Unigene_43609_Transcript_76556	2.527591321	XP_034220016.1serine/threonine-protein phosphatase PP1 isoform X1
CDS_6457_Unigene_17252_Transcript_29665	2.518378881	RWR95464.1zinc finger protein
CDS_39484_Unigene_6165_Transcript_10244	2.51782619	XP_008781778.1ubiquitin-conjugating enzyme E2 22-like
CDS_44869_Unigene_73548_Transcript_131587	2.505972959	KAF2945960.1 DAI22_02g255600
CDS_15852_Unigene_2814_Transcript_4639	2.505864631	XP_021275241.1alpha-galactosidase-like
CDS_18130_Unigene_30821_Transcript_53446	2.504560353	XP_002283348.1: WAT1-related protein At5g07050
CDS_41383_Unigene_6540_Transcript_10934	2.502500341	XP_002533777.1purple acid phosphatase 17
CDS_41637_Unigene_66021_Transcript_117120	2.499495107	No Blast Hit
CDS_12221_Unigene_23902_Transcript_41294	2.499257955	XP_024034688.1uncharacterized protein LOC18032915 isoform X2
CDS_25869_Unigene_40480_Transcript_70720	2.49263062	OMP11194.1 COLO4_03971
CDS_18978_Unigene_31795_Transcript_55206	2.490471866	XP_010259397.1: dnaJ homolog subfamily B member 3 isoform X1
CDS_1831_Unigene_12051_Transcript_20294	2.486782107	XP_010263545.1: heat shock factor protein HSF24-like

Transcript ID	Log2 Fold Change	Hit desc.
CDS_3713_Unigene_1412_Transcript_2398	2.483737032	PWA42418.1tubby C-terminal-like domain-containing protein
CDS_27479_Unigene_42632_Transcript_74780	2.480216044	AAX83417.1gigantea-like protein, partial
CDS_37039_Unigene_57105_Transcript_100934	2.464364162	OVA08593.1Major intrinsic protein
CDS_15803_Unigene_2808_Transcript_4629	2.463333609	XP_021275241.1alpha-galactosidase-like
CDS_46453_Unigene_77853_Transcript_140110	2.452512205	RWR95440.1Para-hydroxybenzoic acid efflux pump subunit AaeB/fusaric acid resistance protein
CDS_38621_Unigene_59992_Transcript_106124	2.442499385	RWR82255.1dirigent protein 22-like protein
CDS_33400_Unigene_51074_Transcript_89932	2.437872506	YP_009408146.1RNA-dependent RNA polymerase
CDS_29134_Unigene_44855_Transcript_78824	2.43278363	THU69225.1 C4D60_Mb08t12170
CDS_50976_Unigene_9331_Transcript_15615	2.432515296	XP_022888150.1transcription factor bHLH66-like
CDS_44280_Unigene_7215_Transcript_12069	2.426419645	XP_017254707.1: AAA-ATPase At3g28580-like
CDS_17040_Unigene_29544_Transcript_51192	2.414670688	OUZ99852.1Glycosyl hydrolases 36
CDS_38330_Unigene_59475_Transcript_105189	2.405582968	XP_034705726.1transcription factor MYB16
CDS_41308_Unigene_6522_Transcript_10905	2.403645485	PON73403.1 PanWU01x14_059070
CDS_12189_Unigene_23866_Transcript_41240	2.398549376	XP_021750146.1MOB kinase activator-like 1A isoform X3
CDS_27466_Unigene_42615_Transcript_74745	2.398549376	KHN10991.1 glysoja_026726
CDS_9171_Unigene_20357_Transcript_35067	2.395443072	KAE8721266.1SPX domain-containing protein 3
CDS_34396_Unigene_52661_Transcript_92828	2.394324791	RWR89594.1D-amino-acid transaminase, chloroplastic isoform X1
CDS_43741_Unigene_7085_Transcript_11858	2.394324791	KDO45654.1 CISIN_1g0152451mg, partial
CDS_2486_Unigene_12771_Transcript_21587	2.393570228	XP_031398942.1 galactinol--sucrose galactosyltransferase 2
CDS_18936_Unigene_31743_Transcript_55111	2.393094946	RWR74286.1Glycoside hydrolase
CDS_7492_Unigene_18418_Transcript_31731	2.389225636	XP_008795112.1sugar transporter ERD6-like 16
CDS_44054_Unigene_71620_Transcript_127762	2.38766106	PON42355.1LRR domain containing protein
CDS_482_Unigene_10546_Transcript_17647	2.379933698	RWR88704.1NAC domain-containing protein 21/22
CDS_8276_Unigene_19331_Transcript_33271	2.378237806	RZB57329.1Zeaxanthin epoxidase, chloroplastic isoform A

Transcript ID	Log2 Fold Change	Hit desc.
CDS_12902_Unigene_24713_Transcript_42719	2.373277142	XP_030439613.1protein RESPONSE TO LOW SULFUR 3-like
CDS_5958_Unigene_16691_Transcript_28665	2.366224389	XP_010256968.1: alanine--glyoxylate aminotransferase 2 homolog 3, mitochondrial
CDS_30404_Unigene_46655_Transcript_82105	2.356983462	XP_010047178.1: uncharacterized protein LOC104436145
CDS_48195_Unigene_83325_Transcript_152109	2.348695654	RWR93589.1protein MOTHER of FT and TFL1-like protein
CDS_17067_Unigene_29573_Transcript_51244	2.347019076	TXG51937.1 EZV62_021106
CDS_35122_Unigene_53840_Transcript_95000	2.347019076	XP_010259986.1: uncharacterized protein LOC104599235
CDS_39485_Unigene_6166_Transcript_10246	2.345764013	XP_008781778.1ubiquitin-conjugating enzyme E2 22-like
CDS_7493_Unigene_18419_Transcript_31737	2.340240543	XP_008795112.1sugar transporter ERD6-like 16
CDS_15806_Unigene_28092_Transcript_48591	2.332110869	XP_010265413.1: AAA-ATPase At3g50940-like
CDS_24250_Unigene_38364_Transcript_66848	2.328581828	KAF2310655.1 GH714_016093
CDS_18071_Unigene_30748_Transcript_53312	2.327670616	XP_012088327.1putative lipid-transfer protein DIR1
CDS_2485_Unigene_12770_Transcript_21584	2.326141936	RWR73774.1Glycosyl hydrolases 36
CDS_25363_Unigene_39818_Transcript_69537	2.324298999	XP_010264071.1: uncharacterized protein LOC104602168
CDS_3308_Unigene_1369_Transcript_2336	2.323303007	RWR77531.1protein GIGANTEA
CDS_7778_Unigene_18764_Transcript_32332	2.317101641	KAF3436417.1 FNV43_RR23509
CDS_34801_Unigene_53358_Transcript_94166	2.311712207	XP_015873986.1zinc transporter 2
CDS_42731_Unigene_6845_Transcript_11465	2.30249235	XP_010263531.1: ABSCISIC ACID-INSENSITIVE 5-like protein 5 isoform X1
CDS_20852_Unigene_34054_Transcript_59212	2.301931186	OUZ99878.1LURP1-like domain
CDS_29126_Unigene_44843_Transcript_78800	2.300368983	RWR89959.1transcription factor bHLH96
CDS_34493_Unigene_52829_Transcript_93147	2.300368983	RWR91431.1 CKAN_02058400
CDS_3311_Unigene_13701_Transcript_23256	2.288000321	XP_021618735.1uncharacterized protein LOC110619533
CDS_7489_Unigene_18415_Transcript_31726	2.275345798	THG11340.1 TEA_027757
CDS_41378_Unigene_6539_Transcript_10933	2.267584608	XP_010241716.1: purple acid phosphatase 17-like
CDS_19004_Unigene_31832_Transcript_55274	2.264057627	RWR80673.1 CKAN_00932500
CDS_39534_Unigene_61740_Transcript_109300	2.255978826	XP_004982014.1basic blue protein
CDS_47584_Unigene_813_Transcript_1365	2.252259934	KAF2314167.1 GH714_023833

Transcript ID	Log2 Fold Change	Hit desc.
CDS_43580_Unigene_7041_Transcript_11790	2.252005961	RWR84153.1putative membrane-associated kinase regulator 1 -like protein
CDS_51035_Unigene_9348_Transcript_15641	2.251469251	XP_010252355.1: protein NRT1/ PTR FAMILY 4.4 isoform X2
CDS_25880_Unigene_40496_Transcript_70744	2.247483402	KAA0042965.1S-norcoclaurine synthase 1-like
CDS_14703_Unigene_26800_Transcript_46352	2.247128015	RWR78560.1putative polyamine oxidase 4 isoform X1
CDS_23565_Unigene_3745_Transcript_6182	2.246622191	XP_020251119.1putative germin-like protein 2-1
CDS_12410_Unigene_24112_Transcript_41668	2.242791707	XP_018679594.1: uncharacterized protein LOC103979672 isoform X1
CDS_18132_Unigene_30823_Transcript_53448	2.239410102	RWR76062.1WAT1-related protein
CDS_17638_Unigene_30221_Transcript_52376	2.233199176	RWR92332.1myb-related protein Hv1-like protein
CDS_39178_Unigene_61048_Transcript_108051	2.22743746	XP_010941684.1VQ motif-containing protein 22
CDS_34924_Unigene_53570_Transcript_94532	2.224763326	KAB5537340.1 DKX38_014873
CDS_30398_Unigene_46647_Transcript_82085	2.224162328	RWW49574.1 BHE74_00044235
CDS_32587_Unigene_49954_Transcript_87973	2.221488194	BAF18856.2Os06g0172800
CDS_1834_Unigene_12054_Transcript_20297	2.218474955	XP_010263545.1: heat shock factor protein HSF24-like
CDS_31895_Unigene_48875_Transcript_86088	2.217736059	RWR84583.1MLO protein 1-like protein
CDS_15405_Unigene_27628_Transcript_47766	2.216800398	KJB63488.1 B456_010G002000
CDS_5095_Unigene_15727_Transcript_26909	2.215335967	PON47775.1Caleosin-related
CDS_14363_Unigene_2638_Transcript_4354	2.209443053	RWR96232.1 CKAN_02560500
CDS_18506_Unigene_31240_Transcript_54181	2.209174045	XP_034675077.1uncharacterized protein LOC117906209
CDS_44628_Unigene_7299_Transcript_12220	2.206857595	OVA17962.1Major intrinsic protein
CDS_47725_Unigene_8191_Transcript_13640	2.205904299	XP_031093344.1alcohol dehydrogenase-like 4
CDS_19102_Unigene_31946_Transcript_55508	2.204061122	XP_010650726.1: BTB/POZ and TAZ domain-containing protein 3
CDS_44140_Unigene_7181_Transcript_12019	2.202510519	XP_010268836.1: F-box protein At1g61340-like
CDS_7250_Unigene_18135_Transcript_31199	2.200904542	XP_010273111.1: uncharacterized protein LOC104608736
CDS_35732_Unigene_54886_Transcript_96858	2.195015982	No Blast Hit
CDS_5318_Unigene_15988_Transcript_27341	2.191576898	PON97075.1Alcohol dehydrogenase superfamily, zinc-type
CDS_22160_Unigene_35640_Transcript_62045	2.190100492	KAA8540212.1 F0562_024225

Transcript ID	Log2 Fold Change	Hit desc.
CDS_33119_Unigene_50671_Transcript_89233	2.184962318	XP_009405364.1: peroxisomal (S)-2-hydroxy-acid oxidase GLO1
CDS_12285_Unigene_23977_Transcript_41414	2.182632258	XP_009419511.1: CASP-like protein 1D1
CDS_21974_Unigene_35417_Transcript_61615	2.18195983	KAB1210503.1Amino acid permease 2
CDS_7779_Unigene_18765_Transcript_32333	2.175804481	KAF3436417.1 FNV43_RR23509
CDS_47769_Unigene_8203_Transcript_13652	2.171932369	XP_031093344.1alcohol dehydrogenase-like 4
CDS_23455_Unigene_37315_Transcript_65052	2.171364714	XP_020103625.1chaperone protein dnaJ 8, chloroplastic-like
CDS_3302_Unigene_1368_Transcript_2334	2.169593386	RWR77531.1protein GIGANTEA
CDS_485_Unigene_10549_Transcript_17652	2.16644683	RWR88704.1NAC domain-containing protein 21/22
CDS_26415_Unigene_41206_Transcript_72117	2.164155019	KAF3436313.1 FNV43_RR23405
CDS_3749_Unigene_14171_Transcript_24090	2.161695909	XP_010259074.1: heparanase-like protein 1
CDS_6431_Unigene_17221_Transcript_29615	2.161463423	XP_008794778.1 polygalacturonase isoform X3
CDS_31800_Unigene_48733_Transcript_85818	2.16074608	XP_034912327.1uncharacterized protein LOC118047209
CDS_1838_Unigene_12058_Transcript_20301	2.160250564	RWR73379.1putative Heat shock transcription factor C1
CDS_20439_Unigene_3355_Transcript_5520	2.15919349	KAE8646573.1 Csa_005623
CDS_25556_Unigene_40068_Transcript_69986	2.155332281	RWR85078.1aspartyl protease family protein 1-like protein
CDS_34383_Unigene_52630_Transcript_92763	2.150178344	KAF5204731.1Udp-glycosyltransferase 74f2
CDS_5696_Unigene_16403_Transcript_28126	2.146106382	PIN19330.1Ubiquitin-protein ligase
CDS_12903_Unigene_24714_Transcript_42721	2.135279766	XP_030439613.1protein RESPONSE TO LOW SULFUR 3-like
CDS_23526_Unigene_3740_Transcript_6169	2.131751089	XP_010251871.1: putative germin-like protein 2-1
CDS_25875_Unigene_40489_Transcript_70734	2.130060541	YP_009270671.1NADH dehydrogenase subunit 5
CDS_42057_Unigene_66960_Transcript_118844	2.129427641	BBE07959.1polyubiquitin
CDS_48371_Unigene_83926_Transcript_153701	2.127901787	No Blast Hit
CDS_17291_Unigene_29841_Transcript_51728	2.127532386	RWR80164.1LURP1-like domain-containing protein
CDS_16440_Unigene_28835_Transcript_49909	2.11401626	No Blast Hit
CDS_103_Unigene_10112_Transcript_16909	2.110343763	PNX75340.1basic leucine zipper 9-like transcription factor, partial
CDS_12305_Unigene_23998_Transcript_41462	2.109899369	BAG15861.1

Transcript ID	Log2 Fold Change	Hit desc.
CDS_48273_Unigene_835_Transcript_1408	2.109848599	XP_034697165.1transcription factor bHLH112-like isoform X1
CDS_34395_Unigene_52660_Transcript_92827	2.109624491	RWR89594.1D-amino-acid transaminase, chloroplastic isoform X1
CDS_2487_Unigene_12772_Transcript_21590	2.103366601	XP_031398942.1 galactinol--sucrose galactosyltransferase 2
CDS_43449_Unigene_70077_Transcript_124761	2.10289778	XP_020570882.1cationic amino acid transporter 1
CDS_18053_Unigene_30728_Transcript_53282	2.100457985	XP_019055634.1: transcription factor ORG2-like
CDS_8613_Unigene_19742_Transcript_34018	2.099926214	KCW50926.1 EUGRSUZ_J00576
CDS_15924_Unigene_28219_Transcript_48800	2.098989095	OVA00651.1Mlo-related protein
CDS_6429_Unigene_17219_Transcript_29613	2.098501174	XP_010255223.1: polygalacturonase isoform X1
CDS_43589_Unigene_7043_Transcript_11793	2.097991528	RWR84153.1putative membrane-associated kinase regulator 1 -like protein
CDS_21970_Unigene_35413_Transcript_61608	2.095480309	RWR90243.1amino acid permease 3
CDS_26361_Unigene_41133_Transcript_71973	2.090485399	XP_010268064.1: calmodulin-binding protein 60 D-like isoform X2
CDS_599_Unigene_10674_Transcript_17887	2.086790726	No Blast Hit
CDS_5041_Unigene_15667_Transcript_26812	2.086081611	XP_020259215.1SUMO-conjugating enzyme SCE1
CDS_23214_Unigene_36988_Transcript_64479	2.085786913	OMO76643.1Regulator of chromosome condensation, RCC1
CDS_21773_Unigene_35163_Transcript_61157	2.079538765	No Blast Hit
CDS_44783_Unigene_73318_Transcript_131104	2.077412016	XP_010260192.1: MLP-like protein 423 isoform X1
CDS_33625_Unigene_51466_Transcript_90663	2.074721749	No Blast Hit
CDS_38804_Unigene_60317_Transcript_106746	2.074721749	KAE8037239.1 FH972_009847
CDS_25933_Unigene_4055_Transcript_6773	2.073025458	XP_010241154.1: 18.2 kDa class I heat shock protein-like
CDS_41015_Unigene_6462_Transcript_10786	2.07281005	XP_009380624.1: putative methyltransferase DDB_G0268948 isoform X1
CDS_29382_Unigene_451_Transcript_738	2.071403153	RWR86835.1late embryogenesis abundant-like protein
CDS_5957_Unigene_16690_Transcript_28664	2.066333963	XP_022722376.1alanine--glyoxylate aminotransferase 2 homolog 2, mitochondrial-like
CDS_50139_Unigene_9008_Transcript_15018	2.057914828	OVA13148.1Myc-type
CDS_18572_Unigene_31314_Transcript_54317	2.056736608	XP_002513994.1purine permease 3
CDS_4103_Unigene_14574_Transcript_24839	2.055347027	No Blast Hit

Transcript ID	Log2 Fold Change	Hit desc.
CDS_22906_Unigene_36537_Transcript_63712	2.052330052	XP_018840848.1: S-norcoclaurine synthase 1-like
CDS_22549_Unigene_36115_Transcript_62878	2.051280505	XP_010243984.1: 9-cis-epoxycarotenoid dioxygenase NCED6, chloroplastic-like
CDS_22627_Unigene_36223_Transcript_63088	2.050626073	XP_010258295.1: casparian strip membrane protein 3
CDS_33549_Unigene_51330_Transcript_90407	2.050626073	RWR73647.1glutaredoxin-C6
CDS_41367_Unigene_6535_Transcript_10928	2.049775845	TKY61094.1Purple acid phosphatase 17
CDS_6388_Unigene_17172_Transcript_29534	2.047862289	No Blast Hit
CDS_48196_Unigene_83326_Transcript_152111	2.047458794	RWR93589.1protein MOTHER of FT and TFL1-like protein
CDS_40853_Unigene_6426_Transcript_10714	2.04465835	PSR84894.1Purple acid phosphatase
CDS_17641_Unigene_30224_Transcript_52379	2.042004364	XP_020703289.1myb-related protein Zm38
CDS_43304_Unigene_69730_Transcript_124102	2.03889678	XP_010061961.1: gibberellin 3-beta-dioxygenase 1
CDS_41362_Unigene_6534_Transcript_10927	2.036678955	TKY61094.1Purple acid phosphatase 17
CDS_19671_Unigene_32645_Transcript_56730	2.033264912	THU48350.1 C4D60_Mb09t25300
CDS_4106_Unigene_14577_Transcript_24842	2.032744554	No Blast Hit
CDS_50138_Unigene_9007_Transcript_15017	2.027841592	OVA13148.1Myc-type
CDS_36998_Unigene_57039_Transcript_100817	2.025090981	XP_021734930.1L-ascorbate peroxidase, cytosolic
CDS_17070_Unigene_29576_Transcript_51247	2.023304361	RWR92977.1 CKAN_02220700
CDS_49654_Unigene_88413_Transcript_169193	2.02143581	ALG05128.1cytochrome P450
CDS_44504_Unigene_7271_Transcript_12177	2.017228863	TXG53256.1 EZV62_022425
CDS_8171_Unigene_19209_Transcript_33069	2.016045841	RWR89359.1BAG family molecular chaperone regulator 1
CDS_25424_Unigene_39885_Transcript_69659	2.01405271	RWR96949.1zinc finger protein
CDS_29330_Unigene_45127_Transcript_79307	2.012151925	No Blast Hit
CDS_46226_Unigene_7717_Transcript_12867	2.012151925	XP_028759077.1PLAT domain-containing protein 3-like
CDS_27067_Unigene_42078_Transcript_73733	2.01115179	MQL98110.1
CDS_5224_Unigene_15879_Transcript_27152	2.006254339	XP_002275288.1: peroxidase 21
CDS_49074_Unigene_8625_Transcript_14348	2.005538184	XP_015879798.1serine carboxypeptidase-like 25
CDS_28274_Unigene_43709_Transcript_76741	2.003831862	XP_019238921.1: uncharacterized protein LOC109218974
CDS_14704_Unigene_26801_Transcript_46353	1.996602424	RWR78560.1putative polyamine oxidase 4 isoform X1

Transcript ID	Log2 Fold Change	Hit desc.
CDS_33968_Unigene_51967_Transcript_91523	1.995220451	RWR75005.1cysteine-rich repeat secretory protein 55
CDS_45855_Unigene_76177_Transcript_136696	1.994717332	XP_009393840.1: LOB domain-containing protein 37-like
CDS_29310_Unigene_450_Transcript_735	1.993713166	NP_001149803.1seed specific protein Bn15D1B
CDS_17206_Unigene_29728_Transcript_51508	1.988565105	XP_010278908.1: protein LURP-one-related 8-like
CDS_50969_Unigene_9329_Transcript_15612	1.982514311	QDH08947.1transcription factor bHLH66 isoform X2
CDS_19101_Unigene_31945_Transcript_55506	1.978649636	RWR84727.1putative carboxylesterase 17
CDS_13263_Unigene_2510_Transcript_4164	1.978392042	XP_007160106.1 PHAVU_002G292900g
CDS_41377_Unigene_6538_Transcript_10932	1.97797575	TKY61094.1Purple acid phosphatase 17
CDS_5226_Unigene_15880_Transcript_27153	1.977262456	XP_002275288.1: peroxidase 21
CDS_18777_Unigene_31566_Transcript_54808	1.976835812	RWR76563.1putative calcium-binding protein CML25
CDS_33762_Unigene_51669_Transcript_91007	1.976835812	RWR76976.1E3 ubiquitin-protein ligase ATL4-like protein
CDS_1835_Unigene_12055_Transcript_20298	1.975050298	XP_010263545.1: heat shock factor protein HSF24-like
CDS_35096_Unigene_53804_Transcript_94944	1.973801752	XP_030971642.1cinnamoyl-CoA reductase 1
CDS_25446_Unigene_39921_Transcript_69740	1.971720692	No Blast Hit
CDS_41852_Unigene_66531_Transcript_118023	1.969456282	XP_020689320.1uncharacterized protein LOC110104510
CDS_40536_Unigene_63640_Transcript_112733	1.967050369	RWR77311.1peroxidase 10-like protein
CDS_6204_Unigene_16961_Transcript_29161	1.966011748	OVA01173.1Basic-leucine zipper domain
CDS_25879_Unigene_40493_Transcript_70740	1.959637919	No Blast Hit
CDS_42380_Unigene_67682_Transcript_120125	1.955828319	OTF90877.1putative NADH:ubiquinone/plastoquinone oxidoreductase, chain 3, Ribosomal protein S12/S23
CDS_16636_Unigene_29077_Transcript_50339	1.953043192	XP_006830282.1uncharacterized protein LOC18425705
CDS_2322_Unigene_125_Transcript_195	1.952445679	PIN21491.1 CDL12_05795
CDS_32835_Unigene_50307_Transcript_88608	1.952445679	THU69745.1 C4D60_Mb08t17640
CDS_34891_Unigene_53509_Transcript_94424	1.949539948	VAH62237.1unnamed protein product
CDS_13931_Unigene_25886_Transcript_44760	1.949158927	XP_022029689.1 aquaporin TIP-type
CDS_19444_Unigene_32360_Transcript_56202	1.942315923	XP_020110151.1uncharacterized protein LOC109725398

Transcript ID	Log2 Fold Change	Hit desc.
CDS_41291_Unigene_6518_Transcript_10899	1.941141576	XP_028114531.1uncharacterized protein LOC114312490
CDS_31099_Unigene_47694_Transcript_83921	1.93821353	No Blast Hit
CDS_4088_Unigene_14558_Transcript_24805	1.931981577	XP_030473411.1nodulation-signaling pathway 1 protein
CDS_47642_Unigene_81636_Transcript_147920	1.931981577	XP_011032644.1: protein TIFY 4A-like isoform X2
CDS_4803_Unigene_15398_Transcript_26311	1.929455702	XP_011458402.1: uncharacterized protein LOC105349702
CDS_35483_Unigene_54445_Transcript_96084	1.927082777	XP_010264010.1: serine incorporator 3 isoform X2
CDS_41851_Unigene_66530_Transcript_118022	1.925095191	KZV21398.1 F511_18564
CDS_30432_Unigene_46687_Transcript_82169	1.92007481	RWR73790.1Protein kinase domain-containing protein
CDS_5071_Unigene_15701_Transcript_26865	1.919755274	RWR72345.1zinc finger protein
CDS_36976_Unigene_57000_Transcript_100750	1.91671482	XP_017217783.1: flowering-promoting factor 1-like protein 3
CDS_47731_Unigene_8193_Transcript_13642	1.913669698	XP_008239269.1: alcohol dehydrogenase-like 4
CDS_18052_Unigene_30727_Transcript_53281	1.913245014	XP_019055634.1: transcription factor ORG2-like
CDS_19767_Unigene_32776_Transcript_56929	1.911709182	XP_008797044.1uncharacterized protein LOC103712332
CDS_47744_Unigene_8197_Transcript_13646	1.910607926	OVA04712.1Alcohol dehydrogenase superfamily
CDS_26646_Unigene_41519_Transcript_72685	1.908134835	RWW76774.1 BHE74_00015125
CDS_46292_Unigene_77384_Transcript_139161	1.900156131	PIA54316.1 AQUCO_00900691v1
CDS_17327_Unigene_29881_Transcript_51804	1.899560099	KAA8519873.1 F0562_014037
CDS_10253_Unigene_21594_Transcript_37273	1.891235234	XP_022139678.1uncharacterized protein LOC111010526
CDS_29233_Unigene_449_Transcript_733	1.890161401	RWR86835.1late embryogenesis abundant-like protein
CDS_39459_Unigene_61615_Transcript_109065	1.890161401	OVA04085.1Squalene/phytoene synthase
CDS_37291_Unigene_57522_Transcript_101656	1.888038229	XP_027348783.1histone H2B isoform X4
CDS_46865_Unigene_79177_Transcript_142811	1.885060529	XP_026404397.1uncharacterized protein LOC113299575 isoform X1
CDS_46452_Unigene_77852_Transcript_140109	1.884913323	OVA18323.1Para-hydroxybenzoic acid efflux pump subunit AaeB/fusaric acid resistance protein
CDS_23960_Unigene_37969_Transcript_66164	1.884675862	No Blast Hit
CDS_43738_Unigene_7084_Transcript_11857	1.884675862	KDO45654.1 CISIN_1g0152451mg, partial

Transcript ID	Log2 Fold Change	Hit desc.
CDS_47763_Unigene_8200_Transcript_13649	1.883651289	OVA04712.1Alcohol dehydrogenase superfamily
CDS_6500_Unigene_17299_Transcript_29758	1.881247594	XP_010915364.1NADP-dependent malic enzyme isoform X2
CDS_35803_Unigene_54_Transcript_89	1.87754997	AGV54733.1dehydration-responsive protein RD22-like protein
CDS_32802_Unigene_50261_Transcript_88532	1.873087888	THU73946.1 C4D60_Mb04t28200
CDS_1588_Unigene_11792_Transcript_19823	1.872839688	XP_006413559.1 aquaporin PIP1-5
CDS_12963_Unigene_24793_Transcript_42863	1.869325969	XP_010932337.1uncharacterized protein LOC105053035
CDS_33536_Unigene_51298_Transcript_90347	1.868835283	No Blast Hit
CDS_23962_Unigene_37970_Transcript_66165	1.865231122	No Blast Hit
CDS_35387_Unigene_54311_Transcript_95839	1.853979065	KAA8526869.1 F0562_008902
CDS_43371_Unigene_69888_Transcript_124412	1.852910006	RWR90084.1thioredoxin-like protein 4, chloroplastic isoform X1
CDS_44128_Unigene_7178_Transcript_12014	1.852910006	XP_010268836.1: F-box protein At1g61340-like
CDS_47768_Unigene_8202_Transcript_13651	1.850984297	XP_010251993.1: alcohol dehydrogenase-like 4
CDS_17640_Unigene_30223_Transcript_52378	1.849880496	RWR92332.1myb-related protein Hv1-like protein
CDS_8170_Unigene_19208_Transcript_33068	1.848840341	RWR89359.1BAG family molecular chaperone regulator 1
CDS_4292_Unigene_14789_Transcript_25206	1.847850596	PON98151.1Mutator
CDS_29720_Unigene_45657_Transcript_80273	1.847092679	QCX36376.1kavalactone reductase 1
CDS_48791_Unigene_85301_Transcript_157331	1.844518735	TKR79661.1 D5086_0000270290
CDS_18934_Unigene_31741_Transcript_55107	1.838872172	RWR74286.1Glycoside hydrolase
CDS_32325_Unigene_49559_Transcript_87293	1.836624603	XP_029120568.1calcium uniporter protein 6, mitochondrial-like
CDS_20464_Unigene_3358_Transcript_5523	1.835986261	OAY78994.1Wound-induced protein 1
CDS_6503_Unigene_17300_Transcript_29759	1.835726621	XP_010915364.1NADP-dependent malic enzyme isoform X2
CDS_64_Unigene_10074_Transcript_16852	1.835081565	RWR96672.1putative aquaporin PIP2-2
CDS_1653_Unigene_11864_Transcript_19958	1.834840418	XP_028125201.1protein SULFUR DEFICIENCY-INDUCED 1-like
CDS_21365_Unigene_34659_Transcript_60251	1.832445903	ESR59989.1 CICLE_v10018257mg
CDS_41494_Unigene_65679_Transcript_116518	1.832445903	KAF5183050.1Ap2-like ethylene-responsive transcription factor ail7, partial
CDS_9713_Unigene_20981_Transcript_36195	1.832445903	EXC02104.1Transcription factor
CDS_38819_Unigene_60342_Transcript_106791	1.82739798	KAA8535068.1 F0562_030071
CDS_11336_Unigene_22875_Transcript_39559	1.825616565	No Blast Hit

Transcript ID	Log2 Fold Change	Hit desc.
CDS_24199_Unigene_38299_Transcript_66715	1.825370386	RWR76451.1bZIP transcription factor 53
CDS_27963_Unigene_43284_Transcript_75966	1.825066373	No Blast Hit
CDS_34517_Unigene_52874_Transcript_93244	1.824393631	XP_010265606.1: omega-6 fatty acid desaturase, chloroplastic-like
CDS_10656_Unigene_22081_Transcript_38117	1.823787542	XP_020672792.1serine--glyoxylate aminotransferase
CDS_5065_Unigene_15697_Transcript_26861	1.822083159	RWR72345.1zinc finger protein
CDS_29748_Unigene_45689_Transcript_80329	1.816504359	RWR93754.1cyclin-P3-1
CDS_461_Unigene_10524_Transcript_17609	1.816504359	OVA08776.1Tafazzin
CDS_34030_Unigene_52068_Transcript_91688	1.812442878	XP_019199014.1: osmotin-like protein
CDS_3137_Unigene_134_Transcript_208	1.812296203	XP_020083486.1vacuolar amino acid transporter 1 isoform X1
CDS_38218_Unigene_59275_Transcript_104841	1.811687343	TKY47271.1Pathogenesis-related transcriptional activator PTI6
CDS_27775_Unigene_43021_Transcript_75468	1.80936229	RWR79680.1ELMO domain-containing protein C isoform X1
CDS_9355_Unigene_20582_Transcript_35494	1.806854189	XP_013617403.1: protein phosphatase 2C 37-like
CDS_15539_Unigene_27776_Transcript_48029	1.80269856	RWR89299.1 CKAN_01835000
CDS_51031_Unigene_9347_Transcript_15640	1.800609816	PIA55277.1 AQUCO_00800178v1
CDS_32915_Unigene_5041_Transcript_8411	1.79812583	XP_015867477.1uncharacterized protein LOC107404979 isoform X1
CDS_16443_Unigene_28838_Transcript_49913	1.796931616	No Blast Hit
CDS_22307_Unigene_35811_Transcript_62367	1.796466606	RWR84321.1Peptidase M16
CDS_16010_Unigene_28328_Transcript_48985	1.791660288	XP_010248357.1: uncharacterized protein LOC104591250
CDS_34246_Unigene_52422_Transcript_92361	1.79122324	GAV85645.1EamA domain-containing protein
CDS_8069_Unigene_19096_Transcript_32867	1.790625727	XP_010920174.1thaumatin-like protein 1b
CDS_48434_Unigene_8414_Transcript_13986	1.789898654	NP_001304057.1NAC transcription factor 29
CDS_24746_Unigene_39000_Transcript_68014	1.788390723	XP_010275723.1: protein ABHD17B-like
CDS_47737_Unigene_8195_Transcript_13644	1.783820549	OVA04712.1Alcohol dehydrogenase superfamily
CDS_7153_Unigene_18023_Transcript_30977	1.782322424	PIA59624.1 AQUCO_00400487v1
CDS_45506_Unigene_7521_Transcript_12570	1.773189317	RWR95446.1histone H2B-like protein
CDS_29407_Unigene_45233_Transcript_79505	1.772992053	AAP83391.1FRUITFULL-like MADS-box, partial
CDS_32693_Unigene_50094_Transcript_88230	1.772324911	YP_009270676.1NADH dehydrogenase subunit 2

Transcript ID	Log2 Fold Change	Hit desc.
CDS_5836_Unigene_16557_Transcript_28440	1.772324911	ESR49892.1 CICLE_v100309252mg, partial
CDS_29551_Unigene_45428_Transcript_79874	1.771045358	XP_016577692.1: protein EARLY FLOWERING 4-like
CDS_35484_Unigene_54446_Transcript_96085	1.770518154	RWR88978.1dirigent protein 18
CDS_20549_Unigene_33690_Transcript_58515	1.769409241	RDX74386.1Expansin-A1, partial
CDS_37195_Unigene_57372_Transcript_101380	1.769252077	No Blast Hit
CDS_1316_Unigene_11489_Transcript_19273	1.767713202	RWR88384.1Galactose-binding protein isoform 1
CDS_102_Unigene_10111_Transcript_16906	1.765571059	XP_002283059.2: basic leucine zipper 9
CDS_35744_Unigene_54899_Transcript_96881	1.765331707	No Blast Hit
CDS_21490_Unigene_34799_Transcript_60508	1.764499751	XP_020248719.1arsenate reductase 2.2-like
CDS_22246_Unigene_35744_Transcript_62251	1.764381628	XP_019417355.1: NAC domain-containing protein 2
CDS_3805_Unigene_14234_Transcript_24219	1.762675625	ESR61409.1 CICLE_v10016627mg
CDS_17517_Unigene_30091_Transcript_52168	1.762056575	No Blast Hit
CDS_14428_Unigene_26475_Transcript_45793	1.760296117	RWR77999.1peroxidase 51-like protein
CDS_21625_Unigene_34974_Transcript_60804	1.759800601	XP_030539968.1pyruvate dehydrogenase (acetyl-transferring) kinase, mitochondrial
CDS_8129_Unigene_19164_Transcript_32974	1.759629838	KAA8523720.1 F0562_010143
CDS_1930_Unigene_12165_Transcript_20492	1.758152121	XP_008800336.1uncharacterized protein LOC103714734
CDS_46222_Unigene_7715_Transcript_12864	1.754597418	TKW03659.1 SEVIR_7G055100v2
CDS_7657_Unigene_18616_Transcript_32089	1.754443391	XP_011014769.1: 60S ribosomal protein L5-like
CDS_9354_Unigene_20581_Transcript_35493	1.754224585	XP_008803118.1 protein phosphatase 2C 24
CDS_17565_Unigene_30147_Transcript_52250	1.753366753	XP_008808992.2aromatic aminotransferase ISS1-like isoform X1
CDS_25378_Unigene_39835_Transcript_69568	1.753011436	RWR79027.1EPIDERMAL PATTERNING FACTOR-like protein 5
CDS_7154_Unigene_18024_Transcript_30979	1.750101442	PIA59624.1 AQUCO_00400487v1
CDS_18740_Unigene_3151_Transcript_5180	1.750029491	TKY61291.1Ubiquitin-conjugating enzyme E2-17 kDa
CDS_20050_Unigene_33114_Transcript_57514	1.747557005	KAF3781496.1 EJ110_NYTH36958
CDS_47757_Unigene_81_Transcript_136	1.746319172	RWR89211.1Crotonase superfamily
CDS_10281_Unigene_21635_Transcript_37350	1.744354573	KAF3976427.1 CMV_000399
CDS_5064_Unigene_15696_Transcript_26859	1.741602477	RWR72345.1zinc finger protein

Transcript ID	Log2 Fold Change	Hit desc.
CDS_10657_Unigene_22082_Transcript_38121	1.740825604	XP_020672792.1serine--glyoxylate aminotransferase
CDS_32109_Unigene_49208_Transcript_86717	1.739039922	No Blast Hit
CDS_36242_Unigene_55726_Transcript_98385	1.734500853	EEF35549.1peptidase, putative
CDS_44064_Unigene_71652_Transcript_127819	1.733435897	No Blast Hit
CDS_36274_Unigene_55774_Transcript_98469	1.728050691	GEY17160.1transcription factor bHLH123-like isoform X2
CDS_50960_Unigene_9326_Transcript_15607	1.726172039	QDL88317.1transcription factor bHLH66 isoform X2
CDS_16779_Unigene_29236_Transcript_50627	1.725530699	XP_010917487.1aldehyde dehydrogenase family 7 member A1 isoform X2
CDS_33121_Unigene_50674_Transcript_89237	1.725070142	GAV89181.1FMN_dh domain-containing protein
CDS_4030_Unigene_14496_Transcript_24677	1.722163848	PSS28737.1Glutathione S-transferase
CDS_33078_Unigene_50628_Transcript_89156	1.721084794	No Blast Hit
CDS_47087_Unigene_79840_Transcript_144203	1.717711195	XP_010250033.1: uncharacterized protein At1g15400
CDS_8424_Unigene_19514_Transcript_33596	1.713980924	RWR73666.1ent-kaurene oxidase
CDS_46504_Unigene_7802_Transcript_13021	1.712971795	AAM00365.1saline responsive OSSRIII protein, partial
CDS_26530_Unigene_41385_Transcript_72434	1.711139607	CDY18845.1BnaAnng03100D
CDS_9146_Unigene_20333_Transcript_35017	1.711139607	XP_010684357.1: mediator of RNA polymerase II transcription subunit 28
CDS_19814_Unigene_32849_Transcript_57041	1.711031129	XP_010907663.1glycerophosphodiester phosphodiesterase GDPD1, chloroplastic
CDS_3480_Unigene_13879_Transcript_23591	1.707865505	XP_021597554.1protein phosphatase 2C 56-like
CDS_46603_Unigene_78314_Transcript_141009	1.705812464	QCX36381.1COMTL6
CDS_6662_Unigene_17476_Transcript_30081	1.70572996	APF31815.1pathogenesis-related protein 1-like protein, partial
CDS_13633_Unigene_2554_Transcript_4229	1.705723928	RWR95105.1protein ASPARTIC PROTEASE IN GUARD CELL 2-like protein
CDS_41300_Unigene_6520_Transcript_10901	1.705401358	No Blast Hit
CDS_24118_Unigene_38193_Transcript_66537	1.705210715	XP_012069670.1polyol transporter 5
CDS_20123_Unigene_33193_Transcript_57657	1.704380864	KAF3775866.1HVA22 protein
CDS_29406_Unigene_45231_Transcript_79503	1.704175659	AAP83391.1FRUITFULL-like MADS-box, partial
CDS_22104_Unigene_35583_Transcript_61933	1.703162886	XP_019223406.1: uncharacterized protein LOC109205179
CDS_44190_Unigene_71926_Transcript_128369	1.703162886	KJB23349.1 B456_004G094300

Transcript ID	Log2 Fold Change	Hit desc.
CDS_19107_Unigene_31950_Transcript_55515	1.702763855	XP_010251393.1: BTB/POZ and TAZ domain-containing protein 3-like
CDS_15932_Unigene_28226_Transcript_48815	1.702101691	PIA51892.1 AQUCO_01000041v1
CDS_23551_Unigene_3743_Transcript_6175	1.701845958	XP_019702338.1putative germin-like protein 2-1
CDS_17702_Unigene_302_Transcript_499	1.698049963	XP_031111289.1uncharacterized protein At5g48480
CDS_9145_Unigene_20332_Transcript_35016	1.696468234	XP_010684357.1: mediator of RNA polymerase II transcription subunit 28
CDS_18977_Unigene_31794_Transcript_55205	1.694942379	XP_010259397.1: dnaJ homolog subfamily B member 3 isoform X1
CDS_25072_Unigene_39425_Transcript_68796	1.690973477	XP_022135125.1PLASMODESMATA CALLOSE-BINDING PROTEIN 3-like
CDS_41372_Unigene_6537_Transcript_10931	1.690741327	XP_010271167.1: purple acid phosphatase 4-like isoform X1
CDS_1711_Unigene_11924_Transcript_20066	1.6905434	XP_030501888.117.9 kDa class II heat shock protein
CDS_12904_Unigene_24715_Transcript_42722	1.689876944	XP_030439613.1protein RESPONSE TO LOW SULFUR 3-like
CDS_48364_Unigene_8390_Transcript_13952	1.689280173	TKY58532.1 E2542_SST15595
CDS_1665_Unigene_11875_Transcript_19982	1.687087157	MQL76237.1
CDS_34220_Unigene_52385_Transcript_92289	1.686002335	XP_011039891.1: UPF0481 protein At3g47200-like
CDS_23574_Unigene_3746_Transcript_6185	1.681505471	RVW53462.1Germin-like protein subfamily 1 member 14
CDS_31444_Unigene_48190_Transcript_84857	1.681312165	RWV88899.1 GW17_00048986
CDS_9599_Unigene_2084_Transcript_3495	1.680680505	PON53612.1BRO1 domain containing protein
CDS_17113_Unigene_29625_Transcript_51326	1.68044281	KAF5189603.1Bzip transcription factor
CDS_31991_Unigene_49020_Transcript_86372	1.67968767	RWR77582.1 CKAN_00607700
CDS_10157_Unigene_21492_Transcript_37096	1.678224984	XP_010277801.1: thiol methyltransferase 2 isoform X1
CDS_9609_Unigene_2085_Transcript_3497	1.67793	PON53612.1BRO1 domain containing protein
CDS_45295_Unigene_74695_Transcript_133748	1.677516449	No Blast Hit
CDS_27814_Unigene_43074_Transcript_75556	1.677167678	No Blast Hit
CDS_31235_Unigene_47898_Transcript_84334	1.677167678	OVA06150.1Protein of unknown function DUF2838
CDS_32222_Unigene_49392_Transcript_87004	1.67665123	No Blast Hit
CDS_5338_Unigene_16016_Transcript_27384	1.676548893	XP_031500153.1uncharacterized protein LOC116264205 isoform X2
CDS_40449_Unigene_6348_Transcript_10566	1.676454707	XP_031116450.1uncharacterized protein LOC116020106

Transcript ID	Log2 Fold Change	Hit desc.
CDS_17639_Unigene_30222_Transcript_52377	1.674183819	RWR92332.1myb-related protein Hv1-like protein
CDS_39431_Unigene_61574_Transcript_108994	1.672941188	RWR87833.1beta-carotene hydroxylase 2, chloroplastic-like protein
CDS_5776_Unigene_1648_Transcript_2766	1.672405491	XP_008451860.1: pectin acetylesterase 8-like isoform X1
CDS_16273_Unigene_28638_Transcript_49533	1.671454026	PKI63948.1 CRG98_015624, partial
CDS_43627_Unigene_70535_Transcript_125631	1.671454026	No Blast Hit
CDS_6284_Unigene_17055_Transcript_29329	1.670595024	XP_020690297.1trihelix transcription factor ASIL1-like
CDS_9584_Unigene_20832_Transcript_35916	1.66983471	No Blast Hit
CDS_48350_Unigene_83861_Transcript_153520	1.667386657	RWR85344.1protein ABA DEFICIENT 4, chloroplastic-like protein isoform X1
CDS_5712_Unigene_1641_Transcript_2759	1.665713309	RWR89660.1pectin acetylesterase 8-like protein
CDS_4637_Unigene_15187_Transcript_25922	1.664209252	XP_022948497.1uncharacterized protein LOC111452156
CDS_42227_Unigene_67329_Transcript_119501	1.663691445	XP_010259661.1: glutathione S-transferase F13
CDS_15454_Unigene_27681_Transcript_47865	1.663164818	XP_026446677.1potassium channel KOR2-like isoform X1
CDS_31687_Unigene_48546_Transcript_85492	1.661892413	XP_010655901.1: pentatricopeptide repeat-containing protein At5g66520-like
CDS_26622_Unigene_41492_Transcript_72639	1.660679555	APQ41676.1ethylene response factor 069-c
CDS_42726_Unigene_6843_Transcript_11462	1.658825282	XP_010263534.1: ABSCISIC ACID-INSENSITIVE 5-like protein 5 isoform X2
CDS_15404_Unigene_27627_Transcript_47765	1.657553905	RWR79246.1Peptidase S8/S53 domain-containing protein
CDS_1839_Unigene_12059_Transcript_20302	1.65533953	RWR73379.1putative Heat shock transcription factor C1
CDS_1841_Unigene_12060_Transcript_20303	1.655141371	RWR73379.1putative Heat shock transcription factor C1
CDS_42742_Unigene_6847_Transcript_11469	1.653861449	XP_010263534.1: ABSCISIC ACID-INSENSITIVE 5-like protein 5 isoform X2
CDS_16009_Unigene_28327_Transcript_48983	1.653774859	XP_010248357.1: uncharacterized protein LOC104591250
CDS_50964_Unigene_9327_Transcript_15608	1.652795765	XP_027331344.1transcription factor bHLH82-like
CDS_3850_Unigene_14285_Transcript_24298	1.650168069	XP_010250328.1: uncharacterized protein LOC104592576
CDS_4900_Unigene_15500_Transcript_26498	1.649581846	XP_010255718.1: myb family transcription factor PHL11 isoform X1

Transcript ID	Log2 Fold Change	Hit desc.
CDS_16437_Unigene_28832_Transcript_49906	1.64720648	No Blast Hit
CDS_42514_Unigene_6799_Transcript_11373	1.646798263	XP_010260385.1: U-box domain-containing protein 4-like isoform X2
CDS_50973_Unigene_9330_Transcript_15614	1.644273782	XP_027331344.1transcription factor bHLH82-like
CDS_30103_Unigene_46216_Transcript_81308	1.643397251	XP_010263413.1: cation transporter HKT7
CDS_5063_Unigene_15695_Transcript_26856	1.640775422	RWR72345.1zinc finger protein
CDS_3482_Unigene_13880_Transcript_23593	1.634869802	XP_021597554.1protein phosphatase 2C 56-like
CDS_11159_Unigene_22683_Transcript_39171	1.634715536	XP_022151039.1extracellular ribonuclease LE-like
CDS_35016_Unigene_53685_Transcript_94735	1.634715536	No Blast Hit
CDS_26319_Unigene_41074_Transcript_71877	1.632773558	RWR79842.1transcription factor ORG2 isoform X1
CDS_12091_Unigene_23747_Transcript_41020	1.631748553	PSS31151.1AT-hook motif nuclear-localized protein
CDS_7407_Unigene_18317_Transcript_31539	1.630397345	RWR87945.1Protein of unknown function DUF506
CDS_7490_Unigene_18416_Transcript_31727	1.628432011	KAA3481016.1sugar transporter ERD6-like 16 isoform X2
CDS_16226_Unigene_28578_Transcript_49415	1.62797539	ABR26122.1s-adenosylmethionine synthetase 1, partial
CDS_13978_Unigene_25936_Transcript_44853	1.626355294	RAL54675.1 DM860_001803
CDS_4586_Unigene_15128_Transcript_25820	1.622877522	No Blast Hit
CDS_12739_Unigene_24517_Transcript_42383	1.621641456	XP_034687178.1(+)-neomenthol dehydrogenase-like isoform X3
CDS_19026_Unigene_31856_Transcript_55334	1.621641456	XP_009400004.1: alanine--glyoxylate aminotransferase 2 homolog 3, mitochondrial
CDS_39460_Unigene_61616_Transcript_109066	1.620622723	RWR92901.1phytoene synthase 2, chloroplastic
CDS_23108_Unigene_36851_Transcript_64242	1.618968206	RWR89814.1putative glycerol-3-phosphate transporter 1
CDS_12090_Unigene_23746_Transcript_41018	1.616566789	No Blast Hit
CDS_20148_Unigene_33226_Transcript_57719	1.615906208	XP_010259762.1: zinc finger protein CONSTANS-LIKE 5-like
CDS_32086_Unigene_49177_Transcript_86657	1.614526958	XP_019442782.1: plant intracellular Ras-group-related LRR protein 6-like
CDS_39432_Unigene_61575_Transcript_108995	1.613159393	EOY23306.1Beta-hydroxylase 1, 1,B1,chy1,BCH1 isoform 1
CDS_7259_Unigene_18143_Transcript_31212	1.612136796	RWR91899.1 CKAN_02107700
CDS_20853_Unigene_34055_Transcript_59213	1.610053482	KAA8540495.1 F0562_024586
CDS_26711_Unigene_41606_Transcript_72828	1.610053482	RWR89401.1mavicyanin

Transcript ID	Log2 Fold Change	Hit desc.
CDS_38820_Unigene_60343_Transcript_106792	1.610053482	RWR77429.1NUDIX hydrolase domain-containing protein
CDS_47779_Unigene_8206_Transcript_13655	1.610053482	XP_031093344.1alcohol dehydrogenase-like 4
CDS_48768_Unigene_85212_Transcript_157087	1.610053482	No Blast Hit
CDS_5384_Unigene_16067_Transcript_27488	1.610053482	RWR87559.1transmembrane protein 64 isoform X1
CDS_9453_Unigene_20688_Transcript_35669	1.610053482	GER42773.1mitochondrial carrier family protein
CDS_21156_Unigene_34398_Transcript_59836	1.607839061	XP_006468457.1protein PHLOEM PROTEIN 2-LIKE A5
CDS_15238_Unigene_27425_Transcript_47426	1.606843925	KDO67367.1 CISIN_1g044409mg
CDS_50339_Unigene_90938_Transcript_183384	1.60359846	XP_024634883.1NADPH-dependent aldehyde reductase-like protein, chloroplastic
CDS_16842_Unigene_29315_Transcript_50778	1.598998293	XP_020087292.1cysteine proteinase inhibitor 12-like
CDS_21767_Unigene_35156_Transcript_61146	1.598912924	OVA02825.1protein of unknown function DUF221
CDS_32005_Unigene_49049_Transcript_86425	1.589589379	XP_003593557.1dof zinc finger protein DOF1.4
CDS_37340_Unigene_57619_Transcript_101829	1.588027175	RZS08652.1 BHM03_00039653
CDS_3751_Unigene_14173_Transcript_24093	1.587800675	XP_010259074.1: heparanase-like protein 1
CDS_9626_Unigene_2087_Transcript_3499	1.587685669	XP_024024470.1uncharacterized protein LOC21388880
CDS_4715_Unigene_1528_Transcript_2576	1.587547715	XP_007012487.2: protein TIFY 3B
CDS_30189_Unigene_46341_Transcript_81541	1.587333405	KAA8537776.1 F0562_027644
CDS_37712_Unigene_58337_Transcript_103131	1.587333405	XP_024964180.1serine carboxypeptidase 1-like isoform X2
CDS_3750_Unigene_14172_Transcript_24091	1.585805935	XP_010259074.1: heparanase-like protein 1
CDS_49715_Unigene_88540_Transcript_169729	1.585391427	RLN09654.1 C2845_PM11G00340
CDS_23109_Unigene_36852_Transcript_64244	1.585178813	RWR89814.1putative glycerol-3-phosphate transporter 1
CDS_16321_Unigene_28698_Transcript_49631	1.584962501	XP_026438474.1uncharacterized protein LOC113336993
CDS_5642_Unigene_16340_Transcript_28000	1.583483761	XP_020267801.1acyl-coenzyme A oxidase 4, peroxisomal-like
CDS_17079_Unigene_29586_Transcript_51263	1.582346553	XP_008792721.1UDP-glycosyltransferase 83A1-like
CDS_30465_Unigene_46724_Transcript_82243	1.578802548	ACN40263.1unknown
CDS_34394_Unigene_52659_Transcript_92819	1.577387293	RWR89594.1D-amino-acid transaminase, chloroplastic isoform X1

Transcript ID	Log2 Fold Change	Hit desc.
CDS_45892_Unigene_76238_Transcript_136820	1.573294932	KAE8100504.1 FH972_018400
CDS_13065_Unigene_24896_Transcript_43040	1.572251449	OAY75040.1Tonoplast dicarboxylate transporter
CDS_51640_Unigene_9928_Transcript_16610	1.572006578	XP_017405735.1: uncharacterized protein LOC108319199
CDS_44587_Unigene_7290_Transcript_12204	1.571579334	No Blast Hit
CDS_15711_Unigene_27986_Transcript_48418	1.569864392	RZC63811.1 C5167_025549
CDS_16004_Unigene_28318_Transcript_48972	1.569768556	TXG49636.1 EZV62_025511
CDS_29037_Unigene_44723_Transcript_78610	1.568233306	XP_010921867.1 calcium-transporting ATPase 8, plasma membrane-type
CDS_19878_Unigene_3291_Transcript_5419	1.567022545	KAA8535783.1 F0562_030783
CDS_21487_Unigene_34795_Transcript_60502	1.565659362	XP_020248719.1arsenate reductase 2.2-like
CDS_29043_Unigene_44734_Transcript_78626	1.565384432	XP_010922827.1protein LURP-one-related 8
CDS_50592_Unigene_91958_Transcript_189653	1.565123218	No Blast Hit
CDS_42728_Unigene_6844_Transcript_11463	1.561457715	XP_010263531.1: ABSCISIC ACID-INSENSITIVE 5-like protein 5 isoform X1
CDS_3877_Unigene_14314_Transcript_24347	1.560665455	XP_010259636.1: extracellular ribonuclease LE-like
CDS_39175_Unigene_6103_Transcript_10152	1.559209804	XP_006837934.2E3 ubiquitin-protein ligase MIEL1
CDS_9356_Unigene_20583_Transcript_35495	1.557930751	BAD06583.1protein phosphatase 2C, partial
CDS_17044_Unigene_29548_Transcript_51199	1.556282225	RWR75655.1putative galactinol--sucrose galactosyltransferase 6 isoform X1
CDS_28272_Unigene_43706_Transcript_76737	1.556013642	No Blast Hit
CDS_25555_Unigene_40067_Transcript_69985	1.555897712	XP_010941346.2uncharacterized protein LOC105059662
CDS_14226_Unigene_26226_Transcript_45376	1.552972386	XP_010924897.1 protein phosphatase 2C 5
CDS_23795_Unigene_37740_Transcript_65779	1.551159793	XP_002281955.1: ras-related protein RABA6b
CDS_24282_Unigene_38408_Transcript_66931	1.550110941	XP_006827190.1trafficking protein particle complex subunit 4 isoform X2
CDS_2966_Unigene_132_Transcript_206	1.548652937	XP_020083486.1vacuolar amino acid transporter 1 isoform X1
CDS_12918_Unigene_24736_Transcript_42759	1.545291107	PIA35944.1 AQUCO_03400083v1
CDS_4070_Unigene_1453_Transcript_2457	1.542678046	MQM12398.1
CDS_18842_Unigene_31627_Transcript_54901	1.542035058	RWR92476.1purine permease 1
CDS_1713_Unigene_11926_Transcript_20068	1.540090924	XP_030501888.117.9 kDa class II heat shock protein

Transcript ID	Log2 Fold Change	Hit desc.
CDS_7715_Unigene_18685_Transcript_32194	1.539398928	RWR96064.1monothiol glutaredoxin-S10
CDS_50135_Unigene_9006_Transcript_15016	1.538816979	OVA13148.1Myc-type
CDS_41370_Unigene_6536_Transcript_10930	1.538500221	XP_018806620.1: purple acid phosphatase 17-like isoform X2
CDS_50708_Unigene_92230_Transcript_190874	1.538500221	KHN30150.1Zinc transporter 1
CDS_41304_Unigene_6521_Transcript_10902	1.536472349	No Blast Hit
CDS_47965_Unigene_825_Transcript_1390	1.533037428	TKY67582.1Ocs element-binding factor 1
CDS_35558_Unigene_5457_Transcript_9114	1.532885621	XP_002527413.1uncharacterized protein LOC8266970
CDS_1710_Unigene_11923_Transcript_20064	1.532648978	XP_004303483.1: 17.9 kDa class II heat shock protein-like
CDS_47461_Unigene_80_Transcript_135	1.532648978	XP_002284547.1: enoyl-CoA delta isomerase 2, peroxisomal
CDS_19643_Unigene_32610_Transcript_56651	1.532516881	XP_026458167.1glutathione S-transferase F9-like
CDS_49339_Unigene_87224_Transcript_162447	1.532432585	No Blast Hit
CDS_30460_Unigene_46719_Transcript_82237	1.530790203	XP_010680204.1: gamma-secretase subunit PEN-2
CDS_9147_Unigene_20334_Transcript_35018	1.530274408	No Blast Hit
CDS_42463_Unigene_6788_Transcript_11353	1.52831493	XP_015901816.1SPX domain-containing protein 1
CDS_42031_Unigene_66909_Transcript_118747	1.528060109	XP_031277613.1uclacyanin-3-like
CDS_34247_Unigene_52423_Transcript_92362	1.522901533	OVA20678.1Drug/metabolite transporter
CDS_23556_Unigene_3744_Transcript_6177	1.52259064	XP_020268784.1putative germin-like protein 2-1
CDS_23720_Unigene_37652_Transcript_65617	1.522377963	RWR81341.1zinc transporter 6, chloroplastic
CDS_23279_Unigene_3706_Transcript_6114	1.520686479	RWR75399.1S-adenosylmethionine decarboxylase proenzyme-like protein
CDS_39415_Unigene_61543_Transcript_108946	1.518905594	RWR85438.1putative carboxylesterase 15
CDS_25510_Unigene_39999_Transcript_69860	1.518364752	XP_014500437.1thioredoxin-like protein Clot
CDS_34760_Unigene_53273_Transcript_94011	1.51583814	XP_010941712.1myb family transcription factor APL isoform X3
CDS_40198_Unigene_6300_Transcript_10477	1.514567314	OMO64817.1Thioredoxin-independent 5'-adenylylsulfate reductase
CDS_29750_Unigene_45690_Transcript_80330	1.514475822	RWR93754.1cyclin-P3-1
CDS_4128_Unigene_14601_Transcript_24874	1.514350536	XP_010941870.1CCG-binding protein 1

Transcript ID	Log2 Fold Change	Hit desc.
CDS_42515_Unigene_67_Transcript_113	1.514026594	XP_010922712.1U-box domain-containing protein 16
CDS_16085_Unigene_28405_Transcript_49118	1.51271648	RWR86975.1NAC domain-containing protein 83-like protein
CDS_20531_Unigene_33669_Transcript_58482	1.510973708	XP_010243401.1: dirigent protein 22-like
CDS_286_Unigene_10299_Transcript_17234	1.510517808	TQD87737.1 C1H46_026741
CDS_47312_Unigene_80558_Transcript_145722	1.510517808	XP_011100260.1uncharacterized protein LOC105178478
CDS_39493_Unigene_6167_Transcript_10247	1.509672892	No Blast Hit
CDS_44704_Unigene_73156_Transcript_130743	1.508633164	XP_022854780.1NADH dehydrogenase
CDS_12735_Unigene_24512_Transcript_42378	1.50457552	XP_006827736.1membrane steroid-binding protein 2
CDS_21104_Unigene_34330_Transcript_59705	1.503925131	No Blast Hit
CDS_6499_Unigene_17298_Transcript_29757	1.503138278	XP_010915357.1NADP-dependent malic enzyme isoform X1
CDS_2275_Unigene_1254_Transcript_2153	1.502607192	KAA8527297.1 F0562_034606
CDS_17718_Unigene_30319_Transcript_52555	1.501993736	No Blast Hit
CDS_50650_Unigene_92077_Transcript_190198	1.497943115	RWR73106.1auxin-responsive protein SAUR71
CDS_47929_Unigene_824_Transcript_1389	1.4963967	RWR82453.1bZIP transcription factor 11-like protein
CDS_44102_Unigene_71729_Transcript_127985	1.49301406	MQL79063.1
CDS_25362_Unigene_39817_Transcript_69536	1.492401893	XP_010264071.1: uncharacterized protein LOC104602168
CDS_5366_Unigene_16044_Transcript_27439	1.491408985	XP_010251048.1: protein DEHYDRATION-INDUCED 19 homolog 5-like
CDS_12854_Unigene_24651_Transcript_42594	1.489519816	XP_026409502.1F-box/FBD/LRR-repeat protein At5g56420-like
CDS_34893_Unigene_53510_Transcript_94425	1.488615354	KAF0919546.1 E2562_029772
CDS_23841_Unigene_37809_Transcript_65881	1.488579186	RWR83318.1U-box domain-containing protein 19-like protein
CDS_6767_Unigene_17597_Transcript_30276	1.485298451	KAE8667976.1Helicase protein with RING/U-box domain
CDS_6318_Unigene_17093_Transcript_29396	1.481351143	XP_022039460.1histone H2A.6-like
CDS_43758_Unigene_7088_Transcript_11862	1.481011537	RWR94126.1putative glutaredoxin-C14
CDS_3115_Unigene_13476_Transcript_22839	1.480973533	KAF5187794.1Nuclear fusion defective
CDS_42615_Unigene_68228_Transcript_121145	1.480216044	XP_030449810.1 2-oxoglutarate-dependent dioxygenase At3g111800
CDS_13672_Unigene_25600_Transcript_44291	1.478587319	XP_002285691.1: protein YLS3
CDS_21215_Unigene_34472_Transcript_59959	1.477206786	OVA18092.1Methyltransferase type 11

Transcript ID	Log2 Fold Change	Hit desc.
CDS_49254_Unigene_8690_Transcript_14468	1.476921449	RWR92016.1transcription factor bHLH155-like protein isoform X1
CDS_43344_Unigene_69828_Transcript_124296	1.476428918	YP_009270683.1ATPase subunit 1
CDS_16638_Unigene_29079_Transcript_50342	1.474864354	RWR87813.1putative aquaporin NIP5-1
CDS_16006_Unigene_28320_Transcript_48974	1.471782363	TXG49636.1 EZV62_025511
CDS_43675_Unigene_7067_Transcript_11831	1.470754444	RWR75704.1 CKAN_00410200
CDS_48299_Unigene_836_Transcript_1410	1.468877419	XP_034697165.1transcription factor bHLH112-like isoform X1
CDS_46809_Unigene_7900_Transcript_13174	1.467508502	RWR74046.1L-galactose dehydrogenase
CDS_3806_Unigene_14235_Transcript_24220	1.466318004	No Blast Hit
CDS_12645_Unigene_24408_Transcript_42196	1.464262217	RCV34753.1 SETIT_7G184300v2
CDS_32296_Unigene_4950_Transcript_8268	1.463296558	KAA8539627.1 F0562_026319
CDS_19908_Unigene_32948_Transcript_57217	1.46261129	ALG05139.1polyphenol oxidase
CDS_30393_Unigene_46642_Transcript_82079	1.462496293	NP_001238595.2ethylene-responsive element binding factor 4
CDS_43343_Unigene_69827_Transcript_124295	1.461190096	No Blast Hit
CDS_2220_Unigene_12482_Transcript_21078	1.460910042	XP_010265415.1: WRKY transcription factor 17
CDS_32108_Unigene_49207_Transcript_86716	1.460787951	No Blast Hit
CDS_37858_Unigene_5860_Transcript_9780	1.460254659	XP_025689906.1peptide methionine sulfoxide reductase B5
CDS_13642_Unigene_2555_Transcript_4231	1.458349423	RWR95105.1protein ASPARTIC PROTEASE IN GUARD CELL 2-like protein
CDS_29747_Unigene_45688_Transcript_80326	1.458050388	RWR93754.1cyclin-P3-1
CDS_22162_Unigene_35642_Transcript_62047	1.456807221	KAA8540212.1 F0562_024225
CDS_15400_Unigene_27623_Transcript_47761	1.455826152	OVA19825.1Peptidase S8/S53 domain
CDS_2420_Unigene_12708_Transcript_21466	1.454582965	XP_010917660.1uncharacterized protein LOC105042235
CDS_14079_Unigene_26052_Transcript_45026	1.452772689	XP_015897751.1cyclin-dependent protein kinase inhibitor SMR6
CDS_18661_Unigene_31429_Transcript_54526	1.451871813	XP_018816632.1: potassium channel SKOR isoform X1
CDS_15754_Unigene_28035_Transcript_48492	1.44895724	RWR75412.1putative steroid-binding protein 3
CDS_10542_Unigene_21947_Transcript_37888	1.448366422	XP_022932006.1 pectinesterase/pectinesterase inhibitor 51
CDS_46866_Unigene_79178_Transcript_142812	1.447500469	XP_026404397.1uncharacterized protein LOC113299575 isoform X1
CDS_47143_Unigene_79_Transcript_133	1.446554749	RWR89211.1Crotonase superfamily

Transcript ID	Log2 Fold Change	Hit desc.
CDS_42693_Unigene_68376_Transcript_121449	1.446445243	MQL79426.1
CDS_935_Unigene_11028_Transcript_18511	1.443632721	XP_027073004.1remorin 4.1-like
CDS_42276_Unigene_67431_Transcript_119690	1.443543145	ACG37316.1
CDS_10540_Unigene_21945_Transcript_37884	1.443061214	XP_017225816.1: uncharacterized protein LOC108201975
CDS_23072_Unigene_36797_Transcript_64156	1.442943496	PKA62582.1Extracellular ribonuclease LE
CDS_29425_Unigene_45253_Transcript_79547	1.441371647	XP_026661593.1RING-H2 finger protein ATL48-like
CDS_2724_Unigene_13029_Transcript_22052	1.44092621	XP_010251199.1: E3 ubiquitin-protein ligase BOI-like
CDS_50330_Unigene_9090_Transcript_15172	1.440418382	XP_010261931.1: protein ELF4-LIKE 4-like
CDS_29169_Unigene_44901_Transcript_78903	1.44012848	RVW55424.1DNA repair protein XRCC4
CDS_43681_Unigene_7068_Transcript_11832	1.44012848	RWR75704.1 CKAN_00410200
CDS_15537_Unigene_27772_Transcript_48025	1.437737933	RWR82950.1somatic embryogenesis receptor kinase 2
CDS_7366_Unigene_18264_Transcript_31460	1.435532952	XP_028097413.1UDP-D-apiose/UDP-D-xylose synthase 2-like
CDS_20500_Unigene_33636_Transcript_58429	1.43537495	RWR85677.1zinc transporter 8
CDS_2746_Unigene_13049_Transcript_22087	1.433673458	XP_034692610.1zinc finger A20 and AN1 domain-containing stress-associated protein 4-like
CDS_33659_Unigene_51521_Transcript_90751	1.431083341	PSR96075.1E3 ubiquitin-protein like
CDS_15455_Unigene_27682_Transcript_47866	1.427723459	XP_026446677.1potassium channel KOR2-like isoform X1
CDS_49693_Unigene_88481_Transcript_169498	1.427400175	XP_008798303.1uncharacterized protein LOC103713226
CDS_5691_Unigene_16399_Transcript_28120	1.427010141	RWR78399.1transcription factor bHLH47-like protein
CDS_22446_Unigene_35977_Transcript_62656	1.425739678	OVA13970.1zinc finger protein
CDS_44829_Unigene_73437_Transcript_131351	1.425723672	No Blast Hit
CDS_25625_Unigene_40144_Transcript_70123	1.42328497	XP_028072141.1vacuolar cation/proton exchanger 3
CDS_936_Unigene_11029_Transcript_18513	1.419589737	XP_027073004.1remorin 4.1-like
CDS_51556_Unigene_9830_Transcript_16439	1.416173748	No Blast Hit
CDS_34134_Unigene_5223_Transcript_8730	1.414174385	RWW22262.1 GW17_00013548
CDS_16637_Unigene_29078_Transcript_50341	1.411618316	RWR87813.1putative aquaporin NIP5-1
CDS_11335_Unigene_22874_Transcript_39558	1.410744673	KAB1669778.1 ES319_1Z011400v1
CDS_3849_Unigene_14284_Transcript_24297	1.409754831	XP_010250328.1: uncharacterized protein LOC104592576

Transcript ID	Log2 Fold Change	Hit desc.
CDS_6317_Unigene_17092_Transcript_29395	1.409499437	XP_022039460.1histone H2A.6-like
CDS_38099_Unigene_5901_Transcript_9850	1.40885833	XP_028122998.1uncharacterized protein LOC114320097
CDS_16686_Unigene_29140_Transcript_50433	1.40706646	PIA30985.1 AQUCO_05300070v1
CDS_8442_Unigene_19535_Transcript_33642	1.406725322	XP_012082976.1autophagy-related protein 8i
CDS_39517_Unigene_6170_Transcript_10254	1.40503616	No Blast Hit
CDS_19032_Unigene_31864_Transcript_55345	1.404734574	XP_021624120.1vacuolar cation/proton exchanger 3
CDS_13237_Unigene_25084_Transcript_43385	1.402565067	GER54030.14-hydroxyphenylpyruvate dioxygenase
CDS_50332_Unigene_9091_Transcript_15174	1.402315879	XP_010261931.1: protein ELF4-LIKE 4-like
CDS_47741_Unigene_8196_Transcript_13645	1.401867553	OVA04712.1Alcohol dehydrogenase superfamily
CDS_8693_Unigene_19827_Transcript_34172	1.39806099	XP_034895094.1abscisic acid receptor PYL8-like
CDS_50335_Unigene_9092_Transcript_15175	1.397004184	XP_010261931.1: protein ELF4-LIKE 4-like
CDS_43629_Unigene_70538_Transcript_125636	1.396798124	XP_030463153.1endochitinase EP3-like
CDS_4022_Unigene_14489_Transcript_24667	1.395155597	XP_022725639.1glutathione S-transferase U10-like
CDS_298_Unigene_10309_Transcript_17252	1.392892124	No Blast Hit
CDS_31846_Unigene_48813_Transcript_85974	1.392661741	ANA09005.1mannose/glucose-specific lectin-like isoform, partial
CDS_38216_Unigene_59272_Transcript_104829	1.391788946	XP_028082692.1cold and drought-regulated protein CORA-like
CDS_6563_Unigene_17371_Transcript_29886	1.390936192	TQD79151.1 C1H46_035279
CDS_1583_Unigene_11788_Transcript_19819	1.388676685	RRT53990.1 B296_00043077
CDS_139_Unigene_10153_Transcript_16974	1.382491958	PON61827.1NAC domain containing protein
CDS_2945_Unigene_1326_Transcript_2273	1.382160882	KAB2092277.1 ES319_A02G018400v1
CDS_35534_Unigene_5453_Transcript_9107	1.381874491	XP_023881521.1transmembrane emp24 domain-containing protein p24beta3-like
CDS_17970_Unigene_30632_Transcript_53116	1.381370581	XP_009415021.1: glutathione S-transferase zeta class
CDS_19641_Unigene_32609_Transcript_56650	1.378827814	RWR81922.1glutathione S-transferase F10-like protein
CDS_2558_Unigene_12854_Transcript_21727	1.377509443	XP_010271685.1: uncharacterized protein LOC104607691
CDS_5066_Unigene_15698_Transcript_26862	1.373277142	RWR72345.1zinc finger protein

Transcript ID	Log2 Fold Change	Hit desc.
CDS_5815_Unigene_16530_Transcript_28402	1.372554168	TXG58573.1 EZV62_016402
CDS_50425_Unigene_9118_Transcript_15224	1.371997944	XP_019702647.1cytochrome b-c1 complex subunit 8
CDS_29376_Unigene_45185_Transcript_79398	1.36826681	XP_011090002.1uncharacterized protein At4g22758-like
CDS_2770_Unigene_13078_Transcript_22127	1.366782331	XP_017243480.1: uncharacterized protein LOC108215483
CDS_42277_Unigene_67432_Transcript_119692	1.366218723	NP_001132837.1uncharacterized protein LOC100194327
CDS_9244_Unigene_20449_Transcript_35238	1.366002179	MQL84186.1
CDS_49402_Unigene_87388_Transcript_163128	1.363847121	PIN23004.1Cyanase
CDS_1853_Unigene_12076_Transcript_20340	1.361972786	KAE9586843.1putative transcription factor C2H2 family
CDS_44101_Unigene_71728_Transcript_127983	1.3594028	MQL79063.1
CDS_16012_Unigene_28331_Transcript_48991	1.359149006	QBM06305.1CAA-type MYB transcription factor 1d, partial
CDS_2750_Unigene_13052_Transcript_22090	1.358129191	XP_034692610.1zinc finger A20 and AN1 domain-containing stress-associated protein 4-like
CDS_19193_Unigene_32052_Transcript_55682	1.352968342	GAV79861.1 CFOL_v3_23324
CDS_633_Unigene_10706_Transcript_17952	1.348715367	XP_010920331.1cyclin-dependent kinase inhibitor 4
CDS_16947_Unigene_29427_Transcript_50978	1.348695654	RWR84591.1 CKAN_01341000
CDS_12911_Unigene_24726_Transcript_42742	1.348095312	RWR82374.1PAN domain-containing protein
CDS_7698_Unigene_18658_Transcript_32151	1.347931885	No Blast Hit
CDS_5690_Unigene_16398_Transcript_28119	1.347890532	XP_022737511.1transcription factor bHLH47
CDS_10276_Unigene_21615_Transcript_37322	1.344632483	XP_010920237.1peptidyl-prolyl cis-trans isomerase Pin1
CDS_28146_Unigene_43546_Transcript_76454	1.344130797	OVA02705.1EF-hand domain
CDS_18017_Unigene_30687_Transcript_53210	1.341973422	KAF5175448.11-aminocyclopropane-1-carboxylate synthase
CDS_7699_Unigene_18662_Transcript_32160	1.340505769	No Blast Hit
CDS_31551_Unigene_48356_Transcript_85153	1.3400039	RWR74685.1nonexpressor of pathogenesis-related protein 1-like 5 protein
CDS_7160_Unigene_18033_Transcript_31006	1.337418306	XP_031501244.1uncharacterized protein LOC116264923
CDS_48354_Unigene_8387_Transcript_13948	1.335546291	RWR95658.1plastid division protein PDV2-like protein
CDS_15483_Unigene_27709_Transcript_47935	1.33227249	PIA53497.1 AQUCO_00900234v1
CDS_17078_Unigene_29585_Transcript_51262	1.331269878	XP_008792721.1UDP-glycosyltransferase 83A1-like

Transcript ID	Log2 Fold Change	Hit desc.
CDS_51537_Unigene_9808_Transcript_16402	1.330233919	APQ41679.1ethylene response factor 11-c
CDS_5722_Unigene_1642_Transcript_2760	1.329017817	XP_008451860.1: pectin acetylesterase 8-like isoform X1
CDS_7738_Unigene_18715_Transcript_32239	1.328827724	TQD80997.1 C1H46_033412
CDS_10277_Unigene_21616_Transcript_37323	1.323413337	XP_009611087.1peptidyl-prolyl cis-trans isomerase Pin1
CDS_16780_Unigene_29237_Transcript_50631	1.323106456	XP_010917487.1aldehyde dehydrogenase family 7 member A1 isoform X2
CDS_18940_Unigene_31749_Transcript_55126	1.321292251	XP_028766219.1F-box/kelch-repeat protein At1g55270-like
CDS_2629_Unigene_12932_Transcript_21902	1.320669788	XP_011089543.1root phototropism protein 2-like
CDS_12915_Unigene_24733_Transcript_42754	1.319603618	PIA35944.1 AQUCO_03400083v1
CDS_19070_Unigene_31904_Transcript_55444	1.31645411	KAF5176390.1Non-specific serine/threonine protein kinase, partial
CDS_4388_Unigene_14914_Transcript_25438	1.313522164	No Blast Hit

Supplementary Table 2

Functional Annotation of Significantly Upregulated DEGs at 28 dpi

Transcript ID	Log2 Fold Change	Hit desc.
CDS_18365_Unigene_31083_Transcript_53907	7.673198585	XP_006363788.1: xyloglucan endotransglucosylase/hydrolase protein 7
CDS_22625_Unigene_36218_Transcript_63081	7.260319098	RWR86677.1proline-rich protein DC2.15-like protein
CDS_46226_Unigene_7717_Transcript_12867	6.803890442	XP_028759077.1PLAT domain-containing protein 3-like
CDS_51351_Unigene_9586_Transcript_16040	6.603647247	RWR86677.1proline-rich protein DC2.15-like protein
CDS_49932_Unigene_8951_Transcript_14921	6.267081146	TVT98964.1 protein EJB05_55700, partial
CDS_21640_Unigene_34997_Transcript_60853	5.972199403	No Blast Hit
CDS_37039_Unigene_57105_Transcript_100934	5.65697703	OVA08593.1Major intrinsic protein
CDS_19004_Unigene_31832_Transcript_55274	5.627482572	RWR80673.1 protein CKAN_00932500
CDS_1827_Unigene_12040_Transcript_20266	5.380707732	RWR83263.1phospholipase A2-alpha isoform X2
CDS_2131_Unigene_12387_Transcript_20901	5.360926582	XP_021910195.1aspartyl protease AED3
CDS_42951_Unigene_6898_Transcript_11543	5.196545704	No Blast Hit
CDS_2948_Unigene_13279_Transcript_22489	5.109830654	XP_007017955.2: L-ascorbate oxidase homolog
CDS_46222_Unigene_7715_Transcript_12864	5.082150079	TKW03659.1 protein SEVIR_7G055100v2
CDS_6431_Unigene_17221_Transcript_29615	5.075453089	XP_008794778.1 polygalacturonase isoform X3
CDS_5642_Unigene_16340_Transcript_28000	4.998360814	XP_020267801.1acyl-coenzyme A oxidase 4, peroxisomal-like
CDS_31846_Unigene_48813_Transcript_85974	4.977431041	ANA09005.1mannose/glucose-specific lectin-like isoform, partial
CDS_21235_Unigene_34498_Transcript_59998	4.95375937	XP_031111220.1uncharacterized protein LOC116015320
CDS_20535_Unigene_33675_Transcript_58492	4.910619455	KAB2086420.1 protein ES319_A04G030500v1
CDS_49953_Unigene_89632_Transcript_176057	4.850278227	XP_021638832.1aspartyl protease AED3-like
CDS_6319_Unigene_17094_Transcript_29397	4.802141123	XP_034692772.1histone H2A
CDS_37291_Unigene_57522_Transcript_101656	4.732425534	XP_027348783.1histone H2B isoform X4
CDS_47584_Unigene_813_Transcript_1365	4.717559353	KAF2314167.1 protein GH714_023833
CDS_47240_Unigene_8033_Transcript_13382	4.711451733	AKR76259.1alpha-tubulin
CDS_6488_Unigene_17285_Transcript_29730	4.628866398	XP_008799243.1LOB domain-containing protein 41
CDS_33772_Unigene_51681_Transcript_91031	4.622188272	KGN60020.1 protein Csa_001829
CDS_11607_Unigene_23191_Transcript_40067	4.59665318	RWR77887.1transcription factor bHLH93

Transcript ID	Log2 Fold Change	Hit desc.
CDS_13747_Unigene_25683_Transcript_44423	4.59456484	RWR71853.1fasciclin-like arabinogalactan protein 7
CDS_35236_Unigene_54068_Transcript_95416	4.576017201	RWR89898.1pollen-specific protein C13-like protein
CDS_13603_Unigene_25513_Transcript_44141	4.572604123	KAE8009448.1 protein FH972_005885
CDS_22627_Unigene_36223_Transcript_63088	4.543199976	XP_010258295.1: casparian strip membrane protein 3
CDS_41504_Unigene_656_Transcript_1086	4.462860659	No Blast Hit
CDS_26711_Unigene_41606_Transcript_72828	4.448007257	RWR89401.1mavicyanin
CDS_41423_Unigene_654_Transcript_1084	4.37354426	No Blast Hit
CDS_41622_Unigene_659_Transcript_1090	4.373082088	No Blast Hit
CDS_1047_Unigene_11165_Transcript_18715	4.367976787	RWR73792.1Nucleolar protein gar2-related isoform 2
CDS_28274_Unigene_43709_Transcript_76741	4.311085591	XP_019238921.1: uncharacterized protein LOC109218974
CDS_6593_Unigene_17402_Transcript_29935	4.291795957	No Blast Hit
CDS_20549_Unigene_33690_Transcript_58515	4.240371257	RDX74386.1Expansin-A1, partial
CDS_41665_Unigene_660_Transcript_1091	4.227729181	CDP14664.1unnamed protein product
CDS_22018_Unigene_3547_Transcript_5838	4.202053629	No Blast Hit
CDS_16795_Unigene_29250_Transcript_50657	4.197923821	XP_013626871.1: pathogenesis-related protein PR-4B-like
CDS_9656_Unigene_20917_Transcript_36084	4.19646849	ABX71220.1osmotin
CDS_29884_Unigene_45873_Transcript_80675	4.19368605	No Blast Hit
CDS_39241_Unigene_61180_Transcript_108309	4.177604744	XP_010261902.1: uncharacterized protein LOC104600570 isoform X1
CDS_15547_Unigene_27787_Transcript_48049	4.138534161	RWR89161.1trifunctional UDP-glucose 4,6-dehydratase/UDP-4-keto-6-deoxy-D-glucose 3,5-epimerase/UDP-4-keto-L-rhamnose-reductase RHM1
CDS_6595_Unigene_17405_Transcript_29940	4.125023171	No Blast Hit
CDS_42946_Unigene_6897_Transcript_11542	4.115521766	No Blast Hit
CDS_12222_Unigene_23903_Transcript_41295	4.107518955	GAY35854.1 protein CUMW_018960
CDS_47243_Unigene_8034_Transcript_13383	4.099898625	KAE8689280.1Tubulin alpha-1 chain
CDS_17113_Unigene_29625_Transcript_51326	4.045479873	KAF5189603.1Bzip transcription factor
CDS_23072_Unigene_36797_Transcript_64156	4.037964668	PKA62582.1Extracellular ribonuclease LE
CDS_3888_Unigene_14324_Transcript_24365	4.030526336	XP_011080226.1omega-6 fatty acid desaturase, endoplasmic reticulum isozyme 2 isoform X1
CDS_6177_Unigene_16934_Transcript_29093	4.022367813	OVA10301.1Peptidase S10
CDS_23565_Unigene_3745_Transcript_6182	4.021964634	XP_020251119.1putative germin-like protein 2-1

Transcript ID	Log2 Fold Change	Hit desc.
CDS_8171_Unigene_19209_Transcript_33069	4.01608155	RWR89359.1BAG family molecular chaperone regulator 1
CDS_18130_Unigene_30821_Transcript_53446	4.01268526	XP_002283348.1: WAT1-related protein At5g07050
CDS_22050_Unigene_3551_Transcript_5843	3.995278468	No Blast Hit
CDS_9679_Unigene_20941_Transcript_36125	3.960351315	RWR90134.1WAT1-related-like protein
CDS_49066_Unigene_8622_Transcript_14344	3.960179192	XP_031267926.1protein NRT1/ PTR FAMILY 3.1-like, partial
CDS_44006_Unigene_7149_Transcript_11962	3.958237476	XP_011037726.1: tubulin beta chain
CDS_30574_Unigene_4690_Transcript_7835	3.948113258	XP_004252814.1tubulin alpha-2 chain-like
CDS_22028_Unigene_3548_Transcript_5839	3.94336066	No Blast Hit
CDS_19908_Unigene_32948_Transcript_57217	3.928456508	ALG05139.1polyphenol oxidase
CDS_11343_Unigene_22881_Transcript_39567	3.902203441	RWR86216.1putative S-adenosyl-L-methionine-dependent methyltransferase
CDS_18301_Unigene_31005_Transcript_53741	3.900461144	OVA05943.1Stress responsive alpha-beta barrel
CDS_24836_Unigene_39121_Transcript_68211	3.898283071	XP_002521130.1 pectate lyase 8
CDS_32813_Unigene_50279_Transcript_88567	3.895292374	No Blast Hit
CDS_14428_Unigene_26475_Transcript_45793	3.881877897	RWR77999.1peroxidase 51-like protein
CDS_19940_Unigene_3298_Transcript_5434	3.879050447	XP_010262132.1: beta-galactosidase isoform X2
CDS_647_Unigene_1071_Transcript_1828	3.866240465	KAF5180549.1Pectinesterase
CDS_6429_Unigene_17219_Transcript_29613	3.84767386	XP_010255223.1: polygalacturonase isoform X1
CDS_7341_Unigene_18237_Transcript_31402	3.839546138	PSR89168.1Boron transporter like
CDS_14427_Unigene_26474_Transcript_45792	3.823785289	RWR82947.1peroxidase 51-like protein
CDS_25933_Unigene_4055_Transcript_6773	3.801105145	XP_010241154.1: 18.2 kDa class I heat shock protein-like
CDS_13746_Unigene_25682_Transcript_44422	3.796011522	RWR71853.1fasciclin-like arabinogalactan protein 7
CDS_34269_Unigene_52468_Transcript_92458	3.764395968	XP_026417945.1bifunctional nitrilase/nitrile hydratase NIT4B
CDS_3887_Unigene_14323_Transcript_24363	3.74413509	XP_021279365.1delta(12)-acyl-lipid-desaturase-like
CDS_24683_Unigene_38923_Transcript_67857	3.730536143	KAE9456085.1 protein C3L33_12025, partial
CDS_12221_Unigene_23902_Transcript_41294	3.723187464	XP_024034688.1uncharacterized protein LOC18032915 isoform X2
CDS_8121_Unigene_19154_Transcript_32957	3.720077738	VAI54365.1unnamed protein product
CDS_26357_Unigene_41125_Transcript_71956	3.71897567	KAA8540552.1 protein F0562_024529
CDS_38525_Unigene_59847_Transcript_105855	3.681571204	PIA62780.1 protein AQUCO_00200653v1
CDS_21302_Unigene_34580_Transcript_60122	3.680409909	NP_001289781.1ceruloplasmin precursor

Transcript ID	Log2 Fold Change	Hit desc.
CDS_17857_Unigene_304_Transcript_503	3.677416586	PHU13619.1 protein BC332_14824
CDS_6576_Unigene_17388_Transcript_29917	3.672020928	NP_001152678.1blue copper protein precursor
CDS_1364_Unigene_11547_Transcript_19382	3.656822962	XP_007019334.2: carboxyvinyl-carboxyphosphonate phosphorylmutase, chloroplastic
CDS_41338_Unigene_652_Transcript_1081	3.640476249	No Blast Hit
CDS_36598_Unigene_56310_Transcript_99484	3.634689285	XP_030956067.1uncharacterized protein LOC115978188
CDS_12223_Unigene_23904_Transcript_41296	3.619821258	XP_016554141.1: bifunctional epoxide hydrolase 2-like
CDS_40569_Unigene_6371_Transcript_10611	3.618805633	XP_030450891.1expansin-A6
CDS_38621_Unigene_59992_Transcript_106124	3.598130595	RWR82255.1dirigent protein 22-like protein
CDS_50732_Unigene_92308_Transcript_191259	3.594383517	XP_031103512.1GDSL esterase/lipase At1g54790
CDS_15711_Unigene_27986_Transcript_48418	3.585335821	RZC63811.1 protein C5167_025549
CDS_1365_Unigene_11548_Transcript_19383	3.578243189	XP_007019334.2: carboxyvinyl-carboxyphosphonate phosphorylmutase, chloroplastic
CDS_17846_Unigene_30487_Transcript_52868	3.573006799	PSS21691.1Natterin-3 like
CDS_27534_Unigene_42705_Transcript_74927	3.567716256	XP_020217317.1polygalacturonase 1 beta-like protein 3
CDS_16816_Unigene_29279_Transcript_50714	3.567495564	RWR88767.1tyrosine/DOPA decarboxylase 2-like protein
CDS_8170_Unigene_19208_Transcript_33068	3.555389385	RWR89359.1BAG family molecular chaperone regulator 1
CDS_13179_Unigene_25024_Transcript_43282	3.550675097	XP_015893811.1ribonucleoside-diphosphate reductase small chain
CDS_6388_Unigene_17172_Transcript_29534	3.543994631	No Blast Hit
CDS_17845_Unigene_30485_Transcript_52866	3.542292678	PSS21691.1Natterin-3 like
CDS_35096_Unigene_53804_Transcript_94944	3.541913579	XP_030971642.1cinnamoyl-CoA reductase 1
CDS_49987_Unigene_89708_Transcript_176416	3.514181083	OVA19654.1Plant disease resistance response protein
CDS_41576_Unigene_658_Transcript_1088	3.504100157	No Blast Hit
CDS_18506_Unigene_31240_Transcript_54181	3.493995978	XP_034675077.1uncharacterized protein LOC117906209
CDS_11159_Unigene_22683_Transcript_39171	3.486314913	XP_022151039.1extracellular ribonuclease LE-like
CDS_14046_Unigene_26018_Transcript_44981	3.480169268	RWR73536.1alpha-xylosidase 1
CDS_34396_Unigene_52661_Transcript_92828	3.476594578	RWR89594.1D-amino-acid transaminase, chloroplastic isoform X1
CDS_18485_Unigene_31215_Transcript_54142	3.473692854	PIA37824.1 protein AQUCO_03000394v1

Transcript ID	Log2 Fold Change	Hit desc.
CDS_13164_Unigene_25006_Transcript_43255	3.473539098	RWR94963.1GDP-fucose protein O-fucosyltransferase
CDS_20334_Unigene_33434_Transcript_58061	3.462279981	RWR90766.1ras-related protein RABA3
CDS_44275_Unigene_7214_Transcript_12066	3.462078922	KMT10440.1 protein BVRB_5g115660
CDS_31450_Unigene_48202_Transcript_84882	3.457179355	RWR90442.1delta24-sterol reductase
CDS_51443_Unigene_9697_Transcript_16215	3.450673361	KAA3485322.1sodium/hydrogen exchanger 2-like
CDS_23574_Unigene_3746_Transcript_6185	3.447410319	RVW53462.1Germin-like protein subfamily 1 member 14
CDS_25174_Unigene_39563_Transcript_69040	3.437405312	RZS23073.1 protein BHM03_00055927, partial
CDS_19494_Unigene_32420_Transcript_56317	3.427467075	XP_010262463.1: thaumatin-like protein isoform X1
CDS_22546_Unigene_36109_Transcript_62871	3.419371389	No Blast Hit
CDS_23551_Unigene_3743_Transcript_6175	3.412175764	XP_019702338.1putative germin-like protein 2-1
CDS_19935_Unigene_3297_Transcript_5433	3.412094224	XP_010262131.1: beta-galactosidase isoform X1
CDS_3877_Unigene_14314_Transcript_24347	3.408283584	XP_010259636.1: extracellular ribonuclease LE-like
CDS_29697_Unigene_45618_Transcript_80205	3.405696453	RWR96656.1zinc finger protein
CDS_14744_Unigene_26849_Transcript_46436	3.402062458	XP_010276659.1: non-specific phospholipase C2-like
CDS_36244_Unigene_5572_Transcript_9291	3.380674186	No Blast Hit
CDS_19851_Unigene_32895_Transcript_57117	3.368049166	AAP92160.2chlorophyllase
CDS_23517_Unigene_37398_Transcript_65183	3.367222305	ARB08605.1caryophyllene synthase
CDS_19774_Unigene_32790_Transcript_56948	3.362303857	XP_010526891.1: aquaporin PIP2-8
CDS_21300_Unigene_34578_Transcript_60118	3.35928042	PIA57899.1 protein AQUCO_00500071v1
CDS_25072_Unigene_39425_Transcript_68796	3.352954991	XP_022135125.1PLASMODESMATA CALLOSE-BINDING PROTEIN 3-like
CDS_20852_Unigene_34054_Transcript_59212	3.35039475	OUZ99878.1LURP1-like domain
CDS_4102_Unigene_14573_Transcript_24838	3.350223906	No Blast Hit
CDS_17702_Unigene_302_Transcript_499	3.328668178	XP_031111289.1uncharacterized protein At5g48480
CDS_49630_Unigene_8833_Transcript_14700	3.328075555	No Blast Hit
CDS_20188_Unigene_33270_Transcript_57779	3.323754839	ARB08606.1cadinene synthase
CDS_7019_Unigene_17887_Transcript_30739	3.322801045	XP_023925763.1tubulin beta-5 chain-like
CDS_4900_Unigene_15500_Transcript_26498	3.313773963	XP_010255718.1: myb family transcription factor PHL11 isoform X1
CDS_3875_Unigene_14312_Transcript_24345	3.311864846	XP_020242243.1ribonuclease 1-like
CDS_7197_Unigene_18075_Transcript_31076	3.310310034	XP_015889813.1protein RALF-like 34

Transcript ID	Log2 Fold Change	Hit desc.
CDS_31071_Unigene_47648_Transcript_83845	3.291363777	XP_022573040.1adenosylhomocysteinase 2-like
CDS_12152_Unigene_23824_Transcript_41172	3.287859962	XP_013736391.1 galactinol--sucrose galactosyltransferase 6
CDS_21643_Unigene_3499_Transcript_5757	3.287838269	MQL85900.1 protein
CDS_3876_Unigene_14313_Transcript_24346	3.282884047	XP_010259636.1: extracellular ribonuclease LE-like
CDS_47246_Unigene_8035_Transcript_13384	3.272548594	KAE8689280.1Tubulin alpha-1 chain
CDS_18131_Unigene_30822_Transcript_53447	3.268879763	XP_020085665.1WAT1-related protein At5g07050-like
CDS_31451_Unigene_48203_Transcript_84883	3.266818279	XP_002315056.1delta(24)-sterol reductase
CDS_14429_Unigene_26476_Transcript_45794	3.258974094	RWR77999.1peroxidase 51-like protein
CDS_21434_Unigene_34733_Transcript_60390	3.255311638	No Blast Hit
CDS_47239_Unigene_8032_Transcript_13380	3.253247483	XP_021998471.1tubulin alpha chain-like isoform X1
CDS_43649_Unigene_70604_Transcript_125752	3.248057824	XP_020092485.1SPARC-like protein 1
CDS_27535_Unigene_42706_Transcript_74929	3.240681365	KAE9467366.1 protein C3L33_00710, partial
CDS_18132_Unigene_30823_Transcript_53448	3.234361881	RWR76062.1WAT1-related protein
CDS_14144_Unigene_26127_Transcript_45186	3.230467419	No Blast Hit
CDS_9525_Unigene_20768_Transcript_35821	3.230211926	RWW24418.1 protein GW17_00011295
CDS_45506_Unigene_7521_Transcript_12570	3.224040085	RWR95446.1histone H2B-like protein
CDS_42031_Unigene_66909_Transcript_118747	3.221151108	XP_031277613.1uclacyanin-3-like
CDS_20189_Unigene_33271_Transcript_57782	3.216132561	ARB08606.1cadinene synthase
CDS_929_Unigene_11019_Transcript_18491	3.214065377	RWR97079.1Protein kinase domain-containing protein
CDS_1366_Unigene_11549_Transcript_19385	3.213967081	XP_007019334.2: carboxyvinyl-carboxyphosphonate phosphorylmutase, chloroplastic
CDS_1367_Unigene_11550_Transcript_19386	3.202940059	XP_007019334.2: carboxyvinyl-carboxyphosphonate phosphorylmutase, chloroplastic
CDS_24252_Unigene_38366_Transcript_66850	3.201824119	XP_023917839.1uncharacterized protein LOC112029389
CDS_23956_Unigene_37960_Transcript_66147	3.199245575	XP_022857079.1laccase-7-like
CDS_15206_Unigene_27389_Transcript_47363	3.196721174	XP_030934219.1uncharacterized protein LOC115959782
CDS_10281_Unigene_21635_Transcript_37350	3.174676854	KAF3976427.1 protein CMV_000399
CDS_29422_Unigene_4524_Transcript_7567	3.169837442	RWR78338.1Cellulose synthase
CDS_4583_Unigene_15125_Transcript_25815	3.169398429	RWR85962.1Plant disease resistance response protein
CDS_12716_Unigene_24495_Transcript_42347	3.152248096	XP_009417284.1: galactan beta-1,4-galactosyltransferase GALS1-like

Transcript ID	Log2 Fold Change	Hit desc.
CDS_1499_Unigene_116_Transcript_178	3.149191433	RWR74326.1xyloglucan endotransglycosylase
CDS_35744_Unigene_54899_Transcript_96881	3.147898695	No Blast Hit
CDS_4104_Unigene_14575_Transcript_24840	3.143254034	No Blast Hit
CDS_35562_Unigene_54589_Transcript_96319	3.137406321	KAA8543456.1 protein F0562_021049
CDS_19680_Unigene_32654_Transcript_56744	3.131702835	OVA01176.1WRC
CDS_5318_Unigene_15988_Transcript_27341	3.126912849	PON97075.1Alcohol dehydrogenase superfamily, zinc-type
CDS_37136_Unigene_57279_Transcript_101210	3.124076346	RWR97387.1GDSL esterase/lipase-like protein
CDS_29216_Unigene_44968_Transcript_79027	3.123296722	XP_010245693.1: stearoyl-
CDS_13643_Unigene_25560_Transcript_44227	3.111538323	XP_034694198.1fasciclin-like arabinogalactan protein 17
CDS_6389_Unigene_17173_Transcript_29535	3.109410241	No Blast Hit
CDS_2085_Unigene_12340_Transcript_20812	3.093267017	XP_012085555.1 pectate lyase 5
CDS_44430_Unigene_72517_Transcript_129555	3.092131831	RWR95123.1arogenate dehydratase/prephenate dehydratase 2, chloroplastic-like protein
CDS_19341_Unigene_32230_Transcript_55979	3.087851845	XP_026386791.1phosphomethylethanolamine N-methyltransferase-like
CDS_24684_Unigene_38924_Transcript_67858	3.083768358	KAE9456085.1 protein C3L33_12025, partial
CDS_25139_Unigene_39513_Transcript_68947	3.081498184	RWR72397.1early nodulin-93-like protein
CDS_37332_Unigene_57605_Transcript_101808	3.057545869	XP_010271938.1: subtilisin-like protease SBT1.7
CDS_24724_Unigene_38979_Transcript_67983	3.05680131	XP_002285068.1: fasciclin-like arabinogalactan protein 11
CDS_15812_Unigene_28098_Transcript_48606	3.050601494	No Blast Hit
CDS_267_Unigene_10280_Transcript_17201	3.048405289	No Blast Hit
CDS_4578_Unigene_15120_Transcript_25805	3.046293652	XP_008447606.1: beta-galactosidase 1
CDS_7672_Unigene_1862_Transcript_3114	3.034380331	XP_010937646.1heat shock cognate 70 kDa protein 2
CDS_47617_Unigene_81561_Transcript_147786	3.03244958	XP_016707131.1: ethylene-responsive transcription factor ERF014-like
CDS_17637_Unigene_30220_Transcript_52375	3.029790737	XP_016695900.1: galactinol synthase 1-like
CDS_27371_Unigene_42486_Transcript_74507	3.028058925	XP_020673332.1gamma conglutin 1-like
CDS_268_Unigene_10281_Transcript_17202	3.027950388	No Blast Hit
CDS_6546_Unigene_1734_Transcript_2885	3.025351671	No Blast Hit
CDS_37290_Unigene_57521_Transcript_101654	3.024248363	XP_011101528.1histone H2B-like
CDS_13165_Unigene_25007_Transcript_43256	3.022367813	RWR94963.1GDP-fucose protein O-fucosyltransferase
CDS_32587_Unigene_49954_Transcript_87973	3.022367813	BAF18856.2Os06g0172800

Transcript ID	Log2 Fold Change	Hit desc.
CDS_11420_Unigene_22977_Transcript_39734	3.020125862	RWR77548.1protein REVERSION-TO-ETHYLENE SENSITIVITY1 isoform X2
CDS_21852_Unigene_35256_Transcript_61341	3.017217165	RWR89525.1peroxidase 5-like protein
CDS_34395_Unigene_52660_Transcript_92827	3.002768636	RWR89594.1D-amino-acid transaminase, chloroplastic isoform X1
CDS_21299_Unigene_34577_Transcript_60116	2.988621043	TKR83436.1peroxidase 42
CDS_38342_Unigene_59499_Transcript_105233	2.987621282	RWR72474.1putative aquaporin TIP4-3
CDS_49869_Unigene_89094_Transcript_172480	2.977777662	XP_018826266.1: protein IQ-DOMAIN 14-like
CDS_23526_Unigene_3740_Transcript_6169	2.97630366	XP_010251871.1: putative germin-like protein 2-1
CDS_5218_Unigene_15873_Transcript_27144	2.975418635	OAY81337.1putative methyltransferase PMT21
CDS_51203_Unigene_9428_Transcript_15767	2.967519688	RWR77480.1extracellular ribonuclease LE-like protein
CDS_29122_Unigene_44838_Transcript_78795	2.961777833	XP_010272971.1: transcription factor bHLH96
CDS_35237_Unigene_54069_Transcript_95417	2.956637148	XP_034692350.1pollen-specific protein C13-like
CDS_5815_Unigene_16530_Transcript_28402	2.952958244	TXG58573.1 protein EZV62_016402
CDS_16637_Unigene_29078_Transcript_50341	2.951480109	RWR87813.1putative aquaporin NIP5-1
CDS_6536_Unigene_1733_Transcript_2882	2.946444262	No Blast Hit
CDS_42282_Unigene_67442_Transcript_119713	2.944690944	AAT37172.1caffeoyl-CoA-O-methyltransferase
CDS_2396_Unigene_12684_Transcript_21423	2.926899509	PIN23985.1Cellulose synthase (UDP-forming)
CDS_49789_Unigene_88768_Transcript_170808	2.923392083	XP_020242649.1non-specific lipid-transfer protein 1-like
CDS_29126_Unigene_44843_Transcript_78800	2.922017288	RWR89959.1transcription factor bHLH96
CDS_13672_Unigene_25600_Transcript_44291	2.92051781	XP_002285691.1: protein YLS3
CDS_4586_Unigene_15128_Transcript_25820	2.920269625	No Blast Hit
CDS_33584_Unigene_51403_Transcript_90547	2.917060069	RWR87539.1LRR receptor-like serine/threonine-protein kinase GSO2
CDS_40485_Unigene_6355_Transcript_10575	2.912632534	XP_020275356.1LOW QUALITY PROTEIN: laccase-6-like, partial
CDS_8688_Unigene_19821_Transcript_34160	2.906422416	XP_028126133.1cytochrome b5
CDS_25363_Unigene_39818_Transcript_69537	2.906073621	XP_010264071.1: uncharacterized protein LOC104602168
CDS_8120_Unigene_19153_Transcript_32956	2.905198465	VAI54365.1unnamed protein product
CDS_35427_Unigene_54368_Transcript_95943	2.904798217	KAF3445133.1 protein FNV43_RR14826
CDS_22036_Unigene_3549_Transcript_5840	2.898587987	No Blast Hit
CDS_45509_Unigene_7522_Transcript_12571	2.898571386	RWR95446.1histone H2B-like protein

Transcript ID	Log2 Fold Change	Hit desc.
CDS_25689_Unigene_40244_Transcript_70287	2.897589875	RWR75996.1blue copper-like protein
CDS_20406_Unigene_33520_Transcript_58230	2.895629359	KAF3943201.1 protein CMV_030218
CDS_22136_Unigene_35617_Transcript_62003	2.89112328	XP_010247189.1: origin of replication complex subunit 1A-like
CDS_16638_Unigene_29079_Transcript_50342	2.890492869	RWR87813.1putative aquaporin NIP5-1
CDS_9279_Unigene_2048_Transcript_3436	2.888559317	XP_010273801.1: pectinesterase
CDS_46838_Unigene_7907_Transcript_13184	2.886486472	RWR80956.1auxin-responsive protein IAA30
CDS_13449_Unigene_25324_Transcript_43832	2.880234964	XP_018725945.1: cellulose synthase A catalytic subunit 3
CDS_38344_Unigene_59500_Transcript_105235	2.878948566	RWR72474.1putative aquaporin TIP4-3
CDS_1831_Unigene_12051_Transcript_20294	2.874444539	XP_010263545.1: heat shock factor protein HSF24-like
CDS_12285_Unigene_23977_Transcript_41414	2.857259828	XP_009419511.1: CASP-like protein 1D1
CDS_29432_Unigene_4526_Transcript_7574	2.853981276	RWR78338.1Cellulose synthase
CDS_2533_Unigene_12827_Transcript_21690	2.852699862	KAF3784605.1putative xyloglucan endotransglucosylase/hydrolase protein 8
CDS_23347_Unigene_37152_Transcript_64766	2.847791781	XP_017432361.1: S-norcoclaurine synthase 2-like
CDS_38785_Unigene_60260_Transcript_106646	2.84672916	RWR95791.1 protein CKAN_02514700
CDS_30567_Unigene_4689_Transcript_7834	2.840203816	WP_151502541.1 protein, partial
CDS_16796_Unigene_29253_Transcript_50664	2.834196212	No Blast Hit
CDS_41093_Unigene_64816_Transcript_114932	2.832908666	RVW12581.1Ethylene-responsive transcription factor ERF062
CDS_1666_Unigene_11876_Transcript_19983	2.827036113	RWR95371.1aluminum-induced protein
CDS_31414_Unigene_48147_Transcript_84785	2.826193542	RWR81339.1pyruvate decarboxylase 2
CDS_17044_Unigene_29548_Transcript_51199	2.819560552	RWR75655.1putative galactinol--sucrose galactosyltransferase 6 isoform X1
CDS_1834_Unigene_12054_Transcript_20297	2.818366937	XP_010263545.1: heat shock factor protein HSF24-like
CDS_20596_Unigene_33737_Transcript_58602	2.817816468	XP_031375183.1two-on-two hemoglobin-3
CDS_24771_Unigene_39029_Transcript_68061	2.817756252	KRY05134.1Tubulin beta-2 chain
CDS_13673_Unigene_25601_Transcript_44292	2.816484479	XP_020096625.1protein YLS3-like
CDS_15892_Unigene_28188_Transcript_48752	2.813502383	XP_026401860.1protein CDI-like
CDS_49710_Unigene_88527_Transcript_169678	2.801318508	XP_018823302.1: osmotin-like protein isoform X1
CDS_29321_Unigene_45115_Transcript_79287	2.796486406	No Blast Hit
CDS_23346_Unigene_37151_Transcript_64765	2.791110077	XP_020083883.1S-norcoclaurine synthase 2-like
CDS_22709_Unigene_36310_Transcript_63264	2.790037155	OVA05555.1zinc finger protein
CDS_265_Unigene_10279_Transcript_17200	2.789687223	No Blast Hit
CDS_15893_Unigene_28189_Transcript_48753	2.784574289	XP_026401860.1protein CDI-like

Transcript ID	Log2 Fold Change	Hit desc.
CDS_2534_Unigene_12828_Transcript_21692	2.779457676	KAF3784605.1putative xyloglucan endotransglucosylase/hydrolase protein 8
CDS_23279_Unigene_3706_Transcript_6114	2.775534532	RWR75399.1S-adenosylmethionine decarboxylase proenzyme-like protein
CDS_47236_Unigene_80320_Transcript_145233	2.774585491	XP_021911467.1protein FAF-like, chloroplastic
CDS_33756_Unigene_51660_Transcript_90984	2.77237093	XP_010271731.1: cytochrome P450 94C1-like
CDS_20531_Unigene_33669_Transcript_58482	2.771384035	XP_010243401.1: dirigent protein 22-like
CDS_13978_Unigene_25936_Transcript_44853	2.770693269	RAL54675.1 protein DM860_001803
CDS_21297_Unigene_34575_Transcript_60113	2.765674111	XP_010278692.1: peroxidase 42-like
CDS_2471_Unigene_12756_Transcript_21562	2.760330378	XP_010259022.1: monocopper oxidase-like protein SKU5
CDS_40216_Unigene_63056_Transcript_111688	2.759546022	KAA8527379.1 protein F0562_034906
CDS_34534_Unigene_52891_Transcript_93280	2.758192486	XP_016486141.1: uncharacterized GPI-anchored protein At3g06035-like
CDS_23455_Unigene_37315_Transcript_65052	2.75412235	XP_020103625.1chaperone protein dnaJ 8, chloroplastic-like
CDS_20876_Unigene_34078_Transcript_59246	2.740210247	XP_002533873.1uncharacterized protein LOC8284795
CDS_15852_Unigene_2814_Transcript_4639	2.737993521	XP_021275241.1alpha-galactosidase-like
CDS_25070_Unigene_39423_Transcript_68794	2.735182508	XP_022135125.1PLASMODESMATA CALLOSE-BINDING PROTEIN 3-like
CDS_27920_Unigene_43230_Transcript_75861	2.732603042	PKI51608.1 protein CRG98_027974
CDS_35294_Unigene_54158_Transcript_95582	2.731466614	No Blast Hit
CDS_16263_Unigene_28623_Transcript_49503	2.726951806	RWR96222.1aspartyl protease family protein 2-like protein
CDS_35484_Unigene_54446_Transcript_96085	2.722410118	RWR88978.1dirigent protein 18
CDS_13947_Unigene_25900_Transcript_44784	2.717896915	XP_034679679.1protein RICE SALT SENSITIVE 3-like
CDS_12286_Unigene_23978_Transcript_41415	2.713124978	XP_026382513.1uncharacterized protein LOC113277702
CDS_28536_Unigene_44036_Transcript_77334	2.710309962	QCX36378.1COMTL2
CDS_5602_Unigene_16300_Transcript_27917	2.710114779	CBI23102.3unnamed protein product, partial
CDS_29427_Unigene_4525_Transcript_7572	2.708573132	RWR78338.1Cellulose synthase
CDS_3038_Unigene_13388_Transcript_22676	2.706622879	XP_010257021.1: laccase-12-like
CDS_29130_Unigene_4484_Transcript_7498	2.69634309	KAF3457614.1 protein FNV43_RR02272
CDS_29748_Unigene_45689_Transcript_80329	2.690149842	RWR93754.1cyclin-P3-1
CDS_17970_Unigene_30632_Transcript_53116	2.689185894	XP_009415021.1: glutathione S-transferase zeta class
CDS_3749_Unigene_14171_Transcript_24090	2.686191828	XP_010259074.1: heparanase-like protein 1
CDS_15210_Unigene_27392_Transcript_47367	2.685332826	THU72040.1 protein C4D60_Mb04t07910

Transcript ID	Log2 Fold Change	Hit desc.
CDS_26122_Unigene_4080_Transcript_6816	2.679111702	XP_010908721.15-methyltetrahydropteroyltriglutamate--homocysteine methyltransferase 1
CDS_10295_Unigene_21652_Transcript_37371	2.676625242	RWR94160.1rapid alkalinization factor-like protein
CDS_11337_Unigene_22876_Transcript_39560	2.670774047	XP_010935030.1WEB family protein At3g02930, chloroplastic
CDS_4061_Unigene_14529_Transcript_24743	2.668730858	XP_008803083.1acyl carrier protein 1, chloroplastic-like isoform X2
CDS_25690_Unigene_40245_Transcript_70288	2.666100602	RWR75996.1blue copper-like protein
CDS_2334_Unigene_12614_Transcript_21286	2.661426058	XP_010918289.1protein EXORDIUM-like 5
CDS_29747_Unigene_45688_Transcript_80326	2.654925059	RWR93754.1cyclin-P3-1
CDS_1665_Unigene_11875_Transcript_19982	2.649796501	MQL76237.1 protein
CDS_48187_Unigene_83297_Transcript_152031	2.645974944	No Blast Hit
CDS_20268_Unigene_33360_Transcript_57925	2.641477249	No Blast Hit
CDS_7651_Unigene_1860_Transcript_3111	2.638953563	EOY07555.1Heat shock cognate protein 70-1 isoform 2, partial
CDS_3883_Unigene_1431_Transcript_2427	2.638761043	XP_009413318.1: tubulin alpha-3 chain-like
CDS_33975_Unigene_51984_Transcript_91546	2.638469643	OVA15235.1Oligopeptide transporter
CDS_43769_Unigene_7091_Transcript_11865	2.63695215	PIA50475.1 protein AQUCO_01300896v1
CDS_29990_Unigene_46046_Transcript_81004	2.606512426	XP_010262784.1: uncharacterized acetyltransferase At3g50280-like
CDS_50396_Unigene_91088_Transcript_184143	2.605305478	XP_034895933.1uncharacterized protein LOC118034697
CDS_15712_Unigene_27987_Transcript_48419	2.605029065	RZC63811.1 protein C5167_025549
CDS_31304_Unigene_47993_Transcript_84505	2.603142517	EEF35153.1conserved protein
CDS_12441_Unigene_24146_Transcript_41730	2.600608137	RWR82793.1putative cytokinin riboside 5'-monophosphate phosphoribohydrolase LOGL1
CDS_286_Unigene_10299_Transcript_17234	2.600598529	TQD87737.1 protein C1H46_026741
CDS_51465_Unigene_9721_Transcript_16253	2.599977168	RWR97281.1Glycoside hydrolase
CDS_34394_Unigene_52659_Transcript_92819	2.595107995	RWR89594.1D-amino-acid transaminase, chloroplastic isoform X1
CDS_21222_Unigene_34481_Transcript_59974	2.593648229	KAF3957516.1 protein CMV_017480
CDS_10448_Unigene_21822_Transcript_37682	2.591698494	XP_022769754.1transcription factor MYC2-like
CDS_28249_Unigene_43675_Transcript_76684	2.589614726	XP_034679489.1kinesin-like protein KIN-14F isoform X1
CDS_20044_Unigene_33106_Transcript_57491	2.586268698	XP_010248147.1: polygalacturonase At1g48100-like, partial
CDS_24251_Unigene_38365_Transcript_66849	2.583528536	XP_023917839.1uncharacterized protein LOC112029389

Transcript ID	Log2 Fold Change	Hit desc.
CDS_23556_Unigene_3744_Transcript_6177	2.582770042	XP_020268784.1putative germin-like protein 2-1
CDS_20875_Unigene_34077_Transcript_59245	2.582221865	XP_002533873.1uncharacterized protein LOC8284795
CDS_39188_Unigene_61074_Transcript_108098	2.577757198	RWR71846.1long-chain-alcohol O-fatty-acyltransferase
CDS_28950_Unigene_4459_Transcript_7460	2.57636684	XP_011624318.1gibberellin-regulated protein 9
CDS_11258_Unigene_22791_Transcript_39410	2.575146074	TXG65198.1 protein EZV62_006473
CDS_17366_Unigene_29923_Transcript_51884	2.567396687	XP_010255326.1: glycerol-3-phosphate acyltransferase 8
CDS_15803_Unigene_2808_Transcript_4629	2.555520248	XP_021275241.1alpha-galactosidase-like
CDS_29331_Unigene_45129_Transcript_79311	2.554398183	No Blast Hit
CDS_26837_Unigene_41761_Transcript_73100	2.549635801	PKI77425.1 protein CRG98_002198
CDS_19489_Unigene_32408_Transcript_56296	2.544265876	XP_010250555.1: serine carboxypeptidase-like 45
CDS_33979_Unigene_51990_Transcript_91554	2.543987165	RWR80661.1proline-rich protein DC2.15-like protein isoform X2
CDS_39485_Unigene_6166_Transcript_10246	2.539012179	XP_008781778.1ubiquitin-conjugating enzyme E2 22-like
CDS_40584_Unigene_6373_Transcript_10615	2.537905677	OVA16518.1Expansin
CDS_33596_Unigene_51425_Transcript_90580	2.531820914	RWR76197.13-oxoacyl-acyl-carrier-protein synthase II, chloroplastic-like protein isoform X1
CDS_10280_Unigene_21631_Transcript_37344	2.527603121	KAF3976427.1 protein CMV_000399
CDS_39950_Unigene_62520_Transcript_110706	2.527002749	No Blast Hit
CDS_545_Unigene_10613_Transcript_17767	2.525761187	GAU43497.1 protein TSUD_92080
CDS_10279_Unigene_21629_Transcript_37339	2.524340949	KAF3976427.1 protein CMV_000399
CDS_19697_Unigene_32686_Transcript_56798	2.522138361	KAA8528523.1 protein F0562_035878
CDS_5548_Unigene_16241_Transcript_27817	2.521814337	XP_010253728.1: receptor-like serine/threonine-protein kinase NCRK
CDS_3039_Unigene_13389_Transcript_22677	2.520644372	XP_022880382.1laccase-12-like
CDS_15209_Unigene_27391_Transcript_47365	2.519867472	XP_020265239.1inositol oxygenase 1-like
CDS_39099_Unigene_6087_Transcript_10129	2.518936204	XP_010243244.1: xyloglucan endotransglucosylase/hydrolase protein 32
CDS_22003_Unigene_3545_Transcript_5836	2.518648542	No Blast Hit
CDS_22764_Unigene_36373_Transcript_63394	2.517469701	No Blast Hit
CDS_41950_Unigene_66729_Transcript_118413	2.51571924	XP_012093337.1protein YLS3
CDS_8613_Unigene_19742_Transcript_34018	2.515407824	KCW50926.1 protein EUGRSUZ_J00576
CDS_13284_Unigene_25132_Transcript_43501	2.515074987	OVA19617.1Glycoside hydrolase family 38
CDS_39484_Unigene_6165_Transcript_10244	2.513619741	XP_008781778.1ubiquitin-conjugating enzyme E2 22-like

Transcript ID	Log2 Fold Change	Hit desc.
CDS_8356_Unigene_19427_Transcript_33454	2.511713341	RWR86285.1Multi antimicrobial extrusion protein
CDS_20592_Unigene_33733_Transcript_58598	2.511332955	XP_031375183.1two-on-two hemoglobin-3
CDS_17432_Unigene_29996_Transcript_52002	2.511049453	AIR07818.1chloroplastic glutamine synthetase GS2, partial
CDS_51449_Unigene_9702_Transcript_16222	2.507234479	XP_010649604.1: nhx1 antiporter isoform X1
CDS_39774_Unigene_6219_Transcript_10342	2.500373152	No Blast Hit
CDS_41831_Unigene_66475_Transcript_117929	2.498805857	GAY69629.1 protein CUMW_289330, partial
CDS_46865_Unigene_79177_Transcript_142811	2.498805857	XP_026404397.1uncharacterized protein LOC113299575 isoform X1
CDS_19660_Unigene_32632_Transcript_56706	2.498416308	PIN08160.1Subunit of Golgi mannosyltransferase complex
CDS_49868_Unigene_8908_Transcript_14844	2.4897804	XP_034888897.1 receptor-like serine/threonine-protein kinase At5g57670
CDS_51464_Unigene_9720_Transcript_16249	2.487842873	RWR97281.1Glycoside hydrolase
CDS_285_Unigene_10298_Transcript_17233	2.486314913	KDP34394.1 protein JCGZ_12788
CDS_41133_Unigene_64881_Transcript_115043	2.480085151	TXG73831.1 protein EZV62_002410
CDS_33454_Unigene_51144_Transcript_90077	2.478627975	RWR97123.1beta-fructofuranosidase, insoluble isoenzyme 3-like protein
CDS_47757_Unigene_81_Transcript_136	2.478244534	RWR89211.1Crotonase superfamily
CDS_8380_Unigene_19462_Transcript_33510	2.475941749	XP_010256924.1: ABC transporter B family member 19
CDS_37435_Unigene_57798_Transcript_102155	2.472810648	No Blast Hit
CDS_17041_Unigene_29545_Transcript_51194	2.47096681	PNS94102.2 protein POPTR_018G126400
CDS_21974_Unigene_35417_Transcript_61615	2.469261581	KAB1210503.1Amino acid permease 2
CDS_33493_Unigene_51207_Transcript_90186	2.463749121	XP_008784028.1alpha carbonic anhydrase 1, chloroplastic-like
CDS_1590_Unigene_11794_Transcript_19825	2.463240497	KAF3968677.1 protein CMV_007459
CDS_27197_Unigene_4225_Transcript_7061	2.46315527	No Blast Hit
CDS_42840_Unigene_68706_Transcript_122060	2.462686431	RWR73763.1cyclin-dependent protein kinase inhibitor SMR9-like protein
CDS_35803_Unigene_54_Transcript_89	2.462468704	AGV54733.1dehydration-responsive protein RD22-like protein
CDS_39857_Unigene_62368_Transcript_110409	2.460036287	XP_034695743.1binding partner of ACD11 1 isoform X1
CDS_14363_Unigene_2638_Transcript_4354	2.45650584	RWR96232.1 protein CKAN_02560500
CDS_1835_Unigene_12055_Transcript_20298	2.44120188	XP_010263545.1: heat shock factor protein HSF24-like
CDS_12139_Unigene_23807_Transcript_41138	2.440253675	XP_034916658.1putative glucose-6-phosphate 1-epimerase isoform X2
CDS_29750_Unigene_45690_Transcript_80330	2.439815831	RWR93754.1cyclin-P3-1
CDS_41891_Unigene_66621_Transcript_118198	2.438684865	KAF3974860.1 protein CMV_001840

Transcript ID	Log2 Fold Change	Hit desc.
CDS_13949_Unigene_25902_Transcript_44789	2.432496512	XP_034679679.1protein RICE SALT SENSITIVE 3-like
CDS_7661_Unigene_1861_Transcript_3112	2.428816351	XP_027353319.1heat shock cognate 70 kDa protein 2-like isoform X1
CDS_41210_Unigene_65016_Transcript_115267	2.428196589	RWR72665.1myosin-9 isoform X1
CDS_6328_Unigene_17101_Transcript_29405	2.425136333	XP_034692772.1histone H2A
CDS_20266_Unigene_33359_Transcript_57924	2.418427011	RWR72857.1protein COBRA-like protein isoform X1
CDS_12182_Unigene_23857_Transcript_41227	2.415611921	PQP92725.1myosin-11
CDS_35766_Unigene_54946_Transcript_96963	2.40999659	XP_010644121.1: epidermis-specific secreted glycoprotein EP1
CDS_17638_Unigene_30221_Transcript_52376	2.409009187	RWR92332.1myb-related protein Hv1-like protein
CDS_30496_Unigene_46783_Transcript_82343	2.405696453	WP_168415041.1 protein, partial
CDS_9612_Unigene_20862_Transcript_35969	2.405696453	XP_010254774.1: mannan endo-1,4-beta-mannosidase 7-like
CDS_9611_Unigene_20861_Transcript_35965	2.40538313	XP_010254774.1: mannan endo-1,4-beta-mannosidase 7-like
CDS_43996_Unigene_7147_Transcript_11960	2.40330986	AQK68709.1Tubulin beta-4 chain
CDS_21590_Unigene_34936_Transcript_60743	2.403196114	XP_010262112.1: uncharacterized protein LOC104600711
CDS_33529_Unigene_51284_Transcript_90326	2.402945842	XP_006644462.1: long chain acyl-CoA synthetase 4-like
CDS_10765_Unigene_22202_Transcript_38340	2.399270183	KDO43303.1 protein CISIN_1g0420481mg, partial
CDS_3108_Unigene_1346_Transcript_2307	2.398482708	XP_010252386.1: peroxidase 72-like
CDS_15783_Unigene_2806_Transcript_4627	2.395712364	KAA8521005.1 protein F0562_011707
CDS_19924_Unigene_3296_Transcript_5431	2.394001119	RWR79133.1beta-galactosidase 3-like protein
CDS_50494_Unigene_9143_Transcript_15270	2.390225044	QGY72664.1piperic acid coenzyme A ligase
CDS_20046_Unigene_33110_Transcript_57498	2.382612839	XP_010248147.1: polygalacturonase At1g48100-like, partial
CDS_9748_Unigene_21016_Transcript_36250	2.380969367	AQY17493.1putative protein S-acyltransferase 22
CDS_29322_Unigene_45116_Transcript_79288	2.378240113	No Blast Hit
CDS_3750_Unigene_14172_Transcript_24091	2.371087416	XP_010259074.1: heparanase-like protein 1
CDS_34949_Unigene_53603_Transcript_94584	2.370798245	XP_010266134.1: protein STRICTOSIDINE SYNTHASE-LIKE 7-like
CDS_22581_Unigene_36155_Transcript_62964	2.370649505	EOY05526.1F28L1.9 protein
CDS_21156_Unigene_34398_Transcript_59836	2.369851254	XP_006468457.1protein PHLOEM PROTEIN 2-LIKE A5
CDS_26477_Unigene_41301_Transcript_72275	2.369819416	XP_010276380.1: glutamate dehydrogenase 1
CDS_8027_Unigene_19051_Transcript_32775	2.369819416	RRT70764.1 protein B296_00030471

Transcript ID	Log2 Fold Change	Hit desc.
CDS_32262_Unigene_49453_Transcript_87108	2.366168088	XP_010255900.1: basic 7S globulin 2-like
CDS_18367_Unigene_31085_Transcript_53909	2.365803725	OVA16067.1Glycoside hydrolase
CDS_26317_Unigene_41071_Transcript_71869	2.358095419	RWR82707.1Ceramide glucosyltransferase
CDS_11123_Unigene_22630_Transcript_39074	2.357844934	RWR76707.1glycerol-3-phosphate acyltransferase 5-like protein
CDS_903_Unigene_10995_Transcript_18454	2.356607245	RWR86285.1Multi antimicrobial extrusion protein
CDS_44002_Unigene_7148_Transcript_11961	2.355963362	AQK68709.1Tubulin beta-4 chain
CDS_43734_Unigene_70837_Transcript_126187	2.351248669	GAU18794.1 protein TSUD_80830
CDS_29872_Unigene_45856_Transcript_80645	2.349994568	XP_008775111.1non-specific lipid transfer protein GPI-anchored 2-like
CDS_11344_Unigene_22882_Transcript_39573	2.34700932	RWR86216.1putative S-adenosyl-L-methionine-dependent methyltransferase
CDS_48226_Unigene_83427_Transcript_152385	2.346802764	XP_021681461.1auxin transporter-like protein 3
CDS_39415_Unigene_61543_Transcript_108946	2.343527631	RWR85438.1putative carboxylesterase 15
CDS_20269_Unigene_33361_Transcript_57926	2.343342469	RWR72857.1protein COBRA-like protein isoform X1
CDS_6097_Unigene_16840_Transcript_28923	2.341189997	XP_015895871.1heavy metal-associated isoprenylated plant protein 37
CDS_11228_Unigene_22762_Transcript_39338	2.340821786	XP_028056275.13-oxoacyl-
CDS_12187_Unigene_23862_Transcript_41233	2.338558769	XP_010273099.1: early endosome antigen 1
CDS_17270_Unigene_29816_Transcript_51677	2.338085546	KAE8022424.1 protein FH972_008226
CDS_17839_Unigene_30475_Transcript_52847	2.334729931	XP_028055634.1(-)-isopiperitenol/(-)-carveol dehydrogenase, mitochondrial-like
CDS_32366_Unigene_4962_Transcript_8287	2.333207132	No Blast Hit
CDS_19661_Unigene_32633_Transcript_56708	2.331191016	XP_011090963.1xyloglucan 6-xylosyltransferase 2
CDS_32770_Unigene_50193_Transcript_88381	2.330928684	No Blast Hit
CDS_32399_Unigene_49691_Transcript_87519	2.330206253	XP_021674747.1peroxidase 11
CDS_25668_Unigene_40209_Transcript_70222	2.329100762	PSR89102.1Isoaspartyl peptidase/L-asparaginase 1 subunit beta like
CDS_31460_Unigene_4821_Transcript_8039	2.326338661	XP_010263063.1: myb family transcription factor EFM-like isoform X2
CDS_17640_Unigene_30223_Transcript_52378	2.325759956	RWR92332.1myb-related protein Hv1-like protein
CDS_43339_Unigene_69817_Transcript_124278	2.325656955	KJB66289.1 protein B456_010G135200
CDS_39107_Unigene_6089_Transcript_10132	2.324805	XP_022766132.1 xyloglucan endotransglucosylase/hydrolase protein 32
CDS_35210_Unigene_54009_Transcript_95321	2.324446132	XP_023926641.1salicylic acid-binding protein 2-like

Transcript ID	Log2 Fold Change	Hit desc.
CDS_36787_Unigene_56637_Transcript_100104	2.319835716	XP_031472843.1beta-glucuronosyltransferase GlcAT14A-like
CDS_7366_Unigene_18264_Transcript_31460	2.318645827	XP_028097413.1UDP-D-apiose/UDP-D-xylose synthase 2-like
CDS_17639_Unigene_30222_Transcript_52377	2.318597882	RWR92332.1myb-related protein Hv1-like protein
CDS_39964_Unigene_62548_Transcript_110757	2.316429114	XP_028552343.1ankyrin repeat-containing protein ITN1
CDS_12739_Unigene_24517_Transcript_42383	2.316099016	XP_034687178.1(+)-neomenthol dehydrogenase-like isoform X3
CDS_22444_Unigene_35975_Transcript_62652	2.31187443	XP_010275692.1: E3 ubiquitin-protein ligase RHA1B-like
CDS_22135_Unigene_35616_Transcript_62002	2.311435721	XP_015571097.1origin of replication complex subunit 1A
CDS_42232_Unigene_67342_Transcript_119532	2.311059578	RWR94235.1GATA transcription factor 16-like protein
CDS_11173_Unigene_22698_Transcript_39196	2.306160779	RWR95279.1 protein CKAN_02461700
CDS_21970_Unigene_35413_Transcript_61608	2.306160779	RWR90243.1amino acid permease 3
CDS_13450_Unigene_25325_Transcript_43834	2.304758061	AAX08057.1UDP-glucose dehydrogenase
CDS_10622_Unigene_22041_Transcript_38046	2.298163324	CBI14856.3unnamed protein product, partial
CDS_19905_Unigene_32945_Transcript_57212	2.296071961	RWR89748.1Plant peroxidase
CDS_14214_Unigene_26213_Transcript_45360	2.293486949	No Blast Hit
CDS_16243_Unigene_285_Transcript_474	2.290164106	No Blast Hit
CDS_10302_Unigene_21663_Transcript_37403	2.288085234	RWR95947.1kinesin-like protein KIN-7K, chloroplastic isoform X2
CDS_1958_Unigene_12191_Transcript_20535	2.287898573	PIN06324.1Pectinesterase
CDS_47932_Unigene_82509_Transcript_149889	2.287723531	KAF5193555.1Dirigent protein
CDS_39540_Unigene_61758_Transcript_109333	2.285812134	RWR96115.1putative inactive linolenate hydroperoxide lyase
CDS_31727_Unigene_48621_Transcript_85637	2.282548222	ERM96041.1 protein AMTR_s00129p00082230
CDS_26990_Unigene_4195_Transcript_7009	2.281449026	XP_010255900.1: basic 7S globulin 2-like
CDS_31530_Unigene_48317_Transcript_85081	2.280524852	PON38590.1HAD hydrolase, subfamily IA
CDS_7052_Unigene_17922_Transcript_30802	2.28016557	OVA04007.1Protein of unknown function DUF761
CDS_26646_Unigene_41519_Transcript_72685	2.275427651	RWW76774.1 protein BHE74_00015125
CDS_23054_Unigene_36759_Transcript_64084	2.274909845	XP_021890475.1 beta-D-xylosidase 6
CDS_26834_Unigene_41759_Transcript_73098	2.272881399	XP_031474446.1endoglucanase 24-like
CDS_8621_Unigene_19750_Transcript_34035	2.272309037	RWR71911.1JHL23J11.5
CDS_43729_Unigene_70820_Transcript_126156	2.271395361	OAY81326.1Serine/threonine-protein kinase Nek5
CDS_8524_Unigene_19632_Transcript_33832	2.270389648	No Blast Hit

Transcript ID	Log2 Fold Change	Hit desc.
CDS_21046_Unigene_34262_Transcript_59581	2.270041353	RWR73374.1mitochondrial arginine transporter BAC2
CDS_21221_Unigene_34480_Transcript_59972	2.2673227	KRH70484.1 protein GLYMA_02G093200
CDS_51200_Unigene_9424_Transcript_15762	2.266671761	RWR77480.1extracellular ribonuclease LE-like protein
CDS_28302_Unigene_43741_Transcript_76804	2.266007282	RWR87342.1glutamate dehydrogenase 2
CDS_35467_Unigene_54416_Transcript_96026	2.260514625	AEL30660.13-hydroxy-3-methylglutaryl-CoA reductase
CDS_15813_Unigene_2809_Transcript_4631	2.259618193	KAA8521005.1 protein F0562_011707
CDS_35307_Unigene_54178_Transcript_95613	2.258542759	XP_006855324.2uncharacterized protein LOC18445117
CDS_3751_Unigene_14173_Transcript_24093	2.250418227	XP_010259074.1: heparanase-like protein 1
CDS_6457_Unigene_17252_Transcript_29665	2.24970029	RWR95464.1zinc finger protein
CDS_2772_Unigene_13080_Transcript_22131	2.249634105	XP_017243480.1: uncharacterized protein LOC108215483
CDS_51192_Unigene_9418_Transcript_15755	2.248827604	XP_010264036.1: pectate lyase 8
CDS_11855_Unigene_23463_Transcript_40544	2.248128658	RWR76482.1Glycoside hydrolase
CDS_29302_Unigene_45091_Transcript_79240	2.24655129	RWR79298.1small heat shock protein, chloroplastic-like protein isoform X2
CDS_51641_Unigene_9929_Transcript_16611	2.245814066	MQL70381.1 protein
CDS_36310_Unigene_55830_Transcript_98572	2.244760234	QIG55755.1PIN1, partial
CDS_9887_Unigene_21173_Transcript_36524	2.243019858	OVA08740.1Calreticulin/calnexin
CDS_27351_Unigene_42464_Transcript_74449	2.24219772	RWR96429.1cellulose synthase-like protein G3
CDS_24353_Unigene_38504_Transcript_67115	2.240374217	No Blast Hit
CDS_15777_Unigene_28061_Transcript_48534	2.238743018	XP_010257021.1: laccase-12-like
CDS_46246_Unigene_77237_Transcript_138896	2.233281899	No Blast Hit
CDS_33931_Unigene_51919_Transcript_91430	2.230609746	TKY64042.1Formin protein 1
CDS_22568_Unigene_36140_Transcript_62938	2.227909333	XP_021631725.1desumoylating isopeptidase 1
CDS_2398_Unigene_12686_Transcript_21425	2.227044027	PKI47156.1 protein CRG98_032448
CDS_29123_Unigene_4483_Transcript_7497	2.225124207	RWR89021.1Protein kinase domain-containing protein
CDS_31083_Unigene_47679_Transcript_83897	2.223171414	RWR89359.1BAG family molecular chaperone regulator 1
CDS_5549_Unigene_16242_Transcript_27818	2.221554513	XP_010253728.1: receptor-like serine/threonine-protein kinase NCRK
CDS_34030_Unigene_52068_Transcript_91688	2.219163448	XP_019199014.1: osmotin-like protein
CDS_50345_Unigene_9095_Transcript_15179	2.217034889	XP_002279914.1: protein ELF4-LIKE 4
CDS_17042_Unigene_29546_Transcript_51197	2.215012891	THU51882.1 protein C4D60_Mb06t35750

Transcript ID	Log2 Fold Change	Hit desc.
CDS_39095_Unigene_6086_Transcript_10127	2.212316992	XP_004304471.1: xyloglucan endotransglucosylase/hydrolase protein 32
CDS_12181_Unigene_23856_Transcript_41226	2.209396036	XP_010273099.1: early endosome antigen 1
CDS_27466_Unigene_42615_Transcript_74745	2.20929924	KHN10991.1 protein glysoja_026726
CDS_2918_Unigene_13236_Transcript_22424	2.207343043	RWR82578.1DnaJ domain-containing protein
CDS_31801_Unigene_48734_Transcript_85819	2.207343043	XP_034912327.1uncharacterized protein LOC118047209
CDS_9888_Unigene_21174_Transcript_36525	2.207256447	BAF02251.1 protein, partial
CDS_30648_Unigene_47030_Transcript_82781	2.203349973	KAA8540484.1 protein F0562_024597
CDS_5219_Unigene_15874_Transcript_27145	2.203134243	OAY81337.1putative methyltransferase PMT21
CDS_25636_Unigene_40162_Transcript_70149	2.202821029	MQM23782.1 protein
CDS_3223_Unigene_135_Transcript_209	2.199245575	KDO39684.1 protein CISIN_1g013919mg
CDS_32755_Unigene_50176_Transcript_88356	2.199245575	RWR82872.1 protein CKAN_01160800
CDS_43589_Unigene_7043_Transcript_11793	2.196536288	RWR84153.1putative membrane-associated kinase regulator 1 -like protein
CDS_43995_Unigene_7146_Transcript_11959	2.19641929	XP_028759390.1tubulin beta chain-like
CDS_8111_Unigene_19143_Transcript_32939	2.196243087	KAF5181367.1U-box domain-containing protein
CDS_40096_Unigene_62805_Transcript_111226	2.194614126	RWR93024.1non-specific lipid-transfer protein-like protein
CDS_14700_Unigene_26799_Transcript_46351	2.192702729	CDP01705.1unnamed protein product
CDS_26831_Unigene_41756_Transcript_73094	2.192702729	XP_010941260.1endoglucanase 24
CDS_20265_Unigene_33358_Transcript_57923	2.189824559	CBI16946.3unnamed protein product, partial
CDS_48123_Unigene_8307_Transcript_13819	2.188401899	XP_010939194.1protein SPIRAL1-like 3
CDS_11126_Unigene_22633_Transcript_39081	2.186861851	XP_028097246.1glycerol-3-phosphate acyltransferase 5-like
CDS_51119_Unigene_9383_Transcript_15704	2.182413204	EOY27986.1Xylem bark cysteine peptidase 3 isoform 2
CDS_30935_Unigene_4744_Transcript_7914	2.181615681	ONI00362.1 protein PRUPE_6G084700
CDS_5938_Unigene_16670_Transcript_28624	2.180978978	XP_024981513.1basic 7S globulin 2-like
CDS_36246_Unigene_55732_Transcript_98395	2.17952734	No Blast Hit
CDS_11172_Unigene_22697_Transcript_39195	2.177836682	RWR95279.1 protein CKAN_02461700
CDS_6007_Unigene_16750_Transcript_28782	2.172529398	XP_010273793.1: protein STRUBBELIG-RECEPTOR FAMILY 6
CDS_37744_Unigene_58397_Transcript_103224	2.172039205	RWR88711.1Galactose mutarotase-like domain-containing protein
CDS_12736_Unigene_24514_Transcript_42380	2.166909593	XP_034687178.1(+)-neomenthol dehydrogenase-like isoform X3
CDS_39976_Unigene_62582_Transcript_110826	2.166757722	XP_026432923.1homeobox-leucine zipper protein ATHB-6-like

Transcript ID	Log2 Fold Change	Hit desc.
CDS_46866_Unigene_79178_Transcript_142812	2.164258276	XP_026404397.1uncharacterized protein LOC113299575 isoform X1
CDS_29425_Unigene_45253_Transcript_79547	2.162817818	XP_026661593.1RING-H2 finger protein ATL48-like
CDS_29751_Unigene_45691_Transcript_80332	2.16177087	RWR93754.1cyclin-P3-1
CDS_3181_Unigene_13554_Transcript_22992	2.160050927	XP_027119113.1adenosylhomocysteinase
CDS_19125_Unigene_31975_Transcript_55559	2.159599771	VAH97389.1unnamed protein product
CDS_30295_Unigene_46510_Transcript_81859	2.159056485	XP_010242974.1: GDSL esterase/lipase At5g22810
CDS_34501_Unigene_52843_Transcript_93176	2.158315311	XP_010243615.1: uncharacterized protein LOC104587627 isoform X1
CDS_48371_Unigene_83926_Transcript_153701	2.158315311	No Blast Hit
CDS_29008_Unigene_44684_Transcript_78536	2.15683182	RVW98443.1BAG family molecular chaperone regulator 3
CDS_15765_Unigene_28046_Transcript_48509	2.155918143	No Blast Hit
CDS_14437_Unigene_26484_Transcript_45808	2.154851456	EOX99118.1Cytochrome P450, family 86, subfamily B, polypeptide 1 isoform 1
CDS_34584_Unigene_52999_Transcript_93494	2.154851456	XP_028083845.1novel plant SNARE 11
CDS_37743_Unigene_58395_Transcript_103221	2.153670371	XP_010257565.1: GDSL esterase/lipase At1g74460-like
CDS_19224_Unigene_32087_Transcript_55747	2.150882554	PSS17867.1Metallothiol transferase
CDS_48101_Unigene_83017_Transcript_151286	2.150882554	No Blast Hit
CDS_8114_Unigene_19146_Transcript_32944	2.149356699	OVA08620.1U box domain
CDS_27372_Unigene_4248_Transcript_7102	2.149059818	PON38817.1Xanthine dehydrogenase C subunit
CDS_38795_Unigene_60300_Transcript_106718	2.147731416	XP_008809715.1plant cysteine oxidase 2-like isoform X2
CDS_12792_Unigene_2457_Transcript_4070	2.14741362	RXI00560.1 protein DVH24_000794
CDS_8112_Unigene_19144_Transcript_32940	2.144445721	OVA08620.1U box domain
CDS_27689_Unigene_42904_Transcript_75273	2.142662047	XP_002263089.2: uncharacterized protein LOC100254361
CDS_28387_Unigene_43854_Transcript_77005	2.140193791	EEF29386.1 protein RCOM_0233610
CDS_2242_Unigene_12512_Transcript_21130	2.139095432	XP_030471382.1protein PGR
CDS_19794_Unigene_32819_Transcript_56986	2.137591057	QCX36374.1KOMT1
CDS_27000_Unigene_4196_Transcript_7012	2.135499521	XP_010255900.1: basic 7S globulin 2-like
CDS_27026_Unigene_42006_Transcript_73608	2.135430478	PIA35168.1 protein AQUCO_03600074v1
CDS_21277_Unigene_34542_Transcript_60072	2.135281299	XP_034706755.1protein SEMI-ROLLED LEAF 2 isoform X3
CDS_39856_Unigene_62367_Transcript_110407	2.133011877	RVW34556.1Binding partner of ACD11 1
CDS_33625_Unigene_51466_Transcript_90663	2.131074072	No Blast Hit
CDS_8725_Unigene_1985_Transcript_3313	2.129838006	PIA38093.1 protein AQUCO_02800023v1

Transcript ID	Log2 Fold Change	Hit desc.
CDS_32974_Unigene_5048_Transcript_8418	2.127190638	RWR95270.1Alpha/beta hydrolase fold-1
CDS_10304_Unigene_21665_Transcript_37405	2.12659733	RWR95947.1kinesin-like protein KIN-7K, chloroplastic isoform X2
CDS_24250_Unigene_38364_Transcript_66848	2.126387992	KAF2310655.1 protein GH714_016093
CDS_2322_Unigene_125_Transcript_195	2.126079163	PIN21491.1 protein CDL12_05795
CDS_35016_Unigene_53685_Transcript_94735	2.124640639	No Blast Hit
CDS_23403_Unigene_37235_Transcript_64905	2.124126095	PSR91212.1Transmembrane ascorbate ferrireductase
CDS_20447_Unigene_3356_Transcript_5521	2.123296722	KCW50407.1 protein EUGRSUZ_J00155, partial
CDS_26563_Unigene_41423_Transcript_72509	2.121113714	THU47312.1 protein C4D60_Mb09t14170
CDS_30573_Unigene_46909_Transcript_82555	2.119902144	PIA47352.1 protein AQUCO_01400195v1
CDS_25095_Unigene_39456_Transcript_68851	2.119392267	PKI42370.1 protein CRG98_037248
CDS_14270_Unigene_26277_Transcript_45467	2.119075226	XP_004508765.1protein IQ-DOMAIN 31 isoform X2
CDS_44280_Unigene_7215_Transcript_12069	2.118157083	XP_017254707.1: AAA-ATPase At3g28580-like
CDS_40270_Unigene_63160_Transcript_111864	2.116935222	No Blast Hit
CDS_41323_Unigene_65254_Transcript_115692	2.116189835	XP_011007843.1: uncharacterized protein LOC105113384
CDS_22930_Unigene_36576_Transcript_63778	2.115477217	QHO09972.1Filament-like plant protein
CDS_38222_Unigene_59282_Transcript_104852	2.115405282	RWR77603.1putative LRR receptor-like serine/threonine-protein kinase
CDS_5919_Unigene_16651_Transcript_28591	2.11518131	RWR77442.1papilin-like protein isoform X1
CDS_19671_Unigene_32645_Transcript_56730	2.11262322	THU48350.1 protein C4D60_Mb09t25300
CDS_50918_Unigene_93189_Transcript_196581	2.11233751	XP_027112574.1uncharacterized protein LOC113731480
CDS_6501_Unigene_1729_Transcript_2878	2.111576553	ADX97326.1actin 9
CDS_33433_Unigene_51106_Transcript_90001	2.110240569	OAO97186.1 protein AXX17_AT4G40530
CDS_21991_Unigene_35447_Transcript_61673	2.109630421	XP_010270661.1: UDP-galactose transporter 2-like
CDS_32964_Unigene_5047_Transcript_8417	2.1076151	XP_024465330.1uncharacterized protein LOC112328798
CDS_28595_Unigene_44105_Transcript_77466	2.106987067	ADA70357.1proliferation cell nuclear antigen
CDS_7365_Unigene_18263_Transcript_31459	2.106136171	PIN00981.1dTDP-glucose 4-6-dehydratase/UDP-glucuronic acid decarboxylase
CDS_18978_Unigene_31795_Transcript_55206	2.105463429	XP_010259397.1: dnaJ homolog subfamily B member 3 isoform X1
CDS_42868_Unigene_68785_Transcript_122235	2.105463429	XP_019054783.1: protein DETOXIFICATION 21-like
CDS_19796_Unigene_32820_Transcript_56987	2.103667915	QCX36374.1KOMT1

Transcript ID	Log2 Fold Change	Hit desc.
CDS_47642_Unigene_81636_Transcript_147920	2.103667915	XP_011032644.1: protein TIFY 4A-like isoform X2
CDS_17040_Unigene_29544_Transcript_51192	2.10315871	OUZ99852.1Glycosyl hydrolases 36
CDS_31149_Unigene_47773_Transcript_84080	2.102946459	OVA01577.1Aldo/keto reductase
CDS_24220_Unigene_38325_Transcript_66767	2.102146887	No Blast Hit
CDS_13281_Unigene_2512_Transcript_4167	2.099821938	XP_020579615.1actin
CDS_5712_Unigene_1641_Transcript_2759	2.098786201	RWR89660.1pectin acetylesterase 8-like protein
CDS_24728_Unigene_38982_Transcript_67993	2.098718699	XP_034224503.1uncharacterized protein LOC117634479
CDS_2355_Unigene_12635_Transcript_21324	2.098195428	No Blast Hit
CDS_6499_Unigene_17298_Transcript_29757	2.095666941	XP_010915357.1NADP-dependent malic enzyme isoform X1
CDS_22747_Unigene_36353_Transcript_63341	2.095065949	RWR86419.1RNA recognition motif domain-containing protein
CDS_51243_Unigene_946_Transcript_1601	2.088800435	XP_010906541.1oryzain alpha chain
CDS_36017_Unigene_55354_Transcript_97705	2.087838022	XP_018846687.1: cytochrome P450 82C4-like
CDS_38207_Unigene_59255_Transcript_104793	2.087223916	XP_010260769.1: organic cation/carnitine transporter 3-like
CDS_594_Unigene_1066_Transcript_1822	2.087150997	RWR76367.1Pectinesterase domain-containing protein/PMEI domain-containing protein
CDS_4245_Unigene_14739_Transcript_25111	2.086182911	Q9FSB7.1RecName: Full=Chalcone synthase 3; AltName: Full=Naringenin-chalcone synthase 3
CDS_38325_Unigene_59467_Transcript_105178	2.086108496	OVA12692.1Methyltransferase FkbM
CDS_180_Unigene_10197_Transcript_17048	2.083942839	XP_010259661.1: glutathione S-transferase F13
CDS_25074_Unigene_39429_Transcript_68801	2.083768358	XP_010268078.1: galacturonosyltransferase-like 7
CDS_36718_Unigene_56511_Transcript_99885	2.083768358	PRQ35660.1 protein RchiOBHm_Chr5g0082391
CDS_9919_Unigene_21213_Transcript_36589	2.08242444	XP_010263050.1: protein IQ-DOMAIN 1 isoform X1
CDS_20604_Unigene_33746_Transcript_58620	2.079159104	XP_002537933.1dirigent protein 22
CDS_34300_Unigene_52517_Transcript_92545	2.07774457	XP_008797454.1bZIP transcription factor 53-like
CDS_4076_Unigene_14546_Transcript_24784	2.077165623	No Blast Hit
CDS_33455_Unigene_51145_Transcript_90079	2.076678933	XP_011628522.1beta-fructofuranosidase, insoluble isoenzyme CWINV1 isoform X2
CDS_30433_Unigene_46688_Transcript_82173	2.075256858	RWR92117.1Cytochrome P450
CDS_35139_Unigene_53882_Transcript_95084	2.070221826	XP_010088559.1aldehyde oxidase GLOX

Transcript ID	Log2 Fold Change	Hit desc.
CDS_22368_Unigene_35882_Transcript_62477	2.069484132	XP_010916428.1ribonucleoside-diphosphate reductase large subunit isoform X2
CDS_36239_Unigene_55723_Transcript_98380	2.066490366	No Blast Hit
CDS_36422_Unigene_55_Transcript_91	2.066490366	AGV54733.1dehydration-responsive protein RD22-like protein
CDS_12184_Unigene_23859_Transcript_41229	2.064659535	PQP92725.1myosin-11
CDS_3389_Unigene_13789_Transcript_23419	2.064507846	XP_010937250.1alanine aminotransferase 2 isoform X1
CDS_19793_Unigene_32818_Transcript_56983	2.060199887	QCX36374.1KOMT1
CDS_13948_Unigene_25901_Transcript_44785	2.052836498	XP_034679679.1protein RICE SALT SENSITIVE 3-like
CDS_21276_Unigene_34541_Transcript_60071	2.04900294	KAF3954206.1 protein CMV_020420
CDS_19603_Unigene_32570_Transcript_56586	2.048492883	XP_002277157.1: protein TIFY 10A
CDS_814_Unigene_10896_Transcript_18298	2.047967636	XP_010246318.1: NADH dehydrogenase
CDS_2140_Unigene_12398_Transcript_20933	2.047027216	XP_021611554.1UDP-arabinopyranose mutase 3-like
CDS_24742_Unigene_38999_Transcript_68012	2.046615359	PON88830.1Alpha/beta hydrolase fold
CDS_21773_Unigene_35163_Transcript_61157	2.046293652	No Blast Hit
CDS_24746_Unigene_39000_Transcript_68014	2.04529421	XP_010275723.1: protein ABHD17B-like
CDS_16488_Unigene_28888_Transcript_49988	2.04396735	PWA40096.1Concanavalin A-like lectin/glucanase, subgroup
CDS_31170_Unigene_47816_Transcript_84158	2.039374238	XP_010255052.1: uncharacterized protein LOC104595834
CDS_18777_Unigene_31566_Transcript_54808	2.03581056	RWR76563.1putative calcium-binding protein CML25
CDS_2478_Unigene_12762_Transcript_21574	2.035794574	RWR79810.1voltage-dependent T-type calcium channel subunit alpha-1G-like protein
CDS_22570_Unigene_36142_Transcript_62941	2.032980248	XP_021631725.1desumoylating isopeptidase 1
CDS_21906_Unigene_35327_Transcript_61453	2.031592893	RWR73284.1putative glucuronoxylan glucuronosyltransferase IRX7
CDS_31659_Unigene_48507_Transcript_85434	2.031300938	XP_009404204.2: UPF0481 protein At3g47200-like
CDS_36285_Unigene_55797_Transcript_98511	2.030526336	KVI03138.1Phloem protein 2-like protein
CDS_22983_Unigene_36653_Transcript_63909	2.030187317	XP_031476820.1calmodulin-like protein 3
CDS_32664_Unigene_50051_Transcript_88165	2.029320574	XP_031286259.1putative disease resistance protein RGA1
CDS_19034_Unigene_31866_Transcript_55347	2.027500138	XP_010679988.1: protein TAPETUM DETERMINANT 1
CDS_19948_Unigene_3299_Transcript_5437	2.024437465	RWR79133.1beta-galactosidase 3-like protein
CDS_24545_Unigene_38754_Transcript_67564	2.022367813	RWR85235.1transcription repressor OFP6-like protein

Transcript ID	Log2 Fold Change	Hit desc.
CDS_3737_Unigene_14154_Transcript_24052	2.018180016	XP_007031572.1: uncharacterized protein LOC18600830
CDS_42404_Unigene_67744_Transcript_120247	2.016654162	No Blast Hit
CDS_42059_Unigene_66963_Transcript_118855	2.015381383	PIA25246.1 protein AQUCO_12100003v1
CDS_8990_Unigene_20152_Transcript_34737	2.013747017	XP_008812548.1stem-specific protein TSJT1
CDS_36633_Unigene_56364_Transcript_99601	2.01337903	No Blast Hit
CDS_45395_Unigene_74927_Transcript_134195	2.01337903	AZM69444.1tyrosine decarboxylase
CDS_22503_Unigene_36057_Transcript_62786	2.012471389	RWR88850.1DJ-1 protein E isoform X1
CDS_19670_Unigene_32643_Transcript_56726	2.011713421	XP_010250299.1: aminotransferase TAT2 isoform X1
CDS_15874_Unigene_28170_Transcript_48720	2.009462799	AZL93827.1flotillin
CDS_41920_Unigene_66670_Transcript_118296	2.007757611	XP_030467795.1GDSL esterase/lipase At5g45960-like
CDS_22060_Unigene_3552_Transcript_5844	2.004606701	No Blast Hit
CDS_21772_Unigene_35162_Transcript_61156	2.001306198	PIA51820.1 protein AQUCO_01000001v1
CDS_39262_Unigene_61231_Transcript_108405	2.000439974	XP_030492067.1cysteine synthase
CDS_6094_Unigene_16838_Transcript_28920	2.000224717	XP_015895871.1heavy metal-associated isoprenylated plant protein 37
CDS_21104_Unigene_34330_Transcript_59705	1.999499441	No Blast Hit
CDS_11204_Unigene_22732_Transcript_39268	1.996856178	XP_026398549.1protein DMR6-LIKE OXYGENASE 2-like
CDS_19605_Unigene_32572_Transcript_56589	1.995481825	KAA8523349.1 protein F0562_009772
CDS_39651_Unigene_61966_Transcript_109713	1.995231683	RWR81748.1Auxin-induced protein
CDS_46515_Unigene_7804_Transcript_13024	1.994425783	No Blast Hit
CDS_24569_Unigene_38788_Transcript_67617	1.993570549	TEY15514.1 protein Saspl_051945
CDS_36515_Unigene_56186_Transcript_99244	1.990658953	No Blast Hit
CDS_5093_Unigene_15725_Transcript_26904	1.990658953	THU48181.1 protein C4D60_Mb09t23530
CDS_9884_Unigene_21170_Transcript_36521	1.990281729	BAF02251.1 protein, partial
CDS_19606_Unigene_32573_Transcript_56590	1.990053923	RWR79480.1protein TIFY 10A
CDS_29303_Unigene_45092_Transcript_79241	1.989131484	XP_019053538.1: LOW QUALITY PROTEIN: small heat shock protein, chloroplastic
CDS_3398_Unigene_13797_Transcript_23434	1.988560051	RWR77171.1Pollen Ole e 1 allergen/extensin
CDS_16842_Unigene_29315_Transcript_50778	1.988291269	XP_020087292.1cysteine proteinase inhibitor 12-like
CDS_9026_Unigene_20193_Transcript_34790	1.986280513	ACJ38671.1farnesyl pyrophosphate synthase
CDS_4961_Unigene_1557_Transcript_2616	1.983964301	RWR88056.1putative disease resistance protein isoform X1
CDS_25469_Unigene_39949_Transcript_69781	1.981198624	XP_021641695.1pathogen-related protein-like
CDS_13642_Unigene_2555_Transcript_4231	1.981056954	RWR95105.1protein ASPARTIC PROTEASE IN GUARD CELL 2-like protein

Transcript ID	Log2 Fold Change	Hit desc.
CDS_13246_Unigene_25092_Transcript_43414	1.979806619	XP_026422045.1uncharacterized protein LOC113318135
CDS_19026_Unigene_31856_Transcript_55334	1.979237774	XP_009400004.1: alanine--glyoxylate aminotransferase 2 homolog 3, mitochondrial
CDS_13979_Unigene_25938_Transcript_44855	1.977538032	XP_010646816.1: non-specific lipid-transfer protein AKCS9
CDS_3937_Unigene_14384_Transcript_24460	1.977220579	XP_027357671.1beta-glucosidase 44-like isoform X2
CDS_50708_Unigene_92230_Transcript_190874	1.975062098	KHN30150.1Zinc transporter 1
CDS_30432_Unigene_46687_Transcript_82169	1.974317215	RWR73790.1Protein kinase domain-containing protein
CDS_20006_Unigene_33061_Transcript_57418	1.973449008	RWR77005.1fasciclin-like arabinogalactan protein 1
CDS_26852_Unigene_41788_Transcript_73161	1.972737045	XP_034681902.17-methylxanthosine synthase 1-like
CDS_42995_Unigene_6906_Transcript_11554	1.972347075	RWR77698.1tRNA-splicing ligase RtcB
CDS_12601_Unigene_2435_Transcript_4034	1.971858616	RWR93851.1putative leucine-rich repeat receptor-like protein kinase
CDS_31677_Unigene_48529_Transcript_85462	1.970267164	RVX20629.1Heat stress transcription factor A-6b
CDS_30867_Unigene_47351_Transcript_83349	1.970111576	KAA8519824.1 protein F0562_014086
CDS_27974_Unigene_43298_Transcript_75998	1.967920029	XP_008812183.1GDSL esterase/lipase At1g31550-like
CDS_5220_Unigene_15875_Transcript_27146	1.96757534	OAY81337.1putative methyltransferase PMT21
CDS_5248_Unigene_15903_Transcript_27198	1.967192781	XP_010275836.1: transmembrane 9 superfamily member 8-like
CDS_27045_Unigene_42038_Transcript_73675	1.965309524	RWR81170.1putative BOI-related E3 ubiquitin-protein ligase 3
CDS_12038_Unigene_23684_Transcript_40927	1.964890962	OVA18734.1Alpha/beta hydrolase fold-1
CDS_6324_Unigene_17099_Transcript_29402	1.964780321	BAH94319.1Os08g0427700
CDS_26091_Unigene_40764_Transcript_71278	1.964410763	XP_010259373.1: uncharacterized protein LOC104598834
CDS_31800_Unigene_48733_Transcript_85818	1.961927235	XP_034912327.1uncharacterized protein LOC118047209
CDS_694_Unigene_10782_Transcript_18092	1.961777833	XP_010277896.1: uncharacterized protein LOC104612242
CDS_38855_Unigene_60401_Transcript_106884	1.961149071	XP_010940972.1myeloid leukemia factor 1 isoform X2
CDS_3287_Unigene_13675_Transcript_23208	1.960458716	RWR95129.1germin-like protein 2 precursor
CDS_43580_Unigene_7041_Transcript_11790	1.95967801	RWR84153.1putative membrane-associated kinase regulator 1 -like protein
CDS_27475_Unigene_42628_Transcript_74772	1.958237476	KAA8527686.1 protein F0562_035445
CDS_42810_Unigene_68645_Transcript_121949	1.958237476	EPS62678.1 protein M569_12114, partial

Transcript ID	Log2 Fold Change	Hit desc.
CDS_1709_Unigene_11921_Transcript_20062	1.956603928	XP_004303483.1: 17.9 kDa class II heat shock protein-like
CDS_4318_Unigene_14826_Transcript_25263	1.954391019	XP_008787716.14-coumarate--CoA ligase-like 5 isoform X3
CDS_28805_Unigene_44385_Transcript_77965	1.953707817	XP_010249361.1: DNA replication licensing factor MCM2
CDS_43741_Unigene_7085_Transcript_11858	1.95337172	KDO45654.1 protein CISIN_1g0152451mg, partial
CDS_50139_Unigene_9008_Transcript_15018	1.953290145	OVA13148.1Myc-type
CDS_25422_Unigene_39883_Transcript_69657	1.95298175	RWR96949.1zinc finger protein
CDS_46032_Unigene_7660_Transcript_12788	1.951318062	RWR72366.1glucan endo-1,3-beta-D-glucosidase
CDS_39977_Unigene_62583_Transcript_110827	1.947266358	KAF3963937.1 protein CMV_011725
CDS_21502_Unigene_34813_Transcript_60529	1.946848507	RWR91480.1GDP-fucose protein O-fucosyltransferase
CDS_31053_Unigene_47614_Transcript_83797	1.946444262	RWR74472.1omega-hydroxypalmitate O-feruloyl transferase-like protein
CDS_6503_Unigene_17300_Transcript_29759	1.945114818	XP_010915364.1NADP-dependent malic enzyme isoform X2
CDS_11176_Unigene_22703_Transcript_39224	1.942204492	RWR84861.1heavy metal-associated isoprenylated plant protein 47-like protein
CDS_27694_Unigene_42914_Transcript_75292	1.941028186	No Blast Hit
CDS_32093_Unigene_49185_Transcript_86673	1.940241046	No Blast Hit
CDS_37323_Unigene_57597_Transcript_101795	1.939378448	XP_020252575.1histone H2B.11-like
CDS_5095_Unigene_15727_Transcript_26909	1.938570442	PON47775.1Caleosin-related
CDS_18476_Unigene_31205_Transcript_54122	1.937917491	RWR81826.1tyrosine/DOPA decarboxylase 2-like protein
CDS_14633_Unigene_26723_Transcript_46231	1.937018046	No Blast Hit
CDS_44508_Unigene_72726_Transcript_129963	1.936426642	MQL76106.1 protein
CDS_19024_Unigene_31854_Transcript_55331	1.936352534	XP_009400004.1: alanine--glyoxylate aminotransferase 2 homolog 3, mitochondrial
CDS_11020_Unigene_22518_Transcript_38868	1.936211169	XP_028079312.1rRNA-processing protein FCF1 homolog
CDS_14703_Unigene_26800_Transcript_46352	1.935445611	RWR78560.1putative polyamine oxidase 4 isoform X1
CDS_4077_Unigene_14547_Transcript_24785	1.935445611	No Blast Hit
CDS_32962_Unigene_50471_Transcript_88892	1.933545271	OVA14062.1C2 calcium-dependent membrane targeting
CDS_14268_Unigene_26275_Transcript_45464	1.933351515	PSR95827.1Protein IQ-DOMAIN like
CDS_22285_Unigene_35791_Transcript_62338	1.93296551	AAA33376.1NADPH thioredoxin reductase, partial
CDS_10652_Unigene_22076_Transcript_38099	1.931447175	RWR96872.1EEIG1/EHBP1 N-terminal domain-containing protein

Transcript ID	Log2 Fold Change	Hit desc.
CDS_13934_Unigene_25889_Transcript_44766	1.931205646	XP_031262629.1 aquaporin TIP2-2
CDS_21004_Unigene_34210_Transcript_59493	1.930445324	TKY66942.1Xyloglucan endotransglucosylase/hydrolase protein 9
CDS_3391_Unigene_13790_Transcript_23420	1.928067996	XP_010937250.1alanine aminotransferase 2 isoform X1
CDS_34801_Unigene_53358_Transcript_94166	1.927649156	XP_015873986.1zinc transporter 2
CDS_31099_Unigene_47694_Transcript_83921	1.926667397	No Blast Hit
CDS_14267_Unigene_26274_Transcript_45461	1.923611132	XP_004508765.1protein IQ-DOMAIN 31 isoform X2
CDS_30404_Unigene_46655_Transcript_82105	1.922743416	XP_010047178.1: uncharacterized protein LOC104436145
CDS_14704_Unigene_26801_Transcript_46353	1.921880675	RWR78560.1putative polyamine oxidase 4 isoform X1
CDS_35122_Unigene_53840_Transcript_95000	1.920048506	XP_010259986.1: uncharacterized protein LOC104599235
CDS_9886_Unigene_21172_Transcript_36523	1.919899656	OVA08740.1Calreticulin/calnexin
CDS_26691_Unigene_41573_Transcript_72776	1.91938154	XP_010681851.1: serine/threonine-protein kinase D6PK
CDS_33128_Unigene_50684_Transcript_89254	1.919137656	XP_012069727.1calmodulin-like protein 11
CDS_2985_Unigene_13326_Transcript_22556	1.918883973	XP_008798468.1uncharacterized protein LOC103713352
CDS_20799_Unigene_33998_Transcript_59099	1.916593967	XP_018730850.1: uncharacterized protein LOC108960255
CDS_44628_Unigene_7299_Transcript_12220	1.915205149	OVA17962.1Major intrinsic protein
CDS_29078_Unigene_44781_Transcript_78705	1.914685806	XP_018855829.1: wall-associated receptor kinase 2-like, partial
CDS_181_Unigene_10198_Transcript_17049	1.914391517	XP_010259661.1: glutathione S-transferase F13
CDS_45492_Unigene_7518_Transcript_12566	1.913749817	XP_011101528.1histone H2B-like
CDS_50318_Unigene_9086_Transcript_15160	1.912982714	XP_020686972.1protein FORGETTER 1 isoform X1
CDS_35595_Unigene_54651_Transcript_96439	1.911973369	RWR94607.1COBRA-like protein 7
CDS_32975_Unigene_50490_Transcript_88918	1.910081437	XP_010243735.1: arogenate dehydratase/prephenate dehydratase 6, chloroplastic-like
CDS_25424_Unigene_39885_Transcript_69659	1.909438177	RWR96949.1zinc finger protein
CDS_33230_Unigene_50818_Transcript_89487	1.908591457	RWR89162.1putative galacturonosyltransferase 15
CDS_6744_Unigene_17572_Transcript_30240	1.906747868	No Blast Hit
CDS_40619_Unigene_63824_Transcript_113066	1.905831542	No Blast Hit
CDS_18816_Unigene_31601_Transcript_54856	1.9056667	RWR75305.1VIN3-like protein 2 isoform X1
CDS_13832_Unigene_25777_Transcript_44585	1.904798217	XP_010263865.1: squalene synthase-like

Transcript ID	Log2 Fold Change	Hit desc.
CDS_23818_Unigene_37781_Transcript_65832	1.902568469	RWR81512.1Pleckstrin domain-containing protein
CDS_9749_Unigene_21017_Transcript_36252	1.901653947	XP_010258671.1: protein S-acyltransferase 22
CDS_7863_Unigene_18873_Transcript_32499	1.901438335	CDY38055.1BnaCnng09160D
CDS_20838_Unigene_34035_Transcript_59165	1.900904301	PKI64591.1 protein CRG98_015023, partial
CDS_42030_Unigene_66907_Transcript_118741	1.900416821	OMO69632.1Plastocyanin-like protein
CDS_3936_Unigene_14383_Transcript_24459	1.900309792	XP_027357671.1beta-glucosidase 44-like isoform X2
CDS_30998_Unigene_47540_Transcript_83656	1.897355233	PSS21510.1Trehalose-phosphate phosphatase
CDS_15208_Unigene_27390_Transcript_47364	1.897048114	XP_010266123.1: uncharacterized protein LOC104603726
CDS_19446_Unigene_32362_Transcript_56205	1.896836931	XP_030943481.1uncharacterized protein LOC115968278 isoform X1
CDS_41201_Unigene_649_Transcript_1075	1.895984747	CDP14664.1unnamed protein product
CDS_42576_Unigene_68129_Transcript_120963	1.893814876	XP_010256147.1: leucine-rich repeat extensin-like protein 6
CDS_20043_Unigene_33105_Transcript_57490	1.892469705	XP_010248147.1: polygalacturonase At1g48100-like, partial
CDS_28272_Unigene_43706_Transcript_76737	1.89112328	No Blast Hit
CDS_20123_Unigene_33193_Transcript_57657	1.889265334	KAF3775866.1HVA22 protein
CDS_30434_Unigene_46689_Transcript_82174	1.889039965	RWR92117.1Cytochrome P450
CDS_3940_Unigene_14387_Transcript_24469	1.887997179	RWR88705.1CASP-like protein 1B2
CDS_44704_Unigene_73156_Transcript_130743	1.886272068	XP_022854780.1NADH dehydrogenase
CDS_34628_Unigene_53062_Transcript_93614	1.881275494	PWZ34714.1Receptor protein kinase-like protein ZAR1
CDS_41088_Unigene_64805_Transcript_114909	1.880234964	RWR97072.1Glycosyl transferase
CDS_7686_Unigene_18642_Transcript_32126	1.878890757	XP_031273992.1mannose-1-phosphate guanylyltransferase 1 isoform X1
CDS_16271_Unigene_28636_Transcript_49530	1.87731748	KAF5206652.1Alpha-galactosidase
CDS_48499_Unigene_84370_Transcript_154746	1.87731748	KAF3974579.1 protein CMV_002109
CDS_47807_Unigene_8213_Transcript_13664	1.874773792	RWR84745.1putative methyltransferase PMT26
CDS_48249_Unigene_83526_Transcript_152659	1.873441002	KAA8532160.1 protein F0562_006698
CDS_2486_Unigene_12771_Transcript_21587	1.872674463	XP_031398942.1 galactinol--sucrose galactosyltransferase 2
CDS_33194_Unigene_50778_Transcript_89425	1.871808136	KAF3779285.1 protein EJ110_NYTH32161
CDS_34086_Unigene_52161_Transcript_91851	1.869368727	TXG60082.1 protein EZV62_014655
CDS_41585_Unigene_6591_Transcript_11015	1.868550989	No Blast Hit
CDS_20853_Unigene_34055_Transcript_59213	1.868039667	KAA8540495.1 protein F0562_024586
CDS_41695_Unigene_66166_Transcript_117384	1.868039667	No Blast Hit

Transcript ID	Log2 Fold Change	Hit desc.
CDS_21931_Unigene_35361_Transcript_61517	1.865847953	OAY78543.1Pyrophosphate-energized vacuolar membrane proton pump
CDS_31001_Unigene_47543_Transcript_83663	1.864933756	QCX36375.1KOMT2
CDS_4871_Unigene_15471_Transcript_26457	1.862872803	RWR72786.1kinesin-like protein KIN-14E isoform X1
CDS_32983_Unigene_5049_Transcript_8419	1.860749631	PIA44332.1 protein AQUCO_01700139v1
CDS_44507_Unigene_72725_Transcript_129962	1.859419739	XP_009405296.2: fatty acyl-CoA reductase 3-like isoform X1
CDS_8005_Unigene_19028_Transcript_32738	1.855740402	RWW45347.1 protein BHE74_00048823
CDS_22284_Unigene_35790_Transcript_62337	1.854010107	XP_002263864.2: thioredoxin reductase NTRB
CDS_19678_Unigene_32652_Transcript_56739	1.853805773	AFN61200.1squalene epoxidase
CDS_7263_Unigene_18147_Transcript_31218	1.853648574	BAK06763.1 protein
CDS_34677_Unigene_53142_Transcript_93751	1.852442812	XP_010939383.1ethylene-responsive transcription factor ERF014
CDS_3402_Unigene_137_Transcript_211	1.847955421	XP_033514312.1amino acid transporter AVT1A-like isoform X7
CDS_26978_Unigene_4193_Transcript_7006	1.845971243	PIA39195.1 protein AQUCO_02700404v1
CDS_22161_Unigene_35641_Transcript_62046	1.84560862	CBI35818.3unnamed protein product, partial
CDS_12474_Unigene_24207_Transcript_41837	1.845456381	XP_017699565.1uncharacterized protein LOC108511488
CDS_24508_Unigene_38697_Transcript_67431	1.845068256	OVA08339.1Peptidase S8/S53 domain
CDS_50952_Unigene_93252_Transcript_196807	1.843884916	RWR92170.1gamma-interferon-inducible lysosomal thiol reductase
CDS_2489_Unigene_12774_Transcript_21595	1.843540726	RWR73773.1Glycosyl hydrolases 36
CDS_31531_Unigene_48318_Transcript_85082	1.84322859	PON38590.1HAD hydrolase, subfamily IA
CDS_50138_Unigene_9007_Transcript_15017	1.842593386	OVA13148.1Myc-type
CDS_11196_Unigene_22725_Transcript_39261	1.842147258	XP_010255099.1: protein DMR6-LIKE OXYGENASE 1-like
CDS_41250_Unigene_65116_Transcript_115443	1.84169357	RWR74798.1heat stress transcription factor B-4b-like protein
CDS_34221_Unigene_52386_Transcript_92291	1.841198054	APA20232.1NADH/NADPH oxidoreductase
CDS_43565_Unigene_70366_Transcript_125326	1.841198054	No Blast Hit
CDS_33428_Unigene_51100_Transcript_89986	1.840099277	No Blast Hit
CDS_10653_Unigene_22077_Transcript_38102	1.83886057	RWR96872.1EEIG1/EHBP1 N-terminal domain-containing protein
CDS_13669_Unigene_25599_Transcript_44290	1.838843332	XP_034672846.1cytochrome P450 71A25-like
CDS_50105_Unigene_8998_Transcript_15004	1.83770703	No Blast Hit
CDS_28596_Unigene_44106_Transcript_77468	1.83760777	ADA70357.1proliferation cell nuclear antigen
CDS_47802_Unigene_8212_Transcript_13663	1.836293426	RWR84745.1putative methyltransferase PMT26

Transcript ID	Log2 Fold Change	Hit desc.
CDS_25425_Unigene_39886_Transcript_69661	1.835089245	RWR96949.1zinc finger protein
CDS_3290_Unigene_13678_Transcript_23211	1.833047213	RWR95129.1germin-like protein 2 precursor
CDS_22160_Unigene_35640_Transcript_62045	1.832463244	KAA8540212.1 protein F0562_024225
CDS_11805_Unigene_23406_Transcript_40444	1.832005064	XP_010249387.1: heparan-alpha-glucosaminide N-acetyltransferase
CDS_11203_Unigene_22731_Transcript_39267	1.831932158	XP_020092748.1protein DMR6-LIKE OXYGENASE 2
CDS_44004_Unigene_71495_Transcript_127502	1.830649421	OMO73551.1 protein CCACVL1_17225
CDS_30423_Unigene_46679_Transcript_82153	1.828726743	XP_022776304.1receptor protein kinase-like protein ZAR1
CDS_33195_Unigene_50779_Transcript_89426	1.828726743	XP_034692977.1uncharacterized protein LOC117919825
CDS_16319_Unigene_28695_Transcript_49628	1.82695439	RWR87194.1Calponin domain-containing protein
CDS_35469_Unigene_54419_Transcript_96034	1.825643866	XP_016208114.1uncharacterized protein LOC107648813 isoform X2
CDS_5315_Unigene_15985_Transcript_27338	1.825437118	PON97075.1Alcohol dehydrogenase superfamily, zinc-type
CDS_6500_Unigene_17299_Transcript_29758	1.823752143	XP_010915364.1NADP-dependent malic enzyme isoform X2
CDS_22369_Unigene_35883_Transcript_62478	1.823675227	XP_010916428.1ribonucleoside-diphosphate reductase large subunit isoform X2
CDS_11231_Unigene_22765_Transcript_39343	1.820733952	XP_027909364.1S-norcoclaurine synthase 2-like
CDS_16273_Unigene_28638_Transcript_49533	1.820733952	PKI63948.1 protein CRG98_015624, partial
CDS_3288_Unigene_13676_Transcript_23209	1.820733952	RWR95129.1germin-like protein 2 precursor
CDS_42120_Unigene_67087_Transcript_119069	1.820733952	No Blast Hit
CDS_44783_Unigene_73318_Transcript_131104	1.820733952	XP_010260192.1: MLP-like protein 423 isoform X1
CDS_19101_Unigene_31945_Transcript_55506	1.816775938	RWR84727.1putative carboxylesterase 17
CDS_21767_Unigene_35156_Transcript_61146	1.816288047	OVA02825.1protein of unknown function DUF221
CDS_48356_Unigene_83881_Transcript_153579	1.816288047	XP_010241075.1: uncharacterized protein C594.04c
CDS_18500_Unigene_31234_Transcript_54174	1.81563308	RWR80825.1protein IQ-DOMAIN 1-like protein
CDS_14047_Unigene_26019_Transcript_44982	1.815008964	PQQ09677.1alpha-xylosidase 1
CDS_19554_Unigene_32499_Transcript_56451	1.815008964	XP_010251385.1: ribonuclease 2-like
CDS_6095_Unigene_16839_Transcript_28921	1.814751794	XP_015895871.1heavy metal-associated isoprenylated plant protein 37
CDS_30628_Unigene_47003_Transcript_82726	1.813679194	XP_010262767.1: transcription factor bHLH30-like
CDS_17495_Unigene_30066_Transcript_52119	1.812346166	OVA01825.1Glutamine amidotransferase

Transcript ID	Log2 Fold Change	Hit desc.
CDS_39697_Unigene_62059_Transcript_109864	1.811688812	RWR93335.1pentatricopeptide repeat-containing protein, mitochondrial isoform X2
CDS_19061_Unigene_31894_Transcript_55414	1.811396087	OVA04557.1Histone deacetylase complex subunit SAP30/SAP30-like
CDS_41370_Unigene_6536_Transcript_10930	1.811396087	XP_018806620.1: purple acid phosphatase 17-like isoform X2
CDS_33129_Unigene_50685_Transcript_89255	1.811242503	XP_021899590.1calmodulin-like protein 8
CDS_2336_Unigene_12616_Transcript_21288	1.810241578	XP_010264172.1: protein EXORDIUM-like 3
CDS_26298_Unigene_41041_Transcript_71817	1.809299057	No Blast Hit
CDS_29138_Unigene_4485_Transcript_7499	1.809145978	RRT53093.1 protein B296_00021198, partial
CDS_17780_Unigene_303_Transcript_502	1.809067891	PSR94971.1Glyoxalase-like domain protein
CDS_40004_Unigene_62628_Transcript_110916	1.808133915	RVX16617.1putative LRR receptor-like serine/threonine-protein kinase
CDS_9119_Unigene_2029_Transcript_3405	1.805467195	ABK93986.1unknown
CDS_41962_Unigene_66754_Transcript_118464	1.80468072	XP_010268114.1: uncharacterized protein LOC104605175 isoform X1
CDS_11414_Unigene_22970_Transcript_39726	1.800302052	MQM13807.1 protein
CDS_19025_Unigene_31855_Transcript_55332	1.800081523	XP_010264475.1: alanine--glyoxylate aminotransferase 2 homolog 3, mitochondrial
CDS_44512_Unigene_72735_Transcript_129977	1.799314968	QCX36391.1RDCT42
CDS_20202_Unigene_33286_Transcript_57811	1.798998022	ADZ76155.1beta-tubulin
CDS_4803_Unigene_15398_Transcript_26311	1.798694704	XP_011458402.1: uncharacterized protein LOC105349702
CDS_50989_Unigene_93354_Transcript_197253	1.797147132	XP_030956557.1uncharacterized protein LOC115978787
CDS_49524_Unigene_87802_Transcript_165234	1.796486406	No Blast Hit
CDS_32839_Unigene_50311_Transcript_88614	1.794738743	XP_010254116.1: uncharacterized protein LOC104595195
CDS_19604_Unigene_32571_Transcript_56588	1.794016613	XP_002277157.1: protein TIFY 10A
CDS_17565_Unigene_30147_Transcript_52250	1.792586623	XP_008808992.2aromatic aminotransferase ISS1-like isoform X1
CDS_31054_Unigene_47615_Transcript_83798	1.79219109	RWR74472.1omega-hydroxypalmitate O-feruloyl transferase-like protein
CDS_21193_Unigene_34449_Transcript_59914	1.791587606	XP_015875080.1dolichyl-diphosphooligosaccharide--protein glycosyltransferase subunit DAD1
CDS_30885_Unigene_47374_Transcript_83386	1.791317464	GER44960.1GDP-mannose transporter
CDS_26950_Unigene_41910_Transcript_73407	1.789707056	XP_010265428.1: afadin- and alpha-actinin-binding protein isoform X1
CDS_854_Unigene_10942_Transcript_18378	1.789198378	VAI47462.1unnamed protein product
CDS_125_Unigene_10137_Transcript_16950	1.789025092	No Blast Hit

Transcript ID	Log2 Fold Change	Hit desc.
CDS_27039_Unigene_42027_Transcript_73659	1.788672743	XP_002520956.12-methyl-6-phytyl-1,4-hydroquinone methyltransferase, chloroplastic
CDS_4842_Unigene_15440_Transcript_26389	1.788425048	OVA11718.1Glycine cleavage system P-protein
CDS_8614_Unigene_19743_Transcript_34020	1.788312474	XP_011076610.1LOB domain-containing protein 15
CDS_8612_Unigene_19741_Transcript_34015	1.787567088	XP_021283467.1uncharacterized protein LOC110415978
CDS_8523_Unigene_19631_Transcript_33831	1.786539032	RWR89477.1putative serine/threonine-protein kinase
CDS_10303_Unigene_21664_Transcript_37404	1.785577506	RWR95947.1kinesin-like protein KIN-7K, chloroplastic isoform X2
CDS_30830_Unigene_47290_Transcript_83246	1.785328616	RWR86042.1 protein CKAN_01492400
CDS_8984_Unigene_20146_Transcript_34726	1.781613936	PKA48341.1Cold-regulated 413 plasma membrane protein 2
CDS_29006_Unigene_44682_Transcript_78533	1.781444821	XP_002280537.1: BAG family molecular chaperone regulator 3
CDS_22639_Unigene_36236_Transcript_63115	1.780156372	KAE9608769.1putative protein kinase RLK-Pelle-LRR-VII-1 family
CDS_29007_Unigene_44683_Transcript_78534	1.778913776	RVW98443.1BAG family molecular chaperone regulator 3
CDS_33093_Unigene_50643_Transcript_89185	1.778913776	XP_006445237.1LOB domain-containing protein 18
CDS_4569_Unigene_1510_Transcript_2540	1.778142075	XP_010277445.1: sugar phosphate/phosphate translocator At1g12500
CDS_8424_Unigene_19514_Transcript_33596	1.777878473	RWR73666.1ent-kaurene oxidase
CDS_33790_Unigene_5169_Transcript_8640	1.777763913	XP_010249715.1: uncharacterized protein LOC104592187
CDS_42277_Unigene_67432_Transcript_119692	1.775865184	NP_001132837.1uncharacterized protein LOC100194327
CDS_26707_Unigene_41601_Transcript_72819	1.775393002	XP_028080768.1leucine-rich repeat extensin-like protein 4 isoform X1
CDS_4971_Unigene_1558_Transcript_2617	1.774686584	RWR88056.1putative disease resistance protein isoform X1
CDS_41383_Unigene_6540_Transcript_10934	1.773538784	XP_002533777.1purple acid phosphatase 17
CDS_37900_Unigene_58673_Transcript_103701	1.773428237	XP_018859030.1: uncharacterized protein LOC109020952
CDS_19104_Unigene_31948_Transcript_55513	1.773168269	XP_010251393.1: BTB/POZ and TAZ domain-containing protein 3-like
CDS_27353_Unigene_42466_Transcript_74451	1.772082091	RWR96431.1cellulose synthase-like protein G3
CDS_170_Unigene_10182_Transcript_17026	1.770351763	KAF5177896.1Hexosyltransferase
CDS_25598_Unigene_40111_Transcript_70082	1.769314971	XP_006422091.1plastidial pyruvate kinase 2
CDS_38808_Unigene_60325_Transcript_106756	1.76889502	No Blast Hit

Transcript ID	Log2 Fold Change	Hit desc.
CDS_4576_Unigene_15119_Transcript_25803	1.76889502	XP_020224994.1beta-galactosidase 1
CDS_3927_Unigene_14375_Transcript_24446	1.767139581	XP_027357671.1beta-glucosidase 44-like isoform X2
CDS_19767_Unigene_32776_Transcript_56929	1.76602806	XP_008797044.1uncharacterized protein LOC103712332
CDS_2936_Unigene_1325_Transcript_2271	1.765592398	No Blast Hit
CDS_74_Unigene_10084_Transcript_16866	1.764880717	XP_026663664.1L-arabinokinase-like isoform X2
CDS_2488_Unigene_12773_Transcript_21593	1.764514397	RWR73774.1Glycosyl hydrolases 36
CDS_9555_Unigene_207_Transcript_337	1.764489841	RWR84579.1protein canopy-1
CDS_21941_Unigene_3537_Transcript_5816	1.760775936	RWR84930.1EMP24_GP25L domain-containing protein/Cellulose_synt domain-containing protein
CDS_35161_Unigene_53917_Transcript_95139	1.760473427	RVW48888.1ABC transporter G family member 25
CDS_19558_Unigene_32504_Transcript_56460	1.760298098	BAT98047.1 protein VIGAN_09166000, partial
CDS_47037_Unigene_79718_Transcript_143934	1.759333407	ACO90256.1tyrosine/dopa decarboxylase-like protein
CDS_14269_Unigene_26276_Transcript_45465	1.75851364	XP_004508765.1protein IQ-DOMAIN 31 isoform X2
CDS_28136_Unigene_43537_Transcript_76436	1.757395603	ABR17957.1unknown
CDS_21741_Unigene_3512_Transcript_5777	1.756727339	XP_012085782.1biotin carboxyl carrier protein of acetyl-CoA carboxylase, chloroplastic isoform X2
CDS_25575_Unigene_40089_Transcript_70032	1.756603614	XP_010244077.1: uncharacterized protein LOC104587988
CDS_26191_Unigene_40883_Transcript_71507	1.756603614	PSR89455.1Protein SHOOT GRAVITROPISM like
CDS_39027_Unigene_60735_Transcript_107482	1.7561937	No Blast Hit
CDS_19651_Unigene_32619_Transcript_56663	1.756132068	XP_023900156.1ABC transporter G family member 5
CDS_35623_Unigene_54707_Transcript_96525	1.75514561	OVA15902.1Peptidase T2
CDS_187_Unigene_10202_Transcript_17059	1.755004633	XP_010259661.1: glutathione S-transferase F13
CDS_2397_Unigene_12685_Transcript_21424	1.754422791	PIN23985.1Cellulose synthase (UDP-forming)
CDS_16226_Unigene_28578_Transcript_49415	1.75430659	ABR26122.1s-adenosylmethionine synthetase 1, partial
CDS_9775_Unigene_21049_Transcript_36310	1.754062912	PON89603.1t-SNARE
CDS_10403_Unigene_2176_Transcript_3630	1.753679755	XP_015885047.1acyl-CoA-binding domain-containing protein 3-like
CDS_21405_Unigene_34699_Transcript_60328	1.753619756	PSR93544.1E3 ubiquitin-protein like
CDS_43155_Unigene_69399_Transcript_123440	1.752146867	QAX90949.1caffeic acid O-methyltransferase

Transcript ID	Log2 Fold Change	Hit desc.
CDS_424_Unigene_10482_Transcript_17532	1.751546369	XP_010253181.1: fasciclin-like arabinogalactan protein 4
CDS_27808_Unigene_43069_Transcript_75548	1.751193019	XP_026457377.1aquaporin SIP1-1-like
CDS_33523_Unigene_51279_Transcript_90317	1.750462873	XP_021685904.1dnaJ homolog subfamily B member 1-like
CDS_25864_Unigene_40473_Transcript_70710	1.750344624	KAF3553695.1 protein F2Q69_00015104
CDS_7134_Unigene_18003_Transcript_30936	1.75029254	XP_010276078.1: uncharacterized protein LOC104610918
CDS_36207_Unigene_55668_Transcript_98283	1.749767431	KAF5178292.1peptidase M50B-like protein
CDS_12751_Unigene_24529_Transcript_42410	1.749572923	RWR79030.1potassium transporter 2-like protein
CDS_41637_Unigene_66021_Transcript_117120	1.747977609	No Blast Hit
CDS_4398_Unigene_14928_Transcript_25468	1.747867841	XP_031277730.1glutathione S-transferase U17-like
CDS_21072_Unigene_34291_Transcript_59626	1.74673337	XP_016554971.1: uncharacterized protein LOC107854477
CDS_35925_Unigene_55196_Transcript_97418	1.746501146	XP_025816395.1bifunctional dTDP-4-dehydrorhamnose 3,5-epimerase/dTDP-4-dehydrorhamnose reductase
CDS_7051_Unigene_17921_Transcript_30800	1.746095151	OVA04007.1Protein of unknown function DUF761
CDS_2091_Unigene_12347_Transcript_20826	1.745019616	XP_010273571.1: beta-glucosidase 18-like
CDS_41364_Unigene_65357_Transcript_115879	1.744880197	RWR77760.1putative Group 2
CDS_29401_Unigene_45227_Transcript_79498	1.744281891	OVA18044.1Alpha carbonic anhydrase
CDS_5920_Unigene_16652_Transcript_28592	1.744171615	XP_010254314.1: papilin-like isoform X1
CDS_23779_Unigene_37721_Transcript_65746	1.743428226	XP_010241161.1: phosphatidylinositol/phosphatidylcholine transfer protein SFH1-like
CDS_35154_Unigene_53907_Transcript_95126	1.742585706	OMO99463.1Plant peroxidase
CDS_42936_Unigene_68954_Transcript_122557	1.742362888	RWR74770.1agmatine coumaroyltransferase-2-like protein
CDS_4982_Unigene_1559_Transcript_2620	1.741477645	RWR88077.1Disease resistance protein
CDS_13061_Unigene_24892_Transcript_43034	1.740748849	XP_034698120.1BTB/POZ domain-containing protein At1g30440
CDS_33781_Unigene_5168_Transcript_8636	1.740720837	XP_010249715.1: uncharacterized protein LOC104592187
CDS_23410_Unigene_37242_Transcript_64914	1.740391844	OVA20092.1TPM domain
CDS_2286_Unigene_12561_Transcript_21205	1.740046106	XP_012067633.1 methyltransferase PMT2 isoform X2
CDS_32396_Unigene_49689_Transcript_87516	1.739813956	GAU42334.1 protein TSUD_242310, partial
CDS_7022_Unigene_17890_Transcript_30748	1.738271792	RZS28733.1 protein BHM03_00062372
CDS_4587_Unigene_15129_Transcript_25821	1.737592717	No Blast Hit

Transcript ID	Log2 Fold Change	Hit desc.
CDS_34924_Unigene_53570_Transcript_94532	1.737210596	KAB5537340.1 protein DKX38_014873
CDS_24939_Unigene_39252_Transcript_68459	1.735845054	KAF2282959.1 protein GH714_043276
CDS_37192_Unigene_57368_Transcript_101372	1.735845054	No Blast Hit
CDS_18355_Unigene_31067_Transcript_53872	1.73400312	RWR84745.1putative methyltransferase PMT26
CDS_20664_Unigene_33818_Transcript_58734	1.73351154	RWR93292.1putative pectinesterase/pectinesterase inhibitor 34
CDS_32072_Unigene_49155_Transcript_86607	1.730131403	PSR94897.1Tyrosine decarboxylase, partial
CDS_32361_Unigene_49614_Transcript_87370	1.729811409	RWR79931.1Glycoside hydrolase
CDS_838_Unigene_10925_Transcript_18336	1.728328581	XP_034701907.1uncharacterized GPI-anchored protein At4g28100
CDS_16095_Unigene_28416_Transcript_49144	1.726234747	ESR47610.1 protein CICLE_v10001502mg
CDS_24789_Unigene_39061_Transcript_68114	1.725314387	XP_019710638.1transcription factor bHLH74 isoform X2
CDS_3933_Unigene_14380_Transcript_24456	1.7220427	XP_027357671.1beta-glucosidase 44-like isoform X2
CDS_34043_Unigene_52089_Transcript_91723	1.721198278	No Blast Hit
CDS_40370_Unigene_63318_Transcript_112141	1.721198278	No Blast Hit
CDS_41478_Unigene_65615_Transcript_116396	1.721198278	PNX84316.1copper-transporting ATPase ran1-like protein
CDS_41552_Unigene_65822_Transcript_116760	1.721198278	No Blast Hit
CDS_1692_Unigene_11902_Transcript_20035	1.719909582	RWR72447.1late embryogenisis abundant protein 6
CDS_35381_Unigene_54300_Transcript_95821	1.718920938	XP_009402731.2: cytochrome b561 and DOMON domain-containing protein At3g25290-like
CDS_11421_Unigene_22978_Transcript_39735	1.715123764	RWR77548.1protein REVERSION-TO-ETHYLENE SENSITIVITY1 isoform X2
CDS_42974_Unigene_69035_Transcript_122700	1.715123764	RWR91357.1histidine kinase 5 isoform X1
CDS_26323_Unigene_41084_Transcript_71894	1.713020135	KAF2307341.1 protein GH714_026474
CDS_6906_Unigene_17754_Transcript_30516	1.712674206	RWR75039.1protein ODORANT1-like protein
CDS_32026_Unigene_49086_Transcript_86482	1.7106445	No Blast Hit
CDS_45445_Unigene_75066_Transcript_134486	1.709572953	XP_023517351.1polygalacturonase inhibitor-like
CDS_43940_Unigene_71333_Transcript_127159	1.709516473	XP_010244646.1: uncharacterized protein LOC104588419
CDS_25073_Unigene_39428_Transcript_68800	1.70896799	NP_001130810.1uncharacterized protein LOC100191914 precursor
CDS_33574_Unigene_51385_Transcript_90514	1.70851076	RWW14482.1 protein GW17_00021743
CDS_43154_Unigene_69398_Transcript_123439	1.707925921	XP_010241050.1: caffeic acid 3-O-methyltransferase 1

Transcript ID	Log2 Fold Change	Hit desc.
CDS_35711_Unigene_5484_Transcript_9171	1.707785561	XP_015885099.1 xyloglucan glycosyltransferase 12
CDS_48355_Unigene_83880_Transcript_153578	1.70724872	RWR80878.13-oxo-5-alpha-steroid 4-dehydrogenase
CDS_21979_Unigene_35421_Transcript_61625	1.70613083	No Blast Hit
CDS_28669_Unigene_4418_Transcript_7394	1.704710156	RWR95277.1dTDP-glucose 4-6-dehydratase/UDP-glucuronic acid decarboxylase
CDS_23181_Unigene_36949_Transcript_64400	1.703496277	OVA11054.1 protein BVC80_1741g28
CDS_47388_Unigene_80818_Transcript_146230	1.703164355	XP_009414128.1: ATP synthase subunit b', chloroplastic
CDS_3392_Unigene_13791_Transcript_23421	1.703065188	XP_010937250.1alanine aminotransferase 2 isoform X1
CDS_26549_Unigene_41410_Transcript_72481	1.70267819	OVA01531.1GDP-fucose protein O-fucosyltransferase
CDS_13063_Unigene_24894_Transcript_43037	1.702269969	XP_034698120.1BTB/POZ domain-containing protein At1g30440
CDS_33121_Unigene_50674_Transcript_89237	1.702260482	GAV89181.1FMN_dh domain-containing protein
CDS_27569_Unigene_42755_Transcript_75012	1.701897722	XP_010252466.1: WRKY transcription factor 31
CDS_29729_Unigene_45667_Transcript_80291	1.700439718	XP_030962250.1glucomannan 4-beta-mannosyltransferase 9-like
CDS_8069_Unigene_19096_Transcript_32867	1.700439718	XP_010920174.1thaumatin-like protein 1b
CDS_32437_Unigene_49744_Transcript_87588	1.699568262	XP_027180539.1UPF0160 protein
CDS_19312_Unigene_32193_Transcript_55921	1.699104507	XP_010255453.1: tetraspanin-10 isoform X1
CDS_21029_Unigene_34242_Transcript_59549	1.699068009	RWR83677.1citrate-binding-like protein
CDS_37983_Unigene_58801_Transcript_103915	1.696251921	XP_010261744.1: peroxidase 11-like isoform X2
CDS_45855_Unigene_76177_Transcript_136696	1.69520307	XP_009393840.1: LOB domain-containing protein 37-like
CDS_41751_Unigene_66292_Transcript_117609	1.69274774	XP_002272243.1: aspartyl protease At4g16563
CDS_12137_Unigene_23804_Transcript_41127	1.691450935	KDO67597.1 protein CISIN_1g020960mg
CDS_12117_Unigene_23778_Transcript_41067	1.691196199	KAA8540670.1 protein F0562_024411
CDS_22469_Unigene_36011_Transcript_62717	1.690880136	No Blast Hit
CDS_21765_Unigene_35154_Transcript_61144	1.690402084	OVA02825.1protein of unknown function DUF221
CDS_36689_Unigene_56465_Transcript_99816	1.689489419	ONM16407.1putative E3 ubiquitin-protein ligase ARI8, partial
CDS_8113_Unigene_19145_Transcript_32943	1.689050843	OVA08620.1U box domain
CDS_40461_Unigene_6351_Transcript_10571	1.686994528	XP_031268216.1laccase-7-like
CDS_27289_Unigene_42389_Transcript_74300	1.68643286	PKI50953.1 protein CRG98_028683, partial

Transcript ID	Log2 Fold Change	Hit desc.
CDS_51121_Unigene_93851_Transcript_199676	1.685957273	PHT34232.1Esterase
CDS_42285_Unigene_67445_Transcript_119718	1.685704906	AAT37172.1caffeoyl-CoA-O-methyltransferase
CDS_18572_Unigene_31314_Transcript_54317	1.684160899	XP_002513994.1purine permease 3
CDS_3935_Unigene_14382_Transcript_24458	1.682709774	XP_027357671.1beta-glucosidase 44-like isoform X2
CDS_2509_Unigene_127_Transcript_197	1.682027681	XP_010278063.1: vacuolar amino acid transporter 1 isoform X1
CDS_423_Unigene_10481_Transcript_17531	1.680915855	XP_010253181.1: fasciclin-like arabinogalactan protein 4
CDS_30886_Unigene_47375_Transcript_83388	1.680556294	GER44960.1GDP-mannose transporter
CDS_37244_Unigene_57449_Transcript_101512	1.679743851	RWR96481.1 protein CKAN_02587000
CDS_14212_Unigene_26211_Transcript_45356	1.679619175	XP_024452631.1uncharacterized protein LOC7456088
CDS_41068_Unigene_6475_Transcript_10806	1.678129556	XP_009611930.1PLASMODESMATA CALLOSE-BINDING PROTEIN 5-like isoform X3
CDS_29663_Unigene_45580_Transcript_80128	1.677775998	XP_008373624.1FCS-Like Zinc finger 2
CDS_2487_Unigene_12772_Transcript_21590	1.677163213	XP_031398942.1 galactinol--sucrose galactosyltransferase 2
CDS_31936_Unigene_4892_Transcript_8158	1.67512863	XP_010278151.1: galacturonosyltransferase 6 isoform X1
CDS_15539_Unigene_27776_Transcript_48029	1.673303588	RWR89299.1 protein CKAN_01835000
CDS_30741_Unigene_47151_Transcript_83013	1.67193329	No Blast Hit
CDS_16096_Unigene_28417_Transcript_49145	1.670041262	XP_006434371.1alcohol dehydrogenase 1
CDS_2984_Unigene_13325_Transcript_22555	1.668730858	XP_008798468.1uncharacterized protein LOC103713352
CDS_23808_Unigene_37757_Transcript_65800	1.667639974	XP_022733100.1uncharacterized protein LOC111287117
CDS_34033_Unigene_52071_Transcript_91694	1.667173713	CBI33549.3unnamed protein product, partial
CDS_983_Unigene_11091_Transcript_18605	1.666071512	OVA02439.1HR-like lesion-inducer
CDS_45170_Unigene_74329_Transcript_133020	1.664717796	XP_034691942.1monocopper oxidase-like protein SKU5 isoform X1
CDS_48400_Unigene_84033_Transcript_153976	1.66461475	RWR92354.1putative cinnamyl alcohol dehydrogenase 6
CDS_2724_Unigene_13029_Transcript_22052	1.664468832	XP_010251199.1: E3 ubiquitin-protein ligase BOI-like
CDS_31464_Unigene_48223_Transcript_84917	1.664143589	XP_020523631.1uncharacterized protein LOC18435522
CDS_1803_Unigene_12016_Transcript_20224	1.663937847	XP_010262243.1: protein YLS9-like
CDS_19792_Unigene_32817_Transcript_56981	1.663865103	QCX36374.1KOMT1
CDS_18911_Unigene_31716_Transcript_55054	1.662925237	XP_022870729.1aspartate aminotransferase, mitochondrial

Transcript ID	Log2 Fold Change	Hit desc.
CDS_15475_Unigene_27701_Transcript_47913	1.662552283	XP_011033568.1: protein RALF-like 1
CDS_35608_Unigene_54677_Transcript_96478	1.662406013	RDX81111.1Auxin-induced protein 22C, partial
CDS_23413_Unigene_37247_Transcript_64924	1.660953508	KAF3957210.1 protein CMV_017759
CDS_11213_Unigene_22741_Transcript_39279	1.66026928	XP_008784965.1peroxidase 72-like
CDS_12534_Unigene_24289_Transcript_41987	1.659270529	KDO86709.1 protein CISIN_1g018568mg
CDS_49074_Unigene_8625_Transcript_14348	1.658832397	XP_015879798.1serine carboxypeptidase-like 25
CDS_33409_Unigene_51083_Transcript_89951	1.658462523	KAF3792823.1B3 domain-containing protein
CDS_33197_Unigene_50780_Transcript_89427	1.656347134	RWR81012.1stellacyanin-like protein
CDS_23577_Unigene_37472_Transcript_65302	1.655443833	RWR78658.1methionine S-methyltransferase
CDS_23412_Unigene_37246_Transcript_64920	1.655384833	XP_027062624.1zinc finger protein MAGPIE-like
CDS_27945_Unigene_4325_Transcript_7235	1.655068689	RWR89744.1protein NRT1/ PTR FAMILY 7.3-like protein
CDS_10459_Unigene_21832_Transcript_37700	1.653174367	RWR96343.1arogenate dehydrogenase 2, chloroplastic-like protein
CDS_7135_Unigene_18004_Transcript_30937	1.653134003	No Blast Hit
CDS_21641_Unigene_34998_Transcript_60858	1.652839486	QCX36384.1RDCT3
CDS_51462_Unigene_9719_Transcript_16247	1.652583196	RWR96046.1Glycoside hydrolase
CDS_36757_Unigene_56595_Transcript_100021	1.652052117	No Blast Hit
CDS_42283_Unigene_67443_Transcript_119715	1.651935616	ABX75853.1caffeoyl-CoA-O-methyltransferase
CDS_14607_Unigene_26697_Transcript_46201	1.65080895	PQQ15433.1putative 3 4-dihydroxy-2-butanone kinase
CDS_47708_Unigene_81859_Transcript_148404	1.64996993	RVW75455.1 protein CK203_061528
CDS_25730_Unigene_40291_Transcript_70369	1.649365534	RWR81903.1CDK-activating kinase assembly factor MAT1
CDS_857_Unigene_10945_Transcript_18382	1.649253484	OVA14081.1Remorin
CDS_37851_Unigene_58599_Transcript_103567	1.648183481	RWR77971.1adenylyl-sulfate kinase 3 isoform X3
CDS_50796_Unigene_9261_Transcript_15489	1.647821869	KZV57513.124-methylenesterol C-methyltransferase 2
CDS_2907_Unigene_13224_Transcript_22398	1.647669243	QCX36383.1RDCT2
CDS_22162_Unigene_35642_Transcript_62047	1.647449938	KAA8540212.1 protein F0562_024225
CDS_354_Unigene_10383_Transcript_17386	1.647197697	RWR76086.1putative sugar phosphate/phosphate translocator
CDS_32295_Unigene_49509_Transcript_87223	1.64669346	XP_031501876.110 kDa chaperonin, mitochondrial-like
CDS_50110_Unigene_8999_Transcript_15005	1.645459325	No Blast Hit
CDS_14952_Unigene_27094_Transcript_46849	1.643969205	XP_010254127.1: kinesin-like protein KIN-13B

Transcript ID	Log2 Fold Change	Hit desc.
CDS_40748_Unigene_64053_Transcript_113484	1.643195766	No Blast Hit
CDS_6322_Unigene_17097_Transcript_29400	1.643195766	XP_009412003.1: histone H2A.2
CDS_22932_Unigene_36582_Transcript_63791	1.642396711	No Blast Hit
CDS_41378_Unigene_6539_Transcript_10933	1.641763811	XP_010241716.1: purple acid phosphatase 17-like
CDS_20931_Unigene_34135_Transcript_59349	1.639818166	XP_010242568.1: protein OPI10 homolog
CDS_21980_Unigene_35425_Transcript_61630	1.639818166	No Blast Hit
CDS_21197_Unigene_34452_Transcript_59922	1.639668393	XP_015875080.1dolichyl-diphosphooligosaccharide--protein glycosyltransferase subunit DAD1
CDS_30398_Unigene_46647_Transcript_82085	1.638983515	RWW49574.1 protein BHE74_00044235
CDS_14151_Unigene_26133_Transcript_45199	1.638736118	OVA03579.1Glycosyl transferase
CDS_33583_Unigene_51401_Transcript_90545	1.638736118	No Blast Hit
CDS_46000_Unigene_76510_Transcript_137400	1.638357209	RWR75485.1DUF868 domain-containing protein
CDS_4172_Unigene_14656_Transcript_24958	1.638177692	XP_010250793.1: adenylate kinase 4-like
CDS_26474_Unigene_41296_Transcript_72261	1.637810364	XP_027111956.1nucleobase-ascorbate transporter 2
CDS_8254_Unigene_19306_Transcript_33236	1.63663805	MQM01222.1 protein
CDS_35705_Unigene_5483_Transcript_9167	1.636309381	RWR82907.1glycosyl transferase family 2 family protein
CDS_15705_Unigene_2797_Transcript_4611	1.63550288	XP_028779756.1LIM domain-containing protein WLIM2b-like
CDS_21825_Unigene_35217_Transcript_61246	1.635468404	XP_021606978.1putative UPF0481 protein At3g02645
CDS_3806_Unigene_14235_Transcript_24220	1.635178299	No Blast Hit
CDS_28742_Unigene_44297_Transcript_77799	1.634523867	No Blast Hit
CDS_18695_Unigene_31467_Transcript_54588	1.633370103	RWR88034.1receptor-like protein kinase THESEUS 1 isoform X1
CDS_12009_Unigene_23652_Transcript_40867	1.63318328	PON87126.1Ribose 5-phosphate isomerase, type A
CDS_32607_Unigene_49976_Transcript_88013	1.632971095	No Blast Hit
CDS_32866_Unigene_50352_Transcript_88692	1.632389011	XP_034697819.1N-acetyl-D-glucosamine kinase
CDS_20798_Unigene_33997_Transcript_59098	1.632072388	XP_018730850.1: uncharacterized protein LOC108960255
CDS_14953_Unigene_27095_Transcript_46850	1.631617685	RWR83089.1kinesin-like protein KIN-13B
CDS_25732_Unigene_40295_Transcript_70375	1.63157786	No Blast Hit
CDS_10521_Unigene_21925_Transcript_37855	1.631463601	XP_010278421.1: uncharacterized protein LOC104612629 isoform X2
CDS_32243_Unigene_49425_Transcript_87053	1.630717532	KAA8523303.1 protein F0562_009726

Transcript ID	Log2 Fold Change	Hit desc.
CDS_11802_Unigene_23403_Transcript_40440	1.630631068	XP_010249387.1: heparan-alpha-glucosaminide N-acetyltransferase
CDS_27281_Unigene_42380_Transcript_74288	1.63040274	XP_006494599.1root phototropism protein 3
CDS_11147_Unigene_22661_Transcript_39129	1.629244108	XP_010270730.1: protein IRX15-LIKE-like
CDS_11606_Unigene_23190_Transcript_40065	1.628799386	RWR77887.1transcription factor bHLH93
CDS_21710_Unigene_35089_Transcript_61012	1.628088874	No Blast Hit
CDS_40515_Unigene_63612_Transcript_112674	1.628088874	XP_010904676.1 ribose-5-phosphate isomerase 4, chloroplastic isoform X2
CDS_44119_Unigene_71770_Transcript_128061	1.628088874	No Blast Hit
CDS_23723_Unigene_37655_Transcript_65623	1.627280415	OVA02910.1SANT/Myb domain
CDS_36601_Unigene_56318_Transcript_99503	1.626514738	RWR86891.1Cytochrome b245
CDS_8004_Unigene_19027_Transcript_32737	1.62506963	RWW45347.1 protein BHE74_00048823
CDS_17053_Unigene_29560_Transcript_51217	1.624764014	XP_010258510.1: uncharacterized protein LOC104598255
CDS_46916_Unigene_7932_Transcript_13223	1.624336739	GER46372.1UDP-D-xylose:L-fucose alpha-1,3-D-xylosyltransferase 1
CDS_35751_Unigene_54919_Transcript_96913	1.623686228	No Blast Hit
CDS_26648_Unigene_41520_Transcript_72686	1.623350955	THU67369.1 protein C4D60_Mb05t23930
CDS_10457_Unigene_21830_Transcript_37697	1.622188272	RWR96343.1arogenate dehydrogenase 2, chloroplastic-like protein
CDS_12163_Unigene_23837_Transcript_41194	1.621916399	RWR72683.1ADP,ATP carrier protein 1, mitochondrial-like protein
CDS_32710_Unigene_50111_Transcript_88255	1.620269369	RWR94135.1protein SRG1-like protein
CDS_50297_Unigene_9080_Transcript_15153	1.619923617	XP_020686972.1protein FORGETTER 1 isoform X1
CDS_47070_Unigene_79806_Transcript_144132	1.619022939	RWR92992.1myotubularin-related protein-like protein
CDS_32490_Unigene_49809_Transcript_87703	1.618104785	XP_026455827.1uncharacterized protein LOC113356812
CDS_2490_Unigene_12775_Transcript_21596	1.617869032	RWR73773.1Glycosyl hydrolases 36
CDS_9499_Unigene_20733_Transcript_35755	1.615012999	No Blast Hit
CDS_51643_Unigene_9930_Transcript_16612	1.614878	MQL70381.1 protein
CDS_21028_Unigene_34241_Transcript_59548	1.614283074	RWR83677.1citrate-binding-like protein
CDS_39901_Unigene_62429_Transcript_110532	1.614283074	XP_023893486.1 transcription-associated protein 1
CDS_29439_Unigene_45281_Transcript_79603	1.611231042	XP_003635420.1: sphingolipid delta(4)-desaturase DES1-like
CDS_10308_Unigene_21670_Transcript_37410	1.611108827	XP_002524363.1light-harvesting complex-like protein 3 isotype 2, chloroplastic
CDS_15537_Unigene_27772_Transcript_48025	1.609129272	RWR82950.1somatic embryogenesis receptor kinase 2

Transcript ID	Log2 Fold Change	Hit desc.
CDS_19966_Unigene_3301_Transcript_5439	1.607642349	XP_010262132.1: beta-galactosidase isoform X2
CDS_657_Unigene_1072_Transcript_1832	1.60603908	RWR95824.1pectinesterase/pectinesterase inhibitor PPE8B
CDS_6520_Unigene_17319_Transcript_29787	1.605721061	KDO47805.1 protein CISIN_1g018854mg
CDS_29170_Unigene_44902_Transcript_78904	1.604600521	RVW55424.1DNA repair protein XRCC4
CDS_44504_Unigene_7271_Transcript_12177	1.604600521	TXG53256.1 protein EZV62_022425
CDS_39534_Unigene_61740_Transcript_109300	1.604555052	XP_004982014.1basic blue protein
CDS_16023_Unigene_28342_Transcript_49004	1.604158857	XP_010265154.1: tetraketide alpha-pyrone reductase 2 isoform X1
CDS_14792_Unigene_26911_Transcript_46537	1.600986252	XP_010254147.1: aldehyde dehydrogenase family 2 member C4-like
CDS_32294_Unigene_49508_Transcript_87222	1.600970915	XP_031501876.110 kDa chaperonin, mitochondrial-like
CDS_16636_Unigene_29077_Transcript_50339	1.598695089	XP_006830282.1uncharacterized protein LOC18425705
CDS_21642_Unigene_34999_Transcript_60859	1.598430254	QCX36384.1RDCT3
CDS_20127_Unigene_3319_Transcript_5469	1.598341531	ABK95605.1unknown
CDS_25599_Unigene_40113_Transcript_70085	1.598341531	No Blast Hit
CDS_39175_Unigene_6103_Transcript_10152	1.597691521	XP_006837934.2E3 ubiquitin-protein ligase MIEL1
CDS_3137_Unigene_134_Transcript_208	1.596940175	XP_020083486.1vacuolar amino acid transporter 1 isoform X1
CDS_33119_Unigene_50671_Transcript_89233	1.59683794	XP_009405364.1: peroxisomal (S)-2-hydroxy-acid oxidase GLO1
CDS_20134_Unigene_3320_Transcript_5470	1.596781017	ABK95605.1unknown
CDS_15806_Unigene_28092_Transcript_48591	1.596542659	XP_010265413.1: AAA-ATPase At3g50940-like
CDS_47641_Unigene_81635_Transcript_147917	1.596416654	XP_011032644.1: protein TIFY 4A-like isoform X2
CDS_26459_Unigene_41267_Transcript_72214	1.595778258	OAY83109.1Polygalacturonase, partial
CDS_1068_Unigene_11195_Transcript_18762	1.595635477	No Blast Hit
CDS_30366_Unigene_46605_Transcript_82014	1.595021172	No Blast Hit
CDS_15474_Unigene_27700_Transcript_47912	1.594832745	XP_011033568.1: protein RALF-like 1
CDS_24443_Unigene_38617_Transcript_67304	1.59456484	MQM18342.1 protein
CDS_33747_Unigene_51650_Transcript_90969	1.594225422	XP_019182095.1: protein DETOXIFICATION 54-like
CDS_26616_Unigene_41484_Transcript_72628	1.59396309	ONK73842.1uncharacterized protein A4U43_C03F140
CDS_31811_Unigene_48753_Transcript_85849	1.592232721	RWR73188.1 protein CKAN_00144400
CDS_32997_Unigene_50519_Transcript_88970	1.591915261	XP_016665515.1: alpha-mannosidase-like isoform X3

Transcript ID	Log2 Fold Change	Hit desc.
CDS_34911_Unigene_53551_Transcript_94495	1.591915261	No Blast Hit
CDS_2287_Unigene_12562_Transcript_21206	1.591502532	XP_012067633.1 methyltransferase PMT2 isoform X2
CDS_26414_Unigene_41205_Transcript_72116	1.589953745	XP_031263816.1antifungal protein ginkbilobin-like protein
CDS_29413_Unigene_45239_Transcript_79517	1.589003666	RWR86899.1DUF761 domain-containing protein
CDS_12249_Unigene_23934_Transcript_41348	1.58869136	No Blast Hit
CDS_29140_Unigene_44861_Transcript_78832	1.588411694	XP_010258982.2: L-lactate dehydrogenase B-like
CDS_47307_Unigene_80536_Transcript_145686	1.588325936	KDO46544.1 protein CISIN_1g015012mg
CDS_10916_Unigene_22387_Transcript_38662	1.588153343	OVA16561.1Glycoside hydrolase
CDS_42303_Unigene_67485_Transcript_119780	1.587463477	XP_010265159.1: uncharacterized protein LOC104602976
CDS_30752_Unigene_47174_Transcript_83056	1.587243822	XP_020231747.1xyloglucan 6-xylosyltransferase 2
CDS_28084_Unigene_43453_Transcript_76254	1.586703835	XP_007022108.2: persulfide dioxygenase ETHE1 homolog, mitochondrial
CDS_27565_Unigene_42749_Transcript_75001	1.586268698	XP_023750131.1VAN3-binding protein-like, partial
CDS_28398_Unigene_43865_Transcript_77029	1.585754277	XP_031401633.1isopentenyl-diphosphate Delta-isomerase I
CDS_19461_Unigene_32378_Transcript_56239	1.584091045	XP_034687201.1photosynthetic NDH subunit of lumenal location 5, chloroplastic
CDS_41593_Unigene_6592_Transcript_11018	1.584000507	No Blast Hit
CDS_18421_Unigene_3114_Transcript_5111	1.583813882	KAF1897440.1 protein Lal_00035145
CDS_38804_Unigene_60317_Transcript_106746	1.582870122	KAE8037239.1 protein FH972_009847
CDS_6907_Unigene_17755_Transcript_30517	1.581268017	RWR95992.1protein ODORANT1-like protein
CDS_17614_Unigene_30199_Transcript_52335	1.580194184	RWR85719.1scarecrow-like protein 23 isoform X1
CDS_14791_Unigene_26910_Transcript_46536	1.579904282	RWR77524.1aldehyde dehydrogenase family 2 member C4
CDS_39224_Unigene_61143_Transcript_108242	1.579725852	XP_027117488.1dCTP pyrophosphatase 1-like
CDS_6995_Unigene_17857_Transcript_30682	1.578976206	TXG52524.1 protein EZV62_021693
CDS_43147_Unigene_6938_Transcript_11612	1.578402683	XP_008786320.1uncharacterized protein At2g38710-like
CDS_1713_Unigene_11926_Transcript_20068	1.577706685	XP_030501888.117.9 kDa class II heat shock protein
CDS_6992_Unigene_17854_Transcript_30679	1.577517833	XP_030528588.1adenine phosphoribosyltransferase 1-like
CDS_15636_Unigene_27902_Transcript_48273	1.577122101	XP_010937626.1glucan endo-1,3-beta-glucosidase

Transcript ID	Log2 Fold Change	Hit desc.
CDS_5963_Unigene_16696_Transcript_28675	1.576808369	RWR72916.1Serine/threonine-protein kinase WNK-related isoform 1
CDS_38649_Unigene_60035_Transcript_106203	1.576048856	XP_010259530.1: blue-light photoreceptor PHR2
CDS_26684_Unigene_41567_Transcript_72767	1.57588208	OVA10738.1Late embryogenesis abundant protein
CDS_12462_Unigene_2417_Transcript_4011	1.575019727	OVA12263.1Mitochondrial carrier protein
CDS_41957_Unigene_66737_Transcript_118428	1.574680724	THU73399.1 protein C4D60_Mb04t22430
CDS_47304_Unigene_80533_Transcript_145683	1.574554409	XP_010551544.1: cytosolic isocitrate dehydrogenase
CDS_30572_Unigene_46905_Transcript_82548	1.57435689	XP_006421608.1expansin-B15
CDS_2966_Unigene_132_Transcript_206	1.574093984	XP_020083486.1vacuolar amino acid transporter 1 isoform X1
CDS_43709_Unigene_70765_Transcript_126051	1.574093984	PQQ13242.1beta-galactosidase protein 2
CDS_36082_Unigene_55464_Transcript_97921	1.572806438	EOX99671.1Jasmonate-zim-domain protein 10, putative
CDS_1805_Unigene_12018_Transcript_20226	1.572386989	XP_010262243.1: protein YLS9-like
CDS_38691_Unigene_60091_Transcript_106320	1.571214352	RVW17335.1 protein CK203_069259
CDS_27221_Unigene_4228_Transcript_7064	1.569977876	No Blast Hit
CDS_32606_Unigene_49975_Transcript_88012	1.569925848	OVA20163.1 protein BVC80_1663g59
CDS_4017_Unigene_1447_Transcript_2449	1.569707779	XP_031270723.1uncharacterized protein LOC116129107
CDS_10298_Unigene_21659_Transcript_37392	1.569195185	XP_018678376.1: 60S ribosomal protein L6-like
CDS_15614_Unigene_27873_Transcript_48221	1.569195185	No Blast Hit
CDS_28521_Unigene_44017_Transcript_77294	1.569195185	No Blast Hit
CDS_8714_Unigene_1984_Transcript_3312	1.569195185	PIA41578.1 protein AQUCO_02200192v1
CDS_13393_Unigene_25255_Transcript_43702	1.569059408	KAA3489229.1transmembrane protein 87A-like
CDS_10862_Unigene_22318_Transcript_38536	1.56870787	RWR85264.1vacuolar iron transporter 4-like protein
CDS_3309_Unigene_136_Transcript_210	1.567230998	XP_020264755.1vacuolar amino acid transporter 1-like
CDS_40005_Unigene_62629_Transcript_110917	1.566550464	KAF3442864.1 protein FNV43_RR16782
CDS_5246_Unigene_15901_Transcript_27194	1.565000081	XP_010275836.1: transmembrane 9 superfamily member 8-like
CDS_45456_Unigene_7509_Transcript_12546	1.56434282	XP_008803802.1histone deacetylase HDT2-like isoform X1
CDS_44123_Unigene_7177_Transcript_12013	1.563900885	XP_010268836.1: F-box protein At1g61340-like
CDS_14500_Unigene_26567_Transcript_45959	1.561646731	XP_034709298.1vacuolar protein 8

Transcript ID	Log2 Fold Change	Hit desc.
CDS_40689_Unigene_63960_Transcript_113307	1.561621965	RWR92778.1dynamin-like protein ARC5 isoform X1
CDS_19120_Unigene_31964_Transcript_55539	1.561541612	No Blast Hit
CDS_21460_Unigene_34762_Transcript_60445	1.561301783	OVA01922.1PMR5 N-terminal domain
CDS_15184_Unigene_27364_Transcript_47314	1.560733606	XP_009386847.1: NAD(P)H:quinone oxidoreductase
CDS_19709_Unigene_32700_Transcript_56823	1.560625906	XP_008777803.1hydroxymethylglutaryl-CoA synthase-like
CDS_24142_Unigene_38229_Transcript_66592	1.560303354	XP_021820609.1 xyloglucan 6-xylosyltransferase 5
CDS_12475_Unigene_24208_Transcript_41838	1.560206402	RWR82495.1 protein CKAN_01121500
CDS_6001_Unigene_16740_Transcript_28757	1.560175669	RWR75225.1Peptidase S8/S53 domain-containing protein
CDS_43569_Unigene_70376_Transcript_125345	1.559688099	BBH06065.1ER-type Ca2+-ATPase 1
CDS_41362_Unigene_6534_Transcript_10927	1.559559888	TKY61094.1Purple acid phosphatase 17
CDS_48251_Unigene_83538_Transcript_152710	1.559010491	XP_006476178.1molybdate transporter 1
CDS_21993_Unigene_35449_Transcript_61675	1.557699546	XP_020268349.1UDP-galactose transporter 2-like isoform X1
CDS_34834_Unigene_53413_Transcript_94259	1.557699546	No Blast Hit
CDS_43737_Unigene_70849_Transcript_126215	1.557699546	No Blast Hit
CDS_44925_Unigene_73735_Transcript_131925	1.557699546	MCH90775.1alpha-14 glucan phosphorylase L isozyme chloroplastic/amyloplastic-like
CDS_2945_Unigene_1326_Transcript_2273	1.556908812	KAB2092277.1 protein ES319_A02G018400v1
CDS_19556_Unigene_32501_Transcript_56455	1.556139032	XP_010251385.1: ribonuclease 2-like
CDS_12220_Unigene_23901_Transcript_41292	1.555836802	PIN23693.1 protein CDL12_03586
CDS_5192_Unigene_15839_Transcript_27080	1.555836802	XP_010250890.1: trihelix transcription factor GTL1 isoform X2
CDS_28444_Unigene_43923_Transcript_77127	1.555389385	XP_010265436.1: NAD(P)H dehydrogenase subunit CRR3, chloroplastic
CDS_21945_Unigene_3538_Transcript_5819	1.555074077	RVW87179.1Cellulose synthase-like protein E1
CDS_15317_Unigene_27520_Transcript_47584	1.554659092	XP_002305442.1bZIP transcription factor 44
CDS_20530_Unigene_33668_Transcript_58481	1.554659092	No Blast Hit
CDS_27158_Unigene_42205_Transcript_73960	1.552577113	PSR89954.1Exosome complex component RRP41-like
CDS_48350_Unigene_83861_Transcript_153520	1.551447337	RWR85344.1protein ABA DEFICIENT 4, chloroplastic-like protein isoform X1
CDS_21712_Unigene_35090_Transcript_61013	1.551273277	RWR90055.1cyclin-dependent kinase inhibitor 1-like protein
CDS_7080_Unigene_17951_Transcript_30852	1.550549432	OVA12971.1Myc-type

Transcript ID	Log2 Fold Change	Hit desc.
CDS_34296_Unigene_52511_Transcript_92535	1.550336158	KAE8664981.1Receptor-like protein kinase HERK 1
CDS_39787_Unigene_62219_Transcript_110155	1.54974626	RWR94287.1nicotianamine synthase
CDS_32116_Unigene_4921_Transcript_8222	1.54943193	No Blast Hit
CDS_42515_Unigene_67_Transcript_113	1.548049376	XP_010922712.1U-box domain-containing protein 16
CDS_37005_Unigene_57054_Transcript_100848	1.547715457	RWR89827.1oxysterol-binding protein-related protein 2A isoform X1
CDS_39725_Unigene_62124_Transcript_109983	1.546458833	KAA8515282.1 protein F0562_018488
CDS_24581_Unigene_38803_Transcript_67648	1.545348443	PIA49523.1 protein AQUCO_01300369v1
CDS_30970_Unigene_47500_Transcript_83594	1.544742141	XP_034685410.11-aminocyclopropane-1-carboxylate oxidase homolog 1-like
CDS_14344_Unigene_26362_Transcript_45593	1.543994631	OVA15933.1 protein BVC80_1821g100
CDS_13062_Unigene_24893_Transcript_43036	1.542783554	XP_034698120.1BTB/POZ domain-containing protein At1g30440
CDS_47305_Unigene_80534_Transcript_145684	1.542008007	XP_010551544.1: cytosolic isocitrate dehydrogenase
CDS_4577_Unigene_1511_Transcript_2541	1.541973716	XP_020226950.1 sugar phosphate/phosphate translocator At1g12500
CDS_16188_Unigene_28537_Transcript_49345	1.541273998	RWR96747.1formin-like protein 1
CDS_12188_Unigene_23864_Transcript_41235	1.540626033	KAF3439787.1 protein FNV43_RR18065
CDS_17923_Unigene_30570_Transcript_53004	1.54002852	KAE8656429.1B-box zinc finger protein 20
CDS_20151_Unigene_3322_Transcript_5472	1.539633361	ABK95605.1unknown
CDS_30656_Unigene_47039_Transcript_82804	1.539321017	RWR83410.1transcription factor FER-LIKE IRON DEFICIENCY-INDUCED TRANSCRIPTION FACTOR-like protein
CDS_34039_Unigene_52078_Transcript_91707	1.538962983	No Blast Hit
CDS_11424_Unigene_22980_Transcript_39737	1.538698584	RWR77548.1protein REVERSION-TO-ETHYLENE SENSITIVITY1 isoform X2
CDS_51118_Unigene_9382_Transcript_15702	1.538407789	RWR96327.1low-temperature-induced cysteine proteinase-like protein
CDS_14588_Unigene_26670_Transcript_46165	1.537799989	AGW21001.1NBS-LRR disease resistance protein, partial
CDS_10458_Unigene_21831_Transcript_37699	1.536202846	RWR96343.1arogenate dehydrogenase 2, chloroplastic-like protein
CDS_20217_Unigene_33303_Transcript_57838	1.535380472	XP_022769142.1uncharacterized protein LOC111312795
CDS_14343_Unigene_26361_Transcript_45592	1.534192793	XP_010266880.1: protein DETOXIFICATION 33-like
CDS_2477_Unigene_12761_Transcript_21573	1.533756161	RWR74748.1voltage-dependent T-type calcium channel subunit alpha-1G-like protein
CDS_30686_Unigene_47084_Transcript_82880	1.533691375	XP_015898171.1 glycosyltransferase STELLO2

Transcript ID	Log2 Fold Change	Hit desc.
CDS_12186_Unigene_23860_Transcript_41231	1.532436635	No Blast Hit
CDS_26324_Unigene_41085_Transcript_71896	1.531972721	KAA8545303.1 protein F0562_020087
CDS_23433_Unigene_37284_Transcript_64988	1.531227335	XP_006475905.1 ADP,ATP carrier protein At5g56450
CDS_42227_Unigene_67329_Transcript_119501	1.531227335	XP_010259661.1: glutathione S-transferase F13
CDS_25750_Unigene_40323_Transcript_70423	1.529832753	RWR95510.1ABC transporter G family member 6
CDS_15299_Unigene_274_Transcript_455	1.528261658	No Blast Hit
CDS_39473_Unigene_61632_Transcript_109101	1.528149819	RWR87427.1NUDIX hydrolase domain-containing protein
CDS_10157_Unigene_21492_Transcript_37096	1.527603121	XP_010277801.1: thiol methyltransferase 2 isoform X1
CDS_13163_Unigene_25005_Transcript_43250	1.526156345	RWR94963.1GDP-fucose protein O-fucosyltransferase
CDS_13064_Unigene_24895_Transcript_43038	1.526027326	XP_034698120.1BTB/POZ domain-containing protein At1g30440
CDS_29960_Unigene_46006_Transcript_80909	1.525278068	XP_020224583.1uncharacterized protein LOC109806552
CDS_12922_Unigene_2473_Transcript_4105	1.524340949	No Blast Hit
CDS_31762_Unigene_48681_Transcript_85742	1.524340949	PKA48395.1Putative glycosyltransferase 2
CDS_2854_Unigene_13167_Transcript_22294	1.524141641	MQM04372.1 protein
CDS_4030_Unigene_14496_Transcript_24677	1.524085265	PSS28737.1Glutathione S-transferase
CDS_7265_Unigene_18149_Transcript_31221	1.52321117	XP_010941633.1protein PHLOEM PROTEIN 2-LIKE A9
CDS_50652_Unigene_9207_Transcript_15385	1.522918313	KAF5184405.1Brevis radix
CDS_303_Unigene_10313_Transcript_17257	1.522879992	XP_010920265.1putative HVA22-like protein g isoform X2
CDS_28659_Unigene_4417_Transcript_7393	1.52188947	RWR95277.1dTDP-glucose 4-6-dehydratase/UDP-glucuronic acid decarboxylase
CDS_25138_Unigene_39510_Transcript_68939	1.521832786	RWR79148.1putative cysteine protease RD19C
CDS_960_Unigene_11063_Transcript_18567	1.521454596	XP_028786496.1chaperonin CPN60-2, mitochondrial-like, partial
CDS_34893_Unigene_53510_Transcript_94425	1.52117367	KAF0919546.1 protein E2562_029772
CDS_41697_Unigene_66169_Transcript_117389	1.52117367	No Blast Hit
CDS_18377_Unigene_31094_Transcript_53924	1.520778056	RWR89884.1PLAT domain-containing protein 3-like protein
CDS_43153_Unigene_69397_Transcript_123438	1.520339019	QAX90949.1caffeic acid O-methyltransferase
CDS_12911_Unigene_24726_Transcript_42742	1.520179508	RWR82374.1PAN domain-containing protein
CDS_43671_Unigene_70661_Transcript_125846	1.519867472	XP_010249378.1: BOI-related E3 ubiquitin-protein ligase 3 isoform X2

Transcript ID	Log2 Fold Change	Hit desc.
CDS_47306_Unigene_80535_Transcript_145685	1.519750985	XP_010551544.1: cytosolic isocitrate dehydrogenase
CDS_11403_Unigene_22955_Transcript_39694	1.51943719	RWR72705.1outer envelope pore protein 16-3, chloroplastic/mitochondrial-like protein isoform X2
CDS_30971_Unigene_47502_Transcript_83596	1.517184386	TYI46743.1 protein E1A91_D13G125500v1
CDS_30655_Unigene_47038_Transcript_82801	1.516727765	KAA8519756.1 protein F0562_014012
CDS_39738_Unigene_62152_Transcript_110035	1.516727765	RWR76985.1lipase
CDS_24143_Unigene_38230_Transcript_66593	1.516617133	XP_021820609.1 xyloglucan 6-xylosyltransferase 5
CDS_8830_Unigene_19991_Transcript_34460	1.516617133	XP_034700059.1uncharacterized protein LOC117925221 isoform X1
CDS_24199_Unigene_38299_Transcript_66715	1.515995618	RWR76451.1bZIP transcription factor 53
CDS_1886_Unigene_12112_Transcript_20402	1.515484598	ACT99428.1unknown, partial
CDS_44371_Unigene_72360_Transcript_129266	1.515107669	XP_018838308.1: folate-biopterin transporter 7, partial
CDS_45733_Unigene_75845_Transcript_136088	1.515026209	RWR90890.1sugar carrier protein C-like protein
CDS_24942_Unigene_39255_Transcript_68463	1.513756198	RWR94961.1restin
CDS_1290_Unigene_11460_Transcript_19228	1.512856119	MQM08793.1 protein
CDS_11200_Unigene_22729_Transcript_39265	1.512437723	XP_020092748.1protein DMR6-LIKE OXYGENASE 2
CDS_12167_Unigene_23841_Transcript_41201	1.512005355	RWR72683.1ADP,ATP carrier protein 1, mitochondrial-like protein
CDS_36720_Unigene_56515_Transcript_99892	1.510393831	PNX82846.1 protein L195_g038881, partial
CDS_38520_Unigene_59835_Transcript_105835	1.510340887	RWR77574.1filament-like plant protein 7
CDS_1782_Unigene_11998_Transcript_20185	1.510150831	XP_028779501.1protein disulfide-isomerase like 2-1-like
CDS_20005_Unigene_33060_Transcript_57416	1.510083263	RWR77005.1fasciclin-like arabinogalactan protein 1
CDS_16804_Unigene_29266_Transcript_50684	1.508958573	XP_026404871.1galacturonokinase-like
CDS_42744_Unigene_68488_Transcript_121660	1.508521012	KHN06269.1 protein glysoja_030335
CDS_5918_Unigene_16650_Transcript_28589	1.508434558	XP_010254314.1: papilin-like isoform X1
CDS_14430_Unigene_26477_Transcript_45796	1.508371834	KAB2029990.1 protein ES319_D05G199800v1
CDS_19460_Unigene_32377_Transcript_56236	1.507684008	KAF2283084.1 protein GH714_043407
CDS_38492_Unigene_59773_Transcript_105727	1.504804598	RWR91098.1deSI-like protein
CDS_12574_Unigene_24329_Transcript_42045	1.503067884	XP_010275992.1: early nodulin-like protein 3
CDS_19659_Unigene_32631_Transcript_56703	1.498805857	XP_023528170.1xyloglucan 6-xylosyltransferase 2
CDS_22076_Unigene_35550_Transcript_61879	1.498805857	PIA38396.1 protein AQUCO_02800239v1
CDS_2261_Unigene_12535_Transcript_21159	1.498805857	XP_010245839.1: peroxidase 43-like

Transcript ID	Log2 Fold Change	Hit desc.
CDS_24144_Unigene_38231_Transcript_66594	1.498805857	XP_021820609.1 xyloglucan 6-xylosyltransferase 5
CDS_24561_Unigene_38775_Transcript_67596	1.498805857	No Blast Hit
CDS_25400_Unigene_39859_Transcript_69619	1.498805857	ART33311.1heterdimeric geranyl diphosphate synthase small subunit protein 1
CDS_28366_Unigene_43832_Transcript_76968	1.498805857	EOY25862.1Disease resistance protein family
CDS_29650_Unigene_45569_Transcript_80116	1.498805857	XP_010240887.1: cinnamoyl-CoA reductase-like SNL6
CDS_35622_Unigene_54706_Transcript_96524	1.498805857	RWR77595.1putative isoaspartyl peptidase/L-asparaginase 2
CDS_41076_Unigene_6477_Transcript_10813	1.498805857	No Blast Hit
CDS_44179_Unigene_71902_Transcript_128321	1.498805857	XP_008775505.1protein LHCP TRANSLOCATION DEFECT
CDS_44747_Unigene_73247_Transcript_130944	1.498805857	XP_010256629.1: BAHD acyltransferase DCR
CDS_5384_Unigene_16067_Transcript_27488	1.498805857	RWR87559.1transmembrane protein 64 isoform X1
CDS_8132_Unigene_19167_Transcript_32977	1.497289625	XP_021852382.1uncharacterized membrane protein At4g09580
CDS_32865_Unigene_50351_Transcript_88691	1.496199361	ERN07672.1 protein AMTR_s00155p00052560
CDS_37168_Unigene_57325_Transcript_101289	1.495940523	OVA16773.1SMP-30/Gluconolactonase/LRE-like region
CDS_6321_Unigene_17096_Transcript_29399	1.495746057	XP_009412003.1: histone H2A.2
CDS_2525_Unigene_12819_Transcript_21675	1.494346209	MQM13305.1 protein
CDS_685_Unigene_10771_Transcript_18076	1.492339261	PON62816.1C2 domain containing protein
CDS_33832_Unigene_51763_Transcript_91168	1.49058535	RWR76507.1dTDP-glucose 4-6-dehydratase/UDP-glucuronic acid decarboxylase
CDS_3929_Unigene_14377_Transcript_24448	1.489982007	No Blast Hit
CDS_36873_Unigene_56797_Transcript_100419	1.489760717	No Blast Hit
CDS_14589_Unigene_26671_Transcript_46168	1.488986796	XP_009395665.2: NAD(P)H dehydrogenase (quinone) FQR1-like 2
CDS_46603_Unigene_78314_Transcript_141009	1.488158613	QCX36381.1COMTL6
CDS_34661_Unigene_53125_Transcript_93717	1.487310218	XP_006446203.1hexokinase-3
CDS_50118_Unigene_9000_Transcript_15006	1.486386598	No Blast Hit
CDS_24490_Unigene_38679_Transcript_67403	1.486169031	BBH00115.1general regulatory factor 3
CDS_13343_Unigene_25203_Transcript_43614	1.485749704	XP_008813513.1serine/threonine-protein kinase RIPK-like isoform X1
CDS_24435_Unigene_38607_Transcript_67286	1.485499601	XP_019705415.1uncharacterized protein LOC105058203 isoform X3
CDS_38820_Unigene_60343_Transcript_106792	1.483698965	RWR77429.1NUDIX hydrolase domain-containing protein

Transcript ID	Log2 Fold Change	Hit desc.
CDS_21827_Unigene_35219_Transcript_61249	1.483485058	PIA41578.1 protein AQUCO_02200192v1
CDS_17882_Unigene_30528_Transcript_52937	1.483422824	XP_026400515.13-hydroxy-3-methylglutaryl-coenzyme A reductase-like
CDS_21976_Unigene_35419_Transcript_61617	1.483038541	RWR90243.1amino acid permease 3
CDS_40322_Unigene_63239_Transcript_111997	1.483038541	XP_023898043.1 serine/threonine-protein kinase ndrA
CDS_33442_Unigene_51127_Transcript_90044	1.482317734	No Blast Hit
CDS_49174_Unigene_86624_Transcript_160700	1.481799432	MCI36713.1microtubule-associated protein 70-2-like
CDS_47010_Unigene_79661_Transcript_143833	1.481527866	KAF3442488.1 protein FNV43_RR16404
CDS_13178_Unigene_25023_Transcript_43281	1.481408807	XP_027352154.1ribonucleoside-diphosphate reductase small chain
CDS_2883_Unigene_131_Transcript_205	1.480957856	XP_020083486.1vacuolar amino acid transporter 1 isoform X1
CDS_3738_Unigene_14155_Transcript_24053	1.480348952	OMO59275.1 protein CCACVL1_24955
CDS_43986_Unigene_71445_Transcript_127401	1.479697034	KAB2047987.1 protein ES319_A13G083600v1
CDS_2485_Unigene_12770_Transcript_21584	1.479587941	RWR73774.1Glycosyl hydrolases 36
CDS_28806_Unigene_44386_Transcript_77968	1.478047297	PIA40645.1 protein AQUCO_02400011v1
CDS_30157_Unigene_46299_Transcript_81460	1.476779551	OVA13739.1Annexin
CDS_2597_Unigene_128_Transcript_198	1.4751933	XP_010278063.1: vacuolar amino acid transporter 1 isoform X1
CDS_12248_Unigene_23933_Transcript_41346	1.474558311	No Blast Hit
CDS_7153_Unigene_18023_Transcript_30977	1.473961786	PIA59624.1 protein AQUCO_00400487v1
CDS_15715_Unigene_27990_Transcript_48422	1.473511837	XP_016507811.1: uncharacterized protein LOC107825453
CDS_25489_Unigene_39978_Transcript_69834	1.472540202	RVX04450.1 protein CK203_018524
CDS_15610_Unigene_27868_Transcript_48214	1.472296227	OVA06662.1C2 calcium-dependent membrane targeting
CDS_6323_Unigene_17098_Transcript_29401	1.4713997	XP_022039460.1histone H2A.6-like
CDS_20286_Unigene_33386_Transcript_57973	1.471325121	RWW07520.1 protein GW17_00029096, partial
CDS_12750_Unigene_24528_Transcript_42407	1.470791481	RXI08714.1 protein DVH24_022858
CDS_5247_Unigene_15902_Transcript_27195	1.470133467	XP_010265569.1: transmembrane 9 superfamily member 10-like
CDS_42343_Unigene_67589_Transcript_119949	1.468793288	PIA34692.1 protein AQUCO_03700165v1
CDS_18607_Unigene_31360_Transcript_54403	1.468432208	XP_010915419.1dehydration-responsive element-binding protein 3
CDS_29070_Unigene_44772_Transcript_78689	1.468432208	XP_025611367.1xyloglucan 6-xylosyltransferase 2
CDS_19419_Unigene_32317_Transcript_56128	1.467554923	KAF3560286.1 protein F2Q69_00014107
CDS_10641_Unigene_22064_Transcript_38082	1.467096997	TMW90087.1 protein EJD97_016219, partial

Transcript ID	Log2 Fold Change	Hit desc.
CDS_30805_Unigene_47257_Transcript_83197	1.46698941	RWR92056.1MLO-like protein 11 isoform X1
CDS_23316_Unigene_3710_Transcript_6119	1.466765591	XP_010647315.1: uncharacterized protein At3g49720
CDS_352_Unigene_10381_Transcript_17383	1.465638993	XP_030457773.1 sugar phosphate/phosphate translocator At3g10290
CDS_42284_Unigene_67444_Transcript_119717	1.465075	ABX75853.1caffeoyl-CoA-O-methyltransferase
CDS_2917_Unigene_13235_Transcript_22423	1.465064374	RWR91246.1chaperone protein dnaJ 8, chloroplastic
CDS_16124_Unigene_28451_Transcript_49200	1.464947053	RWR75219.1Cation-transporting P-type ATPase
CDS_39152_Unigene_60992_Transcript_107943	1.46355501	RWR74770.1agmatine coumaroyltransferase-2-like protein
CDS_26612_Unigene_41480_Transcript_72620	1.463307176	RVX23996.1O-fucosyltransferase 31
CDS_37006_Unigene_57055_Transcript_100849	1.46326174	RWR89827.1oxysterol-binding protein-related protein 2A isoform X1
CDS_2134_Unigene_12390_Transcript_20914	1.463240497	No Blast Hit
CDS_40931_Unigene_64451_Transcript_114219	1.462279981	No Blast Hit
CDS_36193_Unigene_55649_Transcript_98256	1.461524841	No Blast Hit
CDS_2927_Unigene_1324_Transcript_2269	1.461492699	KAB2092277.1 protein ES319_A02G018400v1
CDS_25756_Unigene_40329_Transcript_70436	1.461003824	KAA8536721.1 protein F0562_029199
CDS_10386_Unigene_2174_Transcript_3627	1.460558388	XP_015885047.1acyl-CoA-binding domain-containing protein 3-like
CDS_37416_Unigene_57760_Transcript_102094	1.45963526	PIA39017.1 protein AQUCO_02700297v1
CDS_27102_Unigene_42127_Transcript_73813	1.459492933	XP_012073099.1uncharacterized protein LOC105634792 isoform X2
CDS_36540_Unigene_56228_Transcript_99330	1.45891313	PKU74446.1Ubiquitin-activating enzyme E1 1
CDS_34891_Unigene_53509_Transcript_94424	1.4577432	VAH62237.1unnamed protein product
CDS_34813_Unigene_5337_Transcript_8923	1.457226753	XP_010274674.1: serine carboxypeptidase-like 50
CDS_546_Unigene_10614_Transcript_17769	1.456129172	XP_020261032.1S-norcoclaurine synthase 2-like
CDS_21087_Unigene_34308_Transcript_59653	1.455634023	XP_011088218.1adhesive plaque matrix protein
CDS_37199_Unigene_57376_Transcript_101389	1.455216588	No Blast Hit
CDS_2631_Unigene_12934_Transcript_21909	1.45508448	KAF3774228.1Pyruvate dehydrogenase E1 component subunit alpha
CDS_33531_Unigene_51287_Transcript_90330	1.454215706	KAA8528236.1 protein F0562_035513
CDS_22010_Unigene_35466_Transcript_61702	1.452457117	XP_030955274.1aminomethyltransferase, mitochondrial-like
CDS_30937_Unigene_47453_Transcript_83522	1.451500142	No Blast Hit

Transcript ID	Log2 Fold Change	Hit desc.
CDS_47160_Unigene_80047_Transcript_144648	1.451500142	XP_022724138.1 WRKY transcription factor 14 isoform X1
CDS_41413_Unigene_65476_Transcript_116100	1.450150051	XP_024928185.1calcium permeable stress-gated cation channel 1 isoform X4
CDS_40924_Unigene_64431_Transcript_114193	1.449950566	XP_021604837.1phosphoenolpyruvate carboxylase 2 isoform X1
CDS_41377_Unigene_6538_Transcript_10932	1.449721076	TKY61094.1Purple acid phosphatase 17
CDS_27737_Unigene_42969_Transcript_75375	1.449223828	XP_026404987.1uncharacterized protein At4g28440-like
CDS_18430_Unigene_31158_Transcript_54041	1.449007624	XP_010912576.1dihydrolipoyllysine-residue acetyltransferase component 5 of pyruvate dehydrogenase complex, chloroplastic
CDS_8933_Unigene_20094_Transcript_34637	1.448711291	OVA03699.1Pectinesterase
CDS_23807_Unigene_37756_Transcript_65799	1.44853265	XP_022733100.1uncharacterized protein LOC111287117
CDS_14918_Unigene_27057_Transcript_46782	1.448297955	OVA09400.1putative S-adenosyl-L-methionine-dependent methyltransferase
CDS_38643_Unigene_60026_Transcript_106184	1.447821928	CAN67628.1 protein VITISV_019216
CDS_21358_Unigene_34649_Transcript_60237	1.447690541	XP_010917266.1protein trichome birefringence
CDS_17051_Unigene_29559_Transcript_51216	1.447437466	XP_010258510.1: uncharacterized protein LOC104598255
CDS_21199_Unigene_34454_Transcript_59927	1.446338437	XP_015875080.1dolichyl-diphosphooligosaccharide--protein glycosyltransferase subunit DAD1
CDS_44412_Unigene_72471_Transcript_129469	1.446338437	No Blast Hit
CDS_24740_Unigene_38997_Transcript_68010	1.444912849	PSS08141.1Protein ABHD17C like
CDS_26840_Unigene_41765_Transcript_73117	1.443096424	BAG92142.1unnamed protein product
CDS_29009_Unigene_44685_Transcript_78539	1.442994994	RWR72392.1CRC domain-containing protein
CDS_7685_Unigene_18641_Transcript_32124	1.44207877	XP_031273992.1mannose-1-phosphate guanylyltransferase 1 isoform X1
CDS_28403_Unigene_43870_Transcript_77036	1.441878789	XP_030524837.1serine/threonine-protein kinase SAPK3-like
CDS_18443_Unigene_3116_Transcript_5113	1.440985203	RRT42161.1 protein B296_00057338
CDS_33806_Unigene_51723_Transcript_91102	1.440702902	XP_008799798.1protein trichome birefringence-like 33
CDS_15594_Unigene_27838_Transcript_48167	1.438545332	RWR79201.1cytokinin riboside 5'-monophosphate phosphoribohydrolase LOG1 isoform X1
CDS_27279_Unigene_42379_Transcript_74286	1.438094443	XP_031273821.1root phototropism protein 3
CDS_45560_Unigene_75363_Transcript_135076	1.437702561	No Blast Hit
CDS_8318_Unigene_19383_Transcript_33360	1.437665562	PIA64590.1 protein AQUCO_00100221v1
CDS_29012_Unigene_44688_Transcript_78542	1.437405312	RWR72392.1CRC domain-containing protein

Transcript ID	Log2 Fold Change	Hit desc.
CDS_41363_Unigene_65352_Transcript_115869	1.437405312	No Blast Hit
CDS_4424_Unigene_14954_Transcript_25529	1.437405312	RVX11019.13-hydroxyisobutyryl-CoA hydrolase-like protein 3, mitochondrial
CDS_27212_Unigene_4227_Transcript_7063	1.437015658	No Blast Hit
CDS_14748_Unigene_26852_Transcript_46439	1.43678413	XP_002281406.1: S-adenosylmethionine-dependent methyltransferase At5g37990
CDS_44410_Unigene_7246_Transcript_12136	1.435753686	XP_020241709.1ruBisCO large subunit-binding protein subunit beta, chloroplastic-like
CDS_5491_Unigene_16183_Transcript_27703	1.435406289	XP_021652480.1D-amino-acid transaminase, chloroplastic
CDS_10299_Unigene_21660_Transcript_37393	1.435361628	XP_018678376.1: 60S ribosomal protein L6-like
CDS_46435_Unigene_7778_Transcript_12971	1.435064483	RWR97456.1low-temperature-induced cysteine proteinase-like protein
CDS_32978_Unigene_50495_Transcript_88923	1.434990759	RWR85351.1ecdysone-induced protein 75B-like protein
CDS_11406_Unigene_22962_Transcript_39712	1.433850415	XP_006832965.1mitochondrial import inner membrane translocase subunit TIM8 isoform X2
CDS_14054_Unigene_26027_Transcript_44994	1.433710829	XP_028097476.1KRR1 small subunit processome component
CDS_28137_Unigene_43538_Transcript_76442	1.433584234	ABR17957.1unknown
CDS_5380_Unigene_1605_Transcript_2692	1.432716667	OVA08754.1Nucleotidyl transferase
CDS_15865_Unigene_28162_Transcript_48709	1.432254664	XP_006448965.1putative hydrolase C777.06c
CDS_30105_Unigene_46220_Transcript_81316	1.431691661	No Blast Hit
CDS_41414_Unigene_65481_Transcript_116106	1.431691661	No Blast Hit
CDS_1971_Unigene_1220_Transcript_2082	1.431354196	XP_024165149.1 arabinose 5-phosphate isomerase
CDS_16551_Unigene_28979_Transcript_50176	1.430787434	XP_034679126.1thioredoxin 1
CDS_20722_Unigene_33898_Transcript_58864	1.430571121	OVA01411.1Alpha/beta hydrolase fold-1
CDS_33713_Unigene_51603_Transcript_90889	1.430093107	OVA01922.1PMR5 N-terminal domain
CDS_984_Unigene_11092_Transcript_18606	1.429543195	OVA02439.1HR-like lesion-inducer
CDS_25458_Unigene_39935_Transcript_69762	1.428626208	XP_010244354.1: IAA-amino acid hydrolase ILR1-like 1
CDS_41978_Unigene_66798_Transcript_118535	1.427252596	No Blast Hit
CDS_23184_Unigene_36951_Transcript_64404	1.427015174	OMP10400.1 protein COLO4_04541
CDS_33120_Unigene_50673_Transcript_89236	1.426656071	KDO78207.1 protein CISIN_1g015722mg
CDS_40782_Unigene_64133_Transcript_113620	1.425874335	VAI07605.1unnamed protein product
CDS_47312_Unigene_80558_Transcript_145722	1.424805276	XP_011100260.1uncharacterized protein LOC105178478

Transcript ID	Log2 Fold Change	Hit desc.
CDS_21000_Unigene_34207_Transcript_59488	1.424303992	XP_034703118.1ferroptosis suppressor protein 1-like isoform X1
CDS_28278_Unigene_43713_Transcript_76749	1.42410849	RWR96148.1putative receptor-like protein kinase
CDS_47849_Unigene_8224_Transcript_13684	1.423961347	XP_008792589.1myb family transcription factor EFM
CDS_21766_Unigene_35155_Transcript_61145	1.423662999	OVA02825.1protein of unknown function DUF221
CDS_20869_Unigene_34071_Transcript_59235	1.423544454	XP_027089657.160S ribosomal protein L32-1
CDS_19459_Unigene_32376_Transcript_56234	1.422649586	KAF2283084.1 protein GH714_043407
CDS_21907_Unigene_35328_Transcript_61454	1.422454971	RWR73284.1putative glucuronoxylan glucuronosyltransferase IRX7
CDS_41550_Unigene_6581_Transcript_10996	1.422347693	OWM82819.1 protein CDL15_Pgr029180
CDS_10913_Unigene_22384_Transcript_38659	1.422024622	RWR75140.1lysosomal beta glucosidase-like protein
CDS_2241_Unigene_12511_Transcript_21129	1.422024622	XP_010049937.2: protein PGR
CDS_24145_Unigene_38232_Transcript_66595	1.420803345	XP_019053649.1: xyloglucan 6-xylosyltransferase 5
CDS_27702_Unigene_42924_Transcript_75309	1.420051746	KAE8124359.1 protein FH972_019256
CDS_1816_Unigene_12028_Transcript_20247	1.419844715	KAF5186269.1Adenine nucleotide alpha hydrolases-like superfamily protein
CDS_18388_Unigene_31103_Transcript_53939	1.419371389	XP_022737984.1vacuolar protein sorting-associated protein 25
CDS_19490_Unigene_32409_Transcript_56300	1.419371389	OVA17382.1Peptidase S10
CDS_20086_Unigene_33156_Transcript_57585	1.419371389	No Blast Hit
CDS_37200_Unigene_57377_Transcript_101390	1.419371389	No Blast Hit
CDS_1058_Unigene_11182_Transcript_18742	1.419228866	No Blast Hit
CDS_36772_Unigene_56613_Transcript_100057	1.419188689	No Blast Hit
CDS_2696_Unigene_129_Transcript_199	1.418901991	XP_020083486.1vacuolar amino acid transporter 1 isoform X1
CDS_45051_Unigene_74035_Transcript_132470	1.418822481	XP_010277803.1: endoglucanase 12-like
CDS_22649_Unigene_36246_Transcript_63134	1.418463749	XP_020082413.1 E3 ubiquitin-protein ligase ARI7 isoform X2
CDS_39474_Unigene_61633_Transcript_109102	1.418023202	RWR87427.1NUDIX hydrolase domain-containing protein
CDS_7154_Unigene_18024_Transcript_30979	1.417784848	PIA59624.1 protein AQUCO_00400487v1
CDS_13430_Unigene_25294_Transcript_43778	1.415494803	TQD92549.1 protein C1H46_021885
CDS_23896_Unigene_37880_Transcript_65996	1.414974266	XP_010917610.1UPF0481 protein At3g47200-like
CDS_25468_Unigene_39948_Transcript_69780	1.414974266	XP_031259659.1pathogen-related protein-like
CDS_26265_Unigene_40989_Transcript_71734	1.414741592	RWR82855.1O-FucT domain-containing protein

Transcript ID	Log2 Fold Change	Hit desc.
CDS_39301_Unigene_61310_Transcript_108526	1.414741592	XP_010251861.1: calmodulin-binding protein 25-like
CDS_43359_Unigene_69857_Transcript_124352	1.41441367	XP_022135895.1proline-rich receptor-like protein kinase PERK2
CDS_12166_Unigene_23840_Transcript_41200	1.413580052	RWR72683.1ADP,ATP carrier protein 1, mitochondrial-like protein
CDS_32123_Unigene_4922_Transcript_8223	1.412766026	No Blast Hit
CDS_302_Unigene_10312_Transcript_17256	1.412506011	XP_010920265.1putative HVA22-like protein g isoform X2
CDS_8886_Unigene_20045_Transcript_34552	1.411343016	XP_028759386.1dihydroceramide fatty acyl 2-hydroxylase FAH1-like
CDS_18245_Unigene_30949_Transcript_53659	1.41074968	AEA72605.1mevalonate 5-diphosphate decarboxylase
CDS_49188_Unigene_86658_Transcript_160804	1.41074968	XP_016463977.1: alpha-L-fucosidase 1-like
CDS_34728_Unigene_53220_Transcript_93920	1.410691363	No Blast Hit
CDS_35619_Unigene_54701_Transcript_96517	1.410269182	PIM98415.1Germacradienol synthase
CDS_29563_Unigene_45443_Transcript_79895	1.409872129	No Blast Hit
CDS_20020_Unigene_3307_Transcript_5446	1.40937808	XP_034677299.1uncharacterized protein LOC117907762
CDS_30352_Unigene_4658_Transcript_7790	1.408756252	TXG59860.1 protein EZV62_014433
CDS_27631_Unigene_42834_Transcript_75145	1.408608048	No Blast Hit
CDS_39705_Unigene_62075_Transcript_109895	1.408069307	XP_008776598.1CO(2)-response secreted protease-like
CDS_38647_Unigene_60032_Transcript_106200	1.406827535	XP_010259530.1: blue-light photoreceptor PHR2
CDS_17248_Unigene_29780_Transcript_51615	1.405696453	XP_024462110.1sucrose transport protein SUC3 isoform X3
CDS_30564_Unigene_46897_Transcript_82535	1.405696453	RWR72093.1Alpha crystallin/Hsp20 domain-containing protein
CDS_45052_Unigene_74036_Transcript_132471	1.405124975	XP_010277803.1: endoglucanase 12-like
CDS_40923_Unigene_64430_Transcript_114192	1.404762367	XP_021604837.1phosphoenolpyruvate carboxylase 2 isoform X1
CDS_38368_Unigene_59544_Transcript_105306	1.404724614	No Blast Hit
CDS_73_Unigene_10083_Transcript_16864	1.404672902	XP_012073123.1pyrophosphate-energized vacuolar membrane proton pump
CDS_16120_Unigene_28448_Transcript_49195	1.404288258	KAA8535752.1 protein F0562_030746
CDS_44588_Unigene_72911_Transcript_130277	1.40426022	KAF5181626.1Reticulon-like protein b9
CDS_8253_Unigene_19305_Transcript_33235	1.404135939	XP_010908836.1filament-like plant protein 4 isoform X1
CDS_18636_Unigene_31402_Transcript_54479	1.403946671	KAE8125328.1 protein FH972_020150
CDS_13990_Unigene_25952_Transcript_44874	1.403348698	TYH62498.1 protein ES332_D07G124000v1
CDS_1583_Unigene_11788_Transcript_19819	1.403256032	RRT53990.1 protein B296_00043077

Transcript ID	Log2 Fold Change	Hit desc.
CDS_33977_Unigene_51987_Transcript_91550	1.402945842	THU73434.1 protein C4D60_Mb04t22810
CDS_48694_Unigene_84966_Transcript_156428	1.402343017	XP_010262122.1: zinc transporter 4, chloroplastic isoform X2
CDS_3469_Unigene_13868_Transcript_23559	1.402129838	PSS06150.1Septum-promoting GTP-binding protein
CDS_14606_Unigene_26696_Transcript_46200	1.401738439	PON71269.1Dihydroxyacetone kinase
CDS_36549_Unigene_56240_Transcript_99352	1.400879436	RWR77952.1nucleobase-ascorbate transporter 6
CDS_13094_Unigene_24929_Transcript_43105	1.399672665	RWR77574.1filament-like plant protein 7
CDS_39329_Unigene_61370_Transcript_108626	1.399270183	No Blast Hit
CDS_25648_Unigene_40180_Transcript_70172	1.398278981	No Blast Hit
CDS_37411_Unigene_57753_Transcript_102087	1.397308667	PIA39184.1 protein AQUCO_02700397v1
CDS_32493_Unigene_49813_Transcript_87712	1.397063154	RWR79171.1kinesin-like protein KIN-7E
CDS_31196_Unigene_47854_Transcript_84228	1.396926243	THU51544.1 protein C4D60_Mb06t32150
CDS_39779_Unigene_62209_Transcript_110137	1.396926243	PQM33129.1pentatricopeptide repeat-containing protein
CDS_6113_Unigene_16857_Transcript_28968	1.395857241	XP_018854606.1: ras-related protein RABA2a
CDS_6797_Unigene_17637_Transcript_30345	1.395354508	XP_034911316.1NADH dehydrogenase
CDS_11540_Unigene_23116_Transcript_39950	1.395046673	XP_008804291.2benzoate--CoA ligase, peroxisomal-like
CDS_28397_Unigene_43864_Transcript_77027	1.394530535	XP_031479715.1isopentenyl-diphosphate Delta-isomerase I
CDS_31186_Unigene_47840_Transcript_84205	1.394239937	No Blast Hit
CDS_28303_Unigene_43749_Transcript_76818	1.394108478	XP_034679469.1vascular-related unknown protein 4
CDS_39606_Unigene_61899_Transcript_109592	1.394108478	RWR95893.1fatty-acid-binding protein 2 isoform X2
CDS_18840_Unigene_31624_Transcript_54898	1.392937222	RWR92476.1purine permease 1
CDS_18919_Unigene_31726_Transcript_55075	1.392872412	GAY46225.1 protein CUMW_095350
CDS_6306_Unigene_17082_Transcript_29378	1.392748464	RWR94449.1pectin acetylesterase 10
CDS_9897_Unigene_21185_Transcript_36541	1.391638412	RWR73171.1acetyl-coenzyme A synthetase, chloroplastic/glyoxysomal-like protein
CDS_2558_Unigene_12854_Transcript_21727	1.390992505	XP_010271685.1: uncharacterized protein LOC104607691
CDS_14786_Unigene_26905_Transcript_46531	1.389523639	XP_019702859.1protein ROS1C isoform X7
CDS_26877_Unigene_41815_Transcript_73210	1.388622939	XP_006444469.1uncharacterized protein LOC18050077
CDS_16377_Unigene_2875_Transcript_4732	1.388381867	OMO61652.1 protein CCACVL1_23329
CDS_12305_Unigene_23998_Transcript_41462	1.387549106	BAG15861.1 protein
CDS_15181_Unigene_27361_Transcript_47311	1.386331128	RRT73847.1 protein B296_00021805

Transcript ID	Log2 Fold Change	Hit desc.
CDS_15677_Unigene_2794_Transcript_4605	1.386331128	EOY17918.1GATA type zinc finger transcription factor family protein isoform 3
CDS_16686_Unigene_29140_Transcript_50433	1.386331128	PIA30985.1 protein AQUCO_05300070v1
CDS_44599_Unigene_72933_Transcript_130321	1.386331128	PSS19151.1Protein NUCLEAR FUSION DEFECTIVE 6 like
CDS_10200_Unigene_21537_Transcript_37183	1.386014087	XP_006856410.16-phosphogluconate dehydrogenase, decarboxylating 1, chloroplastic
CDS_10442_Unigene_21814_Transcript_37671	1.385545845	RWR97010.1Glycosyl hydrolases 36
CDS_26828_Unigene_41750_Transcript_73081	1.384937892	No Blast Hit
CDS_27282_Unigene_42381_Transcript_74291	1.384801228	KNA15264.1 protein SOVF_099780
CDS_21935_Unigene_3536_Transcript_5815	1.384457656	RWR84937.1Cellulose synthase
CDS_26361_Unigene_41133_Transcript_71973	1.383813335	XP_010268064.1: calmodulin-binding protein 60 D-like isoform X2
CDS_820_Unigene_10901_Transcript_18307	1.38332864	XP_021687080.1putative lipase YOR059C isoform X4
CDS_50693_Unigene_9218_Transcript_15410	1.38332864	XP_028067444.1UDP-D-xylose:L-fucose alpha-1,3-D-xylosyltransferase MGP4-like
CDS_17993_Unigene_30656_Transcript_53155	1.38307815	XP_009383844.1: ribulose-phosphate 3-epimerase, cytoplasmic isoform
CDS_44112_Unigene_71757_Transcript_128041	1.382957528	XP_008809621.1cytochrome P450 71A1-like
CDS_5372_Unigene_1604_Transcript_2691	1.38288657	OVA08754.1Nucleotidyl transferase
CDS_39346_Unigene_61403_Transcript_108702	1.382291848	RWR92574.1heat stress transcription factor B-4-like protein
CDS_15932_Unigene_28226_Transcript_48815	1.38219667	PIA51892.1 protein AQUCO_01000041v1
CDS_2106_Unigene_12360_Transcript_20846	1.381448906	XP_010941684.1VQ motif-containing protein 22
CDS_3805_Unigene_14234_Transcript_24219	1.381134033	ESR61409.1 protein CICLE_v10016627mg
CDS_23242_Unigene_3701_Transcript_6103	1.381083898	KOM30362.1 protein LR48_Vigan1242s001700
CDS_11729_Unigene_23326_Transcript_40306	1.38016136	KDO72459.1 protein CISIN_1g0016361mg, partial
CDS_7237_Unigene_18121_Transcript_31165	1.379725874	XP_010263991.1: uncharacterized protein LOC104602116 isoform X2
CDS_8029_Unigene_19053_Transcript_32777	1.379658592	RRT70764.1 protein B296_00030471
CDS_21967_Unigene_35410_Transcript_61604	1.379224241	KNA18053.1 protein SOVF_073930 isoform B
CDS_24563_Unigene_38778_Transcript_67603	1.379224241	No Blast Hit
CDS_30243_Unigene_46435_Transcript_81712	1.379224241	XP_015870252.1uncharacterized protein LOC107407482 isoform X1
CDS_33699_Unigene_51579_Transcript_90848	1.379224241	VAI55183.1unnamed protein product
CDS_34569_Unigene_52964_Transcript_93418	1.379092301	No Blast Hit

Transcript ID	Log2 Fold Change	Hit desc.
CDS_31593_Unigene_48421_Transcript_85285	1.379028502	XP_010274121.1: potassium transporter 13
CDS_39527_Unigene_6172_Transcript_10257	1.376704249	XP_009404945.1: cytochrome c
CDS_39034_Unigene_60752_Transcript_107508	1.37632185	OVA16158.1UAA transporter
CDS_3899_Unigene_14336_Transcript_24382	1.375534482	THU51455.1 protein C4D60_Mb06t31230
CDS_22984_Unigene_36654_Transcript_63910	1.375423441	XP_031476820.1calmodulin-like protein 3
CDS_19595_Unigene_32554_Transcript_56555	1.373274975	KAF3772468.1B3 domain-containing protein
CDS_21841_Unigene_35236_Transcript_61288	1.373274975	No Blast Hit
CDS_37810_Unigene_58524_Transcript_103447	1.373274975	PQQ11539.1protein trichome birefringence
CDS_40691_Unigene_63968_Transcript_113316	1.373274975	ESR56190.1 protein CICLE_v100189891mg, partial
CDS_28680_Unigene_4420_Transcript_7397	1.372172418	XP_010269565.1: UDP-glucuronic acid decarboxylase 2-like
CDS_26898_Unigene_41839_Transcript_73271	1.371975835	KAB1227006.1E3 ubiquitin-protein ligase PUB22
CDS_21232_Unigene_34494_Transcript_59992	1.371749121	TYG37710.1 protein ES288_D13G163100v1
CDS_12717_Unigene_24496_Transcript_42348	1.371515805	XP_010260816.1: galactan beta-1,4-galactosyltransferase GALS3
CDS_4884_Unigene_15486_Transcript_26479	1.371255807	XP_016556067.1: mitogen-activated protein kinase homolog NTF4-like
CDS_2729_Unigene_13033_Transcript_22058	1.37105031	XP_010251199.1: E3 ubiquitin-protein ligase BOI-like
CDS_169_Unigene_10181_Transcript_17025	1.370962036	XP_030442845.1 galacturonosyltransferase-like 9
CDS_31911_Unigene_48896_Transcript_86147	1.37043642	PIA51832.1 protein AQUCO_01000011v1
CDS_16844_Unigene_29317_Transcript_50780	1.370341176	PIN17889.1Placental protein 11
CDS_22167_Unigene_35647_Transcript_62052	1.370291116	No Blast Hit
CDS_5497_Unigene_16190_Transcript_27716	1.370072543	AQK57578.1respiratory burst oxidase4
CDS_38179_Unigene_59186_Transcript_104659	1.369819416	ALT07954.1putative geranyl diphosphate synthase small subunit type II.A
CDS_23185_Unigene_36952_Transcript_64405	1.369354606	OMP10400.1 protein COLO4_04541
CDS_16315_Unigene_28691_Transcript_49612	1.369170577	RWR72884.1magnesium transporter MRS2-5
CDS_37716_Unigene_58341_Transcript_103140	1.368624866	No Blast Hit
CDS_23720_Unigene_37652_Transcript_65617	1.367075159	RWR81341.1zinc transporter 6, chloroplastic
CDS_21987_Unigene_35441_Transcript_61657	1.367015984	MQM03969.1 protein
CDS_43002_Unigene_6907_Transcript_11555	1.365921994	RWR77698.1tRNA-splicing ligase RtcB
CDS_9375_Unigene_205_Transcript_335	1.365803725	RWR84579.1protein canopy-1

Transcript ID	Log2 Fold Change	Hit desc.
CDS_45559_Unigene_75362_Transcript_135074	1.365539326	No Blast Hit
CDS_46699_Unigene_78620_Transcript_141685	1.365539326	No Blast Hit
CDS_8256_Unigene_19308_Transcript_33238	1.364712961	RWR79189.1filament-like plant protein 4
CDS_16381_Unigene_28763_Transcript_49772	1.363876277	PNX83792.1DNA-binding protein escarola-like
CDS_34340_Unigene_52566_Transcript_92642	1.363876277	XP_010920325.2BRCA1-associated RING domain protein 1
CDS_9776_Unigene_21050_Transcript_36311	1.36334244	XP_030507951.1syntaxin-132
CDS_1684_Unigene_11895_Transcript_20027	1.362804358	XP_009800428.1: uncharacterized protein LOC104246323
CDS_50701_Unigene_9220_Transcript_15412	1.362744307	XP_028067444.1UDP-D-xylose:L-fucose alpha-1,3-D-xylosyltransferase MGP4-like
CDS_13432_Unigene_25296_Transcript_43780	1.362303857	XP_024027175.1protein RCC2 homolog
CDS_30076_Unigene_46186_Transcript_81257	1.362303857	XP_028054326.1myosin-8-like
CDS_18748_Unigene_31528_Transcript_54732	1.36206952	AEW25885.1phenylalanine ammonia-lyase, partial
CDS_38120_Unigene_59062_Transcript_104434	1.36206952	No Blast Hit
CDS_7432_Unigene_18347_Transcript_31618	1.361989167	OVA00893.1Aminotransferase
CDS_5135_Unigene_15770_Transcript_26977	1.361924051	XP_023540807.1peroxiredoxin-2E-2, chloroplastic-like
CDS_18977_Unigene_31794_Transcript_55205	1.361302333	XP_010259397.1: dnaJ homolog subfamily B member 3 isoform X1
CDS_16994_Unigene_2948_Transcript_4845	1.360654271	OVA02821.1Nonaspanin (TM9SF)
CDS_10093_Unigene_21415_Transcript_36952	1.360285993	No Blast Hit
CDS_21198_Unigene_34453_Transcript_59926	1.360099586	XP_015875080.1dolichyl-diphosphooligosaccharide--protein glycosyltransferase subunit DAD1
CDS_21291_Unigene_34565_Transcript_60102	1.360099586	KAE9588766.1putative diphthine--ammonia ligase
CDS_44128_Unigene_7178_Transcript_12014	1.360099586	XP_010268836.1: F-box protein At1g61340-like
CDS_19284_Unigene_32157_Transcript_55870	1.359619454	RWR77524.1aldehyde dehydrogenase family 2 member C4
CDS_29581_Unigene_45487_Transcript_79971	1.358628199	OVA15930.1Cyclin
CDS_12278_Unigene_23969_Transcript_41403	1.358390738	RWR87463.1cyclin-U2-1-like protein
CDS_32874_Unigene_50365_Transcript_88711	1.357761976	RWR80554.1Mycolic acid cyclopropane synthase
CDS_13317_Unigene_25179_Transcript_43579	1.357416438	RWR79410.1Disease resistance protein TIR-NBS class

Transcript ID	Log2 Fold Change	Hit desc.
CDS_42251_Unigene_67386_Transcript_119601	1.357386102	KAF5183365.1Clt3 protein
CDS_16470_Unigene_28866_Transcript_49956	1.356786852	XP_010242673.1: putative GDP-L-fucose synthase 2
CDS_25972_Unigene_40600_Transcript_70954	1.355278546	PKI78763.1 protein CRG98_000830, partial
CDS_30547_Unigene_46866_Transcript_82476	1.35507038	XP_015871964.1AUGMIN subunit 1-like, partial
CDS_942_Unigene_11037_Transcript_18532	1.354896446	XP_002273970.1: CASP-like protein 5A2
CDS_49548_Unigene_87893_Transcript_165745	1.354415948	RWV99269.1 protein GW17_00037831
CDS_10518_Unigene_21922_Transcript_37852	1.353528627	XP_010278421.1: uncharacterized protein LOC104612629 isoform X2
CDS_8888_Unigene_20048_Transcript_34557	1.353341048	KAA8514817.1 protein F0562_017996
CDS_18926_Unigene_31732_Transcript_55091	1.352954991	CBI34813.3unnamed protein product, partial
CDS_155_Unigene_10169_Transcript_17004	1.352201527	RWR73694.1hydroxyproline O-galactosyltransferase GALT6-like protein
CDS_26772_Unigene_41679_Transcript_72952	1.350960389	RWR93217.1hydroxyproline O-galactosyltransferase HPGT1
CDS_28732_Unigene_44286_Transcript_77784	1.350283332	No Blast Hit
CDS_3411_Unigene_13808_Transcript_23450	1.350005196	XP_020083415.1 signal peptidase complex subunit 2 isoform X1
CDS_681_Unigene_10765_Transcript_18069	1.349158185	XP_030472436.1elicitor-responsive protein 3
CDS_2853_Unigene_13166_Transcript_22293	1.348910426	XP_022959090.1peroxisomal membrane protein PMP22
CDS_7136_Unigene_18005_Transcript_30941	1.34886523	XP_010276078.1: uncharacterized protein LOC104610918
CDS_18898_Unigene_31700_Transcript_55021	1.34745424	RWR89444.1MENTAL domain-containing protein
CDS_15322_Unigene_27535_Transcript_47605	1.347344214	KAE9593220.1putative Ulp1 peptidase
CDS_35309_Unigene_54180_Transcript_95617	1.346802764	No Blast Hit
CDS_39124_Unigene_60944_Transcript_107847	1.346802764	XP_010243795.1: beta-glucuronosyltransferase GlcAT14A
CDS_33849_Unigene_51793_Transcript_91216	1.346307927	XP_030932251.1BTB/POZ domain-containing protein At3g22104 isoform X1
CDS_33390_Unigene_51056_Transcript_89904	1.346195441	XP_010264632.1: delta(7)-sterol-C5(6)-desaturase-like
CDS_29980_Unigene_46032_Transcript_80971	1.345726527	XP_010272145.1: inactive receptor kinase At1g27190
CDS_34358_Unigene_52597_Transcript_92701	1.345096442	No Blast Hit
CDS_37279_Unigene_57509_Transcript_101619	1.343154987	RWR72257.1pistil-specific extensin-like protein

Transcript ID	Log2 Fold Change	Hit desc.
CDS_7031_Unigene_17899_Transcript_30760	1.339149191	ONM54281.1Ras-related protein RABA6a
CDS_43738_Unigene_7084_Transcript_11857	1.339025413	KDO45654.1 protein CISIN_1g0152451mg, partial
CDS_10912_Unigene_22383_Transcript_38656	1.338809973	OVA16561.1Glycoside hydrolase
CDS_816_Unigene_10898_Transcript_18300	1.338765444	XP_010246318.1: NADH dehydrogenase
CDS_49264_Unigene_8694_Transcript_14475	1.33860095	RWR92016.1transcription factor bHLH155-like protein isoform X1
CDS_37251_Unigene_57462_Transcript_101528	1.338341185	XP_010257044.1: UDP-glycosyltransferase 87A1-like
CDS_27241_Unigene_42322_Transcript_74171	1.337869639	XP_008777953.13-oxo-5-alpha-steroid 4-dehydrogenase 2
CDS_29562_Unigene_45442_Transcript_79894	1.33781398	No Blast Hit
CDS_45436_Unigene_75047_Transcript_134458	1.33752495	XP_009402406.1: uncharacterized protein LOC103986202
CDS_42502_Unigene_6797_Transcript_11368	1.337261996	No Blast Hit
CDS_31971_Unigene_48983_Transcript_86305	1.336749099	No Blast Hit
CDS_41448_Unigene_65550_Transcript_116262	1.336076357	XP_002270309.1: xyloglucan galactosyltransferase XLT2
CDS_27818_Unigene_43081_Transcript_75579	1.335800269	XP_011097994.1uncharacterized protein LOC105176787
CDS_26137_Unigene_40824_Transcript_71399	1.335725237	RWR72923.1Glycosyl transferase
CDS_28420_Unigene_43898_Transcript_77087	1.335604557	XP_012456528.1: eukaryotic translation initiation factor isoform 4E-2-like
CDS_18375_Unigene_31092_Transcript_53922	1.3355942	RWR89884.1PLAT domain-containing protein 3-like protein
CDS_38234_Unigene_59309_Transcript_104900	1.334635948	No Blast Hit
CDS_10915_Unigene_22386_Transcript_38661	1.334505405	OVA16561.1Glycoside hydrolase
CDS_33073_Unigene_50618_Transcript_89139	1.334505405	RWR78923.1SAM50-like protein SPAC17C9.06
CDS_39388_Unigene_61486_Transcript_108848	1.334311819	XP_022899246.1uncharacterized protein LOC111412539
CDS_44965_Unigene_73829_Transcript_132104	1.333583474	No Blast Hit
CDS_13347_Unigene_25207_Transcript_43621	1.332795906	PSS25982.1Proline-rich receptor-like protein kinase
CDS_15418_Unigene_27643_Transcript_47791	1.332795906	No Blast Hit
CDS_25640_Unigene_40170_Transcript_70159	1.33263299	OVA10602.1Phosphatidylinositol-4-phosphate 5-kinase
CDS_19553_Unigene_32498_Transcript_56449	1.332512106	MQL86968.1 protein
CDS_38185_Unigene_59193_Transcript_104669	1.332344711	No Blast Hit

Transcript ID	Log2 Fold Change	Hit desc.
CDS_28311_Unigene_43759_Transcript_76836	1.331695871	XP_010101534.1ATP synthase mitochondrial F1 complex assembly factor 1
CDS_19985_Unigene_3303_Transcript_5442	1.329829685	KAF3580873.1 protein DY000_02036139
CDS_49331_Unigene_87209_Transcript_162395	1.328880856	VAI86127.1unnamed protein product
CDS_11120_Unigene_22628_Transcript_39072	1.327039509	OAY82599.1putative gamma-glutamylcyclotransferase
CDS_31675_Unigene_48527_Transcript_85460	1.325656955	PKA64398.1Heat stress transcription factor A-2b
CDS_39076_Unigene_60825_Transcript_107638	1.325656955	RWR77627.1GDSL esterase/lipase APG-like protein
CDS_27703_Unigene_42925_Transcript_75311	1.325235914	KAE8124359.1 protein FH972_019256
CDS_17648_Unigene_30233_Transcript_52404	1.322340706	XP_028053344.1cyclin-D3-1-like
CDS_32356_Unigene_49608_Transcript_87362	1.321928095	POO01861.1sequence-specific DNA binding transcription factor
CDS_6581_Unigene_17392_Transcript_29922	1.321459915	XP_031493368.1proteasome subunit beta type-1
CDS_30403_Unigene_46654_Transcript_82104	1.321267671	RWR75531.1 protein CKAN_00391700
CDS_44060_Unigene_71644_Transcript_127805	1.321162942	No Blast Hit
CDS_48838_Unigene_8545_Transcript_14205	1.320468616	XP_010934325.1oxalate oxidase 1
CDS_21613_Unigene_34961_Transcript_60784	1.32009997	RWR95666.1BTB/POZ domain-containing protein
CDS_48742_Unigene_85115_Transcript_156827	1.319835716	No Blast Hit
CDS_50659_Unigene_9209_Transcript_15392	1.318233611	KAF5184405.1Brevis radix
CDS_51447_Unigene_9700_Transcript_16218	1.318233611	KAA3485322.1sodium/hydrogen exchanger 2-like
CDS_15183_Unigene_27363_Transcript_47313	1.317565542	XP_009386847.1: NAD(P)H:quinone oxidoreductase
CDS_38781_Unigene_60248_Transcript_106631	1.316967534	RWR93019.12,3-bisphosphoglycerate-dependent phosphoglycerate mutase
CDS_15440_Unigene_27669_Transcript_47844	1.315359716	XP_022860843.1ATP-dependent RNA helicase-like protein DB10 isoform X2
CDS_49409_Unigene_87398_Transcript_163185	1.315291791	XP_010277829.1: uncharacterized protein LOC104612189
CDS_30476_Unigene_46742_Transcript_82268	1.314722793	No Blast Hit
CDS_855_Unigene_10943_Transcript_18379	1.314065977	VAI47462.1unnamed protein product
CDS_44282_Unigene_72163_Transcript_128865	1.313773963	RWR76021.1BTB/POZ domain-containing protein
CDS_17870_Unigene_30512_Transcript_52901	1.313091273	XP_023880569.1xyloglucan galactosyltransferase XLT2-like

Transcript ID	Log2 Fold Change	Hit desc.
CDS_28597_Unigene_44107_Transcript_77469	1.310733509	MQM15369.1 protein
CDS_43325_Unigene_69779_Transcript_124211	1.310044214	XP_010266026.1: la-related protein 1C-like isoform X2
CDS_22796_Unigene_36416_Transcript_63465	1.309233613	RWR77896.1transcription factor FER-LIKE IRON DEFICIENCY-INDUCED TRANSCRIPTION FACTOR-like protein
CDS_36132_Unigene_55539_Transcript_98058	1.309144637	XP_010274701.1: peptidyl-prolyl cis-trans isomerase FKBP17-2, chloroplastic
CDS_27471_Unigene_42623_Transcript_74756	1.306160779	XP_028805136.1vacuolar protein sorting-associated protein 60.2
CDS_31619_Unigene_48450_Transcript_85336	1.306160779	KAF5181537.1Mizu-kussei
CDS_38072_Unigene_58962_Transcript_104235	1.306160779	RVW30117.1 protein CK203_083202
CDS_45172_Unigene_74331_Transcript_133023	1.306160779	XP_034691943.1monocopper oxidase-like protein SKU5 isoform X2
CDS_16805_Unigene_29267_Transcript_50686	1.306160779	XP_026404871.1galacturonokinase-like
CDS_26322_Unigene_41083_Transcript_71890	1.306160779	KAF2324054.1 protein GH714_006395
CDS_23754_Unigene_37691_Transcript_65694	1.30277814	PKI67661.1 protein CRG98_011874
CDS_47175_Unigene_80112_Transcript_144799	1.296312993	KAF5193493.15'-nucleotidase SurE

Chapter 6
Summary and Conclusions

Biological control agents like *Pochonia chlamydosporia* are gaining prominence as eco-friendly alternatives to chemical pesticides in sustainable agriculture. This nematophagous fungus not only parasitizes nematode eggs but also promotes plant growth, making it valuable for crops like black pepper. This study investigates the biocontrol potential of *P. chlamydosporia* through its secondary metabolites, assessing their antifungal and nematicidal properties while exploring the fungus's ability to enhance plant growth and defence.

Our research focused on assessing the root colonization ability of *P. chlamydosporia* in the dicotyledonous host plant, black pepper (*Piper nigrum* L.). The findings reveal that the endophytic properties of *P. chlamydosporia* significantly enhance root and shoot growth in black pepper plants. Additionally, the results showed a notable improvement in the uptake of nutrients, including nitrogen, phosphorus, potassium, calcium, magnesium, copper, manganese, iron, and zinc, in treated plants. This underscores the fungus's capacity to mineralize and mobilize both major and minor nutrients in the soil, thus supporting plant growth. Furthermore, the study demonstrated a significant increase in the production of IAA, siderophores, ammonia, extracellular enzymes, and the solubilization of phosphorus and zinc, highlighting the fungus's potential as a plant growth promoter. However, further studies are needed to evaluate potential trade-offs in colonization efficiency under natural field conditions.

The use of real-time PCR in this investigation demonstrated a speedy three-hour quantitative detection approach for the fungus, which was significantly faster than the typical two-week growth period necessary for colony development on selective media. Pot experiments demonstrated that *P. chlamydosporia* not only promotes black pepper growth but also has potential as a biofertilizer for increasing growth and yield in a number of agronomically important crops across diverse soil types. The findings

underscore the importance of integrating this fungus into crop management strategies, such as integrated pest management (IPM) systems, for broader agricultural applications.

This investigation lends support to the concept that *P. chlamydosporia* is a nematophagous fungus with considerable agronomic benefits, particularly its ability to promote plant development and suppress plant-parasitic nematodes. Our ultimate goal is to improve the biocontrol efficacy and crop growth enhancement of *P. chlamydosporia* under a variety of agricultural situations, contributing to sustainable farming methods. Practical field validation remains crucial to optimize its application under diverse environmental and cropping conditions.

The research emphasizes the potential of *P. chlamydosporia* as a source of bioactive secondary metabolites with antiviral, antifungal, and nematicidal characteristics. In this work, all the chemical components that contribute to the isolate's biocontrol function were recovered from *P. chlamydosporia* metabolites using ethyl acetate solvent systems. Our research indicates that *P. chlamydosporia* ethyl acetate extract exhibits a strong nematicidal effect on plant-parasitic nematodes, such as *Radopholus similis*. Quantitative data revealed that crude ethyl acetate extract exhibited the greatest nematicidal activity across all extract concentrations, highlighting its potential as a natural nematicide. However, non-target effects and environmental persistence of these metabolites require further investigation.

The identification of key compounds such as bisevertinol, enniatin I, and enniatin H provides potential leads for the development of novel nematicidal chemicals against plant-parasitic nematodes. These findings indicate that *P. chlamydosporia* could be used effectively in sustainable agricultural methods, notably in black pepper cultivation, to decrease plant-parasitic nematodes and increase crop yield. Further research into the mechanisms of action, as well as extensive field trials, are necessary to optimize the use of these metabolites for agricultural pest management.

Our research reveals that *P. chlamydosporia* colonization alters the transcriptome of black pepper roots, which has two advantages: better growth promotion and stronger

defence responses. The possibility of *P. chlamydosporia* as a biocontrol agent and a biofertilizer is highlighted by the overexpression of genes related to hormone signalling, nutrient absorption, and stress responses. Field trials would be essential to validate these transcriptomic changes and assess the scalability of these benefits in real-world agricultural systems.

Colonization resulted in moderate up-regulation of defence-related genes, notably those associated with the jasmonic acid (JA) and ethylene (ET) signalling pathways, which are critical in plant defence against biotic stress. The increased expression of genes involved in JA production, such as fatty acid desaturases and lipoxygenases, suggests that *P. chlamydosporia* stimulates systemic resistance mechanisms in the host plant. *P. chlamydosporia* has been demonstrated to activate defence mechanisms such as effector-triggered immunity (ETI) and pattern-triggered immunity (PTI), as evidenced by the overexpression of NBS-LRR genes, which are required for pathogen effector recognition.

Significant overexpression of genes involved in the biosynthesis of auxins, gibberellins, cytokinins, and brassinosteroids was found in our transcriptome data, underscoring the diverse ways in which *P. chlamydosporia* aids in the growth and development of plants. Furthermore, our research revealed a notable overexpression of genes related to the absorption of essential nutrients such as calcium, iron, phosphorus, potassium, and nitrogen. This aligns with previous research demonstrating that *P. chlamydosporia* promotes nutrient acquisition, potentially reducing the need for chemical fertilizers.

P. chlamydosporia, which improves plant growth and resilience, provides a promising alternative to chemical treatments consistent with sustainable agriculture practices. Future research should confirm these transcriptome findings in field settings and investigate challenges like potential competition with native microbiota, non-target effects, and environmental factors. This research establishes the groundwork for employing beneficial endophytes to increase crop output while reducing environmental impact.

This study confirms *P. chlamydosporia* as a promising biocontrol agent with dual functions: suppressing plant pathogens and promoting growth in black pepper. Key bioactive compounds, such as bisevertinol, enniatin I, and enniatin H, were identified with potential for nematicidal use. Transcriptomic analysis provided molecular insights into how the fungus boosts plant growth and defence, emphasizing its potential in sustainable pest management and crop resilience strategies.

Chapter 7

Recommendations

7.1 Introduction

The research undertaken on *Pochonia chlamydosporia* has elucidated its multifaceted potential as a biocontrol agent against plant-parasitic nematodes and as a plant growth promoter. This nematophagous fungus demonstrates remarkable adaptability in its saprophytic, parasitic, and endophytic phases, making it a versatile tool for sustainable agriculture. The study revealed its ability to parasitize nematode eggs effectively, significantly reducing nematode populations, while simultaneously enhancing plant growth through improved nutrient uptake and induced systemic resistance. These dual benefits underline its importance as a biological solution to the dual challenges of nematode infestation and suboptimal crop productivity.

The findings also highlight the critical role of *P. chlamydosporia* in modulating plant defense mechanisms, particularly through the upregulation of signaling pathways associated with jasmonic acid and salicylic acid. Moreover, its endophytic colonization of roots contributes to plant health by offering protection against soil-borne pathogens and promoting overall vigor. These attributes, coupled with its compatibility with a range of crops, establish *P. chlamydosporia* as a promising candidate for integration into existing agricultural practices.

Given the growing global demand for sustainable solutions in agriculture, the utilization of *P. chlamydosporia* presents an eco-friendly alternative to chemical nematicides, which are often associated with environmental and health concerns. By leveraging its biocontrol and growth-promoting capabilities, this fungus can contribute to reducing crop losses, enhancing yield, and ensuring long-term soil health. The outcomes of this research provide a solid foundation for its practical application in nematode management and offer a pathway toward sustainable agricultural practices.

The recommendations presented in this chapter aim to translate these findings into actionable strategies, focusing on the implementation of *P. chlamydosporia* in black pepper fields, development of commercial formulations, and identification of future research avenues to maximize its potential.

7.2 Application of *P. chlamydosporia* in Sustainable Agriculture

7.2.1 *Biocontrol potential and nematode management*

- Utilize *P. chlamydosporia* as a biocontrol agent for suppressing plant-parasitic nematodes in crops like black pepper, emphasizing reduced dependence on chemical nematicides.
- Leverage its natural antagonistic properties to manage nematodes while maintaining environmental health and reducing chemical residues in agricultural produce.

7.2.2 *Enhancing plant growth and nutrient uptake*

- Promote its role in improving root architecture, enhancing nutrient uptake, and stimulating systemic resistance.
- Encourage its application to diverse crops and stress-prone environments to boost resilience and productivity.

7.2.3 *Large-scale field trials*

- Conduct multi-location field trials under varied agro-climatic zones to validate its efficacy in real-world conditions.
- Refine its application techniques for different cropping systems based on trial outcomes.

7.2.4 *Development of multi-functional biofertilizers*

- Develop biofertilizer formulations integrating *P. chlamydosporia* with other beneficial microbes for broader action against pests and enhanced nutrient management.

- Prioritize eco-friendly and cost-effective solutions to replace or supplement chemical inputs.

7.3 Enhancing Agricultural Practices

7.3.1 *Integration into farming systems*

- Integrate *P. chlamydosporia* into both conventional and organic farming systems to ensure its adaptability and scalability.
- Reduce chemical input dependence in conventional setups by utilizing this biocontrol agent alongside other sustainable practices.

7.3.2 *Compatibility studies*

- Undertake compatibility studies with other biocontrol agents, biofertilizers, and agrochemicals to design integrated pest and nutrient management protocols.
- Identify synergistic interactions that can enhance its efficacy and broaden its application range.

7.3.3 *Standardization of techniques*

- Standardize inoculum production methods and application techniques such as seed coating, soil drenching, and foliar sprays.
- Develop crop-specific guidelines for dosage, application timing, and repeat treatments for maximum efficacy.

7.3.4 *Farmer training and awareness*

- Organize farmer training programs to familiarize growers with *P. chlamydosporia*-based solutions.
- Launch awareness campaigns and on-field demonstrations to build confidence in its practical benefits and economic viability.

7.4 Future Lines of Research

- Investigate molecular and biochemical mechanisms underlying nematode parasitism and plant growth-promotion traits.
- Identify and analyze genes responsible for endophytic colonization and induced systemic resistance.
- Explore secondary metabolites like bisevertinol and enniatins for potential development as natural pesticides, studying their mode of action, activity spectrum, and non-target effects.
- Perform comparative genomic and transcriptomic analyses of various *P. chlamydosporia* strains to uncover crop-specific and universal functionalities.
- Examine interactions with soil microbiota, environmental factors such as pH and moisture, and plant roots to understand its ecological behavior.
- Conduct multi-season trials to evaluate its sustainability and long-term impact on soil health, nematode populations, and crop yields.
- Extend research to include monocots and economically important dicot crops to establish its broad-spectrum applicability.
- Focus on how *P. chlamydosporia* modulates black pepper's defense mechanisms and identify key genes and pathways activated during fungal colonization and nematode suppression.

7.5 Commercialization and Policy Recommendations

7.5.1 *Product development*

- Facilitate the creation of biofertilizers and biopesticides based on *P. chlamydosporia*, emphasizing its biocontrol and plant growth-promotion properties.

7.5.2 *Regulatory streamlining*

- Advocate for simplified and transparent regulatory frameworks to streamline the registration and commercialization of bio-based products.

7.5.3 *Government Incentives*

- Recommend subsidies and incentives for farmers adopting eco-friendly agricultural solutions, promoting *P. chlamydosporia* as a sustainable alternative to chemical inputs.

7.5.4 *Public-Private Partnerships*

- Encourage collaboration between research institutions, agri-biotech firms, and farmer cooperatives to accelerate the development and dissemination of *P. chlamydosporia*-based products.

7.5.5 *Capacity building*

- Develop infrastructure and expertise for large-scale production and field application of *P. chlamydosporia*.
- Train extension workers and agricultural advisors to support the adoption of biocontrol technologies.

7.6 Conclusion

P. chlamydosporia emerges as a promising cornerstone in the pursuit of sustainable agriculture, offering an effective, eco-friendly solution to the twin challenges of nematode management and soil fertility enhancement. Its dual role as a biocontrol agent and plant growth promoter positions it as a versatile tool for addressing critical agricultural constraints while reducing dependency on chemical inputs. By integrating *P. chlamydosporia* into farming practices, growers can enhance crop productivity, improve soil health, and foster resilience against pests and diseases.

However, unlocking the full potential of *P. chlamydosporia* demands a concerted interdisciplinary effort, combining molecular biology, soil science, agronomy, and

policy-making. Continued research into its molecular mechanisms, secondary metabolites, and interactions with plants and soil microbiomes will deepen our understanding and broaden its applicability. Field trials across diverse agro-climatic zones will help refine its use in real-world conditions, ensuring optimized outcomes for farmers.

Policy support is equally critical. Streamlined regulatory frameworks, incentives for bio-based solutions, and partnerships with agri-biotech firms will facilitate the commercialization and adoption of *P. chlamydosporia*-based products. Awareness campaigns and farmer training programs will empower stakeholders to embrace this biocontrol agent as a core component of integrated pest and nutrient management systems.

The journey toward sustainable agriculture is both urgent and complex. By harnessing the potential of *P. chlamydosporia*, we can make meaningful strides toward achieving this goal, benefiting farmers, ecosystems, and global food security alike.

REFERENCES

Abd-Elgawad, M. M. (2021). Optimizing safe approaches to manage plant-parasitic nematodes. *Plants, 10*(9), 1911.

Abd-Elgawad, M. M., & Askary, T. H. (2015). Impact of phytonematodes on agriculture economy. In *Biocontrol Agents of Phytonematodes* (pp. 3–49). Wallingford, UK: CABI.

Abd-Elgawad, M. M., & Askary, T. H. (2018). Fungal and bacterial nematicides in integrated nematode management strategies. *Egyptian Journal of Biological Pest Control, 28*(1), 1–24.

Abdel-Lateff, A., Fisch, K., & Wright, A. D. (2009). Trichopyrone and other constituents from the marine sponge-derived fungus Trichoderma sp. *Zeitschrift für Naturforschung C, 64*(3–4), 186–192.

Abe, N., Murata, T., Yamamoto, K., & Hirota, A. (1999). Bisorbibetanone, a novel oxidized sorbicillin dimer, with 1, 1-diphenyl-2-picrylhydrazyl radical scavenging activity from a fungus. *Tetrahedron letters*, *40*(28), 5203-5206.

Ahemad, M., & Kibret, M. (2014). Mechanisms and applications of plant growth-promoting rhizobacteria: Current perspective. *Journal of King Saud University-Science, 26*(1), 1–20.

Ahmad, N., Fazal, H., Abbasi, B. H., Farooq, S., Ali, M., & Khan, M. A. (2012). Biological role of Piper nigrum L. (Black pepper): A review. *Asian Pacific Journal of Tropical Biomedicine, 2*(3), S1945-S1953.

Al-Ani, L. K. T., Soares, F. E. D. F., Sharma, A., de Los Santos-Villalobos, S., Valdivia-Padilla, A. V., & Aguilar-Marcelino, L. (2022). Strategy of nematophagous fungi in determining the activity of plant-parasitic nematodes

and their prospective role in sustainable agriculture. *Frontiers in Fungal Biology, 3*, 863198.

Ali, Q., Khan, A. R., Tao, S., Rajer, F. U., Ayaz, M., Abro, M. A., … & Gao, X. (2023). Broad-spectrum antagonistic potential of Bacillus spp. volatiles against Rhizoctonia solani and Xanthomonas oryzae pv. oryzae. *Physiologia Plantarum, 175*(6), e14087.

Aly, A. H., Debbab, A., & Proksch, P. (2011). Fungal endophytes: Unique plant inhabitants with great promises. *Applied Microbiology and Biotechnology, 90*, 1829–1845.

Anandaraj, M. (2000). Diseases of black pepper. In P. N. Ravindran (Ed.), *Black Pepper, Piper nigrum L.* (pp. 239–268). Harwood Academic Publishers.

Anandaraj, M., Jose Abraham, J. A., & Balakrishnan, R. (1989). Crop loss due to foot rot disease of black pepper. *Indian Phytopathology*, *42*, 473-476.

Anandaraj, M., & Sarma, Y. R. (1995). Diseases of black pepper (*Piper nigrum L.*) and their management. *Journal of Spices and Aromatic Crops, 4*(1), 17–23.

Anders, S., & Huber, W. (2012). Differential expression of RNA-Seq data at the gene level–the DESeq package. *Heidelberg, Germany: European Molecular Biology Laboratory (EMBL)*, *10*, f1000research.

Andersson, K. M., Kumar, D., Bentzer, J., Friman, E., Ahrén, D., & Tunlid, A. (2014). Interspecific and host-related gene expression patterns in nematode-trapping fungi. *BMC Genomics, 15*, 1–15.

Angawi, R. F., Swenson, D. C., Gloer, J. B., & Wicklow, D. T. (2003). Lowdenic acid: a new antifungal polyketide-derived metabolite from a new fungicolous Verticillium sp. *Journal of natural products*, *66*(9), 1259-1262.

Aranda-Martinez, A., Lenfant, N., Escudero, N., Zavala-Gonzalez, E. A., Henrissat, B., & Lopez-Llorca, L. V. (2016). CAZyme content of *Pochonia*

chlamydosporia reflects that chitin and chitosan modification are involved in nematode parasitism. *Environmental Microbiology, 18*(11), 4200–4215.

Aravind, R., Kumar, A., Eapen, S. J., & Ramana, K. V. (2009). Endophytic bacterial flora in root and stem tissues of black pepper (*Piper nigrum L.*) genotype: Isolation, identification, and evaluation against *Phytophthora capsici*. *Letters in Applied Microbiology, 48*(1), 58–64.

Aro, N., Pakula, T., & Penttilä, M. (2005). Transcriptional regulation of plant cell wall degradation by filamentous fungi. *FEMS Microbiology Reviews, 29*(4), 719–739.

Askary, T. H., & Martinelli, P. R. P. (Eds.). (2015). *Biocontrol Agents of Phytonematodes*. CABI.

Aver, W. A., & Peña-Rodriguez, L. (1987). Minor metabolites of *Monocillium nordinii*. *Phytochemistry, 26*(5), 1353–1355.

Ayaz, M., Ali, Q., Farzand, A., Khan, A. R., Ling, H., & Gao, X. (2021). Nematicidal volatiles from *Bacillus atrophaeus* GBSC56 promote growth and stimulate induced systemic resistance in tomato against *Meloidogyne incognita*. *International Journal of Molecular Sciences, 22*(9), 5049.

Ayer, W. A., Lee, S. P., Tsuneda, A., & Hiratsuka, Y. (1980). The isolation, identification, and bioassay of the antifungal metabolites produced by *Monocillium nordinii*. *Canadian Journal of Microbiology, 26*(7), 766–773.

Bakshi, M., & Oelmüller, R. (2014). WRKY transcription factors: Jack of many trades in plants. *Plant Signaling & Behavior, 9*(2), e27700.

Barker, K. R., Carter, C. C., & Sasser, J. N. (Eds.). (1985). *An Advanced Treatise on Meloidogyne: Methodology* (Vol. 2). Department of Plant Pathology, North Carolina State University.

Barron, G. L. (1977). Nematophagous fungi: Endoparasites of *Rhabditis terricola*. *Microbial Ecology, 4*, 157–163.

Barron, G. L. (1984). *The Genera of Hyphomycetes from Soil* (Doctoral dissertation, University of Glasgow (United Kingdom).

Barron, G. L., & Onions, A. H. (1966). *Verticillium chlamydosporium* and its relationships to *Diheterospora*, *Stemphyliopsis*, and *Paecilomyces*. *Canadian Journal of Botany*, *44*(7), 861-869.

Batista, A. C., & Fonsêca, O. J. (1965). Publicação: Instituto de Micologia. *Pochonia humicola* n. gen. e n. sp., uma curiosa entidade fungica dos solos do Nordeste do Brasil. Univ. do Recife, Inst. de Micologia.

Benková, E., & Hejátko, J. (2009). Hormone interactions at the root apical meristem. *Plant Molecular Biology, 69*, 383-396.

Bhat, A. I., Biju, C. N., Srinivasan, V., Ankegowda, S. J., & Krishnamurthy, K. S. (2018). Current status of viral diseases affecting black pepper and cardamom. *Journal of Spices and Aromatic Crops, 27*, 1–16.

Bhat, A. I., Hareesh, P. S., & Madhubala, R. (2005). Sequencing of coat protein gene of an isolate of cucumber mosaic virus infecting black pepper (*Piper nigrum L*) in India. *Journal of Plant Biochemistry and Biotechnology, 14*, 37–40.

Bhattarai, K. K., Atamian, H. S., Kaloshian, I., & Eulgem, T. (2010). WRKY72-type transcription factors contribute to basal immunity in tomato and Arabidopsis as well as gene-for-gene resistance mediated by the tomato R gene *Mi-1*. *The Plant Journal, 63*(2), 229–240.

Bibb, M.J. (2005). Regulation of secondary metabolism in streptomycetes. *Current Opinion in Microbiology, 8*(2), 208–215.

Blakeman, J. P., & Parhery, D. G. (1977). Stimulation of appressorium formation in *Colletotrichum acutatum* by phylloplane bacteria. *Physiological Plant Pathology, 11*(3), 313–325.

Bolger, A.M., Lohse, M., & Usadel, B. (2014). Trimmomatic: A flexible trimmer for Illumina sequence data. *Bioinformatics, 30*(15), 2114-2120.

Boller, T., & Felix, G. (2009). A renaissance of elicitors: Perception of microbe-associated molecular patterns and danger signals by pattern-recognition receptors. *Annual Review of Plant Biology, 60*, 379-406.

Bowen, G. D., & Rovira, A. D. (1999). The rhizosphere and its management to improve plant growth. *Advances in Agronomy*, *66*, 1-102.

Brakhage, A.A. (2013). Regulation of fungal secondary metabolism. *Nature Reviews Microbiology, 11*(1), 21–32.

Bruin, G.C.A., & Edgington, L.V. (1981). Adaptive resistance in *Peronosporales* to metalaxyl. *Canadian Journal of Plant Pathology, 3*(4), 201–206.

Brundret, K.M., Dalziel, W., Hesp, B., Jarvis, J.A.J., & Neidle, S. (1972). X-Ray crystallographic determination of the structure of the antibiotic aphidicolin: A tetracyclic diterpenoid containing a new ring system. *Journal of the Chemical Society, Chemical Communications, 18,* 1027–1028.

Buchfink, B., Xie, C., & Huson, D.H. (2015). Fast and sensitive protein alignment using DIAMOND. *Nature Methods, 12*(1), 59-60.

Butler, E. J. (1906). The wilt disease of pigeon pea and pepper. *Agricultural Journal of India, 1*, 23–36.

Campos, M. L., Kang, J. H., & Howe, G. A. (2014). Jasmonate-triggered plant immunity. *Journal of Chemical Ecology, 40*, 657–675.

Cappucino, J., & Sherman, N. (1992). *Microbiology: A Laboratory Manual* (3rd ed.) (pp. 125–179). Benjamin Cumming Pub.

Casneuf, T., Van de Peer, Y., & Huber, W. (2007). In situ analysis of cross-hybridisation on microarrays and the inference of expression correlation. *BMC Bioinformatics, 8*, 1–13.

Castillo, J. D., Lawrence, K. S., & Kloepper, J. W. (2013). Biocontrol of the reniform nematode by *Bacillus firmus* GB-126 and *Paecilomyces lilacinus* 251 on cotton. *Plant Disease, 97*(7), 967–976.

Caverzan, A., Passaia, G., Rosa, S.B., Ribeiro, C.W., Lazzarotto, F., & Margis-Pinheiro, M. (2012). Plant responses to stresses: Role of ascorbate peroxidase in the antioxidant protection. *Genetics and Molecular Biology, 35*, 1011-1019.

Ceiro, W. G., Arévalo, J., Puertas, A. L., & Hidalgo-Díaz, L. (2014). Effect of NaCl concentrations on the mycelial growth of *Pochonia chlamydosporia* (Goddard) Zare and Gams in PDA medium and soil. *Revista de Prot. Veg, 29*, 122–127.

Chaturvedi, B., Tiwari, N., & Nirupama, N.B. (1988). A new insecticidal cyclodepsipeptide from *Beauveria bassiana* and *Verticillium lecanii*. *Agricultural and Biological Chemistry, 42*(3), 1229–1232.

Chaudhry, B., & Riazuddin, S. (2003). The use of CAMB biopesticides to control pests of rice (Oryza sativa). *Asian Journal of Plant Sciences*, *2*(15-16), 1079-1082.

Chaya, M.K., & Rao, M.S. (2012). Bio-management of *Meloidogyne incognita* on okra using a formulation of *Pochonia chlamydosporia*. *Pest Management in Horticultural Ecosystems, 18*(1), 84–87.

Cheong, Y.H., Chang, H.S., Gupta, R., Wang, X., Zhu, T., & Luan, S. (2002). Transcriptional profiling reveals novel interactions between wounding, pathogen, abiotic stress, and hormonal responses in Arabidopsis. *Plant Physiology, 129*(2), 661-677.

Chitwood, D. J. (2003). Research on plant-parasitic nematode biology conducted by the United States Department of Agriculture–Agricultural Research Service. *Pest Management Science, 59*(6-7), 748–753.

Ciancio, A. (1995). Observations on the nematicidal properties of some mycotoxins. *Fundamental and Applied Nematology, 18*(5), 451–454.

Ciancio, A., Colagiero, M., Ferrara, M., Nigro, F., Pentimone, I., & Rosso, L. C. (2013). Transcriptome changes in tomato roots during colonization by the

endophytic fungus *Pochonia chlamydosporia*. In *5th congress of European Microbiologists (FEMS), Leipzig, Germany*.

Ciancio, A., Pentimone, I., Colagiero, M., & Rosso, L. (2017). Regulatory factors in *Pochonia chlamydosporia*-induced gene expression. In R. H. Manzanilla-López & L. V. Lopez-Llorca (Eds.), *Perspectives in Sustainable Nematode Management Through Pochonia chlamydosporia Applications for Root and Rhizosphere Health* (pp. 99–109). Springer.

Ciancio, A., Pieterse, C. M., & Mercado-Blanco, J. (2019). Harnessing useful rhizosphere microorganisms for pathogen and pest biocontrol. *Frontiers in Microbiology, 10*, 1935.

Compant, S., Duffy, B., Nowak, J., Clément, C., & Ait Barka, E. (2005). Biocontrol of plant diseases using plant growth-promoting bacteria (PGPB): Principles, mechanisms of action and future prospects. *Appl. Environ. Microbiol*, *71*, 4951-4959.

Conesa, A., Götz, S., García-Gómez, J.M., Terol, J., Talón, M., & Robles, M. (2005). Blast2GO: A universal tool for annotation, visualization and analysis in functional genomics research. *Bioinformatics, 21*(18), 3674-3676.

Contreras-Cornejo, H. A., Macías-Rodríguez, L., Cortés-Penagos, C., & López-Bucio, J. (2009). *Trichoderma virens*, a plant-beneficial fungus, enhances biomass production and promotes lateral root growth through an auxin-dependent mechanism in Arabidopsis. *Plant Physiology, 149*(3), 1579–1592.

Cronin, D., Moenne-Loccoz, Y., Fenton, A., Dunne, C., Dowling, D. N., & O'Gara, F. (1997). Role of 2,4-diacetylphloroglucinol in the interactions of the biocontrol pseudomonad strain F113 with the potato cyst nematode *Globodera rostochiensis*. *Applied and Environmental Microbiology, 63*(4), 1357–1361.

D'Souza, G.I., Kumar, A.C., Viswanathan, P.K., & Shamanna, H.V. (1970). Relative distribution and prevalence of plant parasitic nematodes in the coffee tracts of South Western India. *Indian Coffee, 34*(12), 330.

Dababat, A. A., Sikora, R. A., & Hauschild, R. (2006). Use of *Trichoderma harzianum* and *Trichoderma viride* for the biological control of *Meloidogyne incognita* on tomato. *Communications in Agricultural and Applied Biological Sciences, 71*(3 Pt B), 953–961.

Dallemole-Giaretta, R., Freitas, L.G.D., Lopes, E.A., Silva, M.D.C.S.D., Kasuya, M.C.M., & Ferraz, S. (2015). *Pochonia chlamydosporia* promotes the growth of tomato and lettuce plants. *Acta Scientiarum. Agronomy, 37*, 417–423.

Davies, K., & Spiegel, Y. (Eds.). (2011). *Biological Control of Plant-Parasitic Nematodes:Building Coherence between Microbial Ecology and Molecular Mechanisms* (Vol. 11). Springer Science & Business Media.

de Oliveira, C. M., Almeida, N. O., Côrtes, M. V. D. C. B., Júnior, M. L., da Rocha, M. R., & Ulhoa, C. J. (2021). Biological control of *Pratylenchus brachyurus* with isolates of *Trichoderma* spp. on soybean. *Biological Control, 152*, 104425.

De Souza, R. A., Alves, F. R., De Oliveira, C. M. G., Rosa, J. M. O., Pinheiro, J. D. A., De Aguiar, G. P., & Moraes, W. B. (2021). Occurrence of *Meloidogyne arenaria* in black pepper (*Piper nigrum* L.) in the extreme south of the State of Bahia, Brazil. *Helminthologia, 58*(2), 213–216.

De Zelicourt Takahashi, H. (2013). Auxin biology in roots. *Plant Root, 7*, 49-64.

De Zelicourt, A., Al-Yousif, M., & Hirt, H. (2013). Rhizosphere microbes as essential partners for plant stress tolerance. *Molecular Plant, 6*(2), 242-245.

Decraemer, W., & Hunt, D. J. (2006). Structure and classification. In *Plant Nematology* (pp. 3–32). Wallingford, UK: CABI.

Deepa, S.P., Subramanian, S., & Ramakrishnan, S. (2011). Biomanagement of citrus nematode *Tylenchulus semipenetrans* Cobb on lemon, *Citrus limonia* L. *Journal of Biopesticides, 4*(2), 205.

Delmotte, P., & Delmotte-Plaquee, J. (1953). A new antifungal substance of fungal origin. *Nature, 171*(4347), 344–344.

Dias-Arieira, C.R., Santana, S.D.M., de Freitas, L.G., da Cunha, T.P., Biela, F., Puerari, H.H., & Chiamolera, F.M. (2011). Efficiency of *Pochonia chlamydosporia* in *Meloidogyne incognita* control in lettuce crop (*Lactuca sativa* L.). *Journal of Food, Agriculture and Environment, 9*(3-4), 561–563.

Dijksterhuis, J., Harder, W., Wyss, U., & Veenhuis, M. (1991). Colonization and digestion of nematodes by the endoparasitic nematophagous fungus *Drechmeria coniospora*. *Mycological Research, 95*(7), 873–878.

Dinesh, R., Anandaraj, M., Kumar, A., Bini, Y.K., Subila, K.P., & Aravind, R. (2015). Isolation, characterization, and evaluation of multi-trait plant growth promoting rhizobacteria for their growth promoting and disease suppressing effects on ginger. *Microbiological Research, 173*, 34–43.

Director, (1990). *Black Pepper- Package of Practices*. National Research Centre for Spices, Calicut, Kerala.

Dodds, P.N., & Rathjen, J.P. (2010). Plant immunity: Towards an integrated view of plant–pathogen interactions. *Nature Reviews Genetics, 11*(8), 539-548.

Drechsler, C. (1937). Some hyphomycetes that prey on free-living terricolous nematodes. *Mycologia, 29*(4), 447–552.

Duarte, M. D. L. R., & Archer, S. A. (2003). In vitro toxin production by *Fusarium solani* f. sp. *piperis*. *Fitopatologia Brasileira, 28*, 229–235.

Eapen, S. J., Beena, B., & Ramana, K. V. (2005). Tropical soil microflora of spice-based cropping systems as potential antagonists of root-knot nematodes. *Journal of Invertebrate Pathology*, *88*(3), 218-225.

Ebadi, M., Fatemy, S., & Riahi, H. (2009). Evaluation of *Pochonia chlamydosporia* var. *chlamydosporia* as a control agent of *Meloidogyne javanica* on pistachio. *Biocontrol Science and Technology, 19*(7), 689–700.

Ebadi, M., Fatemy, S., & Riahi, H. (2018). Biocontrol potential of *Pochonia chlamydosporia* var. *chlamydosporia* isolates against *Meloidogyne javanica* on pistachio. *Egyptian Journal of Biological Pest Control, 28*, 1–6.

Elhamouly, N. A., Hewedy, O. A., Zaitoon, A., Miraples, A., Elshorbagy, O. T., Hussien, S., … & Peng, D. (2022). The hidden power of secondary metabolites in plant-fungi interactions and sustainable phytoremediation. *Frontiers in Plant Science, 13*, 1044896.

Erwin, D. C., & Ribeiro, O. K. (1996). *Phytophthora Diseases Worldwide*. The American Phytopathological Society.

Escudero, N., & Lopez-Llorca, L. V. (2012). Effects on plant growth and root-knot nematode infection of an endophytic GFP transformant of the nematophagous fungus *Pochonia chlamydosporia*. *Symbiosis, 57*, 33–42.

Escudero, N., Ferreira, S. R., Lopez-Moya, F., Naranjo-Ortiz, M. A., Marin-Ortiz, A. I., Thornton, C. R., & Lopez-Llorca, L. V. (2016). Chitosan enhances parasitism of *Meloidogyne javanica* eggs by the nematophagous fungus *Pochonia chlamydosporia*. *Fungal Biology, 120*(4), 572–585.

Escudero, N., Lopez-Moya, F., Ghahremani, Z., Zavala-Gonzalez, E. A., Alaguero-Cordovilla, A., Ros-Ibañez, C., … & Lopez-Llorca, L. V. (2017). Chitosan increases tomato root colonization by *Pochonia chlamydosporia* and their combination reduces root-knot nematode damage. *Frontiers in Plant Science, 8*, 1415.

Esteves, I., & Devonshire, J. (2017). Biology and management of *Pochonia chlamydosporia* and plant-parasitic nematodes. In R. H. Manzanilla-Lopez & L. V. Lopez-Llorca (Eds.), *Perspectives in Sustainable Nematode Management Through Pochonia chlamydosporia Applications for Root and Rhizosphere Health* (pp. 47–76). Springer International Publishing.

Fosu-Nyarko, J., & Jones, M. G. (2016). Advances in understanding the molecular mechanisms of root lesion nematode host interactions. *Annual Review of Phytopathology, 54*(1), 253–278.

Freire, F. (1983). Interactions of Fungi and Nematodes on Black Pepper (*Piper nigrum* L.). Doctoral dissertation, University of London.

Freire, F. C. O., & Bridge, J. (1985). Histopathology of black pepper roots infected with *Radopholus similis*. *Fitopatologia Brasileira, 10*, 475–481.

Freitas, L.G., Dallemole-Giaretta, R., Ferraz, S., Zooca, R.J.F., & Podestá, G.S. (2009). Controle biológico de nematoides: Estudo de casos. In Zambolim, L. & Picanço, M.C. (Eds.), *Controle biológico de pragas e doenças: Exemplos práticos* (Vol. 1, pp. 41–82). Viçosa: Universidade Federal de Viçosa.

Gams, W., & Zare, R. Z. (2001). A revision of *Verticillium* sect. Prostrata. III. Generic classification. *Nova Hedwigia*, *72,* 329 - 337.

Gams, W., & Zare, R. Z. (2003). A taxonomic review of the clavicipitaceous anamorphs parasitizing nematodes and other microinvertebrates. In *Clavicipitalean Fungi* (pp. 26–81). Springer.

Gao, H., Qi, G., Yin, R., Zhang, H., Li, C., & Zhao, X. (2016). *Bacillus cereus* strain S2 shows high nematicidal activity against *Meloidogyne incognita* by producing sphingosine. *Scientific Reports, 6*(1), 28756.

Ghahremani, Z., Escudero, N., Saus, E., Gabaldón, T., & Sorribas, F. J. (2019). *Pochonia chlamydosporia* induces plant-dependent systemic resistance to *Meloidogyne incognita*. *Frontiers in Plant Science, 10*, 945.

Glick, B. R. (2012). Plant growth-promoting bacteria: mechanisms and applications. *Scientifica, 2012*(1), 963401.

Glick, B. R., Cheng, Z., Czarny, J., & Duan, J. (2007). Promotion of plant growth by ACC deaminase-producing soil bacteria. In P. A. H. M. Bakker, J. M. Raaijmakers, G. Bloemberg, M. Höfte, P. Lemanceau, & B. M. Cooke (Eds.),

New Perspectives and Approaches in Plant Growth-Promoting Rhizobacteria Research (pp. 329–341). Springer, Dordrecht.

Goddard, H. N. (1913). Can fungi living in agricultural soil assimilate free nitrogen? *Botanical Gazette*, *56*(4), 249-305.

Gordon, S.A., & Weber, R.P. (1951). Colorimetric estimation of indoleacetic acid. *Plant Physiology, 26*(1), 192.

Gouveia, A. D. S. (2018). *Análise de extratos fúngicos relacionados ao controle biológico de fitonematoides e à promoção de crescimento vegetal*. Universidade Federal de Viçosa, 71–75.

Gouveia, A.D.S., Monteiro, T.S.A., Valadares, S.V., Sufiate, B.L., de Freitas, L.G., Ramos, H.J.D.O., & de Queiroz, J.H. (2019). Understanding how *Pochonia chlamydosporia* increases phosphorus availability. *Geomicrobiology Journal, 36*(8), 747–751.

Gowen, S. R. (1997). Chemical control of nematodes: Efficiency and side-effects. In *Proceedings of the Expert Consultation on Plant Nematode Problems and Their Control in the Near East Region* (pp. 59–65). Karachi, Pakistan.

Gray, N. F. (2018). Fungi attacking vermiform nematodes. In *Diseases of Nematodes* (pp. 13–48). CRC Press.

Grove, J.F. (1984). 23, 24, 25, 26, 27-Pentanorlanost-8-en-3β, 22-diol from *Verticillium lecanii*. *Phytochemistry, 23*(8), 1721–1723.

Haegeman, A., Mantelin, S., Jones, J.T., & Gheysen, G. (2012). Functional roles of effectors of plant-parasitic nematodes. *Gene, 492*(1), 19–31.

Hague, N. G. M., & Gowen, S. R. (1987). Chemical control of nematodes. In R. H. Brown & B. R. Kerry (Eds.), *Principles and practice of nematode control in crops* (pp. 131–178). Academic Press.

Hammouti, B., Dahmani, M., Yahyi, A., Ettouhami, A., Messali, M., Asehraou, A., … & Touzani, R. (2019). Black pepper, the “King of Spices”: Chemical

composition to applications. *Arabian Journal of Chemistry and Environmental Research, 6*, 12–56.

Hamza, S., & Sadanandan, A. K. (2005). Effect of source and method of application of zinc on yield and quality of black pepper (*Piper nigrum* L.). *Journal of Spices and Aromatic Crops, 14*(2), 117–121.

Hayashi, A., Fujioka, S., Nukina, M., Kawano, T., Shimada, A., & Kimura, Y. (2007). Fumiquinones A and B, nematicidal quinones produced by *Aspergillus fumigatus*. *Bioscience, Biotechnology, and Biochemistry, 71*(7), 1697–1702.

Heintz, C. E., & Pramer, D. (1972). Ultrastructure of nematode-trapping fungi. *Journal of Bacteriology, 110*(3), 1163–1170.

Hellwig, V., Mayer-Bartschmid, A., Müller, H., Greif, G., Kleymann, G., Zitzmann, W., … & Stadler, M. (2003). Pochonins A−F, new antiviral and antiparasitic resorcylic acid lactones from *Pochonia chlamydosporia* var. *catenulata*. *Journal of Natural Products, 66*(6), 829–837.

Helmke, P.A., & Sparks, D.L. (1996). Lithium, sodium, potassium, rubidium, and cesium. *Methods of Soil Analysis: Part 3 Chemical Methods, 5*, 551–574.

Henschel, R., Lieber, M., Wu, L.S., Nista, P.M., Haas, B.J., & LeDuc, R.D. (2012). Trinity RNA-Seq assembler performance optimization. In Proceedings of the 1st Conference of the Extreme Science and Engineering Discovery Environment: Bridging from the extreme to the campus and beyond (pp. 1-8).

Hewitt, W. B., Raski, D. J., & Goheen, A. C. (1958). Nematode vector of soil-borne fanleaf virus of grapevines. *Phytopathology, 48*, 586–595.

Hider, R. C., & Kong, X. (2010). Chemistry and biology of siderophores. *Natural Product Reports, 27*(5), 637–657.

Hogenhout, S.A., Van der Hoorn, R.A., Terauchi, R., & Kamoun, S. (2009). Emerging concepts in effector biology of plant-associated organisms. *Molecular Plant-Microbe Interactions, 22*(2), 115–122.

Hoyos-Carvajal, L., Orduz, S., & Bissett, J. (2009). Growth stimulation in bean (*Phaseolus vulgaris* L.) by *Trichoderma*. *Biological Control, 51*(3), 409–416.

Huang, T.C., Chang, H.Y., Hsu, C.H., Kuo, W.H., Chang, K.J., & Juan, H.F. (2008). Targeting therapy for breast carcinoma by ATP synthase inhibitor aurovertin B. *Journal of Proteome Research, 7*(4), 1433–1444.

Huang, X., Zhao, N., & Zhang, K. (2004). Extracellular enzymes serving as virulence factors in nematophagous fungi involved in infection of the host. *Research in Microbiology, 155*(10), 811–816.

Hyun, U., Lee, D.H., Lee, C., & Shin, C.G. (2009). Apoptosis induced by enniatins H and MK1688 isolated from *Fusarium oxysporum* FB1501. *Toxicon, 53*(7–8), 723–728.

Islam, M. T., & Hossain, M. M. (2012). Plant probiotics in phosphorus nutrition in crops, with special reference to rice. In D. K. Maheswari (Ed.), *Bacteria in Agrobiology: Plant Probiotics* (pp. 325–363). Springer.

Jackson, D.S.M., & Johnson-Cicalese, J. (1988). A rapid staining method for detection of endophytic fungi in turf and forage grasses. *Phytopathology, 78*, 237–239.

Jackson, M. A., & Schisler, D. A. (1992). The composition and attributes of *Colletotrichum truncatum* spores are altered by the nutritional environment. *Applied and Environmental Microbiology, 58*(7), 2260–2265.

Jacobs, H., & Crump, D.H. (2003). Interactions between nematophagous fungi and consequences for their potential as biological agents for the control of potato cyst nematodes. *Mycological Research, 107*(1), 47–56.

Jasmer, D. P., Goverse, A., & Smant, G. (2003). Parasitic nematode interactions with mammals and plants. *Annual Review of Phytopathology, 41*(1), 245–270.

Jisha, V. N., Smitha, R. B., & Benjamin, S. (2013). An overview on the crystal toxins from *Bacillus thuringiensis*. *Advances in Microbiology, 3*(05), 462–472.

Jones, J. T., Haegeman, A., Danchin, E. G., Gaur, H. S., Helder, J., Jones, M. G., … & Perry, R. N. (2013). Top 10 plant-parasitic nematodes in molecular plant pathology. *Molecular Plant Pathology, 14*(9), 946–961.

Jones, L. M., Koehler, A. K., Trnka, M., Balek, J., Challinor, A. J., Atkinson, H. J., & Urwin, P. E. (2017). Climate change is predicted to alter the current pest status of *Globodera pallida* and *G. rostochiensis* in the United Kingdom. *Global Change Biology, 23*(11), 4497–4507.

Jones, M. G. K., & Goto, D. B. (2011). Root-knot nematodes and giant cells. In J. Jones, G. Gheysen, & C. Fenoll (Eds.), *Genomics and molecular genetics of plant–nematode interactions* (pp. 83–102). Dordrecht, The Netherlands: Springer.

Junior, A.F.C., Chagas, L.F.B., Martins, A.L.L., de Oliveira, R.S., & Luz, L.L. (2021). Phosphate solubilization, synthesis of Indole Acetic Acid, and effect on biomass soybean inoculated with *Pochonia*. *Brazilian Journal of Development, 7(7)*, 72919–72934.

Kadam, S. S., Rasam, D. V., Joshi, K. H., & Jadhav, A. D. (2020). Micropropagation of black pepper, cv. Panniyur-1: Standardization of sterilization protocol and media composition. *Global Journal of Bioscience and Biotechnology, 9*(2), 45–49.

Kamaruzzaman, M., Zheng, L., Zhou, S., Ye, W., Yuan, Y., Qi, Q., … & Wang, X. (2024). Evaluation of the novel endophytic fungus *Chaetomium ascotrichoides* 1-24-2 from *Pinus massoniana* as a biocontrol agent against pine wilt disease caused by *Bursaphelenchus xylophilus*. *Pest Management Science, 80*(10), 4924–4940.

Kantor, M., Handoo, Z., Kantor, C., & Carta, L. (2022). Top ten most important US-regulated and emerging plant-parasitic nematodes. *Horticulturae, 8*(3), 208.

Keeney, D.R., & Nelson, D.W. (1982). Nitrogen—inorganic forms. *Methods of Soil Analysis: Part 2 Chemical and Microbiological Properties, 9*, 643–698.

Keller, N. P., Turner, G., & Bennett, J. W. (2005). Fungal secondary metabolism—from biochemistry to genomics. *Nature Reviews Microbiology, 3*(12), 937–947.

Kepler, R. M., Humber, R. A., Bischoff, J. F., & Rehner, S. A. (2014). Clarification of generic and species boundaries for *Metarhizium* and related fungi through multigene phylogenetics. *Mycologia, 106*(4), 811–829.

Kerry, B. R. (1988). Two microorganisms for the biological control of plant parasitic nematodes. In *Proceedings British Crop Protection Conference-Pests and Diseases* (pp. 603–607). Brighton.

Kerry, B. R. (2000). Rhizosphere interactions and the exploitation of microbial agents for the biological control of plant-parasitic nematodes. *Annual Review of Phytopathology, 38*(1), 423–441.

Kerry, B. R., & Crump, D. H. (1977). Observations on fungal parasites of females and eggs of cereal cyst-nematode, *Heterodera avenae* and other cyst nematodes. *Nematologica, 23*(2), 193.

Kerry, B. R., & Irving, F. (1986). Variation between strains of the nematophagous fungus, verticillium chlamydosporium Goddard. Ii. Factors affecting parasitism of cyst nematode eggs. *Nematologica*, *32*(4), 474-485.

Kerry, B. R., Kirkwood, I. A., De Leij, F. A. A. M., Barba, J., Leijdens, M. B., & Brookes, P. C. (1993). Growth and survival of *Verticillium chlamydosporium* Goddard, a parasite of nematodes, in soil. *Biocontrol Science and Technology, 3*(3), 355–365.

Khabbaz, S. E., Ladhalakshmi, D., Babu, M., Kandan, A., Ramamoorthy, V., Saravanakumar, D., … & Kandasamy, S. (2019). Plant growth-promoting bacteria (PGPB)—a versatile tool for plant health management. *Canadian Journal of Pesticides and Pest Management, 1*(1), 1.

Khambay, B. P. S., Bourne, J. M., Cameron, S., Kerry, B. R., & Zaki, M. J. (2000). A nematicidal metabolite from *Verticillium chlamydosporium*. *Pest Management Science, 56*(12), 1098–1099.

Khan, A., Williams, K. L., & Nevalainen, H. K. (2004). Effects of *Paecilomyces lilacinus* protease and chitinase on the eggshell structures and hatching of *Meloidogyne javanica* juveniles. *Biological Control, 31*(3), 346–352.

Khan, M.R., Mohiddin, F.A., Ejaz, M.N., & Khan, M. (2012). Management of root-knot disease in eggplant through the application of biocontrol fungi and dry neem leaves. *Turkish Journal of Biology, 36(2)*, 161–169.

Khan, T.A., & Husain, S.I. (1989). Effect of culture filtrates of soil fungi on the mortality and hatching of reniform nematodes (*Rotylenchulus reniformis*). *Indian Journal of Nematology, 19*, 35–40.

Kifelew, H., & Adugna, G. (2018). Study on *Phytophthora capsici* cause of foot rot disease on black pepper (*Piper nigrum L.*), Tepi, Ethiopia. *International Journal of Research Studies in Agricultural Sciences, 4*(5), 1–7.

Kiontke, K., & Fitch, D. H. (2013). Nematodes. *Current Biology, 23*(19), R862–R864.

Klosterman, S. J., Rollins, J. R., Sudarshana, M. R., & Vinatzer, B. A. (2016). Disease management in the genomics era—Summaries of focus issue papers. *Phytopathology, 106*(10), 1068–1070.

Kohl, J., Kolnaar, R., & Ravensberg, W. J. (2019). Mode of action of microbial biological control agents against plant diseases: Relevance beyond efficacy. *Frontiers in Plant Science, 10,* 845.

Koshy, P. K., Eapen, S. J., & Pandey, R. P. (2005). Nematode parasites of spices, condiments, and medicinal plants. In *Plant Parasitic Nematodes in Subtropical and Tropical Agriculture* (pp. 751–791). Wallingford, UK: CABI Publishing.

Krasnoff, S. B., & Gupta, S. (1994). Identification of the antibiotic phomalactone from the entomopathogenic fungus *Hirsutella thompsonii* var. synnematosa. *Journal of Chemical Ecology, 20*(2), 293–302.

Krohn, K., Elsässer, B., Antus, S., Kónya, K., & Ammermann, E. (2003). Synthesis and structure-activity relationship of antifungal coniothyriomycin analogues. *The Journal of Antibiotics, 56*(3), 296–305.

Krohn, K., Sohrab, M.H., Draeger, S., & Schulz, B. (2008). New pyrenocines from an endophytic fungus. *Natural Product Communications, 3*(10), 1934578X0800301022.

Kroschel, J. (Ed.). (2002). *A Technical Manual for Parasitic Weed Research and Extension*. Springer Science & Business Media.

Kuć, J. (2001). Concepts and direction of induced systemic resistance in plants and its application. *European Journal of Plant Pathology, 107*(1), 7–12.

Kueh, T. K. (1990). Major diseases of black pepper and their management. *The Planter, 66*(772), 59–69.

Kumar, J., Schäfer, P., Hückelhoven, R., Langen, G., Baltruschat, H., Stein, E., … & Kogel, K. H. (2002). Bipolaris sorokiniana, a cereal pathogen of global concern: cytological and molecular approaches towards better control. *Molecular Plant Pathology, 3*(4), 185–195.

Kumari, P. S., & Gopalan, B. R. (2000). Status of fungal foliar diseases of black pepper in Kerala. In Ramana, K. V., Eapen, S. J., Babu, K. N., Krishnamurthy, K. S., & Kumar, A. (Eds.) *Spices and Aromatic Plants: Challenges and Opportunities in the New Century* (pp. 274–275). Indian Society for Spices.

Kuźniak, E., Kopczewski, T., & Chojak-Koźniewska, J. (2017). Ascorbate-glutathione cycle and biotic stress tolerance in plants. In: Hossain M., Munné-Bosch S., Burritt D., Diaz-Vivancos P., Fujita M., Lorence A. (eds.) *Ascorbic Acid in Plant Growth, Development and Stress Tolerance* (pp. 201-231). Springer; Cham, Switzerland.

Larriba, E., Jaime, M. D., Carbonell-Caballero, J., Conesa, A., Dopazo, J., Nislow, C., … & Lopez-Llorca, L. V. (2014). Sequencing and functional analysis of the genome of a nematode egg-parasitic fungus, *Pochonia chlamydosporia*. *Fungal Genetics and Biology, 65*, 69–80.

Larriba, E., Jaime, M. D., Nislow, C., Martín-Nieto, J., & Lopez-Llorca, L. V. (2015). Endophytic colonization of barley (*Hordeum vulgare*) roots by the nematophagous fungus *Pochonia chlamydosporia* reveals plant growth promotion and a general defense and stress transcriptomic response. *Journal of Plant Research, 128*(4), 665–678.

Larriba, E., Martín-Nieto, J., & Lopez-Llorca, L. V. (2012). Gene cloning, molecular modeling, and phylogenetics of serine protease P32 and serine carboxypeptidase SCP1 from nematophagous fungi *Pochonia rubescens* and *Pochonia chlamydosporia*. *Canadian Journal of Microbiology, 58*(7), 815–827.

Lasserre, F., Rivoal, R., & Cook, R. (1994). Interactions between *Heterodera avenae* and *Pratylenchus neglectus* on wheat. *Journal of Nematology, 26*(3), 336–340.

Lau, E. T., Tani, A., Khew, C. Y., Chua, Y. Q., & San Hwang, S. (2020). Plant growth-promoting bacteria as potential bio-inoculants and biocontrol agents to promote black pepper plant cultivation. *Microbiological Research, 240*, 126549.

Lawless, H. (1989). Pepper potency and the forgotten flavor sense. *Food Technology (Chicago), 43*(11), 52–58.

Leong, S. S., Leong, S. C. T., Pau, C. G., & Beattie, G. A. C. (2021). In vitro bioassay of *Purpureocillium lilacinum* and *Bacillus thuringiensis* for control of *Meloidogyne incognita* on black pepper (*Piper nigrum L.*) in Sarawak, Malaysia, Northern Borneo. *Journal of the Entomological Research Society, 23*(1), 41–59.

Li, C., Liu, G., Xu, C., Lee, G.I., Bauer, P., Ling, H.Q., & Howe, G.A. (2003). The tomato suppressor of prosystemin-mediated responses2 gene encodes a fatty acid desaturase required for the biosynthesis of jasmonic acid and the production of a systemic wound signal for defense gene expression. *The Plant Cell, 15*(7), 1646-1661.

Li, G-H., & Zhang, K-Q. (2014). Nematode-toxic fungi and their nematicidal metabolites. In Hyde, K.D., & Zhang, K-Q. (Eds.), *Nematode-Trapping Fungi* (pp. 313–375). Springer, Dordrecht Heidelberg, New York, London.

Li, J., Xu, C., Yang, S., Chen, C., Tang, S., Wang, J., & Xie, H. (2021). A venom allergen-like protein, RsVAP, the first discovered effector protein of *Radopholus similis* that inhibits plant defense and facilitates parasitism. *International Journal of Molecular Sciences, 22*(9), 4782.

Li, J., Yu, L., Yang, J., Dong, L., Tian, B., Yu, Z., … & Zhang, K. (2010). New insights into the evolution of subtilisin-like serine protease genes in Pezizomycotina. *BMC Evolutionary Biology, 10*, 1–14.

Li, Y., Hyde, K. D., Jeewon, R., Cai, L., Vijaykrishna, D., & Zhang, K. (2005). Phylogenetics and evolution of nematode-trapping fungi (Orbiliales) estimated from nuclear and protein-coding genes. *Mycologia, 97*(5), 1034–1046.

Lindsay, W.L., & Norvell, W. (1978). Development of a DTPA soil test for zinc, iron, manganese, and copper. *Soil Science Society of America Journal, 42(3)*, 421–428.

Liu, S. Q., Meng, Z. H., Yang, J. K., Fu, Y. X., & Zhang, K. Q. (2007). Characterizing structural features of cuticle-degrading proteases from fungi by molecular modeling. *BMC Structural Biology, 7*, 33.

Liu, X., Xiang, M., & Che, Y. (2009). The living strategy of nematophagous fungi. *Mycoscience, 50*(1), 20–25.

Lopez-Llorca, L. V. (1990). Purification and properties of extracellular proteases produced by the nematophagous fungus *Verticillium suchlasporium*. *Canadian Journal of Microbiology, 36*(8), 530–537.

Lopez-Llorca, L. V., & Robertson, W. M. (1992). Immunocytochemical localization of a 32-kDa protease from the nematophagous fungus *Verticillium suchlasporium* in infected nematode eggs. *Experimental Mycology, 16*(4), 261–267.

Lopez-Llorca, L. V., Gómez-Vidal, S., Monfort, E., Larriba, E., Casado-Vela, J., Elortza, F., … & Martín-Nieto, J. (2010). Expression of serine proteases in egg-parasitic nematophagous fungi during barley root colonization. *Fungal Genetics and Biology, 47*(4), 342–351.

Lopez-Llorca, L. V., Maciá-Vicente, J. G., & Jansson, H. B. (2008). Mode of action and interactions of nematophagous fungi. In *Integrated Management and Biocontrol of Vegetable and Grain Crops Nematodes* (pp. 51–76). Dordrecht: Springer Netherlands.

Lopez-Llorca, L. V., Olivares-Bernabeu, C., Salinas, J., Jansson, H. B., & Kolattukudy, P. E. (2002). Pre-penetration events in fungal parasitism of nematode eggs. *Mycological Research, 106*(4), 499–506.

Luambano, N. D., Manzanilla-López, R. H., Kimenju, J. W., Powers, S. J., Narla, R. D., Wanjohi, W. J., & Kerry, B. R. (2015). Effect of temperature, pH, carbon, and nitrogen ratios on the parasitic activity of *Pochonia chlamydosporia* on *Meloidogyne incognita*. *Biological Control, 80*, 23–29.

Lumsden, R.D., Frias, T.G., Gracia, E.R., & Dunn, M.T. (1982). Biocontrol of *Pythium aphanidermatum* on cucumber by microbial isolates from Mexican soils. *Phytopathology, 72*, 1010.

Maciá-Vicente, J. G., Rosso, L. C., Ciancio, A., Jansson, H. B., & Lopez-Llorca, L. V. (2009a). Colonization of barley roots by endophytic *Fusarium equiseti* and

Pochonia chlamydosporia: Effects on plant growth and disease. *Annals of Applied Biology, 155*(3), 391–401.

Maciá-Vicente, J.G., Jansson, H.B., Talbot, N.J., & Lopez-Llorca, L.V. (2009b). Real-time PCR quantification and live-cell imaging of endophytic colonization of barley (*Hordeum vulgare*) roots by *Fusarium equiseti* and *Pochonia chlamydosporia*. *New Phytologist, 182*(1), 213–228.

Magaldi, S., Mata-Essayag, S., De Capriles, C.H., Pérez, C., Colella, M.T., Olaizola, C., & Ontiveros, Y. (2004). Well diffusion for antifungal susceptibility testing. *International Journal of Infectious Diseases, 8*(1), 39–45.

Manohara, D., Mulya, K., & Wahyuno, D. (2004). Phytophthora disease on black pepper and the control measures. *Focus on Pepper, 1*, 37–49.

Manzanilla-López, R. H., Esteves, I., Finetti-Sialer, M. M., Hirsch, P. R., Ward, E., Devonshire, J., & Hidalgo-Díaz, L. (2013). *Pochonia chlamydosporia*: Advances and challenges to improve its performance as a biological control agent of sedentary endo-parasitic nematodes. *Journal of Nematology, 45*(1), 1.

Manzanilla-López, R. H., Esteves, I., Powers, S. J., & Kerry, B. R. (2011). Effects of crop plants on abundance of *Pochonia chlamydosporia* and other fungal parasites of root-knot and potato cyst nematodes. *Annals of Applied Biology, 159*(1), 118–129.

Manzanilla-López, R.H., & Lopez-Llorca, L.V. (Eds.). (2017). *Perspectives in Sustainable Nematode Management Through Pochonia chlamydosporia Applications for Root and Rhizosphere Health.* Springer.

Maruyama, Y., Yamoto, N., Suzuki, Y., Chiba, Y., Yamazaki, K.I., Sato, T., & Yamaguchi, J. (2013). The *Arabidopsis* transcriptional repressor ERF9 participates in resistance against necrotrophic fungi. *Plant Science, 213*, 79-87.

Mauchline, T.H., Kerry, B.R., & Hirsch, P.R. (2002). Quantification in soil and the rhizosphere of the nematophagous fungus *Verticillium chlamydosporium* by

competitive PCR and comparison with selective plating. *Applied and Environmental Microbiology, 68*(4), 1846–1853.

McClure, M. A., & Bird, A. F. (1976). The tylenchid (Nematoda) egg shell: Formation of the egg shell in *Meloidogyne javanica*. *Parasitology, 72*(1), 29–39.

McGlacken, G. P., & Fairlamb, I. J. (2005). 2-Pyrone natural products and mimetics: Isolation, characterization, and biological activity. *Natural Product Reports, 22*(3), 369–385.

Medeiros, H. D., Resende, R. S., Ferreira, F. C., Freitas, L. G., & Rodrigues, F. Á. (2015). Induction of resistance in tomato against *Meloidogyne javanica* by *Pochonia chlamydosporia*. *Nematoda, 2*, 10015–10022.

Meng, J., Wang, X., Xu, D., Fu, X., Zhang, X., Lai, D., … & Zhang, G. (2016). Sorbicillinoids from fungi and their bioactivities. *Molecules, 21*(6), 715.

Mesa-Valle, C. M., Garrido-Cardenas, J. A., Cebrian-Carmona, J., Talavera, M., & Manzano-Agugliaro, F. (2020). Global research on plant nematodes. *Agronomy, 10*(8), 1148.

Mhatre, P. H., Malik, S. K., Kaur, S., Singh, A. K., Mohan, S., & Sirohi, A. (2015). Histopathological changes and evaluation of resistance in Asian rice (*Oryza sativa* L.) against rice root-knot nematode, *Meloidogyne graminicola* Golden and Birch. *Indian Journal of Genetics and Plant Breeding, 75*(1), 41–48.

Mi, Q., Yang, J., Ye, F., Gan, Z., Wu, C., Niu, X., … & Zhang, K. Q. (2010). Cloning and overexpression of *Pochonia chlamydosporia* chitinase gene *pcchi44*, a potential virulence factor in infection against nematodes. *Process Biochemistry, 45*(5), 810–814.

Mian, I. H. (1998). *Introduction to Nematology*. IPSA, Gazipur, Bangladesh, 29–66.

Migunova, V. D., & Sasanelli, N. (2021). Bacteria as a biocontrol tool against phytoparasitic nematodes. *Plants, 10*(2), 389.

Milagres, A.M., Machuca, A., & Napoleao, D. (1999). Detection of siderophore production from several fungi and bacteria by a modification of chrome azurol S (CAS) agar plate assay. *Journal of Microbiological Methods, 37*(1), 1–6.

Minato, H., Matsumoto, M., & Katayama, T. (1973). Studies on the metabolites of *Verticillium* sp. Structures of verticillins A, B, and C. *Journal of the Chemical Society, Perkin Transactions 1,* 1819–1825.

Mingot-Ureta, C., Lopez-Moya, F., & Lopez-Llorca, L. V. (2020). Isolates of the nematophagous fungus *Pochonia chlamydosporia* are endophytic in banana roots and promote plant growth. *Agronomy, 10*(9), 1299.

Mo, M., Xu, C., & Zhang, K. (2005). Effects of carbon and nitrogen sources, carbon-to-nitrogen ratio, and initial pH on the growth of the nematophagous fungus *Pochonia chlamydosporia* in liquid culture. *Mycopathologia, 159*, 381–387.

Mohanakumaran, B., & Cheeran, A. (1981). Nutritional requirement of pepper vine trailed on living and dead standards. *Agricultural Research Journal of Kerala, 19*, 3–5.

Mohandas, C., & Ramana, K. V. (1987). Slow wilt disease of black pepper and its control. *Indian Cocoa, Arecanut and Spices Journal, 11*, 10–11.

Mohandas, C., & Ramana, K. V. (1991). Pathogenicity of *Meloidogyne incognita* and *Radopholus similis* on black pepper (*Piper nigrum* L.). *Journal of Plantation Crops, 19*(1), 41–53.

Molinari, S., & Leonetti, P. (2019). Bio-control agents activate plant immune response and prime susceptible tomato against root-knot nematodes. *PloS One, 14*(12), e0213230.

Monfort, E., Lopez-Llorca, L. V., Jansson, H. B., Salinas, J., Park, J. O., & Sivasithamparam, K. (2005). Colonization of seminal roots of wheat and barley by egg-parasitic nematophagous fungi and their effects on *Gaeumannomyces graminis* var. *tritici* and development of root-rot. *Soil Biology and Biochemistry, 37*(7), 1229–1235.

Monteiro, T. S. A. (2013). Controle biológico do nematoide das galhas, *Meloidogyne javanica*, e promoção de crescimento vegetal com os fungos *Pochonia chlamydosporia* e *Duddingtonia flagrans*. MSc Dissertation, Universidade Federal de Viçosa, MG, Brazil.

Monteiro, T. S. A., Valadares, S. V., de Mello, I. N. K., Moreira, B. C., Kasuya, M. C. M., de Araújo, J. V., & de Freitas, L. G. (2018). Nematophagous fungi increasing phosphorus uptake and promoting plant growth. *Biological Control, 123*, 71–75.

Moosavi, M. R., & Zare, R. (2020). Fungi as biological control agents of plant-parasitic nematodes. In J.-M. Mérillon & K. G. Ramawat (Eds.), *Plant Defence: Biological Control* (pp. 333–384). Springer Cham.

Morgan-Jones, G., White, J. F., & Rodriguez-Kabana, R. (1984). Phytonematode pathology: Ultrastructural studies. I. Parasitism of *Meloidogyne arenaria* eggs by *Verticillium chlamydosporium*. *Nematropica, 13*, 245–260.

Moriya, Y., Itoh, M., Okuda, S., Yoshizawa, A.C., & Kanehisa, M. (2007). KAAS: an automatic genome annotation and pathway reconstruction server. *Nucleic Acids Research, 35*(suppl_2), W182-W185.

Morozova, O., Hirst, M., & Marra, M. A. (2009). Applications of new sequencing technologies for transcriptome analysis. *Annual Review of Genomics and Human Genetics, 10*(1), 135–151.

Morris, G.M., Goodsell, D.S., Halliday, R.S., Huey, R., Hart, W.E., Belew, R.K., & Olson, A.J. (1998). Automated docking using a Lamarckian genetic algorithm and an empirical binding free energy function. *Journal of Computational Chemistry, 19*(14), 1639–1662.

Morton, C. O., Hirsch, P. R., Peberdy, J. P., & Kerry, B. R. (2003). Cloning of and genetic variation in protease VCP1 from the nematophagous fungus *Pochonia chlamydosporia*. *Mycological Research, 107*(1), 38–46.

Moulin, E., Barluenga, S., & Winssinger, N. (2005). Concise synthesis of pochonin A, an HSP90 inhibitor. *Organic Letters, 7*(25), 5637–5639.

Muller, H. R. A. (1937). The Phytophthora foot rot of black pepper (*Piper nigrum* L.) in the Netherlandish Indies. Cited in *Review of Applied Mycology, 16*, 559.

Murali, M., Amruthesh, K. N., Sudisha, J., Niranjana, S. R., & Shetty, H. S. (2012). Screening for plant growth-promoting fungi and their ability for growth promotion and induction of resistance in pearl millet against downy mildew disease. *Journal of Phytology, 4*(5), 30–36.

Muthulakshmi, M., Kumar, S., Subramanian, S., & Anita, B. (2012). Compatibility of *Pochonia chlamydosporia* with other biocontrol agents and carbofuran. *Journal of Biopesticides, 5*, 243.

Mutz, K. O., Heilkenbrinker, A., Lönne, M., Walter, J. G., & Stahl, F. (2013). Transcriptome analysis using next-generation sequencing. *Current Opinion in Biotechnology, 24*(1), 22–30.

Nagesh, M., Hussaini, S. S., Ramanujam, B., & Rangeswaran, R. (2007). Molecular identification, characterization, variability, and infectivity of Indian isolates of the nematophagous fungus *Pochonia chlamydosporia*. *Nematologia Mediterranea, 35*, 47–56.

Nahar, K., Kyndt, T., De Vleesschauwer, D., Höfte, M., & Gheysen, G. (2011). The jasmonate pathway is a key player in systemically induced defense against root-knot nematodes in rice. *Plant Physiology, 157*(1), 305-316.

Nahar, P., Ghormade, V., & Deshpande, M. V. (2004). The extracellular constitutive production of chitin deacetylase in *Metarhizium anisopliae*: Possible edge to entomopathogenic fungi in the biological control of insect pests. *Journal of Invertebrate Pathology, 85*(2), 80–88.

Nambiar, K. K. N., & Sarma, Y. R. (1977). Wilt diseases of black pepper. *Journal of Plantation Crops, 5*, 92–98.

Nasu, É. D. G. C., Amora, D. X., Monteiro, T. S. A., Alves, P. S., de Podestá, G. S., Ferreira, F. C., & de Freitas, L. G. (2018). *Pochonia chlamydosporia* applied via seed treatment for nematode control in two soil types. *Crop Protection, 114*, 106–112.

Nicholson, R. L., & Moraes, W. B. (1980). Survival of *Colletotrichum graminicola*: Importance of the spore matrix. *Phytopathology, 70*(3), 255–261.

Nicol, J. M., Elekçioğlu, I. H., Bolat, N., & Rivoal, R. (2007). The global importance of the cereal cyst nematode (*Heterodera* spp.) on wheat and international approaches to its control. *Communications in Agricultural and Applied Biological Sciences, 72*(3), 677–686.

Nicol, J. M., Turner, S. J., Coyne, D. L., Nijs, L. d., Hockland, S., & Maafi, Z. T. (2011). Current nematode threats to world agriculture. In J. Jones, G. Gheysen, & C. Fenoll (Eds.), *Genomics and Molecular Genetics of Plant-Nematode Interactions* (pp. 21–43). Springer, Dordrecht.

Nilanonta, C., Isaka, M., Kittakoop, P., Saenboonrueng, J., Rukachaisirikul, V., Kongsaeree, P., & Thebtaranonth, Y. (2003). New diketopiperazines from the entomopathogenic fungus *Verticillium hemipterigenum* BCC 1449. *The Journal of Antibiotics, 56*(7), 647–651.

Nirmal Babu, K., Minoo, D., Geetha, S. P., Sumathi, V., & Praveen, K. (2007). Biotechnology of turmeric and related species. In *Turmeric: The Genus Curcuma* (pp. 107–127). CRC Press, Boca Raton, FL, USA.

Nisha, M. S., Anusree, S. S., & Sooraj, S. (2019). Efficacy of *Andrographis paniculata* (*Burm. f.*) Nees against root-knot nematode in pepper, *Piper nigrum* L. *Journal of Entomology and Zoology Studies, 7*, 539–545.

Niu, X. M. (2017). Secondary metabolites from *Pochonia chlamydosporia* and other species of *Pochonia*. In R. H. Manzanilla-López & L. V. López-Llorca (Eds.), *Perspectives in Sustainable Nematode Management through Pochonia*

chlamydosporia - Applications for Root and Rhizosphere Health (pp. 131–168). Springer International Publishing AG, Cham.

Niu, X. M., & Zhang, K. Q. (2011). *Arthrobotrys oligospora*: A model organism for understanding the interaction between fungi and nematodes. *Mycology, 2*(2), 59–78.

Niu, X. M., Wang, Y. L., Chu, Y. S., Xue, H. X., Li, N., Wei, L. X., … & Zhang, K. Q. (2010). Nematodetoxic aurovertin-type metabolites from a root-knot nematode parasitic fungus *Pochonia chlamydosporia*. *Journal of Agricultural and Food Chemistry, 58*(2), 828–834.

O'Bannon, J.H. (1977). Worldwide dissemination of *Radopholus similis* and its importance in crop production. *Journal of Nematology, 9*(1), 16.

Oberegger, H., Schoeser, M., Zadra, I., Abt, B., & Haas, H. (2001). SREA is involved in regulation of siderophore biosynthesis, utilization, and uptake in *Aspergillus nidulans*. *Molecular Microbiology, 41*(5), 1077–1089.

Olanrewaju, O. S., Glick, B. R., & Babalola, O. O. (2017). Mechanisms of action of plant growth-promoting bacteria. *World Journal of Microbiology and Biotechnology, 33*(11), 197.

Olivares-Bernabeu, C. M., & López-Llorca, L. V. (2002). Fungal egg-parasites of plant-parasitic nematodes from Spanish soils. *Revista Iberoamericana de Micología, 19*(2), 104–110.

Olsen, S.R., & Sommers, L.E. (1982). Phosphorus. In A.L. Page, R.H. Miller, & D.R. Keeney (Eds.), *Methods of Soil Analysis, Part 2: Chemical and Microbiological Properties* (2nd ed., Agronomy Monograph, 9, pp. 421–422). Madison, WI: ASA and SSSA.

Owen, S.P., & Bhuyan, B.K. (1965). Biological properties of a new antibiotic, U-13,933. *Antimicrobial Agents and Chemotherapy, 5,* 804–807.

Ozalvo, R., Cabrera, J., Escobar, C., Christensen, S.A., Borrego, E.J., Kolomiets, M.V., … & Brown Horowitz, S. (2014). Two closely related members of *Arabidopsis* 13-lipoxygenases (13-LOXs), LOX3 and LOX4, reveal distinct functions in response to plant-parasitic nematode infection. *Molecular Plant Pathology, 15*(4), 319-332.

Paily, P. V., Devi, L. R., Nair, V. G., Menon, M. R., & Nair, M. R. G. K. (1981). Malformation of leaves in black pepper. *Journal of Plantation Crops, 9*, 61–62.

Palma-Guerrero, J., Gómez-Vidal, S., Tikhonov, V. E., Salinas, J., Jansson, H. B., & Lopez-Llorca, L. V. (2010). Comparative analysis of extracellular proteins from *Pochonia chlamydosporia* grown with chitosan or chitin as main carbon and nitrogen sources. *Enzyme and Microbial Technology, 46*(7), 568–574.

Pande, A., Pandey, P., Mehra, S., Singh, M., & Kaushik, S. (2017). Phenotypic and genotypic characterization of phosphate solubilizing bacteria and their efficiency on the growth of maize. *Journal of Genetic Engineering and Biotechnology, 15*(2), 379–391.

Patten, C.L., & Glick, B.R. (1996). Bacterial biosynthesis of indole-3-acetic acid. *Canadian Journal of Microbiology, 42*(3), 207–220.

Peachey, D., Roberts, J.L., & Scot-Baker, J. (1973). Rapid colorimetric determination of phosphorus in geochemical survey samples. *Journal of Geochemical Exploration, 2*(2), 115–120.

Peachey, J. E. (1969). Nematodes of tropical crops. *Commonwealth Bureau of Helminthology Technical Communication, 40*, 355.

Pentimone, I., Colagiero, M., Ferrara, M., Nigro, F., Rosso, L.C., & Ciancio, A. (2019). Time-dependent effects of *Pochonia chlamydosporia* endophytism on gene expression profiles of colonized tomato roots. *Applied Microbiology and Biotechnology, 103*, 8511-8527.

Pentimone, I., Lebrón, R., Hackenberg, M., Rosso, L.C., Colagiero, M., Nigro, F., & Ciancio, A. (2018). Identification of tomato miRNAs responsive to root colonization by endophytic *Pochonia chlamydosporia*. *Applied Microbiology and Biotechnology, 102*(2), 907-919.

Petch, T. (1939). Notes on entomogenous fungi. *Transactions of the British Mycological Society, 23*(2), 127–148.

Pieterse, C.M.J., Zamioudis, C., Does, D.V., der and Van Wees, S.C.M. (2014). Signalling networks involved in induced resistance. In: D.R. Walters, A.C. Newton and G.D. Lyon (eds.) *Induced Resistance for Plant Defense* (pp. 58-80). Wiley.

Pires, D., Vicente, C. S., Menéndez, E., Faria, J. M., Rusinque, L., Camacho, M. J., & Inácio, M. L. (2022). The fight against plant-parasitic nematodes: Current status of bacterial and fungal biocontrol agents. *Pathogens, 11*(10), 1178.

Pires, D.E.V., Blundell, T.L., & Ascher, D.B. (2015). pkCSM: Predicting small-molecule pharmacokinetic and toxicity properties using graph-based signatures. *Journal of Medicinal Chemistry, 58*(9), 4066–4072.

Podestá, G. S., Dallemole-Giaretta, R., Freitas, L. G., Lopes, E. A., Ferraz, S., & Zooca, R. J. (2009). Atividade nematófaga de *Pochonia chlamydosporia* em solo natural ou autoclavado sobre *Meloidogyne javanica*. *Nematología Brasileira, 33*(2), 191–193.

Podestá, G. S., de Freitas, L. G., Dallemole-Giaretta, R., Zooca, R. J. F., Caixeta, L. D. B., & Ferraz, S. (2013). *Meloidogyne javanica* control by *Pochonia chlamydosporia*, *Gracilibacillus dipsosauri*, and soil conditioner in tomato. *Summa Phytopathologica, 39*, 122–125.

Poinar, G. O., & Jansson, H. B. (Eds.). (1988). *Diseases of Nematodes* (Vol. 1). Boca Raton, Calif, USA: CRC Press.

Proença, D. N., Schwab, S., Vidal, M. S., Baldani, J. I., Xavier, G. R., & Morais, P. V. (2019). The nematicide *Serratia plymuthica* M24T3 colonizes *Arabidopsis*

thaliana, stimulates plant growth, and presents plant beneficial potential. *Brazilian Journal of Microbiology, 50*, 777–789.

Puertas, A., De la Noval, B., Martínez, B., Miranda, I., Fernández, F., & Hidalgo, L. (2006). Interacción de *Pochonia chlamydosporia* var. *catenulata* con *Rhizobium* sp., *Trichoderma harzianum* y *Glomus clarum* en el control de *Meloidogyne incognita*. *Rev Protección Veg, 21*(2), 80–89.

Qin, F., Li, Y., Lin, R., Zhang, X., Mao, Z., Ling, J., … & Xie, B. (2019). Antibacterial radicicol analogues from *Pochonia chlamydosporia* and their biosynthetic gene cluster. *Journal of Agricultural and Food Chemistry, 67*(26), 7266–7273.

Ramakrishnan Nair, R., & Dutta Gupta, S. (2003). Somatic embryogenesis and plant regeneration in black pepper (*Piper nigrum* L.): I. Direct somatic embryogenesis from tissues of germinating seeds and ontogeny of somatic embryos. *The Journal of Horticultural Science and Biotechnology, 78*(3), 416–421.

Ramana, K. V., & Eapen, S. J. (1995). Parasitic nematodes and their management in major spices. *Journal of Spices and Aromatic Crops, 4*(1), 1-16.

Ramana, K. V., & Eapen, S. J. (2000). Nematode induced disease of black pepper. In P. N. Ravindran (Ed.), *Black Pepper, Piper nigrum L.* (pp. 269-295). Harwood Academic Publishers.

Ramana, K. V., & Mohandas, C. (1987). Plant parasitic nematodes associated with black pepper (*Piper nigrum* L.) in Kerala. *Indian Journal of Nematology, 17*(1), 62-66.

Ramana, K. V., Mohandas, C., & Balakrishnan, R. (1987). Role of plant parasitic nematodes in the slow wilt disease complex of black pepper (*Piper nigrum* L.) in Kerala. *Indian Journal of Nematology, 17*(2), 225–230.

Ravindra, H., Sehgal, M., Manu, T. G., Murali, R., Latha, M., & Narasimhamurthy, H. B. (2014). Incidence of root-knot nematode (*Meloidogyne incognita*) in

black pepper in Karnataka. *Journal of Entomology and Nematology, 6*(4), 51-55.

Ravindran, P. N. (2000). Introduction on black pepper. In *Black Pepper (Piper nigrum L.)* (pp. 1–22). Harwood Academic Publishers.

Ravindran, P. N., Babu, K. N., Sasikumar, B., & Krishnamurthy, K. S. (2000). Botany and crop improvement of black pepper. In *Black Pepper* (pp. 43–164). CRC Press.

Reeves, C. D., Hu, Z., Reid, R., & Kealey, J. T. (2008). Genes for the biosynthesis of the fungal polyketides hypothemycin from *Hypomyces subiculosus* and radicicol from *Pochonia chlamydosporia*. *Applied and Environmental Microbiology, 74*(16), 5121–5129.

Rosana, O.B., Eapen, S.J., & Krishna, P.B. (2016). Cloning and characterization of genes encoding two detoxifying enzymes, glutathione transferase and carboxylesterase, from burrowing nematode (*Radopholus similis*). *International Journal of Parasitology Research, 8*(1), 173–183.

Rosso, L. C., Finetti-Sialer, M. M., Hirsch, P. R., Ciancio, A., Kerry, B. R., & Clark, I. M. (2011). Transcriptome analysis shows differential gene expression in the saprotrophic to parasitic transition of *Pochonia chlamydosporia*. *Applied Microbiology and Biotechnology, 90*, 1981–1994.

Saad, A. M., Salem, H. M., El-Tahan, A. M., El-Saadony, M. T., Alotaibi, S. S., El-Shehawi, A. M., … & Swelum, A. A. (2022). Biological control: An effective approach against nematodes using black pepper plants (*Piper nigrum* L.). *Saudi Journal of Biological Sciences, 29*(4), 2047-2055.

Sabu, S. S., Kuruvila, A., & Manojkumar, K. (2020). Status of production and export of Indian black pepper. *Indian Journal of Arecanut, Spices and Medicinal Plants, 22*(4), 9–20.

Sadanandan, A. K. (2000). Agronomy and nutrition of black pepper. In P. N. Ravindran (Ed.), *Black Pepper - Piper nigrum* (pp. 163–223). Harwood Academic Publishers.

Sarker, M. S., Mohiuddin, K. M., Al-Ani, L. K. T., Hassan, M. N., Akter, R., Hossain, M. S., & Khand, M. (2020). Effect of bio-nematicide and bau-biofungicide against root-knot (*Meloidogyne* spp.) of soybean. *Malaysian Journal of Sustainable Agriculture, 4*, 44.

Sarma, Y. R., Kiranmai, G., Sreenivasulu, P., Anandaraj, M., Hema, M., Venkatramana, M., … & Reddy, D. V. R. (2001). Partial characterization and identification of a virus associated with stunt disease of black pepper (*Piper nigrum*) in South India. *Current Science, 80*(3), 459–462.

Sasanelli, N., Ciccarese, F., & Papajova, I. (2008). *Aphanocladium album* via sub-irrigation in the control of *Pyrenochaeta lycopersici* and *Meloidogyne incognita* on tomato in a plastic-house. *Helminthologia, 45*, 137–142.

Satou, T., Kaneko, K., Li, W., & Koike, K. (2008). The toxin produced by *Pleurotus ostreatus* reduces the head size of nematodes. *Biological and Pharmaceutical Bulletin, 31*(4), 574–576.

Schmeda-Hirschmann, G., Hormazabal, E., Rodriguez, J.A., & Theoduloz, C. (2008). Cycloaspeptide A and pseurotin A from the endophytic fungus *Penicillium janczewskii*. *Zeitschrift für Naturforschung C, 63*(5–6), 383–388.

Schmidt, A.R., Dörfelt, H., & Perrichot, V. (2007). Carnivorous fungi from Cretaceous amber. *Science, 318*(5857), 1743–1743.

Schmitt, D. P., Riggs, R. D., & Wrather, J. A. (Eds.). (2004). *Biology and Management of Soybean Cyst Nematode* (Vol. 11). Marceline, Mo.: Schmitt & Associates of Marceline.

Schwyn, B., & Neilands, J. (1987). Universal chemical assay for the detection and determination of siderophores. *Analytical Biochemistry, 160*(1), 47–56.

Segers, R. (1996). The nematophagous fungus *Verticillium chlamydosporium*: Aspects of pathogenicity. Doctoral dissertation, University of Nottingham.

Segers, R., Butt, T. M., Keen, J. N., Kerry, B. R., & Peberdy, J. F. (1995). The subtilisins of the invertebrate mycopathogens *Verticillium chlamydosporium* and *Metarhizium anisopliae* are serologically and functionally related. *FEMS Microbiology Letters, 126*(3), 227–231.

Segers, R., Butt, T. M., Kerry, B. R., & Peberdy, J. F. (1994). The nematophagous fungus *Verticillium chlamydosporium* produces a chymoelastase-like protease which hydrolyses host nematode proteins *in situ*. *Microbiology, 140*(10), 2715–2723.

Segers, R., Butt, T. M., Kerry, B. R., Beckett, A., & Peberdy, J. F. (1996). The role of the proteinase VCP1 produced by the nematophagous *Verticillium chlamydosporium* in the infection process of nematode eggs. *Mycological Research, 100*(4), 421–428.

Shahnazi, S., Meon, S., Vadamalai, G., Ahmad, K., & Nejat, N. (2012). Morphological and molecular characterization of Fusarium spp. associated with yellowing disease of black pepper (*Piper nigrum* L.) in Malaysia. *Journal of General Plant Pathology, 78*, 160-169.

Shamarao Jahagirdar, S. J., & Siddaramaiah, A. L. (2002). Prevalence of foot rot of black pepper in Karnataka. *Agricultural Science Digest, 22*, 45–47.

Shanmugam, G., Lee, S.K., & Jeon, J. (2018). Identification of potential nematicidal compounds against the pine wood nematode, *Bursaphelenchus xylophilus* through an *in-silico* approach. *Molecules, 23*(7), 1828.

Sharma, O.P., Pan, A., Hoti, S.L., Jadhav, A., Kannan, M., & Mathur, P.P. (2012). Modeling, docking, simulation, and inhibitory activity of the benzimidazole analogue against β-tubulin protein from *Brugia malayi* for treating lymphatic filariasis. *Medicinal Chemistry Research, 21*, 2415–2427.

Shendure, J., & Ji, H. (2008). Next-generation DNA sequencing. *Nature Biotechnology, 26*(10), 1135–1145.

Shinonaga, H., Kawamura, Y., Ikeda, A., Aoki, M., Sakai, N., Fujimoto, N., & Kawashima, A. (2009a). The search for a hair-growth stimulant: New radicicol analogues as WNT-5A expression inhibitors from *Pochonia chlamydosporia* var. *chlamydosporia*. *Tetrahedron Letters, 50*(1), 108–110.

Shinonaga, H., Kawamura, Y., Ikeda, A., Aoki, M., Sakai, N., Fujimoto, N., & Kawashima, A. (2009b). Pochonins K–P: new radicicol analogues from *Pochonia chlamydosporia* var. *chlamydosporia* and their WNT-5A expression inhibitory activities. *Tetrahedron, 65*(17), 3446–3453.

Siddiqui, Z. A., & Mahmood, I. (1996). Biological control of plant parasitic nematodes by fungi: A review. *Bioresource Technology, 58*(3), 229-239.

Siddiqui, Z. A., & Mahmood, I. (2001). Effects of rhizobacteria and root symbionts on the reproduction of *Meloidogyne javanica* and growth of chickpea. *Bioresource Technology, 79*(1), 41–45.

Singh, S., Rai, A.B., Singh, R.K., Singh, S., Rai, A.B., & Singh, R.K. (2011). Bio-management of root-knot disease of Chili (*Capsicum annum*) caused by *Meloidogyne incognita*. *Vegetable Science, 38*(1), 63–67.

Sitepu, D., & Mustika, I. (2000). Diseases of black pepper and their management in Indonesia. In P. N. Ravindran (Ed.), *Black Pepper - Piper nigrum*. Harwood Academic Publishers: 297–308.

Skidmore, A.M., & Dickinson, C.H. (1976). Colony interactions and hyphal interference between *Septoria nodorum* and phylloplane fungi. *Transactions of the British Mycological Society, 66*(1), 57–64.

Sparace, S.A., Reeleder, R.D., & Khanizadeh, S. (1987). Antibiotic activity of the pyrenocines. *Canadian Journal of Microbiology, 33*(4), 327–330.

Sparks, D.L., Page, A.L., Helmke, P.A., & Loeppert, R.H. (Eds.). (2020). *Methods of Soil Analysis, Part 3: Chemical Methods* (Vol. 14). John Wiley & Sons.

Sreeja, K., Anandaraj, M., & Bhai, R. S. (2019). Documentation of fungal endophytes of black pepper (*Piper nigrum* L.) and their seed transmission studies. *Journal of Spices and Aromatic Crops, 28*(2), 113–121.

Sreeja, T. P., Eapen, S. J., & Ramana, K. V. (1996). Occurrence of *Verticillium chlamydosporium* Goddard in a black pepper (*Piper nigrum* L.) garden in Kerala. *Journal of Spices and Aromatic Crops, 5*(2), 143–147.

Stadler, M., Anke, H., & Sterner, O. (1993). Linoleic acid—The nematicidal principle of several nematophagous fungi and its production in trap-forming submerged cultures. *Archives of Microbiology, 160*, 401-405.

Stadler, M., Mayer, A., Anke, H., & Sterner, O. (1994). Fatty acids and other compounds with nematicidal activity from cultures of Basidiomycetes. *Planta Medica, 60*(02), 128-132.

Stadler, M., Sterner, O., & Anke, H. (1993). New biologically active compounds from the nematode-trapping fungus *Arthrobotrys oligospora* Fresen. *Zeitschrift für Naturforschung C, 48*(11-12), 843-850.

Suarez, D.L. (1996). Beryllium, magnesium, calcium, strontium, and barium. In *Methods of Soil Analysis: Part 3 Chemical Methods* (Vol. 5, pp. 575–601).

Sudeep, K.C., Upadhyaya, J., Joshi, D.R., Lekhak, B., Chaudhary, D.K., Pant, B.R., … & Raghavan, V. (2020). Production, characterization, and industrial application of pectinase enzyme isolated from fungal strains. *Fermentation, 6*(2), 59.

Sundararaju, P., Koshy, P. K., & Sosamma, V. K. (1979). Plant parasitic nematodes associated with spices. *Journal of Plantation Crops, 7*(1), 15–26.

Sung, G. H., Spatafora, J. W., Zare, R., Hodge, K. T., & Gams, W. (2001). A revision of *Verticillium* sect. *Prostrata*. II. Phylogenetic analyses of SSU and LSU

nuclear rDNA sequences from anamorphs and teleomorphs of the *Clavicipitaceae*. *Nova Hedwigia, 72*(3-4), 311-328.

Sutherland, E.D., & Papavizas, G.C. (1991). Evaluation of oospore hyperparasites for the control of *Phytophthora* crown rot of pepper. *Journal of Phytopathology, 131*(1), 33–39.

Sy-Cordero, A. A., Pearce, C. J., & Oberlies, N. H. (2012). Revisiting the enniatins: a review of their isolation, biosynthesis, structure determination and biological activities. *The Journal of antibiotics*, *65*(11), 541-549.

Tamariz-Angeles, C., Huamán, G. D., Palacios-Robles, E., Olivera-Gonzales, P., & Castañeda-Barreto, A. (2021). Characterization of siderophore-producing microorganisms associated with plants from high-Andean heavy metal polluted soil from Callejón de Huaylas (Ancash, Perú). *Microbiological Research, 250*, 126811.

Taylor, C.M., Wang, Q., Rosa, B.A., Huang, S.C.C., Powell, K., Schedl, T., … & Mitreva, M. (2013). Discovery of anthelmintic drug targets and drugs using chokepoints in nematode metabolic pathways. *PLoS Pathogens, 9*(8), e1003505.

Thirugnanasambantham, K., Durairaj, S., Saravanan, S., Karikalan, K., Muralidaran, S., & Islam, V.I.H. (2015). Role of ethylene response transcription factor (ERF) and its regulation in response to stress encountered by plants. *Plant Molecular Biology Reporter, 33*, 347-357.

Thuy, T. T. T., Yen, N. T., Tuyet, N. T. A., Te, L. L., & De Waele, D. (2012). Plant-parasitic nematodes and yellowing of leaves associated with black pepper plants in Vietnam. *Archives of Phytopathology and Plant Protection, 45*(10), 1183–1200.

Tian, Y.Q., Lin, X.P., Wang, Z., Zhou, X.F., Qin, X.C., Kaliyaperumal, K., … & Liu, Y. (2015). Asteltoxins with antiviral activities from the marine sponge-derived fungus *Aspergillus* sp. SCSIO XWS02F40. *Molecules, 21*(1), 34.

Tikhonov, V. E., Lopez-Llorca, L. V., Salinas, J., & Jansson, H. B. (2002). Purification and characterization of chitinases from the nematophagous fungi *Verticillium chlamydosporium* and *V. suchlasporium*. *Fungal Genetics and Biology, 35*(1), 67–78.

Timper, P. (2014). Conserving and enhancing biological control of nematodes. *Journal of Nematology, 46*(2), 75.

Trifonov, L., Bieri, J.H., Prewo, R., Dreiding, A.S., Rast, D.M., & Hoesch, L. (1982). The constitution of vertinolide, a new derivative of tetronic acid, produced by *Verticillium intertextum*. *Tetrahedron, 38*(3), 397–403.

Trifonov, L.S., Bieri, J.H., Prewo, R., Dreiding, A.S., Hoesch, L., & Rast, D.M. (1983). Isolation and structure elucidation of three metabolites from *Verticillium intertextum*: sorbicillin, dihydrosorbicillin, and bisvertinoquinol. *Tetrahedron, 39*(24), 4243–4256.

Trifonov, L.S., Hilpert, H., Floersheim, P., Dreiding, A.S., Rast, D.M., Skrivanova, R., & Hoesch, L. (1986). Bisvertinols: A new group of dimeric vertinoids from *Verticillium intertextum*. *Tetrahedron, 42*(12), 3157–3179.

Trudgill, D. L., & Blok, V. C. (2001). Apomictic, polyphagous root-knot nematodes: exceptionally successful and damaging biotrophic root pathogens. *Annual Review of Phytopathology, 39*(1), 53–77.

Truong, N. V., Burgess, L. W., & Liew, E. C. Y. (2008). Prevalence and aetiology of Phytophthora foot rot of black pepper in Vietnam. *Australasian Plant Pathology, 37*, 431–442.

Tucker, S. L., & Talbot, N. J. (2001). Surface attachment and pre-penetration stage development by plant pathogenic fungi. *Annual Review of Phytopathology, 39*(1), 385–417.

Tunlid, A., Rosén, S., Ek, B. O., & Rask, L. (1994). Purification and characterization of an extracellular serine protease from the nematode-trapping fungus *Arthrobotrys oligospora*. *Microbiology, 140*(7), 1687–1695.

Umadevi, P., Suraby, E.J., Anandaraj, M., & Nepolean, T. (2019). Identification of stable reference gene for transcript normalization in black pepper-*Phytophthora capsici* pathosystem. *Physiology and Molecular Biology of Plants, 25*, 945-952.

Unnikrishnan Nair, P. K., Sasikumaran, S., & Sukumara Pillai, V. (1987). Time of application of fungicide for control of anthracnose disease of pepper (fungal pollu). *Agriculture Research Journal, 25*, 136–139.

Usman, M., Gulzar, S., Wakil, W., Wu, S., Piñero, J. C., Leskey, T. C., … & Shapiro-Ilan, D. (2020). Virulence of entomopathogenic fungi to *Rhagoletis pomonella* (Diptera: Tephritidae) and interactions with entomopathogenic nematodes. *Journal of Economic Entomology, 113*(6), 2627–2633.

Valadon, L.R.G., & Mummery, R.S. (1977). Natural β-apo-4′-carotenoic acid methyl ester in the fungus *Verticillium agaricinum*. *Phytochemistry, 16*(5), 613-614.

Van Berkum, J. A., & Hoestra, H. (1979). Practical aspects of the chemical control of nematodes in soil. In D. Mulder (Ed.), *Developments in Agricultural and Managed Forest Ecology* (Vol. 6, pp. 53-134). Elsevier.

Veenhuis, M., Nordbring-Hertz, B., & Harder, W. (1985). An electron-microscopical analysis of capture and initial stages of penetration of nematodes by *Arthrobotrys oligospora*. *Antonie van Leeuwenhoek, 51*, 385–398.

Venkitesan, T. S., & Setty, K. G. H. (1977). Pathogenicity of *Radopholus similis* to black pepper (*Piper nigrum*). *Indian Journal of Nematology, 7*, 17–26.

Verdejo-Lucas, S., Sorribas, F. J., Ornat, C., & Galeano, M. (2003). Evaluating *Pochonia chlamydosporia* in a double-cropping system of lettuce and tomato in plastic houses infested with *Meloidogyne javanica*. *Plant Pathology, 52*(4), 521–528.

Vieira Dos Santos, M. C., Horta, J., Moura, L., Pires, D., Conceicao, I., Abrantes, I., & Costa, S. R. (2019). An integrative approach for the selection of *Pochonia*

chlamydosporia isolates for biocontrol of potato cyst and root-knot nematodes. *Phytopathologia Mediterranea, 58*(1), 187–199.

Viggiano, J. R., de Freitas, L. G., & Lopes, E. A. (2014). Use of *Pochonia chlamydosporia* to control *Meloidogyne javanica* in cucumber. *Biological Control, 69*, 72–77.

Wan, J., Dai, Z., Zhang, K., Li, G., & Zhao, P. (2021). Pathogenicity and metabolites of endoparasitic nematophagous fungus *Drechmeria coniospora* YMF1.01759 against nematodes. *Microorganisms, 9*(8), 1735.

Wang, K., Riggs, R.D., & Crippen, D. (2005). Isolation, selection, and efficacy of *Pochonia chlamydosporia* for control of *Rotylenchulus reniformis* on cotton. *Phytopathology, 95*(8), 890–893.

Wang, R., Wang, M., Chen, K., Wang, S., Mur, L.A.J., & Guo, S. (2018). Exploring the roles of aquaporins in plant–microbe interactions. *Cells, 7*(12), 267.

Wang, Y. L., Li, L. F., Li, D. X., Wang, B., Zhang, K., & Niu, X. (2015). Yellow pigment aurovertins mediate interactions between the pathogenic fungus *Pochonia chlamydosporia* and its nematode host. *Journal of Agricultural and Food Chemistry, 63*(29), 6577–6587.

Wang, Y., Zhao, Z., Liu, F., Sun, L., & Hao, F. (2020). Versatile roles of aquaporins in plant growth and development. *International Journal of Molecular Sciences, 21*(24), 9485.

Wang, Z., Gerstein, M., & Snyder, M. (2009). RNA-Seq: a revolutionary tool for transcriptomics. *Nature Reviews Genetics, 10*(1), 57–63.

Ward, E., Kerry, B. R., Manzanilla-Lopez, R. H., Mutua, G., Devonshire, J., Kimenju, J., & Hirsch, P. R. (2012). The *Pochonia chlamydosporia* serine protease gene *vcp1* is subject to regulation by carbon, nitrogen, and pH: implications for nematode biocontrol. *PLoS One, 7*(4), e35657.

Wasternack, C., & Hause, B. (2013). Jasmonates: biosynthesis, perception, signal transduction and action in plant stress response, growth and development. An update to the 2007 review in *Annals of Botany*. *Annals of Botany, 111*(6), 1021-1058.

Weil, M., PockTsy, J. M. L., & Razafimandimby, H. (2021). Authenticating wild *Piper* species (peppers) originating from islands in the Indian Ocean on the basis of morphological, genetic and chemical characteristics. *Phytochemistry, 190*, 112886.

Westphal, A., & Becker, J. O. (2001). Components of soil suppressiveness against *Heterodera schachtii*. *Soil Biology and Biochemistry, 33*(1), 9–16.

Whipps, J. M. (1997). Developments in the biological control of soil-borne plant pathogens. *Advances in Botanical Research, 26*, 1-134.

Wright, D. J. (1981). Nematicides: Mode of action and new approaches to chemical control. In B. M. Zuckerman & R. A. Rohde (Eds.), *Plant-Parasitic Nematodes* (pp. 421-449). Academic Press.

Wu, Q., Peng, Z., Zhang, Y., & Yang, J. (2018). COACH-D: Improved protein–ligand binding sites prediction with refined ligand-binding poses through molecular docking. *Nucleic Acids Research, 46*(W1), W438-W442.

Wubben, M. J., Callahan, F. E., & Scheffler, B. S. (2010). Transcript analysis of parasitic females of the sedentary semi-endoparasitic nematode *Rotylenchulus reniformis*. *Molecular and Biochemical Parasitology, 172*(1), 31–40.

Yan, Y., Mao, Q., Wang, Y., Zhao, J., Fu, Y., Yang, Z., … & Ahammed, G. J. (2021). *Trichoderma harzianum* induces resistance to root-knot nematodes by increasing secondary metabolite synthesis and defense-related enzyme activity in *Solanum lycopersicum* L. *Biological Control, 158*, 104609.

Yang, J., Tian, B., Liang, L., & Zhang, K. Q. (2007). Extracellular enzymes and the pathogenesis of nematophagous fungi. *Applied Microbiology and Biotechnology, 75*, 21–31.

Yang, Y., Yang, E., An, Z., & Liu, X. (2007). Evolution of nematode-trapping cells of predatory fungi of the Orbiliaceae based on evidence from rRNA-encoding DNA and multiprotein sequences. *Proceedings of the National Academy of Sciences, 104*(20), 8379-8384.

Yao, Y., Huo, J., Ben, H., Gao, W., Hao, Y., Wang, W., & Xu, J. (2023). Biocontrol efficacy of endophytic fungus, *Acremonium sclerotigenum*, against *Meloidogyne incognita* under *in vitro* and *in vivo* conditions. *Biologia, 78*(11), 3305–3313.

Yao, Y.R., Tian, X.L., Shen, B.M., Mao, Z.C., Chen, G.H., & Xie, B.Y. (2015). Transformation of the endophytic fungus *Acremonium implicatum* with GFP and evaluation of its biocontrol effect against *Meloidogyne incognita*. *World Journal of Microbiology and Biotechnology, 31*, 549-556.

Ye, J., Fang, L., Zheng, H., Zhang, Y., Chen, J., Zhang, Z., & Wang, J. (2006). WEGO: a web tool for plotting GO annotations. *Nucleic Acids Research, 34*(suppl_2), W293-W297.

Yen, J. H., Niblack, T. L., Karr, A. L., & Wiebold, W. J. (1996). Seasonal biochemical changes in eggs of *Heterodera glycines* in Missouri. *Journal of Nematology, 28*(4), 442.

Zachariah, T. J., & Parthasarathy, V. A. (2008). Black pepper. In *Chemistry of Spices* (pp. 21–40). Wallingford, UK: CABI.

Zakaria, S. N. S., & Noor, N. M. (2020). A review on major fungus associated with black pepper (*Piper nigrum* L.) diseases in Malaysia. *International Journal of Scientific & Engineering Research, 11*(10), 6.

Zare, R., Gams, W., & Culham, A. (2000). A revision of *Verticillium* sect. *Prostrata*. I. Phylogenetic studies using ITS sequences. *Nova Hedwigia, 71*, 465–480.

Zare, R., Gams, W., & Evans, H. C. (2001). A revision of *Verticillium* section *Prostrata*. V. The genus *Pochonia*, with notes on *Rotiferophthora*. *Nova Hedwig, 73*, 51–86.

Zavala-Gonzalez, E. A., Escudero, N., Lopez-Moya, F., Aranda-Martinez, A., Exposito, A., Ricaño-Rodríguez, J., … & Lopez-Llorca, L. V. (2015). Some isolates of the nematophagous fungus *Pochonia chlamydosporia* promote root growth and reduce flowering time of tomato. *Annals of Applied Biology, 166*(3), 472–483.

Zavala-Gonzalez, E. A., Rodríguez-Cazorla, E., Escudero, N., Aranda-Martinez, A., Martínez-Laborda, A., Ramírez-Lepe, M., … & Lopez-Llorca, L. V. (2017). *Arabidopsis thaliana* root colonization by the nematophagous fungus *Pochonia chlamydosporia* is modulated by jasmonate signaling and leads to accelerated flowering and improved yield. *New Phytologist, 213*(1), 351–364.

Zhang, J., Li, Y., Yuan, H., Sun, B., & Li, H. (2016). Biological control of the cereal cyst nematode (*Heterodera filipjevi*) by *Achromobacter xylosoxidans* isolate 09X01 and *Bacillus cereus* isolate 09B18. *Biological Control, 92*, 1–6.

Zhang, S., & Klessig, D.F. (2001). MAPK cascades in plant defense signaling. *Trends in Plant Science, 6*(11), 520-527.

Zhao, D., Zhao, H., Zhao, D., Zhu, X., Wang, Y., Duan, Y., … & Chen, L. (2018). Isolation and identification of bacteria from rhizosphere soil and their effect on plant growth promotion and root-knot nematode disease. *Biological Control, 119*, 12–19.

Zhou, B., Mural, R.V., Chen, X., Oates, M.E., Connor, R.A., Martin, G.B., & Zeng, L. (2017). A subset of ubiquitin-conjugating enzymes is essential for plant immunity. *Plant Physiology, 173*(2), 1371-1390.

APPENDIX

APPENDIX

Potato Dextrose Broth

Potato	:	200 g
Dextrose	:	20 g
Distilled water	:	1000 ml

Peel the potato and cut it into small pieces. Boil in 500 ml distilled water and take the extract. Add dextrose to the extract. Make up to 1000ml.

Potato Dextrose Agar

Potato	:	200 g
Dextrose	:	20 g
Agar	:	17 g
Distilled water	:	1000 ml

Peel the potato and cut it into small pieces. Boil in 500 ml distilled water and take the extract. Add dextrose and agar to the extract and mix well. Make up to 1000ml.

Yeast Peptone Dextrose broth

Yeast extract	:	10 g
Peptone	:	20 g
Dextrose	:	20 g
Distilled water	:	1000 ml

Mineral salts agar medium

Dextrose	:	10 g
Ammonium sulfate	:	1 g
Potassium chloride	:	0.2 g
Dipotassium hydrogen phosphate	:	0.1 g
Magnesium sulfate, heptahydrate	:	0.2 g
Zinc oxide	:	1 g
Agar	:	17 g
Distilled water	:	1000 ml

Starch Agar

Meat extract	:	3 g
Peptic digest of animal tissue	:	5 g
Soluble starch	:	2 g
Agar	:	17 grams
Distilled water	:	1000 ml

Bray-1 reagent (0.025 M HCl in 0.04 M NH_4F)

Ammonium fluoride	:	11.1 g
HCl	:	21ml
Distilled water	:	10 l

CTAB buffer

1 M Tris	:	100 ml
5 M NaCl	:	280 ml
0.5 M EDTA	:	40 ml
CTAB	:	20 g
Distilled water	:	1000 ml
pH	:	8.0

PUBLICATIONS

1. **Rincy, M.K.**, Praveena, R., & Eapen, S.J. (2021). A modified semi-selective medium for isolation and enumeration of Pochonia chlamydosporia (Goddard) Zare & W. Gams. *Journal of Spices & Aromatic Crops*, *30*(1): 117-125. https://doi.org/10.25081/josac.2021.v30.i1.6923

2. **Rincy, M.K.**, Praveena, R., & Eapen, S.J. (2018) Development of a semi-selective medium for the isolation and quantification of the nematophagous fungus, *Pochonia chlamydosporia.* In abstracts *:* National Symposium on "Cutting edge approaches for sustainable plant disease management and ensuring farmer's profit", Tiruchirapalli.

3. **Rincy, M.K.**, Praveena, R., & Eapen, S.J. (2019) Plant growth promotion by a nematophagous fungus, *Pochonia chlamydosporia,* on black pepper (*Piper nigrum* L.). In abstracts: XIX International Plant Protection Congress (IPPC 2019) on "Crop protection to outsmart climate change for food security & Environmental Conservation", Hyderabad.

Journal of Spices and Aromatic Crops
Vol. 30 (1) : 117-125 (2021)
doi : 10.25081/josac.2021.v30.i1.6923

Indian Society for Spices

A modified semi-selective medium for isolation and enumeration of *Pochonia chlamydosporia* (Goddard) Zare & W. Gams

M K Rincy[1, 2], R Praveena[1*], S J Eapen[1]
[1]*Division of Crop Protection, ICAR-Indian Institute of Spices Research, Kozhikode - 673 012, Kerala, India*
[2]*University of Calicut, Malappuram - 673635, Kerala, India*
**E-mail: Praveena.R@icar.gov.in*

Received 24 February 2021; Revised 11 June 2021; Accepted 22 June 2021

Abstract

Pochonia chlamydosporia, is one of the most promising biological control agents for managing phytoparasitic nematodes. Isolation and enumeration of viable colonies of *P. chlamydosporia* from soil and other substrates without contamination is a major limitation, when commonly available nutrient media are used. Development of a suitable selective/semi-selective media by incorporating one or more inhibitors of microbial growth can facilitate isolation of the fungus. *In vitro* studies were carried out to test the compatibility of commonly used pesticides, namely, metalaxyl, metalaxyl-mancozeb, carbendazim, copper oxychloride, and chlorpyrifos with *P. chlamydosporia*. The fungus showed relatively high tolerance to higher doses of metalaxyl and carbendazim and was used in the modified medium for better suppression of other soil borne fungi. In the present study, Kerry's semi-selective medium was modified and evaluated by counting the viable fungal propagules in different substrates (rice, farmyard manure, maize, rice bran, barley, and sorghum) and soil artificially inoculated with the fungus. The results showed that the modified Kerry's semi-selective medium can effectively be used for isolation and quantification of *P. chlamydosporia* in routine studies.

Keywords: biological control, *Pochonia chlamydosporia*, quantification, semi-selective medium.

Introduction

Currently, phytoparasitic nematode management strategies are mainly based on nematicides, host plant resistance and crop rotation. Intensive use of nematicides results in critical environmental hazards (Aravind *et al.* 2009). The need for alternatives to chemical nematicides has accelerated research on eco-friendly measures to manage parasitic nematodes (Fourie *et al.* 2016). Biological control is an alternative management technique that can minimize the population of nematodes directly through parasitism or indirectly through the production of toxic metabolites and thus can address the possible environmental problems associated with chemical control of phytoparasitic nematodes (Dong & Zhang 2006).

ICAR-NATIONAL RESEARCH CENTRE FOR BANANA

&

INDIAN PHYTOPATHOLOGICAL SOCIETY (SOUTH ZONE)

भाकृअनुप
ICAR

Certificate

This is to certify that ~~Dr.~~ /~~Mr.~~ /Ms. MERY RINCY. K, PRAVEENA. R, SANTHOSH has participated and presented ~~Lead~~ / ~~Oral~~ / Poster entitled Development of a Semi Selective nematophagous fungus, pochonia Chlamydosporia in the *National Symposium on Cutting Edge Approaches for Sustainable Plant Disease Management and ensuring Farmers' Profit* held during 21-23 December 2018 at Tiruchirapalli, Tamil Nadu, India

S.Uma	R.Selvarajan	R.Thangavelu
Director, ICAR-NRCB	President, IPS (SZ)	Councillor IPS (SZ)
Chairperson	Organizing Secretary	Co-organizing Secretary


IPPC2019
XIX International Plant Protection Congress
IPPC2019
10-14 November 2019, Hyderabad, Telangana, India
IAPPS
Certificate of Participation
The XIX International Plant Protection Congress
is pleased to present a certificate to
Ms . MERY RINCY K
for Poster/Oral Presentation
Dr H C Sharma
President IPPC2019
Dr Rajan Sharma
Organizing Secretary IPPC2019